UNIVERSITAT DE BARCELONA

Molecular Evolution of Unicellular Eukaryote Metallothioneins: Tandem Repetition of Coordinating Domains

Anna Espart Herrero

Doctoral Program in Biotechnology
Universitat de Barcelona

MOLECULAR EVOLUTION OF UNICELLULAR EUKARYOTE METALLOTHIONEINS: TANDEM REPETITION OF COORDINATING DOMAINS

Thesis report supported by
Anna Espart Herrero

For the award of the degree of
Doctor by the Universitat de Barcelona

Thesis work carried out under the supervision of
Dr. Sílvia Atrian i Ventura
in the Department of Genetics of the Faculty of Biology
Universitat de Barcelona

Dr. Sílvia Atrian i Ventura
Supervisor

Anna Espart Herrero
Candidate

Barcelona, June 2015

This PhD thesis has been possible thanks to a FPI grant awarded by the *Ministerio de Economía y Competitividad. Secretaría de Estado de Investigación, Desarrollo e Innovación*.
2010-2014

ACKNOWLEDGEMENTS

Fa gairebé 5 anys que vaig iniciar aquest projecte que ara culmina amb la defensa d'aquesta tesi doctoral. Durant tot aquest temps, a més d'adquirir una gran quantitat de coneixements i experiència, he compartit el meu dia a dia amb un grapat de persones a qui vull mostrar el meu agraïment.

A la Dra. Sílvia Atrian per la supervisió d'aquesta tesi doctoral i la transmissió de tants coneixements durant aquests anys.

Al *Ministerio de Economía y Competitividad; Secretaría de Estado de Investigación, Desarrollo e Innovación*, per la concessió de la beca FPI (2010-2014) i els ajuts atorgats per a la realització de l'estada breu als Estats Units, que m'han permès realitzar la tesi doctoral. A la Universitat de Barcelona per la formació predoctoral i els cursos de formació continuada.

Als companys del grup METMET per tots els bons moments i tot el que hem après junts. A la María, l'Elena, la Mireia, el Sebas, la Mari, el Wei, la Sara i el Paul, i tota la gent que ha anat passant pel laboratori. Gràcies pels ànims quan feien falta i pels nostres cafès, moltes vegades impossibles. María, gracias por tu inestimable ayuda y por esas charlas que nos permitieron viajar a Cuba o a Colombia en un segundo. Elena i Mireia, gràcies per tota la vostra ajuda en llevats i en MTs i les converses valenciano-catalanes. Sebas y Mari, gracias por todo vuestro apoyo físico y moral; sin vosotros el lab no sería lo que es.

Als companys de la Universitat Autònoma per la seva col·laboració.

A tots els companys de la planta 2 del Departament de Genètica, especialment a tots els del lab 4, a les noies del lab 6 i els nois del lab 7, i a les administratives de la secretaria del departament: Rosa M, Vicky, Susi i Mercè, per estar sempre a punt per ajudar-me a resoldre qualsevol dubte burocràtic.

A la colla xerinol·la per ser com sou. Sou els millors i per res del món us canviaria. Amb els nostres defectes i virtuts ens enriquim dia a dia i el més important, ens ho passem genial. Gràcies per tots els sopars temàtics que ens permeten enfortir l'amistat. I que en vinguin molts més!

I més sincerament, agrair als meus pares i les meves germanes tot el que representen per mi. Gràcies per les vostres paraules d'ànim a qualsevol moment del dia. A la meua mare per tantes i tantes xerrades i les paraules reconfortants. Al meu pare per ajudar-me a treure "ferro a l'asunto" quan de vegades les coses semblaven complicar-se, a cada moment. A la Laura i la Gemma perquè no podria desitjar tenir unes germanes millors; sempre esteu aquí per escoltar qualsevol pensament, comentari o tonteria i això no es paga amb tot l'or del món.

Finalmente a ti Edinson, simplemente gracias por todo, por estar aquí, por todos tus "cambia esa carita", cuando a veces los ánimos no acompañaban; pero sobre todo, gracias por el día a día y por mostrarme una parte del mundo que no deja de maravillarme.

Us estic molt agraïda.

SUMMARY

Metallothioneins (MTs) are a superfamily of ubiquitous and small cysteine rich metalloproteins present in all eukaryotes and some prokaryotes organisms, that exhibit preferences to coordinate divalent or monovalent heavy metal ions such as Zn(II), Cd(II) or Cu(I), respectively; this property is used by MTs to participate in toxic metal detoxification, metal ion homeostasis and protection against oxidative stress. Features of MT sequences, as well as their structural arrangement, are be crucial to determine the metal-abilities and the related functions. In this PhD thesis we tried to expand the knowledge of some specific MTs, which are characterized by their unusual longer sequence, their Cys-distribution and their modular structuration. Thus, initially, the five *Tetrahymena thermophila* MTs (MTT1 to MTT5), which represent one of the longest MTs reported so far, were characterized to decipher their divalent or monovalent metal preferences. The modular structure of MTT1, MTT3 and MTT5 isoforms which contain high occurrence of doublets and triplets confer a clear Zn-character to these MTs. Contrarily, MTT2 and MTT4 in which not modular structures, nor Cys doublets and triplets were detected, present a specific Cu-thionein character. The gradation of metal-binding preferences from Zn-thionein to Cu-thionein shown by each MT, as well as the sequence features, constitute an important information source for MT evolutionary studies. Later, two other MTs from the human pathogenic opportunistic fungus *Cryptococcus neoformans* (CnMT1 and CnMT2) were characterized. The unusual long sequence, not known in fungal MTs so far, together with high Cys content, revealed the extraordinary Cu detoxification ability of both. The modular structure of CnMTs in which three and five Cys-containing regions, respectively, separated by cysteine free spacer regions, is crucial to conform Cu_5 clusters and improve the detoxification capacity of CnMTs; this extraordinary talent becomes decisive in *C. neoformans* virulence to avoid copper toxicity induced by macrophages cells during infection. The sequence analysis of these Cys-rich regions in CnMTs revealed their homology to other well characterized fungal MT models as *Neurospora crassa* and *Agaricus bisporus* MTs whose Cys pattern almost exactly coincides with those found in CnMTs, supporting the emergence of the long *C. neoformans* MTs by ancient tandem repetitions of a primeval fungal MT unit. Other hypothetical fungal MTs were identified *in silico* among which, *Fusarium* genus MTs. The strategy used in our group to characterize MTs, allowed us to identify a new fungal MT, whose results are extensible to *F. graminearum* and *F. oxysporum* MTs and contribute to increase the knowledge of fungal MTs.

ABBREVIATIONS

ARE	Antioxidant Response Element
CD	Circular Dichroism
Da	Dalton
ESI-MS	Electrospray Ionization Mass Spectrometry
EST	Expressed Sequence Tag
GSH	Glutathione
GSSG	Glutathione disulfide
GST	Glutathione S-transferase
ICP-AES	Inductively Coupled Plasma Atomic Emission Spectroscopy
IFI	Invasive Fungal Infection
MRE	Metal Response Element
MT(s)	Metallothionein(s)
NCBI	National Center for Biotechnology Information
PC	Phytochelatin
PDA	Potato Dextrose Agar
PDB	Protein Data Bank
rtPCR	Real-time Polymerase Chain Reaction
ROS	Reactive Oxygen Species
UV-vis	Ultraviolet-visible Spectroscopy

TABLE OF CONTENTS

INTRODUCTION

1. INTRODUCTION

1.1. METALS IN LIFE

Proteins carry out a vast range of chemical reactions inside cells. Structure building, cell signalling, immunological response or enzymatic reactions are only some of the functions that they specifically performed. Their structural features, determined by the amino acid sequence as well as their final 3D structure, explain part of the great diversity of proteins, but also the interaction with other molecules of distinct nature including cofactors, other proteins, metal ions, etc. will finally define the protein behaviour.

Enzymes are probably one of the main cell macromolecules, due to their heterogeneity (*i.e.* different structures) and their ability to bind additional components, to allow them to catalyse a large number of diverse chemical reactions. One of the most typical cofactors required by enzymes in order to be fully active are metal ions. Enzymes, as well as other metal, binding proteins, conform the group of metalloproteins. It is estimated that a nearly half of total proteins contain metal ions (Thomson & Gray, 1998) and around a 30% need them to perform their functions (Waldron & Robinson, 2009). Hence, metals are considered as essential elements for life, being in the core of multiple biological functions. The function of other metalloproteins, besides the catalytic reactions performed by enzymes, are principally metal storage and transport and signal transduction.

Among all the metal ions, transition metals as: iron, zinc, copper, nickel, manganese and cobalt, are required in small concentrations by the cell. A non-appropriate metal concentration (by default or excess), as much as the presence of non-physiological metals such as cadmium, mercury or lead, may cause cellular damage and jeopardize the lifespan of the cell. Throughout the evolution, cells have developed complex homeostatic systems to control the fragile equilibrium between needed and harmful transient metal concentrations, as well as the management of toxic metal ions (Bleackley & MacGillivray, 2011).

Among metalloproteins, metallothioneins (MTs) (which are deeply introduced below, *cf*. section 1.2.) constitute a very peculiar subset. MTs are able to interact with a wide range of metal ions, being zinc, copper and cadmium the most important, and are able to form homometallic or heterometallic complexes. Hence, the most claimed function of MTs is to help the cell to control a non-appropriate cellular concentration of these metals. Features of zinc, copper and cadmium are set out below.

1.1.1. ZINC

Zn is an indispensable element for life. After iron, it is the second transition metal most present from oceans to humans (Outten & O'Halloran, 2001). Over the evolution, the percentage of the genome encoding for proteins requiring zinc, has increased; in prokaryotes it is around 5 to 6%, whereas it increases until 9% in eukaryotes (Andreini et al., 2009). Zn acts as structural or catalytic cofactor in an important range of regulatory proteins and enzymes; being present as cofactor in all the six major classes of enzymes (oxidoreductases, transferases, hydrolases, lyases, isomerases and ligases), which catalyse more than 300 enzymatic reactions (Coleman, 1998) (Berg & Shi, 1996) (Tapiero et al., 2003), being paradigmatic examples the carbonic anhydrase and most alcohol dehydrogenases. Zn-finger domains, which are present in DNA transcription factors, as well as in protein-protein interactions (Sriram & Lonchyna, 2009), are the main representative of Zn-regulatory functions. So, the four main functions in which zinc is involved in proteins are: structural, regulatory, catalytic and antioxidant (King, 2011). Cysteines are one of the major amino acids acting as Zn-ligands in structural and catalytic proteins. Zn coordination in the protein involves a specific geometry, being the tetrahedral coordination geometry Zn the most usual (Patel et al., 2007).

Under biological conditions, zinc does not undergo redox changes and in consequence, it cannot be involved in electron transfer reactions (Sinclair & Krämer, 2012); this is the reason why zinc cellular toxicity is markedly lower than that of other physiological metals as copper or iron, which can transfer electrons (Outten & O'Halloran, 2001) or participate in Fenton reactions. In order to ensure a correct amount of this metal to all the proteins that require it, cells have developed a complex homeostatic system, comprising Zn-transporters, low affinity ligand and metallochaperones, as well as chelators as MTs (Sinclair & Krämer, 2012).

1.1.1.1. Zinc in archaea and prokaryotes

In prokaryotic organisms, zinc homeostasis involve a set of proteins responsible for the uptake, chelation and export of this metal. The zinc import is performed by different proteins: Znu, which is a high-affinity protein belonging to the ABC-transporter family; the Nramp (natural resistance-associated macrophage protein); the ZIP protein family, which include ZupT and IRT-like proteins; and other non-specific Zn-transporters that can import different metal ions. Related to chelators and chaperones, an heterogenic group of these proteins has been identified, which varies depending on the organism. In *Synechococcus elongatus*, SmtA, an MT that natively coordinates Zn^{2+}, was characterized, and it has been proposed that it is used by the cyanobacterium for zinc chelation and storage (Shi et al., 1992); in *E. coli*, Zn-binding is performed by other proteins, like YdaE, whose primary structure is similar to that of SmtA (Blindauer et al., 2002); and finally in *Haemophilus influenza*, a periplasmic Zn-chaperone called PZP1 has been reported (Lu et al., 1998). Related to zinc export, P-type ATPases (*e.g*. ZntA & ZiaA), nodulation and cell division (RND)-driven transporters, and cation diffusion facilitator (CDF) proteins super-family perform the efflux of zinc outside bacterial cells (Blencowe & Morby, 2003).

1.1.1.2. Zinc in eukaryotes

The zinc homeostatic system is highly conserved in all the eukaryotic species, which also share most of the Zn-proteins with prokaryotes. The requirement of this metal in multicellular eukaryotes (basically animals and plants) can be different depending on the considered cell types or tissues, which increases the complexity of studying the zinc proteomes. Nevertheless, the following sections are aimed at illustrating a general overview of zinc homeostatic proteins in some model organisms.

1.1.1.2.1. Zinc in yeast

In *Saccharomyces cerevisiae,* the yeast model par excellence, the proteins responsible to import Zn^{2+} into the cell are the Zrt1 (high affinity) and Zrt2 (low affinity) transporters, which belong to the ZIP protein family (Zhao & Eide, 1996a) (Zhao & Eide, 1996b), as well as Fet4 that although import iron, it can also import zinc and copper (Waters & Eide, 2002). When cellular concentrations of zinc are high, Ztr1 decreases at the same time that surplus

zinc is stored in vacuoles; Zrc1 and Cot1 are the transporters that mobilize the metal from the cytoplasm to the vacuole. When the cytoplasmic zinc requirements increase, Zrt3 is the responsible to recover it from the vacuole (MacDiarmid et al., 2002). All these proteins are synthesized under the control of the two transcription factors Zap1 and MTF-1 which respond to low zinc concentrations through multiple zinc regulations, and in which MTF-1 can be regulated at several levels and in which zinc-fingers and phosphorylation events are involved (Westin et al., 1998) (Rutherford & Bird, 2004).

1.1.1.2.2. Zinc in mammals

Zinc homeostasis in mammals follows generally the same rules that those explained for yeast, although new functions are required for biological mechanisms non existing in unicellular organisms. Hence, in mammals, zinc is essential, besides the basic cellular functions, for the successful functioning of the immune system, including the development of macrophages, neutrophils and natural killers, among others. Zinc deficiency may results in severe disorders (Prasad, 2009) because mammalian cells do not possess storage vacuoles, other structures or molecules are needed to store zinc when the concentration is high, and deliver it to the Zn-proteins when cellular concentration decreases. This function has been proposed for MTs, precisely for the human MT-1 and MT-2 isoforms, which are able to bind seven Zn^{2+} ions and to deliver then when/where it is needed (Rutherford & Bird, 2004). The synthesis of these MTs is controlled by MTF-1, that at the same time regulates the expression of the *hZTL1*, which synthesizes an enterocyte protein that import zinc from diet, and also can regulate the zinc efflux system by the *ZnT-1* gene (Rutherford & Bird, 2004) (Langmade et al., 2000).

1.1.1.2.3. Zinc in plants

In plants, zinc enters through the roots and depending on the zinc level status, it will reach the xylem directly from soil (this happening under zinc deficiency) or will be first stored and later transported (under normal zinc conditions). Once in the xylem, Zn^{2+} enters cells through ZIP (ZRT1 and ZRT2) transporters. In *Arabidopsis thaliana*, for instance, until 15 ZIP transporters have been reported, among which the IRT family is outstanding. Although IRT proteins are characterized to transport iron, they can also transport other divalent metals, among which zinc is included. Not much is known about other roles of ZIP proteins in plants (Sinclair & Krämer, 2012). Related to the zinc export, in *A. thaliana* three

proteins of the p-type ATPase HMA family (HMA2, HMA3 and HMA4) export the metal out of the cytoplasm, whereas HMA2 and HMA4 carry it out of the cell, and HMA3 mobilize zinc to the vacuoles. Also MTPs proteins belonging to CDF family, are able to import Zn^{2+} from the cytoplasm to the vacuole; and finally, also one of the protein of Nramp family, Nramp4, is able to export it from vacuole to cytoplasm (Sinclair & Krämer, 2012). Regarding zinc chelators, no exclusively proteins are identified as zinc-chelators in plants. MTs can natively bind different metals depending on the species; for instance, Ec-1 which is the MT of embryogenic wheat (*Triticum aestivum*) has been reported as a Zn^{2+} storage protein for seed development (Robinsonet al., 1993) as well as the MT2b of the plant *Colocasia esculenta* (Kim et al., 2012).

1.1.2. COPPER

Copper is a transition metal also essential for biochemical processes. The cellular copper requirements are low; for instance the human cell contains around 100 μg of this element and may vary from a tissue to another (Linder & Hazegh-Azam, 1996). It possess a redox activity which is determinant in a wide range of cellular functions, from microbes to plants or animals. Very often, copper is coordinated to proteins with the aid of another chemical ligand such as oxygen or nitrogen, providing the required assistance to induce a conformational change, a catalytic reaction or a protein-protein interaction (Kim et al., 2008). Copper ions are mainly found in two oxidation states: Cu(II) (oxidized) and Cu(I) (reduced), which consequently will exhibit different coordination geometries. Thus, it is known that Cu^{2+} coordinates better to nitrogen or oxygen donors, such as histidine or glutamate, respectively, whereas Cu^{+} does the same with sulphur donors such as cysteine or methionine (Lippard & Berg, 2007).

An important number of enzymes requiring Cu are mainly oxidative or enzymes involved in obtaining energy, localized in mitochondria and chloroplasts (Bleackley et al., 2011). A small group of copper-proteins are localized in the cytoplasm and are involved in protection and detoxification of the potential cellular damage that this metal can produce (Bleackley & MacGillivray, 2011). Due to their ability to donate and accept electrons, the uncontrolled redox Cu activity induces oxidative stress by the production of reactive oxygen species (ROS), via Fenton-like reaction, jeopardizing the well functioning of the cell (Rees &

Thiele, 2004). This is why a complex mechanism in which copper may be internalized, distributed and detoxified across the cell is needed, to ensure that environmental scarcity or abundance will not cause copper imbalance (Rees & Thiele, 2004). Copper management by different organism groups is listed below.

1.1.2.1. Copper in archaea and prokaryotes

Since many centuries ago it is known the ability that Cu plays as antimicrobial agent. Unicellular organisms are particularly sensitive to Cu ion toxicity; although this, archaea and prokaryotes, encode Cu-related proteins. Currently, it is estimated that only the 0.3% of the bacterial genome encodes for Cu-proteins (Dupont et al., 2011), showing that the role of copper in prokaryotes is significantly lower than in other eukaryotic organisms. However, nearly all bacteria possess some Cu-proteins related with copper export and protection against toxicity, through their chaperone activity. Besides, other bacterial lineages, presumably more specialized, possess Cu-proteins related with sensing, transport and export (Dupont et al., 2011) (Festa & Thiele, 2011).

Little is known about the copper uptake in bacteria. Nevertheless, they present enzymes containing copper, as cytochrome c oxidase (Cox), NADH dehydrogenase-2 or tyrosinases, localized in the periplasm where they are loaded with copper ions (Festa & Thiele, 2011). The general model of copper homeostasis that protects bacteria of its toxicity is based on three main protein families: Cop, Cue and Cus, which are highly conserved in Gram-positive and Gram-negative organisms. The Cop family, whose synthesis is copper-dependent, are P-type ATPases that export copper out of the cytoplasm and transfer it to the periplasm. The Cue proteins are multicopper oxidases. *e.g.* in *E. coli*, CueO, which is present in the periplasm, oxidizes Cu(I) to Cu(II). Finally, the Cus family is responsible to efflux the periplasmic copper out of the cell. Not all the bacteria encode all these types of proteins; for instance, in *Salmonella* spp. no Cus-like proteins has been reported, whereas in *Mycobacterium tuberculosis* other efflux copper proteins, such as MctB, are described (Dupont et al., 2011) (Festa & Thiele, 2011) (Grass & Rensing, 2001).

All the anaerobic archaea are limited copper users. Although the percentage of genome encoding Cu-proteins in archaea is slightly higher than that in bacteria (around 0.35%), only copper exporters (which maintain a no clear homology with other prokaryotic or

eukaryotic Cu-proteins) have been described (Festa & Thiele, 2011) (Dupont et al., 2011).

1.1.2.2. Copper in eukaryotes

The complexity of eukaryotic cells require more complex homeostasis mechanisms in order to uptake, distribute and detoxify copper. This is why these organisms encode: i) several proteins to specifically transport copper across cell membranes; ii) proteins involved in copper homeostasis, the synthesis of which is regulated by intracellular copper to respond to high or low concentrations; and iii) proteins able to maintain a communication system between cellular copper levels, their homeostasis in organelles, the external environment and other cellular processes (Rees & Thiele, 2004). Besides, multicellular organisms possess copper regulation mechanisms that are tissue-specific due to their particular needs. The main mechanisms in copper homeostasis in eukaryotes are discussed below.

1.1.2.2.1. Copper in yeast

S. cerevisiae is a well studied model, in which the main copper homeostasis mechanisms, also present in other species, are identified (Figure 1). The copper uptake in *S. cerevisiae* initiates when the metallo-reductases Fre1/2 reduce extracellular copper from Cu^{2+} to Cu^{+}. Then these metal ions are mobilized inside the cell by means of the high-affinity copper transports Ctr1, Ctr3 whose genes are induced in low copper concentrations (Puig et al., 2002). Evenly, some low-affinity copper transport proteins participate in copper mobilization; they are Ctr2, which also belongs to the CTR family and acts specifically transporting Cu^{+} to vacuolar copper storage (Rees & Thiele, 2004), and Fet4 which is able to transport not only copper but also iron and zinc (Puig & Thiele, 2002) (Festa & Thiele, 2011).

Once inside the cell, copper ions must be readily bound, to avoid the potential damage they can cause if free, and will be then transferred to specific targets. In yeast, this role is performed by different metallochaperones. One of them is Atx that will deliver the bound Cu to Ccc2, a copper transporter P-type ATPase (similar to those found in prokaryotes) localized on the Golgi membrane. Later the copper ions will be transported into the lumen of the secretory compartment, where they can be incorporated as ligands in Cu-proteins such as laccase, or the multicopper ferroxidase Fet3 (Rees & Thiele, 2004). Other Cu-chaperones are Cox17 and CCs. Cox17 delivers the Cu ions to mitochondria, where its membrane proteins such as Sco1, Sco2 and cytochrome c oxidase (Cox) will bind them; on the other hand, CCs

transports copper to Cu,Zn superoxide dismutase (Sod1), which consequently, will download Cu^{+} into mitochondrial intermembrane space to catalyse the disproportionation of superoxide ($O_2^{-\bullet}$) to hydrogen peroxide (H_2O_2) and oxygen to protect cell against oxidative stress (Festa & Thiele, 2011) (Puig & Thiele, 2002) (Bleackley & MacGillivray, 2011).

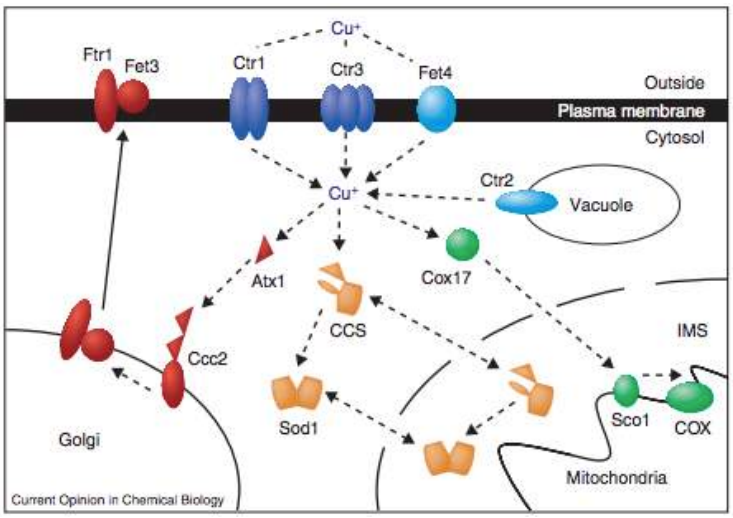

Figure 1. Proteins involved in Cu^{+} uptake and distribution in *S. cerevisiae*. Copper ions can be internalized by Ctr1/3 after being reduced from Cu^{2+} to Cu^{+}. After that, three different metallochaperones transport Cu^{+} to other Cu-proteins. Atx delivers copper to Ccc2, CCs to Sod1 and Cox17 to Sco1 and Cox. Each pathway is devoted to a specific activity in which copper can be used as cofactor of other Cu-proteins required in the cytoplasm (Atx1-Ccc2 pathway) or the mitochondria (Cos17-Sco1/Cox pathway) or the metal ion can be modified to avoid cell damage (Ccs-Sod1 pathway). IMS: intermembrane space (adapted from Puig et al., 2002).

Finally, in *S. cerevisiae*, the strategies to protect cells against copper toxic effects, involve two principal actions. On the one hand, the performance of Cup1 and Crs5 MTs, whose synthesis is induced by the copper transcription factor Ace1, and are able to scavenge copper ions when their cellular concentration is high. On the other hand, the vacuolar storage of these metal ions, mediated by Ctr2, in order to enclose them and avoid oxidative stress (Festa & Thiele, 2011) (Rees & Thiele, 2004).

1.1.2.2.2. Copper in mammals

Copper homeostasis in mammals involves similar proteins to those found in yeast. However, some differences are significant. Ctr1/3 proteins which are highly conserved in eukaryotic species, are distinctly induced in mammals than in yeast; specifically Ctr1, which is synthesized when the levels of Cu-induced endocytosis and degradation increase (Festa & Thiele, 2011). Atox (Atx, in yeast cells) and Ccs chaperones act in the same way as in yeast. Furthermore, ATP7A, which is a P-type ATPase, plays an important role by pumping copper to the portal circulation in the liver, as well as in other copper requiring tissues, such as the placenta or the brain, or proteins as ceruloplasmin, which is involved in iron homeostasis (Festa et al., 2008). Among the mammalian MTs, MT3 and MT4 are most probably related with Cu homeostasis; MT3 (expressed in the central nervous system) have a dual behaviour in which the N-terminus domain or β-domain, is able to coordinate Cu^{+} ions efficiently and the C-terminus or α-domain, shows a preference binding Zn^{2+}. Moreover, MT4 (expressed in epithelial tissue) presents a greater preference for Cu-binding in front of divalent metal ions (Artells et al., 2014) (Tió et al., 2004) (Atrian & Capdevila, 2013).

1.1.2.2.3. Copper in plants

Copper homeostasis presents a more complex system in plants than in other organisms. Specific copper proteins have been identified, probably in relation to the presence of plant-specific organelles that require copper, such as chloroplasts. and also to the excess of copper in their environment (mainly localized in soil), on which plants are dependent (Burkhead et al., 2009). Hence, it is worth to note that in the plant model *Arabidopsis thaliana* it has been found six Ctr proteins, named as COPT1-6 that are involved in several functions, from copper uptake in roots to vacuolar copper storage among others. Evenly the P-type ATPases that are known as group, present different functions in copper mobilization, which include Cu^{+} export outside the cell, transport inside the chloroplasts and also into their inner structures (Hussain et al., 2004) (Burkhead et al., 2009).

1.1.2.3. Copper and virulence

As explained, copper is present in all organisms, from prokaryotes to eukaryotes. But at high concentrations Cu^{+} acts as anti-microbial, as well as it is toxic for all cells. When

mammalian organisms are infected by microorganisms, their immune system recruits copper and uses it, as a defense strategy. Macrophages cells phagocyte the pathogen and create a hostile environment inside the phagolysosome to fight and kill the microorganism. CTR1 gene expression increases and start to import more extracellular copper which will be transported from the cytoplasm to the phagolysosome by ATP7A. Once inside the lumen, Cu^{+} will react with other elements to increases ROS, nitric oxide, proteases and decrease pH and iron concentration (Festa & Thiele, 2012).

Consequently, pathogenic bacteria and fungi have evolved copper resistance mechanisms. Bacteria manage copper toxicity basically with copper sensing and export proteins. Cu,Zn SOD, chaperones and P-type ATPases, as well as copper efflux pumps and copper resistance operons are present in different Gram-positive and Gram-negative species (Festa & Thiele, 2012).

Pathogenic fungi also possess copper toxicity defense mechanisms. For instance, *Cryptococcus neoformans,* which is a human opportunistic fungal pathogen, uses Cu,Zn SOD and cupro-laccases. Laccase is required in the synthesis of melanin, which plays a crucial role in the protection against oxidative stress induced by macrophages during the infection (Rees & Thiele, 2004). Furthermore, in the experimental work performed by Ding et al. (Ding et al., 2011) it has been also demonstrated the role of Cuf1 in the induction of several genes in response to the micro-environmental copper excess, usual in the infection stages (Ding et al., 2011) (Festa & Thiele, 2012). Two of these genes encode the *C. neoformans* copper MTs, which are the subject of part of this thesis work.

1.1.3. CADMIUM

Cadmium is a divalent transition (also considered post-transition) metal that is not physiological, while, in fact constituting an important environmental pollutant and toxic for life. Its presence in all the terrestrial surfaces represents a potential interaction with it, because it is internalized by living organisms. Virtually all organisms need to remove the cellular cadmium to avoid its toxicity and consequential irreversible damages. Cd^{2+} is related with increased levels of ROS, although it seems that it can not produces ROS directly. Hence, the action of Cd^{2+} is more related with the interference of cell metabolism as a deleterious substitute of Zn, than in radical production (Deckert, 2005).

Only the marine diatom *Thalassiosira weissflogii* is known to need cadmium in its cells (Tang et al., 2014). Nevertheless, some organisms are able to tolerate better than others a certain amount of this heavy metal. In general terms, algae, cyanobacteria and animals are more sensitive to cadmium than bacteria, fungi and plants (Trevors et al., 1986) (Clemens et al., 2009).

Despite that the physical properties of Cd^{2+} are different from Zn^{2+}, cadmium benefits from the chemical properties that shares with zinc, so that it is able to replace this ion in several proteins, altering biological systems, and resulting in dysfunctions, mutagenesis and cell death (Tang et al., 2014). Organisms have developed multiple mechanisms to respond to this toxicity and the induced oxidative stress, regulating the cellular homeostasis, activating the efflux cellular pumps and chelating cadmium through cysteine-rich ligands such as MTs, glutathione (GSH) or phytochelatins (PCs), obtained from reduced GSH (Bertin & Averbeck, 2006) (Vido et al., 2001).

1.1.3.1. Cadmium in archaea and prokaryotes

Mechanisms that confer resistance to cadmium have been described in some archaea and bacteria. For instance in the archae *Thermococcus gammatolerans,* the exposition to cadmium induces the activation of several mechanisms involved in redox homeostasis, oxygen detoxification and repair mechanisms (Lagorce et al., 2012). On the other hand, bacteria contains in most cases, cadmium efflux systems that are plasmid-encoded; thus, in the gram-positive *Staphylococcus aureus*, three proteins are involved in Cd^{2+} homeostasis. A P-type ATPase localized in the membrane-bound, CadA, is the responsible to Cd^{2+} efflux; CadC is required for full resistance, whereas CadR is supposed to regulate this resistance (Nies, 1992). Although few MTs have been described in bacteria, they do not seem to show high affinity for Cd^{2+}; for instance, SmtA which belong to the cyanobacterium *Synechococcus elongatus* has been preferably related to Zn metabolism than to Cd detoxification (Shi et al., 1992).

1.1.3.2. Cadmium in eukaryotes

Exposure to cadmium not only alters proteins, DNA or cellular structures directly (Zhou et al., 2013) (Gałazyn-Sidorczuk et al., 2009), it can be also bioaccumulated and affect progressively the cell. In lower eukaryotes cadmium toxicity will result to irreparable cell damage and its death. However, in higher eukaryotic organisms the bioaccumulation and toxicity can be initially confined to a specific tissue to result in a disorder that will affect the whole organism, only if the exposure to cadmium persist.

1.1.3.2.1. Cadmium in yeast

Cadmium is able to enter *S. cerevisiae* cells using proteins such as Zrt1p, Fet4 , Sm1p or Mid1p that usually transport zinc, iron, manganese or calcium, respectively. Once inside the cell, it will be removed by different mechanisms to avoid the toxicity. The ubiquitous Pca1p, which is a P-type ATPase, exports cadmium out of the cell and contributes to reduce their intracellular levels. Vacuolar sequestration is also usual as strategic mechanism and is carried out by three different Cd-transporters: Zrc1p, Bpt1p and Ycf1p (Wysocki & Tamás, 2010). Finally, metal chelation is performed by cysteine-rich agents able to bind the ions; they are basically MTs and PCs. Cup1 and Crs5 MTs do not present a special preference to bind Cd^{2+}, though they are able to effectively coordinate it (Winge et al., 1985) (Wysocki & Tamás, 2010). PCs, which are polymers of (γ-Glu-Cys)n-Cys units synthesized from GSH, do not present any cadmium affinity in *S. cerevisiae*; however in the fission yeast *Schizosaccharomyces pombe*, where they are called cadystins, PCs are the principal cadmium detoxification pathway (Clemens, 2006b).

1.1.3.2.2. Cadmium in mammals

Mammal exposure to cadmium may result in health problems: blood, respiratory, bone or kidney disorders are probably the most frequent, but it also inhibits cell proliferation and induces apoptosis. Additionally, it is considered a human carcinogen and mutagen by the International Agency for Research on Cancer (IARC) (Martelli et al., 2006) (Clemens et al., 2009) (Deckert, 2005). After cadmium is introduced into the body through inhalation or ingestion, it enters cells, basically through DMT1, a proton-metal co-transporter or calcium channels. Unlike what happens in yeast, it seems that in mammals, cadmium do not use Zn-importers to be internalized (Martelli et al., 2006). Once inside cells, the detoxification machinery represented by MTs and GSH will scavenge the toxic metal. MTs, the synthesis of

which is strongly induced by cadmium, can harbour Cd^{2+} through Zn^{2+} ions replacement in Zn-MT species (Clemens, 2006a) (Hamer, 1986); whereas the thiol chelating scavenger GSH, can bind Cd and excrete the complexes into the bilis and the renal tubules to facilitate its removal (Martelli et al., 2006).

1.1.3.2.3. Cadmium in plants

Plants acquire heavy metals through mychorrizas, roots and cell walls (Das et al., 1997) (Hall, 2002). The uptake of cadmium alters the metabolism of plants, leading to different disorders, such as the inhibition of photosynthesis or the reduction of water and minerals uptake; these finally will result in chlorosis and plant growth inhibition (Deckert, 2005) (Perfus-Barbeoch et al., 2002).

Cadmium uptake in plants is performed across plasma membrane and by proteins that are related with the uptake of other metal ions: ZIP proteins (Zn/Fe-importers such as IRT1 and ZNT1), Ca^{2+} and K^{+} channels and Nramp, which uptake cadmium from vacuole to cytoplasm (Pence et al., 2000) (Clemens, 2001) (Hall & Williams, 2003) (Perfus-Barbeoch et al., 2002). Once in the cytoplasm, cadmium must be chelated to be immobilized or removed. Sequestration occurs in vacuoles, or cells remove cadmium to xylem. There are two main ways by which Cd^{2+} can arrive to vacuoles: i) after the uptake it is bound to GSH as ligand to form GS_2-Cd, which will result in the complex PC-Cd, after the action of the PC synthase; then, ABC-type transporters will translocate the PC-Cd complex from cytosplasm to vacuole (Clemens, 2006b); ii) cadmium can be transported directly to vacuoles by the Cd^{2+}/H^{+} antiport activity pathway (Salt & Wagner, 1993). Furthermore, the P-type ATPases HMA4 can export cadmium to xylem and remove it from the cell (Clemens, 2006b). Finally, cadmium chelation in cell plants is performed by PCs and MTs. PCs which are the principal cadmium detoxifying pathway in plants, can be induced after a short exposure of different metals, although not all of these metals are the substrate of PCs (Clemens, 2006a) (Clemens, 2006b). In relation to the participation of MTs, although according to Clemens, the role of MTs in the detoxification of Cd^{2+} is not clear (Clemens, 2006a); *in vitro* experiments in some MT plants have shown their ability to coordinate Cd^{2+}, such as *Quercus suber* and *Glycine max* MTs (Pagani et al., 2012) (Domènech et al., 2007), suggesting a probably role of them in cadmium detoxification.

1.2. METALLOTHIONEINS

Metallothioneins (MTs) are conserved metalloproteins present in all the eukaryotes and a important number of prokaryotes, but not reported in archaea. They are extremely heterogeneous but are characterized by: i) small size (normally, up to 10 kDa); ii) high content of cysteine residues (15-30%) with practically no aromatic residues; and iii) ability to coordinate metal ions through metal-thiolate bonds (Hamer, 1986) (Capdevila & Atrian, 2011) (Blindauer & Leszczyszyn, 2010).

In 1957, Margoshes and Vallee identified the first MT in the horse kidney cortex, although they not named it as *metallothionein* initially, but as *cadmium-binding protein* (Margoshes & Vallee, 1957). The *metallothionein* name appeared for the first time in 1960 when Kägi and Vallee confirmed its unusually high metal and sulphur content (Kägi & Vallee, 1960). Since then, and until early 2015, more than 8,000 protein sequences respond to *metallothionein* and *metallothionein-like* queries in the NCBI database, although that number decreases to 4,000 if we consult more specific protein databases, such as UniProtKB. As Capdevila and Atrian indicate (Capdevila & Atrian, 2011), more than 20,000 scientific papers are devoted to MT studies, most of them appearing in the last decades and focusing mainly on animal and plant MTs, although the studies on fungal and bacterial MTs are also increasing, due to their growing importance in crops and human diseases, or as biomarkers (Capdevila et al., 2012) (Blindauer, 2014).

1.2.1. STRUCTURE

Contrarily to what is observed in the evolution of a wide range of conserved proteins, MTs have evolved in a heterogeneous way, so it is no easy to classify them according to their sequence. Furthermore, most of the typical structure elements are absent, this increasing the difficulty in characterizing MTs. However differences in primary and three-dimensional structures provide the biggest peculiarities in these proteins.

1.2.1.1. Primary structure

Primary structure of MTs can be extremely diverse among the different species, in terms of length, amino acid composition, Cys patterns or number of isoforms per species. Nevertheless some attributes are common, being part of the defining features of MTs:

i. The distribution of the cysteine residues in the MT sequences is greatly conserved; CXC and CXXC patterns are the most frequents, but they are not unique. Also Cys doublets and triplets (CC, CCC) are present in some sequences, though they are less common (Blindauer & Leszczyszyn, 2010) (Guo et al., 2008).
ii. The remaining residues that compose the MT sequences are mostly small amino acids, such as alanine and glycine, providing a flexible structure which allows a better protein folding to harbour the metal ions inside the formed cluster.
iii. A scarce percentage of aromatic residues (phenylalanine, tryptophan, histidine or tyrosine) can be present in some MTs, being histidine the most frequent among them. One of the properties that aromatic amino acids provide in proteins is the structural stability; hence, their absence or poor presence in MTs do not contribute to this feature, being the metal-thiolate bonds who fulfill this (Blindauer & Leszczyszyn, 2010).

1.2.1.2. Secondary structure

A few secondary structure elements have been identified in MTs. Analytical techniques, such as Infrared-, Circular Dichroism- and Raman-spectroscopy have been used to this end. Until now, only β-turns have been reported in some plant MTs, in the rat MT2 or even in recombinant human MT2 (Freisinger, 2008) (Luber & Reiher, 2010) (Rigby & Stillman, 2004). Nonetheless, not much else is known about it, suggesting that this structure does not play a crucial role in MTs.

1.2.1.3. Three-dimensional or Tertiary structure

The metal-free MT polypeptide (apo-MT) shows a random-coil structure that becomes folded only after metal ion binding (Romero-Isart & Vasák, 2002). Thus, the three-dimensional structure of MTs (in fact of metal-MT complexes) depend at the end on the cysteine arrangement in the protein chain, and on the metal ions harboured, through metal-thiolate clusters. The variety of metal ions that some MTs are able to coordinate contributes to a high heterogeneity in the three-dimensional structure of the metal-MT complexes. Despite this, few MTs have been analyzed at this level. In the Protein Data Bank (PDB), the NMR solution and the X-ray crystallography techniques have allowed analysing the cluster formed with different metals by 14 complete or partial (*i.e.* separated domains) MTs. The differences of the coordinated metal ions or the specific MT domain analyzed have been taken into account to reveal particularities in each three-dimensional metal-MT complex, resulting in a total of 35 different PDB entries (Table 1).

Table 1. MTs with solved metal-complex three-dimensional structures, available in PDB database.

ORGANISM	MT	METAL	PDB ENTRY
Homo sapiens	MT2	Cd	1MHU, 2MHU
	MT3	Cd	2F5H, 2FJ4, 2FJ5
Mus musculus	MT1	Cd	1DFT, 1DFS
	MT3	Cd	1JI9
Rattus rattus	MT2	Cd	1MRT, 2MRT
		Cd-Zn	4MT2
Oryctolagus cuniculus	MT2A	Cd	1MRB, 2MRB
Notothenia coriiceps	MT	Cd	1M0G, 1M0J
Homarus americanus	β-MT1	Cd	1J5L, 1J5M
Callinectes sapidus	β-MT1	Cd	1DMC, 1DMD, 1DME, 1DMF
Strongylocentrotus purpuratus	MTA	Cd	1QJK, 1QJL
Triticum aestivum	E_c-1	Zn	2L62, 2KAK
		Cd	2MFP, 2L61
Saccharomyces cerevisiae	Cup1	Cu	1AQR, 1AQS, 1FMY, 1RJU
		Ag	1AOO, 1AQQ
Neurospora crassa	NcMT	Cu	1T2Y
Synechococcus elongatus	SmtA	Zn	1JJD

These results reveal the presence of two domains for the vertebrate MTs when coordinating divalent metal ions (Zn(II) or Cd(II)): one so-called β-domain (N-terminus) and one so-called α-domain (C-terminus). Each domain folds into a metal-thiolate cluster, in β containing 3 divalent metal ions, and in α, 4 divalent metal ions (Figure 2). This is common to all mammalian MTs; for instance, all the isoforms analysed for human, mouse, rat and rabbit share 20 cysteines, of which 9 are in the β-domain ($M(II)_3(SCys)_9$) and the remaining 11 in the α-domain ($M(II)_4(SCys)_{11}$). It is worth noting that this does not occurs in all MTs, such is the case of the cyanobacteria *S. elongatus* SmtA, which folds into a single domain, when it coordinates Zn(II) ions (Blindauer et al., 2001).

On the other hand, single domains are supposed to be common in metal-MT complexes with monovalent metal ions, such as Cu(I) or Ag(I). This is the case of the yeast *S. cerevisiae* Cu-, Ag-Cup1 complex, whose 12 cysteines are suggested to coordinate 7 copper ions (Cu_7-Cup1) (Romero-Isart & Vasák, 2002), or the fungus *N. crassa*, whose 7 cysteines more efficiently coordinating 6 ions (Cu_6-NcMT) (Cobine et al., 2004).

A

B

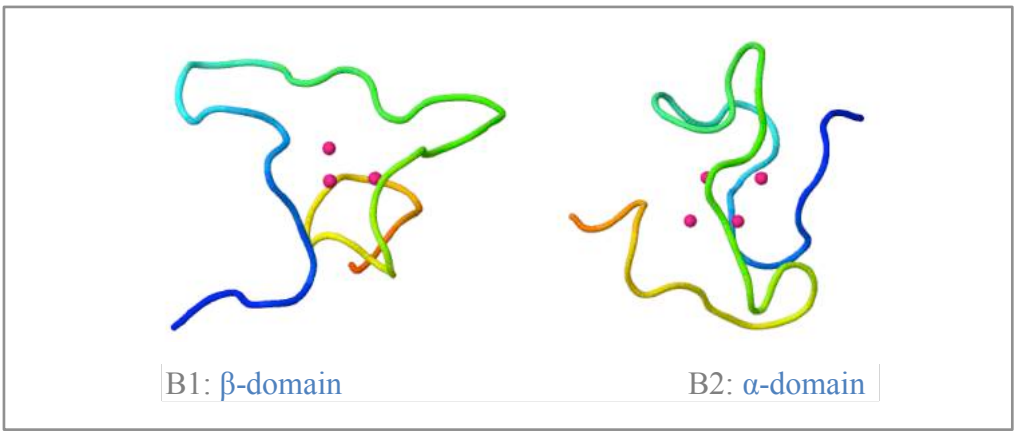

Figure 2. A. Alignment of the β- and α-domain from mouse MT1 (P02802), human MT2 (P02795) and rabbit MT2A (P18055); cysteine residues are highlighted to show their total conservation in each domain (sequences recovered from UniprotKB). **B**. 3D cluster structures from mouse MT1 domains; **B1**. $Cd_3(SCys)_9$ β-domain (1DFT) and **B2**. $Cd_4(SCys)_{11}$ α-domain (1DFS); the pink coloured spots correspond to Cd^{2+} metal ions. (Images from PDB).

The divalent metal ions are bound to mammalian MTs according to a tetrahedral coordination geometry, while monovalent ions usually are trigonally- or digonally-coordinated (Ngu & Stillman, 2009). The metal-thiolate MT complexes show a high thermodynamic stability associated to a kinetic lability depending on the cell requirements. All this give to the three-dimensional structure an important role in the cellular function of the MT (Romero-Isart & Vasák, 2002) (Vasák & Hasler, 2000) (Vasák, 2005).

1.2.1.4. Quaternary structure

There is no clear evidence of quaternary structures in MTs, although some sporadic studies have identified weak dimers in mammalian MTs, via chemical modification or under metal excess (Templeton & Cherian, 1984) (Carpenè et al., 2007). Currently, the quaternary structure is not considered as an important factor for biological MT functions.

1.2.2. CLASSIFICATION

30 years after the first MT report by Margoshes and Vallee, and because the identified MTs were increasing in number and heterogeneity, it was considered necessary to establish a MT classification. In 1987, Kägi & Kojima developed a metallothionein nomenclature in order to attempt a coherent MT grouping. From then, three systems of MT classifications have been proposed:

1.2.2.1. First classification

The empirical system proposed by Kägi & Kojima, established three classes of MTs according to the Cys pattern and distribution in the polypeptide sequence (Kägi & Kojima, 1987) (Blindauer, 2014).

Class I: comprises MTs homologous to the equine MT-1B. All the vertebrate MTs were in this group, but also the crustacean, some molluscs and the fungus *N. crassa* MTs.

Class II: all the MTs with no sequence homology to the equine MT were grouped in this class. Plant, fungal or invertebrate MTs, as well as cyanobacteria MTs are in this category.

Class III: integrated by enzymatically-synthesized cysteine-rich polypeptides that although do not share sequence similarity with MTs, are functionally and phenotypically related. The main examples are PCs and cadystins present in plants and fungi, respectively, which are polymers of (γ-Glu-Cys)n-Cys units.

The main problem of this classification was that it did not differentiate among the many MT sequences that were being included in Class II owing to new MT discoveries. That is why another classification system was proposed by the same authors some years later.

1.2.2.2. Second classification

At the end of the last century, the previous classification became insufficient to classify MTs due to the increasing number of new MT identified. Then Binz & Kägi proposed a new classification based on phylogenetic relationships, in addition to sequence similarity (Binz & Kägi, 1999) (Blindauer, 2014). A total of 15 families were arranged according to a set of specific features. This led to place a huge number of MTs of different taxa in a same family, whereas others from organisms of the same kingdom were grouped into different families. It is the case for instance, of the fungal MTs, which are classified in six different families (Table 2).

Table 2. Binz & Kägi MT classification. It is shown an example of each of the 15 represented families.

FAMILY	GROUP	EXAMPLE	SEQUENCE	UNIPROTKB ENTRY
1	**Vertebrates**	*H. sapiens* MT2	MDPNCSCAAGDSCTCAGSCKCKECKCTSCKKSCCSCCPVGCAKCAQGCICKGAS DKCSCCA	P02795
2	**Molluscs**	*M. edulis* MT-10-IV	MPAPCNCIETNVCICDTGCSGEGCRCGDACKCSGADCKCSGCKVVCKCSGSCAC EGGCTG PSTCKCAPGCSCK	P80249
3	**Crustaceans**	*H. americanus* MT1	PGPCCKDKCECAEGGCKTGCKCTSCRCAPCEKCTSGCKCPSKDECAKTCSKPCS CCXX	P29499
4	**Echinoderms**	*S. purpuratus* SpMTA	MPDVKCVCCKEGKECACFGQDCCKTGECCKDGTCCGICTNAACKCANGCKCGS GCSCTEGNCAC	P04734
5	**Diptera**	*D. melanogaster* MTNB	MVCKGCGTNCQCSAQKCGDNCACNKDCQCVCKNGPKDQCCSNK	P11956
6	**Nematodes**	*C. elegans* MT1	MACKCDCKNKQCKCGDKCECSGDKCCEKYCCEEASEKKCCPAGCKGDCKCANCH CAEQKQCGDKTHQHQGTAAAH	P17511
7	**Ciliates**	*T. thermophila* MTT1	MDKVNSCCCGVNAKPCCTDPNSGCCCVSKTDNCCKSDTKECCTGTGEGCKCVNCK CCKPQANCCCGVNAKPCCFDPNSGCCCVSKTNNCCKSDTKECCTGTGEGCKCTSCQ CCKPVQQGCCCGDKAKACCTDPNSGCCCSNKANKCCDATSKQECQTCQCCK	Q8WSW3
8	**Fungi 1**	*N. crassa* MT	MGDCGCSGASSCNCGSGCSCSNCGSK	P02807
9	**Fungi 2**	*C. glabrata* MT1	MANDCKCPNGCSCPNCANGGCQCGDKCECKKQSCHGCGEQCKCGSHGSSCHGSCG CGDKCECK	P15113
10	**Fungi 3**	*C. glabrata* MT2	MPEQVNCQYDCHCSNCACENTCNCCAKPACACTNSASNECSCQTCKCQTCKC	P15114
11	**Fungi 4**	*Y. lipolitica* MT3	MEFTTAMLGASLISTTSTQSKHNLVNNCCCSSSTSESSMPASCACTKCGCKTCKC	Q9HFD0
12	**Fungi 5**	*S. cerevisiae* Cup1	MFSELINFQNEGHECQCQCGSCKNNEQCQKSCSCPTGCNSDDKCPCGNKSEETKKSC CSGK	P0CX80
13	**Fungi 6**	*S. cerevisiae* Crs5	MTVKICDCEGECCKDSCHCGSTCLPSCSGGEKCKCDHSTGSPQCKSCGEKCKCETTCT CEKSKCNCEKC	P41902
14	**Prokaryotes**	*Synechococcus sp* SmtA	MTSTTLVKCACEPCLCNVDPSKAIDRNGLYYCSEACADGHTGGSKGCGHTGCNCHG	P30331
15	**Plants**	Type 1: *P. sativum* MT Type 2: *L. esculetum* MT Type 3: *A. thaliana* MT3 Type 4: *T. aestium* MT	MSGCGCGSSCNCGDSCKCNKRSSGLSYSEMETTETVILGVGPAKIQFEGAEMSAASED GGCKCGDNCTCDPCNCK	P20803

1.2.2.3. Third classification

More recently, our research group proposed another criterion, more functional, to classify MTs, which is based on their metal-binding preferences, *i.e*. the preference to conform homometallic, well-shaped divalent (Zn(II) or Cd(II)) or monovalent (Cu(I)) metal-MT complexes. At the beginning, two categories, Zn-thioneins and Cu-thioneins, were proposed (Valls et al., 2001). Hence, depending on the preference to yield a unique, well-folded homometallic complex with a specific kind of metal ions, MTs were classified in one group or in another. However, due to the existence of MTs that exhibit partial, or shared, metal preferences (*i.e*. not genuine Zn-thionein nor genuine Cu-thionein), it was necessary to set up a gradation among these two groups (Figure 3) (Bofill et al., 2009). For instance, in the yeast *S. cerevisiae,* Cup1 is considered a genuine Cu-thionein, forming single well-folded Cu-species; whereas Crs5 forms heterometallic Zn,Cu-Crs5 when it folds in the presence of regular Cu. Obviously, it is known that a genuine Cu-thionein is also able to bind divalent metal ions in an enriched media with Zn^{2+} or Cd^{2+}; however the formed complexes will be a mixture of oxidized, partially metalated species, and they will contain S^{2-} ions as additional ligands, mainly when synthesized as Cd-complexes (Palacios et al., 2011). Similar results are observed when a Zn-thionein is synthesized with Cu^{+}, in this case a mixture of heterometallic species, folded into poorly stable structures will be detected (Palacios et al., 2011).

A

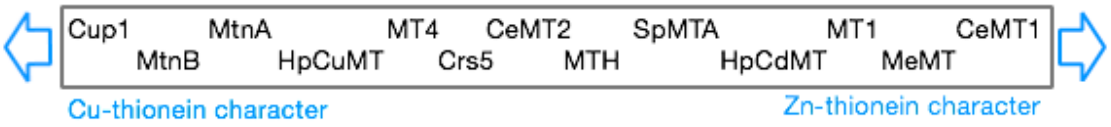

B

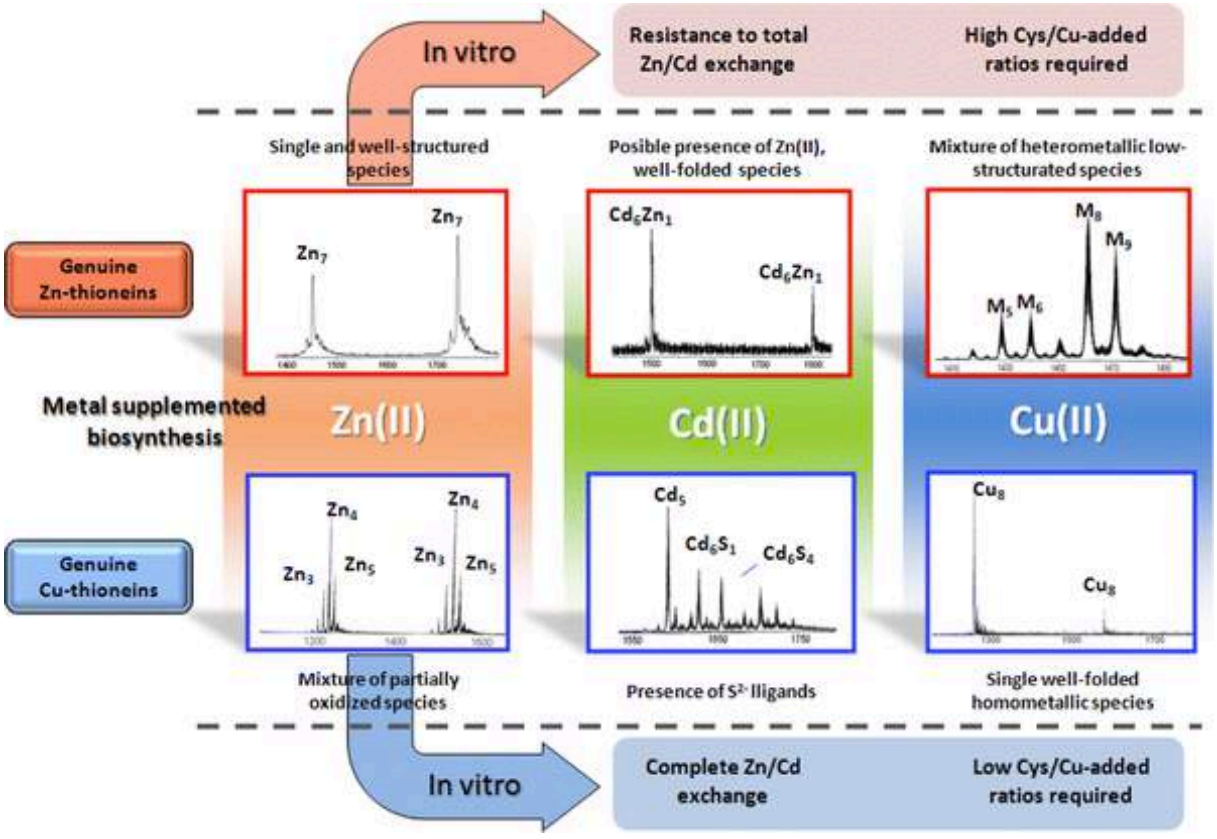

Figure 3. MT classification according to their metal preferences. **A**. Different MTs placed according to their metal preference; the ends are occupied as the most genuine Cu-thioneins (left) and Zn-thioneins (right). (Adapted from Palacios et al. 2011). **B**. Metal complexes features of synthesizely recombinant genuine Cu- and Zn-thioneins in metal supplemented media, and observed metal species in Cd and Cu titration from Zn-MT complexes. (Adapted from Palacios et al. 2011).

1.2.2.3.1 *Obtaining recombinant metal-MT complexes. A successful approach*

MTs classification according the criterion of metal-binding preference, is subordinate to the availability of the corresponding metal-MT complexes. One of the most successful approaches, was the developed in our group, in which a recombinant synthesis and further purification of a specific MT, allows to recover and characterize the obtained metal-MT (Cols et al., 1997) (Capdevila et al., 1997) and classify them as Zn- or Cu-thionein (Palacios et al., 2011). The experimental procedures required to achieve this approach are a combination of Bioinformatics searches, Genetic and Molecular Engineering strategies and a set of spectroscopic and spectrometric analysis, allowing to go from an hypothetical MT sequence, to the complete characterization of its metal-binding abilities.

The first step of this approach, consists in the *in silico* analysis of the hypothetical MT. The identification of the annotated genome, coding cDNA and protein sequences in the databases, is required in order to establish the genomic and protein sequence features. Knowing the presence or absence of introns/exons in MT-encoding genes, as occurs in *S. cerevisiae* CUP1 gene, which is an intronless sequence (Winge et al., 1985) or *N. crassa MT* gene, possessing a short intron (Münger et al., 1985); but also, understanding other events as the alternative splicing phenomenon, identified in *Branchiostoma floridae* MT2 cDNA (Guirola et al., 2012); the presence of multiple isoforms, as occur in the *Glycine max* MT system (Pagani et al., 2012); or even, the presence of misannotated genes and protein sequences, bring us a comprehensive information about the features of the metal-MT complex characterized.

The following summary presents all the genetic and molecular procedures involved in our experimental approach. Hence, the corresponding mRNA isolation from the studied organism is required to perform an rtPCR reaction from which the total cDNA is obtained. A further PCR amplification, using the total cDNA as template and specific MT oligonucleotides, hopefully yields the MT encoding cDNA, which is then cloned into an expression vector to synthesize a fusion Glutathione S-transferase-MT (GST-MT) in the *E. coli* recombinant system. The synthesis of the GST-MT in Zn-, Cd- and Cu-supplemented cultures, yield metal-MT complexes that are purified from the rest of total proteins; excised of the GST protein by thrombin cleavage and finally purified by liquid chromatography (FPLC) obtaining pure metal-MT preparations.

The analytical steps consist in spectroscopic (ICP-AES, UV-vis and CD) and spectrometric (ESI-MS) analyses, which provide the required data to describe the MT behaviour in front divalent (Zn(II) and Cd(II)) and monovalent (Cu(I)) metal ions, through the characterization of the obtained metal-MT species. A considerable list of MTs from different organisms has been characterized according to this approach. For instance, the coordination abilities of the model *Helix pomatia* MTs binding cognate and noncognate metal ions have been thoroughly described (Palacios et al., 2014b); also the metal-binding differences of the two identified MTs in sea urchin (*Strongylocentrotus purpuratus*), in which SpMTA presents better abilities to coordinate divalent metal ions, whereas SpMTB exhibits a preference for monovalent metal ions, suggesting a specific role for each MT in the echinoderm metal homeostasis (Tomàs et al., 2013); and even, the existing differences in the mammalian MT system, in which it is suggested that the specific metal-binding abilities presented by the four MTs, would respond to different metal homeostasis requirements in the tissues were these MTs are most expressed (Artells et al., 2014) (Artells et al., 2013).

This successfully approach provides not only valuable data about the Zn- or Cu-thionein behaviour of a specific MT (Capdevila & Atrian, 2011), but also the understanding how the cysteines, as well as the non-coordinating residue distribution can be involved in a specific behaviour, and also helps to suggest putative evolving events of this MT.

1.2.3. REGULATION OF MT GENE EXPRESSION

Generally, *MT* genes are commonly expressed at basal levels. It is known that their expression can increase in the presence of metals, but these are not the only inducer agents identified. The agents causing the increase of MT synthesis can be principally divided in inorganic (metal) and organic (non-metals) inducers. The transcription factors are the responsible to activate MT expression and for that, the inducers will interact with them. The MT expression can vary depending on the organism, but generally the expression regulation patterns are similar (Andrews, 2000) (Haq et al., 2003).

1.2.3.1. Inorganic inducers

The main *MT* gene inducer is the exposure to heavy metal concentrations, among which, the most usual are Zn, Cd and Cu but also Ag and Hg (Bourdineaud et al., 2006). Although mammalian MT-1 and MT-2 are mainly induced by Zn(II) and Cu(I), they can be also induced by Hg or Bi (Haq et al., 2003). Metal regulatory elements (MRE) are required in MT expression induction by metals, and even in absence of exogenous metal ions to maintain the MT basal levels. At the same time, the Zn-responsive transcription factor MTF-1, which is activated by zinc, is interrelated with MRE and participates in the induction of MT expression through the MT promoter activation (Haq et al., 2003). MTF-1 is the predominant transcription factor that mediates the induction of MT expression, although is also required at basal levels. It is ubiquitously present in mammalian cells and insects, but curiously *Drosophila* MTF-1 is not activated by zinc, but for copper. Hence, it has been reported that in *Drosophila* species this transcription factor induces *MT* expression in low and high copper concentrations ensuring a minimum copper level to maintain the physiological function and avoiding high concentrations that can lead the cell to a lethal toxicity (Balamurugan & Schaffner, 2006).

In *S. cerevisiae* this function is performed by the Cu-responsive transcription factor ACE1, which induces *CUP1* expression in presence of Cu(I) and Ag(I) (Casas-Finet et al., 1991) (Thiele, 1988). Evenly, ACE1 regulates *CRS5* expression at basal and high copper levels, as well as it trans-activates SOD1, which encodes the Cu,Zn SOD and whose role is to supress copper toxicity through ion buffering (Culotta et al., 1994).

Metals can also indirectly trigger *MT* expression by inducing oxidative stress in higher, but no in lower eukaryotes (Kumar et al., 2005). Cadmium is one of the major heavy metals causing oxidative stress through redox activity. Antioxidant responsive elements (ARE) are activated by the reactive oxygen species (ROS), produced by cadmium and other oxidative molecules such as H_2O_2, which finally increases *MT* gene expression. A synergic action of MRE and ARE to increase MT expression was also identified in rodents hepatotoxicity produced by cadmium (Sabolić et al., 2010).

So the presence of metals activates different transcription factors that not only regulate the MT expression, but can also control the expression of other genes that at the same time regulate the presence of metals inside the cell.

1.2.3.2. Organic inducers

Other inducers not related to metals may also trigger *MT* gene expression, preferably in higher eukaryotic organisms. Glucocorticoids activate the dimerization of their cellular receptors, which translocate into the nucleus and bind to the glucocorticoid response elements (GRE), which are common in the *MT* regulatory region, producing the activation of mammalian MT-1 and MT-2 (Collingwood et al., 1999) (Di Croce et al., 1999). Other cases of reported non-metal MT inducers are cytokines, growth factors, irradiation and bacterial lipopolysaccharides, whose activity induces hepatic *MT* expression in rats (Haq et al., 2003). On the contrary, the DNA methylation observed in some tumour cells down regulates the *MT-1* gene in mammals (Sabolić et al., 2010).

1.2.4. FUNCTIONS

Since the horse kidney MT identification, one of the main issues concerning MTs has been to elucidate their principal biological functions. Dozens of scientific papers have addressed the topic, exposing diverse functions and concluding that it does not exist a unique function for MTs (Palmiter, 1998). The huge diversity in MT sequences and the ability to coordinate different metal ions, may contribute to their multipurpose nature (Coyle et al., 2002) (Blindauer & Leszczyszyn, 2010). Moreover, the cellular functions performed by MTs, may produce not only a result on the cell, but also to the whole organism when it is a high eukaryotic organism. For instance, it has been confirmed that the downregulation of a specific isoform may result, in some cases, in a systemic disease that may endangers life (Simpkins, 2000). Three main functions have been proposed at cellular level: i) toxic metal detoxification; ii) metal ion homeostasis; and iii) protection against oxidative stress.

1.2.4.1. Toxic metal detoxification

MTs play an important role in toxic metal detoxification. Precisely, the first MT was initially described as a cadmium-binding protein, showing already from the first moment, the characteristic property of binding non-physiological metal ions. Cadmium, which is a xenobiotic element, possess a great affinity for thiol groups and may displace easily zinc ions,

that are forming a Zn-MT complex (Chiaverini & De Ley, 2010). According to Sutherland & Stillman, MTs seams to have more ability to bind toxic metals, since the association constant of metal ions for thiolate ligands correlates as: $Hg^{2+} > Cu^{+} > Cd^{2+} > Zn^{2+}$ (Sutherland & Stillman, 2011). In fact, this is a coherent situation if we take into account the need of the cell to maintain a physiologic situation as much as possible and avoid cell damage. This is why when Cd^{2+} is presents inside the cell, MTs sequester them to buffer its toxicity.

But not only toxic metals *per se* can cause cell damage; all the physiologic metals, as Cu^{+} or Zn^{2+} can be poisonous in high concentrations. For example, mice with deleted MT genes and with a rich Zn^{2+} diet present pancreatic cell degeneration (Kelly et al., 1996). These and other results taken together show that MTs act as provisional storage agents of zinc ions. Copper is an special case, because it is considered a physiological metal, it stimulates free radical production when present at high concentration, hence being considered also a toxic metal ion (Sutherland & Stillman, 2011). Not only MTs participate in cellular Cu^{+} control; copper transport proteins as ATP7 are crucial in the transport of this metal. Major alterations in these or other implicated copper molecules can cause severe diseases, as in human are Wilson and Menkes diseases (Prohaska, 2008).

1.2.4.2. Metal ion homeostasis

The main metal-MT complexes natively isolated that have been analyzed are Zn-MT, Cu-MT, Cd-MT or a mixture of species such as Zn,Cu-MT and Zn,Cd-MT. While in mammals and plants, any of them can be encountered, in yeast and fungi the predominant native complex is Cu-MT (Sutherland & Stillman, 2011); but in some cases, such as in the aquatic fungus *Heliscus lugdunensis*, MT has been natively isolated as a Cd-complex (Loebus et al., 2013a).

Scientific evidence has shown the role of MTs in Zn^{2+} and Cu^{+} homeostasis. The importance of the appropriate metal concentrations has been exposed in different experiments. Specific studies conducted for Zn-dependant transcription factors, such as Sp1, showed that the apo-MT removes Zn^{2+} easily from them. MTs also act as reservoir of this metal in the metalloprotein synthesis and also behave as metallochaperone in the transcription of DNA to RNA, for which metal ions are required (Chiaverini & De Ley, 2010). There are a lot of examples for MTs acting as metal reservoirs and possible transfer reactions. Hence, in

mammals, four MT isoforms have been described, among them MT2, MT3 and MT4 present metal-binding abilities compatible with a role in housekeeping metal ion homeostasis (Tió et al., 2004), while MT1 is suggested to be rather involved in Cd detoxifying events (Artells et al., 2013). MT3, localized specifically in the central nervous system, has been related with Zn/Cu equilibrium and content control in brain (Atrian & Capdevila, 2013) (Artells et al., 2014). Finally, MT4, exclusively expressed in epithelial differentiating tissue, has been suggested to play a role in physiological Cu-homeostasis, due to its partial Cu-thionein character (Tió et al., 2004).

In some cases, MTs are not limited to chelate metal ions to maintain an appropriate metal balance, but they can also interact physically with some proteins. Thus, *Drosophila* and mammalian MTs have been shown to establish MT-protein interactions, in which mammalian MT1, MT2 and MT3 interact with proteins of different tissues to swap or exchange metal ions, nearly always zinc. Contrastingly, Zn-MtnA and Zn-MtnB complexes from *Drosophila*, have been shown to interact with the peroxiredoxin system, probably to perform a redox recycling function (Atrian & Capdevila, 2013).

1.2.4.3. Protection against oxidative stress

Scientific studies corroborate not only that metals such as cadmium, can induce the expression of MTs, but in general molecules producing ROS are MT gene inducers through ARE activation, as it is saw in cardiac MTs in mice (Sabolić et al., 2010) (Sutherland & Stillman, 2011) (Blindauer, 2014). Moreover, the relevant amount of cysteine residues that possess all the MTs implies a large number of chemically reactive thiol groups, meaning that they can be oxidized or reduced by redox molecules. This, indicate that MTs can play an important role in the cellular protection against oxidative stress either by protein overexpression and sequestration of toxic metals, either by direct involvement of free radical binding activity of MTs to avoid DNA, RNA and cell structures damage (Chiaverini & De Ley, 2010) (Ruttkay-Nedecky et al., 2013) (Blindauer, 2014).

In case of mammals, the cysteine ligands of Zn-thioneins can be chemically distinguished in three states: metal-bound, reduced (thionein or T_R) and oxidized (thionin or T_O). The redox cycle of MTs is depending on ROS and also the glutathione (GSH)/glutathione disulfide (GSSG) ratio. So, when significant concentrations of ROS and

GSSG are the cell environment, the T_R becomes T_O; this characterized T_O has disulphide bounds that release Zn^{2+} from MT complex. The free zinc will bind others proteins and MTF-1 inducing the overexpression of the MT gene that synthesize more proteins, whereas the T_O will be reduced to T_R again by selenium catalyst and avoiding thereby the protein degradation (Figure 3) (Kang, 2006) (Quesada et al., 1996) (Krezel & Maret, 2007) (Chiaverini & De Ley, 2010).

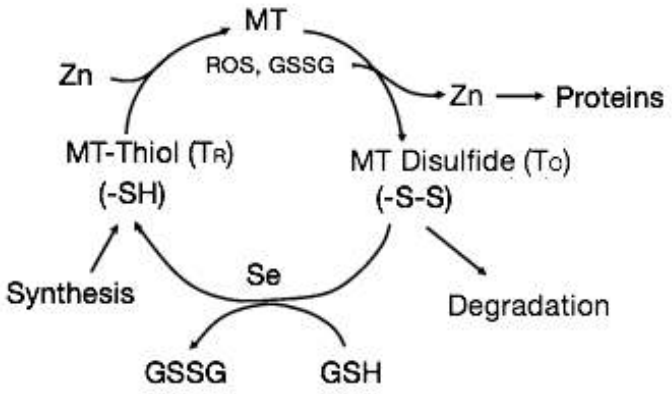

Figure 3. MT redox cycle scheme. MT-thiol (–SH bounds) is oxidized by ROS or GSSG becoming MT disulfide (-S-S-) releasing Zn^{2+}. Through the selenium catalyst, the MT is reduced and is able to bind Zn^{2+} again. (Adapted from Kang, 2006).

In plants, ROS production is related with pathogen attack (Kuźniak et al., 2013), senescence (Buchanan-Wollaston, 1994) (Guo et al., 2003) and response to wounds (Razem & Bernards, 2002), besides the ROS production by copper ions through Fenton reaction (Valko et al., 2005). Works on *Quercus suber* MT (QsMT) reveals the significant role of plants MTs in the protection against oxidative stress, probably through two principal ways: the balance of the local redox by oxygen radical sequestration, and the Cu^{+} coordination to avoid the cellular damage (Mir et al., 2004). At the same time, studies in soybean (*Glycine max*) and sunflower (*Helianthus annuus*) corroborate that plant MTs respond to the oxidative stress, among other stresses (metal ions, salts, temperature, pathogen invasions and abscisic acid), through the ubiquitous expression of the corresponding genes (Pagani et al., 2012) (Tomàs et al., 2014) (Tomàs et al., 2015).

Also yeast MTs are involved in oxidative stress protection (Liu & Thiele, 1996). In *S. cerevisiae*, CUP1 gene expression can be induced, besides ACE, by heat shock transcription factor (HSF) (Tamai et al., 1994). Glucose starvation, which is considered as equivalent to the generation of oxidative stress as well as heat shock, may activate HSF, specifically its C-terminus trans-activation domain, inducing the synthesis of CUP1 (Liu & Thiele, 1996) (Tamai et al., 1994). On the other hand, the main ROS source able to increase the fungal MT genes expression is copper, but no other factors. For instance, in *N. crassa* MT only copper toxicity and its following cell effects induce the MT synthesis, but not other stimuli (Kumar et al., 2005).

1.2.5. UNICELLULAR EUKARYOTE MTS

MT knowledge is constantly increasing; the obtained new data allow us to know better the heterogeneous structures and the functions in which these proteins are involved. A large number of scientific works have been devoted to eukaryote MTs and more specifically to multicellular eukaryote (animal and plants) MTs. Unfortunately unicellular eukaryote MTs (*i.e.* those from protists and fungi) have not been studied so well, except in the case of the yeast *S. cerevisiae* MTs, which has been adopted as model for these group of MTs. However, current studies in this issue are becoming more frequent, and they are providing unexpected information about MT structure and their cell function.

This PhD thesis will provide new information about unicellular eukaryote MTs: the protozoan *Tetrahymena thermophila* MTs, and the fungal *Cryptococcus neoformans* and *Fusarium verticillioides* MTs. Also new fungal MT sequences will be also communicated. Therefore, a detailed account on the knowledge of these MTs at the beginning of this thesis work is here presented.

1.2.5.1. Ciliate MTs

Ciliated protozoa are adapted to live in terrestrial and aquatic ecosystems. Two of the main representatives ciliate model organisms are *Paramecium tetraurelia* and *Tetrahymena spp.* (Gutiérrez et al., 2011); they possess some metabolic traits and some conserved

functional genes that resemble more to those of human cells, than to yeast or other microorganisms (Gutiérrez et al., 2009). Two of the *Tetrahymena* species, *T. thermophila* and *T. pyriformis* are considered remarkable models to study environmental pollution, due to their absence of cell wall in the vegetative stage, what make them sensitive to some contaminants (Díaz et al., 2007).

In 1994, Piccinni et al., identified the first *Tetrahymena* MTs in *T. pigmentosa* (TpigMT-1 and TpigMT-2) and in *T. pyriformis* (TpMT-1), which were induced by Cd^{2+} (TpigMT-1 and TpMT-1) or Cu^{+} (TpigMT-2). All these MTs were surprisingly longer than any MT described so far, suggesting possible gene duplication events throughout evolution as their origin (Piccinni et al., 1994). Few years later, two MTs from *T. thermophila* were also identified, MTT1, which is inducible by Cd^{2+} (Shang et al., 2002), and MTT2, inducible by Cu^{+} (Boldrin et al., 2006). The percentage of cysteine residues in these sequences is similar to any other MT, but not the total amount of them; the large number of this amino acid in each sequence allows the MT to bind more metal ions. Moreover, three common cysteine patterns -CXC-, -C- and -CC-, found also in other MTs, were identified in *Tetrahymena* MTs, together with three less usual patterns -CCC-, -CXCC- and -CXCXC- (Gutiérrez et al., 2011).

1.2.5.1.1. Subfamilies in ciliate MTs

According to Binz & Kägi classification, ciliate MTs are placed in family 7. Nonetheless, Díaz et al. have characterized two *Tetrahymena* MT subfamilies, in which take into account: i) the kind of metal inducing the *Tetrahymena MT* gene; ii) the percentage of CCC and CC patterns; iii) the presence of lysine residues juxtaposed to cysteine; and iv) the modular organization of the MT (Díaz et al., 2007). Combining all these data, it is feasible to obtain two differentiated subgroups that Díaz et al. named as 7a and 7b. 7a contains those MTs whose genes are inducible by Cd^{2+}, possess a higher percentage of -CCC- and -CC-, a minor percentage of Lys next to Cys and their sequences are composed by modular stretches. On the contrary, MTs placed in 7b group, their genes are induced by Cu^{+}, only sporadic sequences possess -CC- but never -CCC- motifs, have more Lys residues next to Cys in the cluster CKC, and they are not clearly identifiable modular structures. A total of twenty one *Tetrahymena* MT sequences known so far have been classified according to these features (Table 3).

SPECIES		CXC	C	CC	CCC	CXCC	CXCXC	Total Cys	% Cys	CKC
Subfamily 7a (CdMT)										
T. pyriformis	MT-1	1	1	5	4	2	-	31	28.9	2
	CdMT-2	4	1	6	6	5	-	54	29.8	2
T. thermophila	MTT1	2	1	8	6	3	-	48	29.6	3
	MTT3	4	3	9	2	2	1	42	25.9	3
	MTT5	1	6	5	1	1	-	24	24.2	1
T. tropicalis	TMCd1	2	-	8	6	3	-	47	30.1	4
T. rostrata	MTT1	2	-	6	4	2	-	34	28.5	3
T. pigmentosa	MT-1	2	-	6	4	2	-	34	28.8	3
T. vorax	MT1	2	1	8	6	3	-	48	28.4	3
T. hegewischi	MT1	2	-	6	4	2	-	34	27.8	3
	MT2	7	4	8	4	1	-	49	25.6	-
	MT3	3	-	9	6	3	-	51	28.6	5
	MT4	6	4	8	5	1	-	50	25.9	1
T. mobilis	MT1	3	-	9	6	3	-	51	28.4	5
T. malaccensis	MT1	2	1	8	6	3	-	48	29.6	3
Subfamily 7b (CuMT)										
T. thermophila	MTT2	15	2	-	-	-	-	32	29.6	9
	MTT4	15	2	-	-	-	-	32	29.6	10
T. rostrata	MTT2	12	2	1	-	-	-	22	28.2	7
T. pigmentosa	MT-2	9	2	1	-	-	-	28	29.1	9
T. tropicalis	MT1	12	2	1	-	-	-	28	28	8
	MT2	15	2	-	-	-	-	32	29.6	9
T. pyriformis	CuMT-2	12	2	1	-	-	-	28	29.1	9

Table 3. *Tetrahymena* MT species classified according to the subfamily to which they belong. Cysteine patterns and their total amount and percentage in the respective sequences, as well as the number of times that Lys is juxtaposed with Cys, are shown. Adapted from (Chaudhry & Shakoori, 2010) (Gutiérrez et al., 2011) (Shuja & Shakoori, 2007).

1.2.5.1.2. Modular structures in Tetrahymena MTs

The alignment of the subfamily 7a sequences revealed the existence of a hierachical modular arrangement in these MTs (Díaz et al., 2007), in which two principal motifs (motif 1: $C_3X_6C_2X_6$ and motif 2: $C_2X_6CXCX_2CXCCX_3$) are the basis of the submodules; the sum of three submodules -two motif 1 and one motif 2- will conform a module; the whole MT is conformed by two, three, four, and until five of these modules. Although some exceptions exist and not all MTs, possess the complete motifs, a large number of them follow the same pattern (Table 4) (Gutiérrez et al., 2011).

Tetrahymena MT	Linker	Module			N
		Motif 1 submodule	Motif 1 submodule	Motif 2 submodule	
TrostMTT1	MDKNS····	CCCGENAKPCCTDPNSG	CCCSSKTNNCCQSDTKE	CCTGTGP··GCKCTSCKCCKPA	2
TmobiMT1	MDKVT····	CCCGENAKPCCTDPNSG	CCCSSKTNNCCKSEVKD	CCTGTGQ··GCKCTGCKCCQPV	3
TpyriMT-1	MDKVNNN··	CCCGENAKPCCTDPNSG	CCCVSETNNCCKSDKKE	CCTGTGE··GCKCTGCKCCEPA	2
TpyriMT-2	MDKVNNNN·	CCCVESTQTCCSGVASG	···	··········CQCTNCQCCKKT	5
ThegewMT1	MDKVENKQT	CCCGENAKPCCFDPNSG	CCCSSKEDNCCKSDTKD	CCSGDKQENGCKCTSCKCCQPT	3
ThegewMT2	MDKVDNKQT	CCCGENAKPCCFDPRTG	CSCASKDNNCCTSENQG	··········NCKNCLCCQPT	4
TtherMTT1	MDKVNNN··	CCCGENAKPCCTDPNSG	CCCVSETNNCCKSDKKE	CCTGTGE··GCKWTGCKCCQPA	2
TtherMTT3	MEKINNS··	CC·GENTKICCTDLNRQ	CNCACKTDNCCKPETNE	CCTDTLE··GCKCVDCKCCKSH	3
TtherMTT5	MDKIS····	···GESTKICSKTEEKW	CCCPSETQNCCNSDDKQ	CCVGSGE··GCIYVCCKCCKVQ	2

Table 4. Basic modules of *Tetrahymena* MTs of subfamily 7a. The sequences are formed by linker plus two, three, four or five modules, which are composed by three submodules (two motif 1 and one motif 2). Here are shown the N-terminus MTs. N: number of modules repetitions in each MT (Adapted from (Gutiérrez et al., 2011) (Díaz et al., 2007)).

On the contrary, these modular structures are missing in the subfamily 7b, where only repetitions of the unit $CKCX_{2\text{-}5}CXC$ are found (Gutiérrez et al., 2011), and the juxtaposition of Lys to Cys is very common; however this is not so in family 7a, where only motif 2 contains this juxtapositions (Díaz et al., 2007). Taken all this information together, it was proposed the theory of the modular structure evolution, in where gene tandem duplications were the explanation of the generation and evolution of current *Tetrahymena* MTs has been proposed (Gutiérrez et al., 2011).

1.2.5.1.3. Tetrahymena MT gene expression and protein characterization

The identified inducers of *Tetrahymena MT* gene expression are diverse. Although it is clear that Cd^{2+} and Cu^{+} are inducers of subfamily 7a and 7b, respectively, other metal ions and agents have been found to induce specific *Tetrahymena* MT genes (Gutiérrez et al., 2009).

Thus, depending on the species, the synthesis of the protein can be activated *in vitro* by Zn^{2+}, Hg^{2+}, Ni^{2+}, Pb^{2+} or even arsenate (As^{5+}) (Gutiérrez et al., 2011). Among metal influence, other non-metal agents can induce *Tetrahymena* MT genes expression: H_2O_2, paraquat, starvation or heat-shock stress are usual inducers, even though not all these agents are able to induce all the *Tetrahymena* MTs and at the same rate (Gutiérrez et al., 2009). No clear evidence of metal responsive elements are found in these genes. Evenly, some other possible regulatory elements have been related with specific *Tetrahymena* genes different from MTs. However, a conserved motif (MTMC1) has been described in the 5' flanking regions in *T. thermophila* MTT1, MTT3 and MTT5 and also in *T. pyriformis* MT-1, suggesting a possible specific function on these genes (Díaz et al., 2007).

Despite the characterization of some *T. thermophila* MTs at protein level, no studies are devoted to the complete MT system at protein level. Thus, the vast majority of available information is related to the *MTT* gene induction (Boldrin et al., 2006) (Boldrin et al., 2008) (Formigari et al., 2010) (Santovito et al., 2007), the features of the MTT peptide sequences (Díaz et al., 2007) (Gutiérrez et al., 2011) or the potential use of *T. thermophila* MTs as biosensors (Amaro et al., 2011) (Gutiérrez et al., 2009). A single study from 25 years ago, dealt with the Cd-binding abilities of two *T. thermophila* MTs (named as MT1 and MT2), that probably correspond to the currently known as MTT1 and MTT3 or MTT5 (Piccinni et al., 1990). No other studies about the precise metal preferences of the five MT isoform of the *Tetrahymena* system have been performed. In following sections of this PhD thesis, a complete study of the metal-binding abilities of the *T. thermophila* MT system members is presented.

1.2.5.2. Yeast and fungal MTs

The first MTs identified in the large fungal kingdom, were Cup1 and Crs5 from *S. cerevisiae* (Winge et al., 1985). Since then, an interesting collection of fungal MTs, has been gathered. Currently, MTs have been reported in: yeast (*e.g. S. cerevisiae*, *Schizosaccharomyces pombe*), yeast-like (*e.g. Candida* spp), multicellular fungi (*e.g. Agaricus bisporus*, *Lentinula edodes*), unicellular fungi (*e.g. N. crassa*, *Heliscus lugdunensis*) or specifically unicellular pathogenic fungi (*e.g. C. neoformans*, *Magnaporthe grisea*).

In last two decades, the list of fungal MTs described has largely increased. Their increasing characterization allowed establishing the principal features of these metallopeptides. Classified into six different families (from Family 8 -or Fungal 1- to Family 13 -or Fungal 6-) according to Binz & Kägi's classification (Table 2) (Binz & Kägi, 1999), they show a genuine Cu-thionein character in almost all the cases, in accordance with the report by Palacios et al. (Palacios et al., 2011). The study of fungal *MT* gene induction, the analysis of their coding sequence lengths, the differences in the cysteine pattern distributions, and the metal-binding abilities of these MTs have revealed interesting singularities. Thus, *Y. lipolytica* MTs present a unusual -CCC- motif, not identified in other fungal MTs (García et al., 2002), *H. lugdunensis* MT shows a clear preference for binding Cd rather than Cu (Loebus et al., 2013b), or the human opportunistic pathogenic fungus *C. neoformans* presents extraordinary long MT sequences (CnMTs) not observed in any other kingdom (Ding et al., 2011). Precisely, the marked expression of the *CnMT* genes in Cu excess conditions, suggests a Cu detoxification role through these two long metalloproteins during the infection process in mammalian cells, in which the macrophages fight against fungi creating a Cu-rich microenvironment (Ding et al., 2011) (Ding et al., 2014b).

C. neoformans is the causing agent of cryptococcosis, affecting especially immunocompromised people and causing 600,000 deaths/year according to the Centers for Disease Control and Prevention (CDC). The interesting results obtained for *CnMT* gene induction patterns encouraged going further in the CnMTs studies at protein level and understand their hypothetical role in infection process. In coming sections of this PhD thesis, more comprehensive studies about sequence features and metal-binding abilities of CnMTs are included. Finally, a manuscript in preparation presents a review of described fungal MTs, related to their gene inducer agents, sequence features and metal-binding abilities. At the same time, other more recently described fungal MTs, some coming from pathogenic fungi, are described.

OBJECTIVES

2. OBJECTIVES

This PhD thesis has as objective the study of the structure and the metal binding behaviour of the metallothioneins (MTs) of two unicellular eukaryote model organisms, both of them harbouring an MT system including extremely long MT proteins.

1. Study of the metal binding preferences of the five MT isoforms of the ciliate model *Tetrahymena thermophila*.
2. Characterization of two MTs of the human opportunistic pathogen fungus *Cryptococcus neoformans*; metal binding abilities and analysis of their modular structure. Comparison with other fungal MTs.

2.1 METAL BINDING PREFERENCES OF *T. thermophila* MTS.

T. thermophila possesses, like other ciliate, the largest characterized MTs reported so far. The five isoforms encoded by *T. thermophila* (MTTs) are suggested to play different roles in metal binding. This hypothesis is supported in different publications (Chang et al., 2011) (Díaz et al., 2007) (Gutiérrez et al., 2011) that study divers *Tetrahymena* species, after

Consideration of two criteria: the gene induction response of their genes, or the cysteine motifs and their distribution in the MT sequences. Hence, we aimed at the characterization of the metal binding properties of MTTs by:

1.1. Construction of modified cDNAs for recombinant synthesis in *E.coli*, taking into account the peculiar codon usage in this ciliate, different in some cases (TAA and TAG triplets) to the Genetic Universal Code.
1.2. Synthesis and characterization of recombinant Zn-, Cd- and Cu-MTTs complexes.

2.2 METAL BINDING ABILITIES AND MODULAR STRUCTURE ANALYSIS OF THE TWO *C. neoformans* MTS. COMPARISON WITH OTHER FUNGAL MTS.

The two MTs identified in *C. neoformans* (CnMTs) resulted to be long proteins which differed significantly from the short MTs long ago reported as mode MT of fungi, such as

Neuropora crassa and *Agaricus bisporus* (26 aa each). It was likely that these CnMTs participated somehow in the virulence mechanism of the fungus. The CnMTs metal-cluster analysis, the description of their metal abilities and their comparison with other pathogenic and non-pathogenic fungal MTs, as well as a new pathogenic fungal MT in *Fusarium verticillioides*, should help us to discern the implication of these proteins in fungus metal metabolism as well as their implications on virulence. In this scenario, we proposed:

2.1. CnMTs and other fungal MTs *in silico* analysis.

2.1.1. Study of CnMT1 and CnMT2 at genomic, DNA, and protein level, to solve the existing ambiguity between annotated *C. neoformans* genome and experimentally obtained sequences.

2.1.2. Description of the modular blocks forming CnMTs, identification of cysteine distribution patterns, and their homology to the *N. crassa* fungal MT model.

2.1.3. Identification of new pathogenic and non-pathogenic fungal MT sequences, and comparison with the existing fungal MT models, as well as with CnMTs as example of specialized MTs.

2.2. Characterization of metal binding abilities of CnMTs.

2.2.1. Study of the metal coordination capacity of CnMTs and their respective forming blocks, by recombinant synthesis of Zn-, Cd- and Cu-MT complexes.

2.2.2. Analysis of the capacity in recovery copper tolerance by CnMT1 and its different building blocks, inserted in a copper-resistance defective yeast strain.

2.3. Characterization of a new fungal pathogenic MT.

2.3.1. Localization of a new *F. verticilloides* MT, and study of their metal binding properties by synthesis of their recombinant Zn-, Cd- and Cu-MT complexes.

RESULTS

REPORT ISSUED BY DR. SÍLVIA ATRIAN I VENTURA, PROFESSOR OF GENETICS, AS SUPERVISOR OF THE PHD THESIS PRESENTED BY MS. ANNA ESPART HERRERO.

The doctoral thesis report of Ms. Anna Espart Herrero entitled, **"Molecular Evolution of Unicellular Eukaryote Metallothioneins: Tandem Repetition of Coordinating Domains"**, is presented as a compilation of five publications; four of them as finished papers (published or submitted) and one as publication in preparation (manuscript).

PUBLICATION #1:

"Hints for metal-preference protein sequence determinants: different metal binding features of the five *Tetrahymena thermophila* metallothioneins"

Anna Espart, Maribel Marín, Selene Gil-Moreno, Òscar Palacios, Francisco Amaro, Ana Martín-González, Juan C. Gutiérrez, Mercè Capdevila and Sílvia Atrian.

International Journal of Biological Science 18, 456-471, 2015. (IF 2014: 4.372)

This work have been performed in collaboration with the group of Dr. Mercè Capdevila, in the department of Chemistry of the Universitat Autònoma de Barcelona (UAB), and thanks to Prof. J.C. Gutiérrez, from the Universidad Complutense de Madrid, who is a specialist in *Tetrahymena* MTs, who supplied us with the cDNA clones of the five *T. thermophila* MTTs. The personal contribution of the author of this thesis was: i) the mutagenesis of the five *T. thermophila* MTT cDNAs to adapt them for *E.coli* heterologous expression, because of the special meaning of some codons in *Tetrahymena*, different to the Universal Genetic Code; ii) cloning the five MTT cDNAs into suitable expression vector; and iii) the recombinant synthesis and purification of the five *Tetrahymena* MTTs, in *E. coli* cultures supplemented with Zn, Cd or Cu; all the purified metal-MTT complexes were then analysed by spectroscopy and spectrometry at the UAB; and iv) the synthesis of further Zn-MTT complexes, so that the UAB team performed *in vitro* metal (Cd and Cu) exchange reactions.

PUBLICATION #2:

"*Cryptococcus neoformans* copper detoxification machinery is critical for fungal virulence"

Chen Ding, Richard A. Festa, Ying-Lien, **Anna Espart**, Òscar Palacios, Jordi Espín, Mercè Capdevila, Sílvia Atrian, Joseph Heitman, Dennis J. Thiele.

Cell Host Microbe 13, 265-276, 2013 (IF 2013: 13.570)

This work has been performed in collaboration with the group of Prof. Dennis J. Thiele, in his laboratory at Duke University (Durham, North Carolina, USA), and our regular collaborator group of Dr. Mercè Capdevila, in the department of Chemistry, in the Universitat Autònoma de Barcelona (UAB). The personal work of the author of this thesis included: i) the protein similarity studies of CnMTs, to examine their homology and evolutionary relationships with fungal MTs; ii) the construction of the suitable *E. coli* expression vectors for both CnMT; and iii) the subsequent recombinant synthesis and purification of both CnMTs, as well as the CnMTala mutant, from *E. coli* cultures supplemented with Zn and Cu. All the purified metal-CnMT complexes were then analysed by spectroscopy and spectrometry at the UAB.

PUBLICATION #3:

"Full characterization of the Cu-, Zn-, and Cd-binding properties of CnMT1 and CnMT2, two metallothioneins of the pathogenic fungus *Cryptococcus neoformans* acting as virulence factors"

Òscar Palacios[*], **Anna Espart**[*], Jordi Espín, Chen Ding, Dennis J. Thiele, Sílvia Atrian, Mercè Capdevila (*co-authored).

Metallomics 6, 279-291, 2014 (IF 2014: 4.000)

This work has been carried out in collaboration with the group of Dr. Mercè Capdevila, in the department of Chemistry of the Universitat Autònoma de Barcelona (UAB).

The author of this thesis contributed personally performed: i) the *in silico* study of cDNAs sequences of CnMTs as entries retrieved in the databases were wrongly annotated, and the gene regions were wrongly delimited; ii) the construction of the suitable *E. coli* expression vectors for both CnMTs, and the subsequent recombinant synthesis and purification of CnMT1 and CnMT2 mutants, from *E. coli* cultures supplemented with Zn, Cd and Cu. All the purified metal-CnMT complexes were then analysed by spectroscopy and spectrometry at the UAB; and iii) the synthesis of further Zn-CnMT1 and CnMT2 preparations, so that the UAB team performed *in vitro* metal (Cd and Cu) exchange reactions.

PUBLICATION #4:

"Understanding the internal architecture of long metallothioneins: 7-Cys building blocks in fungal (*C. neoformans*) MTs"

Anna Espart, Selene Gil-Moreno, Òscar Palacios, Mercè Capdevila, Sílvia Atrian.

Submitted for publication

This work has been performed in collaboration with the group of Dr. Mercè Capdevila, in the department of Chemistry of the Universitat Autònoma de Barcelona (UAB).

The personal contribution of the author of this thesis was: i) the participation in the design of the studied cDNA fragments; ii) the construction of the suitable *E. coli* expression vectors for the seven CnMT1-Sx, and the subsequent recombinant synthesis and purification of CnMT1-Sx mutant, from *E. coli* cultures supplemented with Zn and Cu. Purification of the metal-CnMT1-Sx complexes and spectroscopic analyses; and iii) the performing of the Cu tolerance test by yeast complementation assays.

MANUSCRIPT:

"The unexplored universe of fungal MTs: review and new data"

Anna Espart *et al*.

Publication in preparation.

This document has been completely written by the author of this thesis work. In this report, a review of the features of fungal MTs are discussed, from the firstly reported fungal MTs, to the recently identified MT sequences in pathogenic and non-pathogenic fungal MTs. The role of some of those MTs in virulence, the frequent mis annotation of MT sequences in databases, or the new long fungal MTs identified, are also put in debate in this manuscript.

Barcelona, 19st of June, 2015.

Dr. Sílvia Atrian i Ventura
PhD Supervisor

Publication # 1

Hints for metal-preference protein sequence determinants: different metal binding features of the five *Tetrahymena thermophila* metallothioneins.

PUBLICATION #1:

TITLE

"Hints for metal-preference protein sequence determinants: different metal binding features of the five *Tetrahymena thermophila* metallothioneins"

AUTHORS

Anna Espart, Maribel Marín, Selene Gil-Moreno, Òscar Palacios, Francisco Amaro, Ana Martín-González, Juan C. Gutiérrez, Mercè Capdevila and Sílvia Atrian.

REFERENCE

International Journal of Biological Science (2015) 18: 456-471 (IF: 4.372)

SUMMARY

Metallothionein (MT) polymorphism is present in virtually all animal and plants, entailing the presence of isoforms likely due to progressive gene duplication. Thus evolution has allowed a high diversification in metal-binding ability of MT isoforms. *Tetrahymena* species contain several isoforms in the same organism, which were classified as Cd-thioneins and Cu-thioneins. They were the longest MTs identified so far. Some *Tetrahymena* MTs have already been studied according to the metal regulation pattern of their gene and their protein sequence similarity to other MTs, but almost nothing was known about their metal-binding behaviour. This work is focused on elucidating the metal-binding features behaviour of the five *T. thermophila* MTs (MTTs).

To achieve this, the corresponding cDNAs of MTT1 to MTT5 were cloned into an *E.coli* expression vector; MTT2 and MTT4 were directly cloned, but MTT1, MTT3 and MTT5 required a previously site-directed-mutagenesis strategy to modify specific codons that in *T. thermophila* codify for glutamine residues but are stop codons in the Universal Genetic Code. Them suitable cDNA sequences were cloned in the *E. coli* expression vector and were synthesized as Zn-, Cd- and Cu-complexes. Finally these were characterized by spectroscopic and spectrometric analysis.

Results concluded that MTTs could be classified from Zn/Cd-thioneins to Cu-thioneins in a gradation: MTT1>MTT5>MTT3>MMT4>MTT2 being MTT1, the one that has higher preference for divalent metal ions (Zn and Cd), whereas MTT2 shows The most extreme Cu-thionein character. On the other hand, MTT3 can be considered as an MT with undefined metal-binding preference, due to its ambiguous behaviour binding Zn, Cd and Cu ions. Looking at their protein sequences, Cys triplets and doublets are present in Zn/Cd MTTs and non in Cu-thionein MTTs.

Taking this information together, we concluded that *Tetrahymena* MTs are a good model to understand how MTs have evolved by elongating their sequences, through tandem repetition of fragments, and by adapting to different preferences of metal ion binding, which is a advantageous strategy for cell metabolism and survival.

Contribution to this work

This work have been performed in collaboration with the group of Dr. Mercè Capdevila, in the department of Chemistry of the Universitat Autònoma de Barcelona (UAB), and thanks to Prof. J.C. Gutiérrez, from the Universidad Complutense de Madrid, who is a specialist in *Tetrahymena* MTs, who supplied us with the cDNA clones of the five *T. thermophila* MTTs. My contribution was: i) the mutagenesis of the five *T. thermophila* MTT cDNAs to adapt them for *E.coli* heterologous expression, because of the special meaning of some codons in *Tetrahymena*, different to the Universal Genetic Code; ii) cloning the five MTT cDNAs into suitable expression vector; and iii) the recombinant synthesis and purification of the five *Tetrahymena* MTTs, in *E. coli* cultures supplemented with Zn, Cd or Cu. All the purified metal-MTT complexes were then analysed by spectroscopy and spectrometry at the UAB; and iv) the synthesis of further Zn-MTT complexes, so that the UAB team performed *in vitro* metal (Cd and Cu) exchange reactions.

Int. J. Biol. Sci. 2015, Vol. 11 456

IVYSPRING INTERNATIONAL PUBLISHER

International Journal of Biological Sciences

2015; 11(4): 456-471. doi: 10.7150/ijbs.11060

Research Paper

Hints for Metal-Preference Protein Sequence Determinants: Different Metal Binding Features of the Five Tetrahymena thermophila Metallothioneins

Anna Espart[1], Maribel Marín[2], Selene Gil-Moreno[2], Òscar Palacios[2], Francisco Amaro[3], Ana Martín-González[3], Juan C. Gutiérrez[3], Mercè Capdevila[2] and Sílvia Atrian[1]✉

1. Departament de Genètica, Facultat de Biologia, Universitat de Barcelona, 08028-Barcelona, Spain;
2. Departament de Química, Facultat de Ciències, Universitat Autònoma de Barcelona, 08193-Cerdanyola del Vallès (Barcelona), Spain;
3. Departamento de Microbiología-III, Facultad de Biología, Universidad Complutense, 28040-Madrid, Spain.

✉ Corresponding author: Departament de Genètica, Facultat de Biologia, Universitat de Barcelona, Av. Diagonal 643, 08028-Barcelona, Spain, Phone: +34 934021501, FAX: +34 934034420, E-mail: satrian@ub.edu

Received: 2014.11.14; Accepted: 2015.01.21; Published: 2015.03.18

Abstract

The metal binding preference of metallothioneins (MTs) groups them in two extreme subsets, the Zn/Cd- and the Cu-thioneins. Ciliates harbor the largest MT gene/protein family reported so far, including 5 paralogs that exhibit relatively low sequence similarity, excepting MTT2 and MTT4. In *Tetrahymena thermophila*, three MTs (MTT1, MTT3 and MTT5) were considered Cd-thioneins and two (MTT2 and MTT4) Cu-thioneins, according to gene expression inducibility and phylogenetic analysis. In this study, the metal-binding abilities of the five MTT proteins were characterized, to obtain information about the folding and stability of their cognate- and non-cognate metal complexes, and to characterize the *T. thermophila* MT system at protein level. Hence, the five MTTs were recombinantly synthesized as Zn^{2+}-, Cd^{2+}- or Cu^{+}-complexes, which were analyzed by electrospray mass spectrometry (ESI-MS), circular dichroism (CD), and UV-vis spectrophotometry. Among the Cd-thioneins, MTT1 and MTT5 were optimal for Cd^{2+} coordination, yielding unique Cd_{17}- and Cd_8- complexes, respectively. When binding Zn^{2+}, they rendered a mixture of Zn-species. Only MTT5 was capable to coordinate Cu^{+}, although yielding heteronuclear Zn-, Cu-species or highly unstable Cu-homometallic species. MTT3 exhibited poor binding abilities both for Cd^{2+} and for Cu^{+}, and although not optimally, it yielded the best result when coordinating Zn^{2+}. The two Cu-thioneins, MTT2 and MTT4 isoforms formed homometallic Cu-complexes (major Cu_{20}-MTT) upon synthesis in Cu-supplemented hosts. Contrarily, they were unable to fold into stable Cd-complexes, while Zn-MTT species were only recovered for MTT4 (major Zn_{10}-MTT4). Thus, the metal binding preferences of the five *T. thermophila* MTs correlate well with their previous classification as Cd- and Cu-thioneins, and globally, they can be classified from Zn/Cd- to Cu-thioneins according to the gradation: MTT1>MTT5>MTT3>MTT4>MTT2. The main mechanisms underlying the evolution and specialization of the MTT metal binding preferences may have been internal tandem duplications, presence of doublet and triplet Cys patterns in Zn/Cd-thioneins, and optimization of site specific amino acid determinants (Lys for Zn/Cd- and Asn for Cu-coordination).

Key words: Metallothionein, Functional Differentiation, Metal specificity, Zinc, Copper, *Tetrahymena thermophila*.

Introduction

The massive explosion of Genome and Proteome projects in the last decades demonstrated the wide existence of gene/protein families, instead of single-copy elements, in all types of genomes along the tree of life. A broadly accepted Molecular Evolution principle considers gene duplication events and subsequent specialization of paralogs as the optimal scenario for the acquisition of novel and differentiated

functions, from the unicellular Eukaryote organisms and first Metazoa ([1,2]) up to the Chordates/Vertebrates ([3]). Consequently, the characterization of the protein structure/function relationships in any polymorphic gene/protein system, and precisely the features of the specialized paralogous forms, should shed light to determine the evolutionary determinants that had caused the differentiation of the initially identical duplicates. Unfortunately, in many gene/protein families this basis for paralogous differentiation cannot be analyzed because even the function of every family member is unknown.

Metallothioneins (MTs) are small, ubiquitous, proteins exhibiting an extraordinary Cys content (*ca.* 30 %), which allows them the coordination of heavy-metal ions through the corresponding metal-thiolate bonds ([4,5]). They are polymorphic in practically all the organisms (plants and animals) studied up to now. It is supposed that the diversification of MT isoforms had its origin in successive gene duplication events ([6,7]) occurred independently in different taxa, where they constitute different homology groups. In each case, the MT function may have evolved to serve different molecular metal-related functions, such as essential metal ion homeostasis (Zn^{2+} or Cu^{+}), the defense in front of toxic metal ions (*i.e.* Cd^{2+}, Pb^{2+} or Hg^{2+}), the scavenging of free radicals and ROS, and a wide range of cell stresses ([8,9]). Therefore, MTs are a very useful model to study function (in this case, *metal-binding*) differentiation and specificity. MT isoforms in a given organism exhibit either equivalent or opposite preferences for divalent (Zn^{2+} and Cd^{2+}) *vs.* monovalent (Cu^{+}) metal ion coordination ([5,10]), independently of the degree of their similarity at protein sequence level. At present, there is no clear clue about the molecular determinants of this specificity, a question that is framed in the more global subject of protein/metal interaction specificity in living systems ([11,12]). Sequence/function relationship evolution is best investigated in gene/protein families that simultaneously include highly differentiated members. In the case of MTs, this assumes the coexistence in the same organism of MTs optimized for Zn/Cd-binding (Zn/Cd-thioneins) and for Cu-binding (Cu-thioneins). Significantly, our recent thorough analysis of the MT system in pulmonate gastropod Molluscs (the *Helix pomatia* and *Cantareus aspersus* snails), which consists of highly similar MT paralogs with extreme opposite metal ion binding specialization (Cd *vs.* Cu), revealed that this "metal specificity" lies in their protein sequence attributes and not in other possible factors, such as gene expression inducibility, metal availability, or cell environment ([13]). Precisely, the specific constraints imposed by the coordination geometry of each metal ion should be in accordance with the number and disposition of ligands (*i.e.* thiolate groups or alternative amino acid side chains) in the MT polypeptide sequences. As a consequence, the MT protein synthesis and folding about their cognate metal ions results in a unique, energetically optimized complex, while when taking place about non-cognate metal ions, a mixture of species is produced, none of them representing an energy well conformation, but principally reflecting the amount of metal ions available in its molecular environment ([14]).

The first studies of function and structure in metallothioneins took for granted that the most primitive eukaryotic MTs might have been extremely short peptides of Cu-thionein character, represented nowadays by the fungal *N. crassa* and *A. bisporus* MTs, which evolved to produce all the ß-like domains of MTs in higher Eukaryotes, including Vertebrates ([15]). Since then, this hypothesis has been superseded by multiple experimental evidence, among which the molecular characterization of the *Tetrahymena* (Ciliophora, Protozoa) MT system in several species of the genus offers a most striking example. In fact, *Tetrahymena* MTs are among the longer MTs reported (up to 191 amino acids) and include MTs classified both as Cd-thioneins (Family 7a in the Kägi's classification ([16])), and as Cu-thioneins (Family 7b) ([17,18]), while the evolutionary origin of Ciliates has been proposed for around 10^9 years ago, thus, notably before the emergence of fungi and other major eukaryotic lineages ([19]). These features triggered a more extensive study of the MT system in different *Tetrahymena* species in terms of molecular evolution and differentiation (*T. thermophila* ([20,21,22,23,24]), *T. pigmentosa* ([20,25,26,27,28]), *T. pyriformis* ([25,29,30,31]), *T. rostrata* ([32]), *T. tropicalis lahorensis* ([33,34,35]) and lately *T. hegewischi, T. malaccensis* and *T. mobilis* ([36])), all of them exhibiting a high degree of polymorphism. At this point, it is worth remembering that the classification of a given MT peptide as Zn/Cd- or Cu-thionein can be performed according to three different criteria, that logically converge in their results: gene expression inducibility, protein sequence similarity, and protein metal-binding behavior ([37]). The wealth of information gathered from the above mentioned literature refers almost exclusively to the first two criteria. Hence, on the one hand, all the reported *Tetrahymena* MTs have been so far classified according to the type of metal ion that provokes or enhances the expression of its gene, and the promoter response to different metals and stresses has been deeply characterized, also in view of biotechnological applications ([38,39,40,41,42]). On the other hand, the origin, relationships and evolution of the corresponding protein sequences has been the object of deep and

thorough analyses that have revealed close internal relationships in the Cd- and Cu-thioneins clades, as well as an interesting modular organization of the MT Cd-thionein sequences showing their more than probable origin from tandem duplications of primeval amino acid stretches ([17,18]). However, it is striking that studies on the third criterion, *i.e.* metal binding behavior or metal preference, are almost absent. Hence, only the metal ion binding features of the *T. pyriformis* MT1 isoform were shown in full concordance with its Cd-thionein character ([43]), and a partial attempt to compare the *T. thermophila* MTT1 and MTT2 isoforms has been recently published ([44]).

Thus, to fill the gap of protein functional studies on *Tetrahymena* MTs, we present here the full characterization of the Zn-, Cd- and Cu-binding abilities of the five *T. thermophila* MT isoforms (named MTT1 to MTT5 ([17]), *cf.* Figure 1 for polypeptide features). The MTT1, MTT3 and MTT5 Cd-thioneins exhibit Cys patterns typical of MTs (XCCX, CXC, XXCXX), and also some atypical Cys arrangements, such as CCC, CXCC, and CXCXC, while the MTT2 and MTT4 isoforms only enclose typical CXC motifs. Comprehensive interpretation of our results, obtained from the spectrometric and spectroscopic analyses of the recombinantly synthesized, as well as *in vitro*-reconstituted, metal-MTT complexes confirm that the MTT1 and MTT5 isoforms are optimized for divalent metal binding, MTT2 and MTT4 forms behave as clear Cu-thioneins and MTT3 shows an undefined behavior. However, clear differences can be defined among the coordination abilities of the five isoforms. This allows some relationships between the metal preference traits and the amino acid composition of the *Tetrahymena* MTs to be proposed, which will contribute to the understanding of the factors determining metal preference in proteins. Finally, the correspondence of a modular sequence structure, as proposed for the Cd-isoforms, and the metal clusters formed, is examined. Overall, it remains clear that from the first steps of the eukaryotic world, two complementary forces have driven the evolution of metallothioneins: a qualitative one, for metal specificity; and a quantitative one, to enlarge the metal binding capacity of a basic peptide fragment. This resulted in protein lengthening by internal tandem repeats (as the case of *Tetrahymena*, or the recently reported fungal MTs (*cf. C. neoformans* Cu-thioneins ([45,46])), or in entire gene duplication events, as is reported for *S. cerevisiae* Cup1 ([47]).

A

```
MTT2  GSMDT-----------------------------------QTQTKVTVGCSCNPCKCQPLCKCGTTAACNCQPCEN-------------
MTT4  GSMDT-----------------------------------QTQTKVTVGCSCNPCKCQPLCKCGTTAACNCQPCEN-------------
MTT5  GSMDKIS----GESTKICSKTEEKWCCCPSETQNCCNSDDKQCCVGSGEGCIYVCCKCCK-----------------------------
MTT1  GSMDKVNSCCCGVNAKPCCTDPNSGCCCVSKTDNCCKSDTKECCTGTGEGCKCVNCKCCKPQANCCCGVNAKPCCFDPNSGCCCVSKTNN
MTT3  GSMEKINNSCCGENTKICCTDLNRQCNCACKTDNCCKPETNECCTDTLEGCKCVDCKCCKSHVTCCHGVNVKSSCLDPNSGYQCASKTDN

MTT2  CDPCSCNPCKCGATESCGCNPCKCAE-----CKCGSHTE-----KTSACKCNPCACNPCNCGSTSNCKCNPCKCAECKC
MTT4  CDPCSCNPCKCGATESCGCNPCKCAE-----CKCGSHTE-----KTSACKCNPCACNPCKCGSTSNCKCNPCKCAECKC
MTT5  ---------------------------VQAECKCGPNAKYCCIDPNTGNCCVCKTKPCSKSDSKECCPGGSC
MTT1  CCKSDTKECCTGTGEGCKCTSCQCCKPVQQGCCCGDKAKACCTDPNSGCCCSNKANKCCDATSKQECQTCQCCK
MTT3  CCKSDTKECCTGTQEGCKCTNCQCYKQAQQGCCCGDKAKACCTDPNSGCCCSNKANKCCDATSKKECQVCQCCK
```

B

	subfamily	NCBI reference sequence	length	Cys	Met	His	Cys triplets	Cys doublets	Single Cys
MTT1	7a (Cd-thionein)	XP_001024888.1	162 aa	48	1	0	6	11	8 (7 in CXC motives)
MTT3	7a (Cd-thionein)	XP_001024889.1	162 aa	42	1	2	2	11	14 (11 in CXC motives)
MTT5	7a (Cd-thionein)	XP_001020086.1	99 aa	24	1	0	1	7	7 (3 in CXC motives)
MTT2	7b (Cu-thionein)	AAQ55281.1	108 aa	32	1	1	0	0	32 (30 in CXC motives)
MTT4	7b (Cu-thionein)	XP_001011379.1	108 aa	32	1	1	0	0	32 (30 in CXC motives)

Figure 1. (A) Multiple sequence alignment (Clustal Omega) of the five *Tetrahymena thermophila* MT isoforms. The Cys residues are in grey. The unique amino acid substitution between MTT2 and MTT4 is marked in bold. The Glu (Q) residues encoded by mutated codons are marked in bold italics. The initial GS residues (in italics) result from the recombinant synthesis rationale. (B) Comparison of the main sequence features of the five *Tetrahymena thermophila* MT isoforms.

Materials and Methods

Construction of MTT cDNAs and *E.coli* expression vectors.

The cDNAs corresponding to the five *T. thermophila* MT isoforms were obtained by mRNA retrotranscription, from cultures previously treated with Cd^{2+} (27 μM), Zn^{2+} (870 μM) or Cu^{2+} (80 μM) for 1h, and subcloned in PCR2.1-TOPO-TA vectors (Invitrogen), as previously reported ([17]). Since in *Tetrahymena* nuclear genes, the TAA and TAG triplets encode a glutamine instead of being stop codons (as in the Universal Gene Code) ([48]), the cDNAs of the MTT1, MTT3 and MTT5 isoforms had to be site-directed-mutated before cloning in the bacterial expression plasmid (pGEX-4T1). MTT2 and MTT4 cDNAs include no TAA or TAG codons, thus they could be directly subcloned. Two different site-directed-mutagenesis methods were used, owing to the different location of the bases to be mutated inside the cDNA length; hence the MTT1 and MTT5 cDNAs were mutated through Megaprimer PCR reactions ([49]) and the QuickChange Lightning Multi Site-Directed Mutagenesis Kit (Agilent Technologies) was used for the MTT3 cDNA mutagenesis. In all cases the T position of the TAA and TAG codons was changed to C, the CAA and CAG codons encoding Gln in the Universal Genetic Code.

In the MTT1 cDNA, four TAA (encoding Gln110, Gln116, Gln117 and Gln159) and one TAG (encoding Gln156) triplets were present. The first PCR amplified a MTT1 cDNA fragment which included the five target codons, by using as primer oligonucleotides: 5'AAATGTACAAGTTGCCAATGCTGCAAACCTGT TCAACAAGGATGTTGTTGTG-3' (forward) and 5'-GGAACTCGAGTCATTTACAACATTGACAAGT CTGACACTCTTGCTTTGA-3' (reverse). An *Xho*I restriction site (underlined) was added to the reverse primer for cloning purposes. 30-cycle amplification reactions were performed with a thermo-resistant Taq DNA polymerase (Expand High Fidelity PCR System, Roche) under the conditions: 2 min at 94 °C (initial denaturation), 15 s at 94°C (denaturation), 30 s at 57°C (annealing) and 30 s at 72°C (elongation). The second PCR reaction was required to amplify the whole cDNA sequence of MTT1, using a new oligonucleotide 5'-GGGGAGGATCCATGGATAAAGTTAATA GC-3' (forward) and the product of the first PCR (reverse) as primers. Now, the *BamH*I restriction site (underlined) was added to the forward primer for cloning purposes. The 30-cycle amplification reactions were performed with the same Taq DNA polymerase as before, under the conditions: 2 min at 94°C (initial denaturation), 15 s at 94°C (denaturation), 30 s at 52°C (annealing) and 30 s at 72°C (elongation).

The MTT5 cDNA included only one TAA (encoding Gln36) that had to be mutated. Here, the first PCR amplified a MTT5 cDNA fragment using as primers: 5'-GCCGGGGATCCATGGATAAAATTTC TGGTGA-3' (forward *BamH*I site underlined) and 5'-TCTCCTGAACCGACACAACATTGTTTATCATC AGAATTGCAGCAA-3' (reverse). The 30-cycle amplification reactions were performed with the same Taq DNA polymerase as for MTT1, under the following conditions: 2 min at 94°C (initial denaturation), 15 s at 94°C (denaturation), 30 s at 57°C (annealing) and 30 s at 72°C (elongation). The second PCR was performed using the product of the previous PCR as forward megaprimer and the oligonucleotide 5'-AAAAGCTCGAGTCAGCAACTACCTCCAGGGC -3' (*Xho*I restriction site underlined) as reverse primer. The procedure and reagents in the second PCR were the same as for the first reaction.

As mentioned before, the MTT3 cDNA was mutagenized by using the QuickChange Lightning Multi Site-Directed Mutagenesis Kit (Agilent Technologies), because the location of the involved codons (one TAG, encoding Glu81) and four TAA (encoding Gln102, Gln111, Gln117, Gln118 and Gln159)) made it impossible to use the megaprimer strategy. Four oligonucleotides were required to introduce the desired mutations: *ol-1:* (to mutate the T nucleotide in the 159-TAA triplet) 5'-ACTTCAAAGAAAGAGTG TCAGGTATGTCAATGTTGTAAATGA-3';

ol-2: (to mutate the T nucleotide in the 111-, 117- and 118-TAA triplet) 5'-CACTAATTGTCAATGC TACAAACAAGCTCAACAAGGATGTTGTTG-3';

ol-3: (to mutate the T nucleotide in the 102-TAA triplet) 5'-CTAAAGAATGTTGTACTGGCACTCAA GAAGGATG-3'; and *ol-4:* (to mutate the T nucleotide in the 81-TAG triplet) 5'-TTAGATCCAAATA GTGGATATCAGTGTGCAAGTAAAACTG-3'. The 30-cycle amplification reactions were performed following the kit instructions: 20 s at 95°C (initial denaturation), 30 s at 55°C (annealing) and 30 s at 65°C (elongation). Finally, an additional PCR reaction added the suitable restriction sites for cloning into the expression vector (*BamH*I in forward and *Xho*I in reverse, underlined), to the fully mutated cDNA product. The designed primers were: 5'-GGGAAGGATCCATGGAAAAAATTAATAAC-3' (forward) and 5'-GGGGACTCGAGTCATTTACA ACATTGACA-3' (reverse) and the PCR conditions were the same as before.

The MTT2 and MTT4 cDNA sequences were directly amplified using the following oligonucleotides as primers: 5'- GGGGAGGATCCATGGACACTCA-3' (forward) and 5'-GAAACTCGAGTCAGCATTTGC ATT-3' (reverse) for MTT2; and 5'-GGGGAGGA TCCATGGACACCCA-3' (forward) and 5'-GGGG

ACTCGAGTCAGCATTTGC-3′ (reverse) for MTT4. These primers introduced the 5′ *BamH*I and 3′ *Xho*I restriction sites required for subsequent subcloning. The PCR conditions and reagents were the same as before.

In all cases, the final PCR products were analyzed by 1% agarose gel electrophoresis and the expected bands were excised and purified (Genelute™ Gel Extraction Kit, Sigma Aldrich) to be subcloned into the *BamH*I/*Xho*I sites of the pGEX-4T1 *E.coli* expression vector (GE Healthcare) by ligation using the DNA Ligation Kit 2.1 (Takara Bio Inc.). The recombinant vectors were transformed into *E. coli MachI* strains. All the mutated MTT cDNAs were sequenced before expression, using the Big Dye Terminator 3.1 Cycle Sequencing Kit (Applied Biosystems). The recombinant clones were then transformed into BL21 *E. coli* protease deficient cells for GST-MTT fusion protein synthesis.

Synthesis and purification of recombinant and *in vitro*-constituted metal-MTT complexes.

5-l Luria-Bertani (LB) cultures of the transformed BL21 *E. coli* strains were the source of recombinant metal-MTT complexes. Gene induction was switched on with 100 µM (final concentration) of isopropyl β-D-thiogalactopyranoside (IPTG) 30 min before the addition of the suitable metal supplement (300 µM $ZnCl_2$, 300 µM $CdCl_2$ or 500 µM $CuSO_4$, final concentrations) to allow the synthesis of the corresponding metal complex. The cultures grew for 3 h, and in the case of Cu-supplementation, cultures were aerated to obtain either a normal oxygenation (1-l of LB media in a 2-l Erlenmeyer flask at 250 rpm) or a low oxygenation (1.5-l of LB media in a 2-l Erlenmeyer flask at 150 rpm), since this condition highly determines the level of intracellular copper in the host cells, as described in ([50]). It is worth noting that to prevent oxidation of the metal–MTT complexes, argon was bubbled in all the subsequent steps of the purification protocol. The 2.5-h cultures were centrifuged and the recovered cell mass was resuspended in ice-cold PBS (1.4 M NaCl, 27 mM KCl, 101 mM Na_2HPO_4, 18 mM KH_2PO_4)-0.5% v/v β-mercaptoethanol, and disrupted by sonication. The total protein extract was obtained in the supernatant of a 12,000 x*g*, 30 min centrifugation, which was then incubated with Glutathione-Sepharose 4B (GE Healthcare) beads at gentle agitation for 1 h at room temperature, for GST–MTT purification by batch affinity chromatography. After three washes in PBS, the GST-MTT proteins were digested with thrombin (10 u per mg of fusion protein, overnight at 17 °C) to separate the metal-MTT complexes from the GST fragment, which remains bound to the gel matrix. The recovered solution was concentrated using Centriprep 3 kDa cut-off Microcons (Amicon) and finally fractionated through a Superdex-75 FPLC column (GE Healthcare) equilibrated with 50 mM Tris-HCl, pH 7.0, and run at 0.8 ml min^{-1}. Aliquots of the protein-containing fractions were identified by their absorbance at 254 and 280 nm, and later analyzed in 15% SDS-PAGE gels stained with Coomassie Blue. MTT-containing samples were pooled and stored at -80 °C until further use. Due to the pGEX recombinant expression system specificities, the five synthesized MTT isoforms contained two additional residues (Gly-Ser) as their N-termini, but these amino acids have been shown not to alter the MT metal-binding features ([51]). Further details about the synthesis and purification procedures can be found in our previous publications ([51, 52]).

The so-called "*in vitro* complexes", to differentiate them from the "*in vivo*" recombinantly synthesized complexes, were prepared *via* metal replacement by adding the corresponding metal ions (Cd^{2+} or Cu^{+}) to the recombinant Zn-MTT samples. These reactions were performed at pH 7.0 following the procedures previously reported for mammalian MTs ([52, 53]). Characterization of the *in vitro* complexes was performed by UV–Vis and CD spectroscopies, as well as ESI-MS analysis, as explained below for the recombinant complexes. All assays were carried out in an Ar atmosphere, and the pH remained constant throughout all the experiments, without the addition of any extra buffers.

Spectroscopic characterization of the metal-MTT complexes

The S, Zn, Cd and Cu content of all the metal-MTT preparations was analyzed by Inductively Coupled Plasma Atomic Emission Spectroscopy (ICP-AES), using a Polyscan 61E (Thermo Jarrell Ash) spectrometer, measuring S at 182.040 nm, Zn at 213.856 nm, Cd at 228.802 nm, and Cu at 324.803 nm. Samples were routinely treated as reported in ([54]). Alternatively their incubation in 1 M HCl at 65 °C for 15 min prior to analyses allowed the elimination of labile sulfide ions ([55]). Protein concentrations were calculated from the ICP-AES sulfur measurement, assuming that all S atoms were contributed by the MTT peptides. CD spectra were recorded in a Jasco spectropolarimeter (Model J-715) interfaced to a computer (J700 software), where a 25 °C temperature was maintained constant by a Peltier PTC-351S equipment. Electronic absorptions measurements were performed on an HP-8453 Diode array UV-visible spectrophotometer. 1-cm capped quartz cuvettes were used to record all the spectra, which were corrected for the dilution effects and processed using the GRAMS 32 program.

ElectroSpray ionization mass spectrometry (ESI-MS) analyses of the metal-MTT complexes

Electrospray ionization time-of-flight mass spectrometry (ESI-TOF MS) was performed on a Micro TOF-Q instrument (Bruker) interfaced with a Series 1200 HPLC Agilent pump, equipped with an autosampler, all of which controlled by the Compass Software. The ESI-L Low Concentration Tuning Mix (Agilent Technologies) was used for equipment calibration. For the analysis of Zn- and Cd-MTT complexes, samples were run under the following conditions: 20 µl of protein solution injected through a PEEK (polyether heteroketone) tubing (1.5 m x 0.18 mm i.d.) at 40 µl min^{-1}; capillary counter-electrode voltage 5 kV; desolvation temperature 90-110 °C; dry gas 6 l min^{-1}; spectra collection range 800-2500 m/z. The carrier buffer was a 5:95 mixture of acetonitrile:ammonium acetate (15 mM, pH 7.0). Instead, the Cu-MTT samples were analyzed as follows: 20 µl of protein solution injected at 40 µl min^{-1}; capillary counter-electrode voltage 3.5 kV; lens counter-electrode voltage 4 kV; dry temperature 80 °C; dry gas 6 l min^{-1}. Here, the carrier was a 10:90 mixture of acetonitrile:ammonium acetate, 15 mM, pH 7.0. Acidic-MS conditions, which causes the demetalation of the peptides loaded with divalent metal ions, but keeps the Cu^+ ions bound to the protein, were used to generate the apo-MTT forms and to analyze the Cu-containing MTT samples. For it, 20 µl of the preparation were injected under the same conditions described previously, but using a 5:95 mixture of acetonitrile:formic acid, pH 2.4, as liquid carrier. For all the ESI-MS results, the error associated with the mass measurements was always inferior to 0.1%. Masses for the holo-species were calculated according the rationale previously described ([56]).

Results and Discussion

MTT1 to MTT5 peptide identity and classification

The MTT1 to MTT5 cDNAs constructed by site-directed mutagenesis according to the standard genetic code were confirmed by DNA sequencing. In total, nine TAA and two TAG triplets (coding for Gln in *Tetrahymena* and Stop in the standard genetic code) had been replaced by CAA and CAG codons: five in MTT1, five in MTT3, and one in MTT5 (protein positions indicated in Figure 1). SDS-PAGE analyses of total protein extracts from BL21 cells transformed with each one of the pGEX-MTT plasmids revealed the presence of bands corresponding to the expected GST-MTT sizes (data not shown). Homogeneous metal-MTT complex preparations were obtained from 5-l *E. coli* cultures at final concentrations varying in the 10^{-4} M range, as detailed in Table 1. Firstly, Zn-MTT and Cd-MTT aliquots were acidified to pH 2.4 to verify the molecular weight of the corresponding apo-forms, since this acid pH conventionally results in demetalation of the complexes formed by MTs and divalent metal ions. Some unusual results were already obtained at this stage. Since it was impossible to recover the corresponding Zn- or Cd-complexes for MTT2, no apo-MTT2 could be characterized. Nevertheless, the coherent results obtained for the Cu-MTT2 species (which will be analyzed in a following section) led to assuming the correct identity and integrity of the MTT2 peptide. For MTT4 and MTT5, the molecular masses of the acidified samples were in accordance with the expected values calculated from their respective amino acid sequences (Figure 1 and Table 1). Strikingly, the MTT1 and MTT3 isoforms, those first classified as Cd-thioneins according to gene induction criteria, yielded both Zn- and Cd-complexes that were extremely resistant to demetalation (Figure 2 and Table 1). Hence, the Zn-MTT1 preparation acidified to pH 2.4 yielded a mixture of almost equimolar apo-MTT1 and Zn_4-MTT1 forms, while in the acidified Cd-preparations, a major Cd_{12}-MTT1 and minor Cd_{11}-MTT1 were detected. In contrast, the Zn-MTT3 complexes exhibited the usual complete demetalation at pH 2.4, yielding an apo-form with the expected molecular weight, and only the Cd-MTT3 preparation was reluctant to yield the corresponding apo-form, yielding Cd_8-MTT3 complexes instead (Figure 2). Since the Cys content of MTT1 (48 Cys/162 aa) is considerably higher than that of MTT3 (42 Cys/162 aa) it is sensible to hypothesize that the resistance to acid demetalation exhibited by the Cd-MTT1 in relation to the Cd-MTT3 complexes may be related to the capacity of the former to fold into a more compact cluster, which would be stabilized by a higher number of Cd-thiolate bonds, the Cd content of both, Cd-MTT1 and Cd-MTT3, being roughly equivalent (*cf.* Table 2). Also the fact that, for both isoforms, the Zn species are more prone to demetalation than the Cd species is concordant with the higher strength of Cd-thiolate than Zn-thiolate bonds. These results suggest that the Cd-MTT1 and Cd-MTT3 complexes include highly stable Cd-SCys cores, which are formed by coordination of 4, or multiples of 4, Cd^{2+}, and that the bound Cd^{2+} ions are only released under harsh acidification conditions. Therefore, the incubation of the Zn-MTT1, Cd-MTT1, and Cd-MTT3 preparations with increasing strength of formic acid (final pH of 1.82) yielded the expected apo-MTT1 and apo-MTT3 polypeptides, as shown in both cases by the single ESI-MS peak corresponding to the expected molecular size (Figure 2).

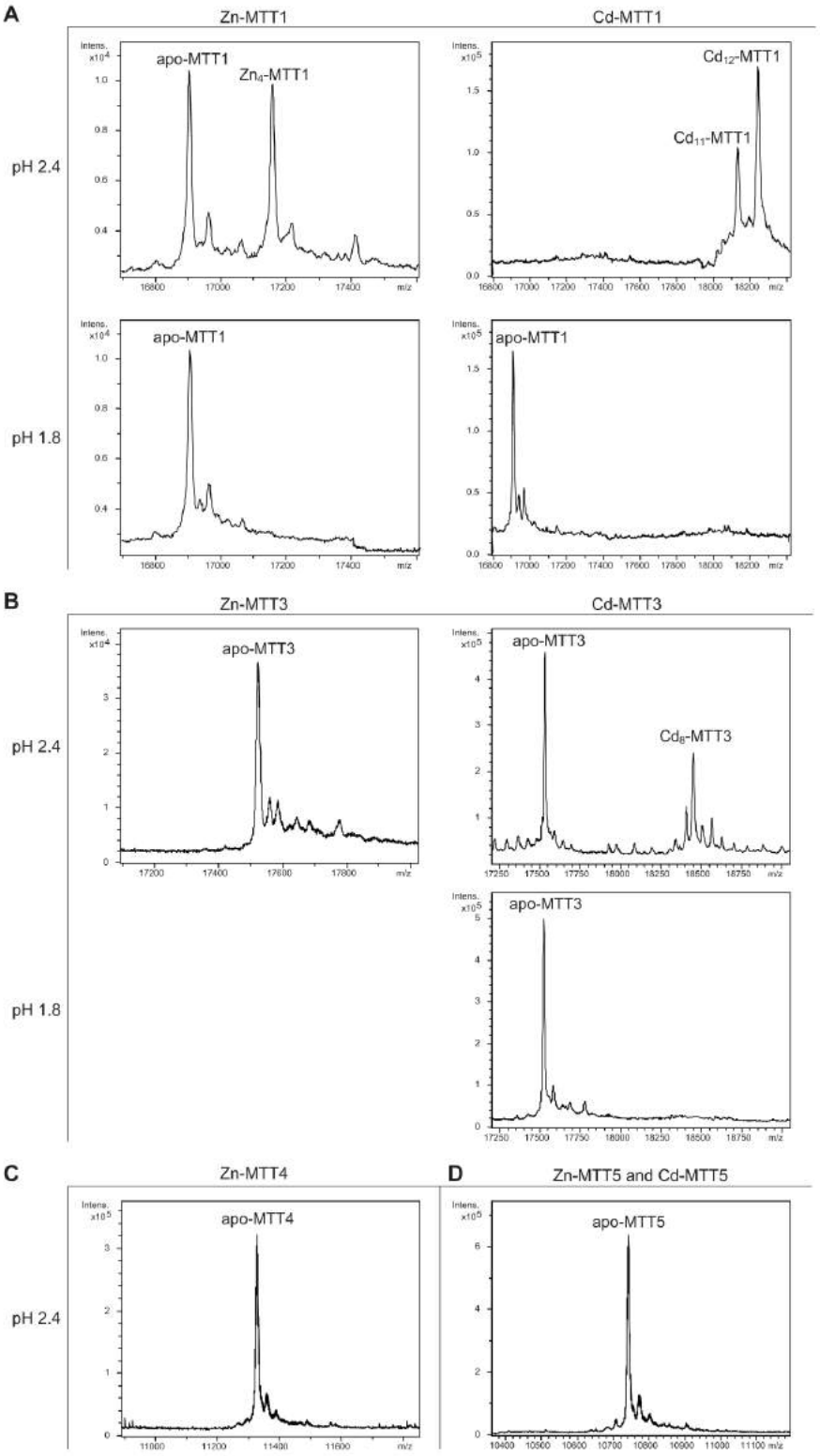

Figure 2. Deconvoluted ESI-MS spectra of the demetalated Zn- and Cd-MTT complexes, recorded at acidic pH. The spectra correspond to the demetalated preparations in Zn- and/or Cd-enriched cultures of (A) MTT1, (B) MTT3, (C) MTT4, and (D) MTT5. For those isoforms that were resistant to demetalation, the ESI-MS was run at pH 2.4 and pH 1.8.

Table 1. General features of the recombinant MTT syntheses. Total protein yield of the recombinant metal-MTT preparations. The molecular weight of the acidified (pH 2.4) Zn-, and Cd- MTT preparations compared to the expected theoretical MW of the respective apo-MTT polypeptides.

	[MT][a] (mg per L of culture)			Molecular Weight (Da)		
Isoform	**Zn supplemented in culture**	**Cd supplemented in culture**	**Cu supplemented in culture**	**Acidified (pH 2.4) Zn- and Cd-complexes[b]**	**Acidified (pH 1.8)**	**Theoretical value for the apoforms**
MTT1	1.21-1.62	2.55	0.54	16903.0 + Zn_4-MTT1 Cd_{12}- > Cd_{11}-MTT1	16903.0 16903.0	16901.5
MTT2[c]	---	---	0.32-3.15	---	---	11316.0
MTT3	1.90-2.27	6.31-7.36	0.11	17530.0 Cd_8-MTT3	17530.0 17530.0	17529.9
MTT4	0.49-1.47	0.21	0.32-1.14	11328.0	---	11330.1
MTT5	1.67	1.72-2.36	0.86-2.40	10739.6	---	10741.4

a The values were calculated from the sulphur content in normal ICP-AES measurements.
b Acidification of complexes with divalent metal ions commonly renders the demetalated polypeptides, as observed for MTT3, MTT4 and MTT5. The cases of MTT1 and MTT3 are fully commented in the text.
c MTT2 failed to yield Zn- and Cd-complexes.

Table 2. Summary of the metal-to-protein-stoichiometries found in the recombinant metal-MTT preparations.

MT Isoform	Zn supplemented in culture	Cd supplemented in culture	Cu supplemented in culture (normal aeration)	Cu supplemented in culture (low aeration)
MTT1	Zn_{17}- Zn_{16}-, Zn_{18}-	**Cd_{17}-** Cd_{12}-	---	---
MTT3	**Zn_{12}-** **Zn_{11}-, Zn_{13}-** Zn_{10}-, Zn_{14}-	**$Cd_{15}S$-, $Cd_{16}S$-,Cd_{18}-** several Cd_x- and Cd_yS-	**$Zn_x(Cu_8, Cu_4, Cu_{12})$**	---
MTT5	**Zn_6-, Zn_5-** Zn_7-, Zn_4- Zn_8-, Zn_3-	**Cd_8-** Cd_9-	**M_{12}-** M_9-, M_8- $Zn_x(Cu_8, Cu_9, Cu_{12})$	**(Cu_8, Cu_4)**
MTT2	---	---	**Cu_{20}-** Cu_{16}- Zn_5Cu_{12}-	**Cu_{20}-** Cu_{23}- Cu_{21}-, Cu_{22}-
MTT4	**Zn_{10}-** Zn_{11}-, Zn_9- Zn_{12}-, Zn_8-	---	**M_{16}-, M_{13}-** $Zn_x(Cu_8, Cu_4, Cu_{12})$	**Cu_{20}-** Cu_{23}-, Cu_{24}- Cu_{21}-, Cu_{22}-

Major species are highlighted in bold. (---) means that neither protein nor metal complexes were recovered.

Zn-, Cd- and Cu-binding abilities of the Cd-MTT isoforms (family 7a): MTT1, MTT3 and MTT5

The metal binding abilities of the *T. thermophila* MTs previously described as Cd-thioneins (*i.e.* family 7a, including MTT1, MTT3 and MTT5) ([17]) were studied using ESI-MS and spectroscopic characterization of their corresponding recombinant Zn^{2+}, Cd^{2+} and Cu^{+}-complexes (Figure 3 and 4, respectively).

MTT1 could only be recovered from Zn^{2+}- and Cd^{2+}-supplemented cultures, this pointing to a complete inability of the protein for folding *in vivo* into stable Cu-complexes. MTT1 yielded a major Zn_{17}-MTT1, together with minor Zn_{18}-, Zn_{16}- and other much minor complexes of lower and higher stoichiometry, when synthesized in the presence of Zn^{2+} (Table 2, Figure 3). Conversely, an almost unique peak was detected as the result of the synthesis by Cd^{2+}-enriched bacteria, which corresponded to Cd_{17}-MTT1, accompanied only by a very minor Cd_{12}-complex, in total coincidence with the major Zn_{17}- stoichiometry found for the Zn-MTT1 preparation (Table 2, Figure 3). Interestingly, although both syntheses yielded major M_{17} complexes, their CD fingerprints are quite different, and reflect the nature of the samples. Zn-MTT1 shows a practically featureless CD envelope, mainly contributed by the protein, and where the absorptions expected at *ca.* 240 nm for the $Zn(SCys)_4$ chromophores are not perceptible, it is probably as a consequence of the mixture of coexisting species. Conversely, Cd-MTT1 gives rise to a very intense CD spectrum with maxima at 245(+) and 260(-) that can be attributed to the major Cd_{17}-MTT1 species. This fingerprint could be contributed by a Gaussian band centered at the characteristic wavelength of the $Cd(SCys)_4$ chromophores, 250 nm, and an exciton coupling at the same wavelength. The presence of two types of Cd-thiolate entities could be hypothesized, so that perhaps the exciton coupling signal arises from the Cd_{12} "robust cluster", while the remaining Cd-SCys units forming the Cd_{17}-MTT1 complex just generate a Gaussian band in the spectrum. Finally, it is worth noting that the results reported here are highly consistent with the stoichiometric data recently reported after apo-MTT1 metal reconstitution experiments, which showed the formation of Cd_{16}-MTT1 ([44]), and the theoretical Cd_{17} maximum capacity, estimated from the available coordinating Cys residues of the polypeptide ([18]).

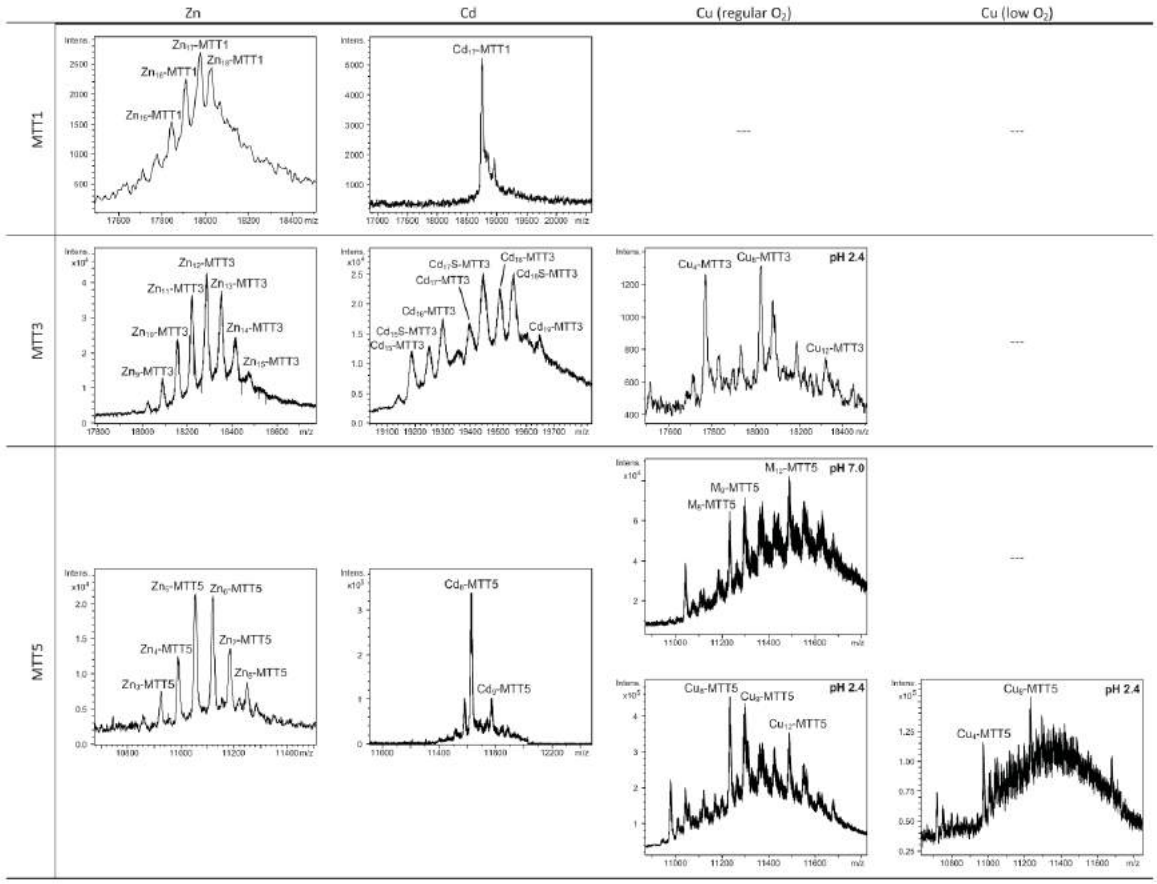

Figure 3. Deconvoluted ESI-MS spectra of the recombinant preparations of MTT1, MTT3 and MTT5. The metal-MTT complexes were synthesized in recombinant cultures supplemented with Zn, Cd, or Cu, and in the case of Cu-enriched media, the synthesis was carried out under regular and low aeration conditions. (---) denotes that no metal-MTT complexes could be purified from the corresponding cultures.

MTT3 could be recovered from Zn^{2+}, Cd^{2+} and also Cu^{2+}-supplemented cultures, but the latter only if they had been grown under normal aeration (normal cell Cu content), so that high Cu may be assumed to preclude the folding into stable complexes. Synthesis of MTT3 in Zn-supplemented *E. coli* cells yielded a mixture of species ranging from major Zn_{12}-MTT3 complexes to minor Zn_9- to Zn_{15}-MTT3 species (Table 2, Figure 3), and this sample showed a CD spectrum such as that expected for an apo-MT, *i.e.* a silent to CD above 250 nm (Figure 4), once again reflecting the mixture of species in the sample. Although this multiplicity of Zn species resembled the behavior of MTT1, MTT3, unlike the former isoform, also yielded a mixture of complexes when synthesized under Cd supplementation, which, most significantly, included sulfide-containing species as major components (Table 2, Figure 3). Hence, $Cd_{16}S$-, $Cd_{15}S$-, and Cd_{18}-MTT3 were predominant, but $Cd_{13}S$-, $Cd_{14}S$-, Cd_{15}-, Cd_{16}-, Cd_{17}- and Cd_{19}-MTT3 were also clearly identifiable. The presence of sulfide-containing species was confirmed by the corresponding ICP measurements, in which the S content proved to be significantly different depending on whether or not the sample had been subjected to acid treatment prior to analysis (data not shown). Additionally, the recombinant Cd-MTT3 sample exhibited a CD profile very similar to that of the Cd-MTT1 preparation, but the latter including the typical absorption of the $Cd\text{-}S^{2-}$ binding motifs absorbing at *ca.* 280 nm(-) (Figure 4). The synthesis in Cu^{2+}-supplemented media also yielded poor results, consisting of heterometallic complexes (ICP-AES results of almost equimolar Zn:Cu content) where only Cu_8- and Cu_4- and minor Cu_{12}- cores were stable enough to resist ESI-MS analysis conditions. Furthermore, these complexes were invariably CD silent at the metal-to-protein transition wavelength range (*cf.* Table 2, Figures 3 and 4). Therefore, MTT3 had a very atypical behavior, since it yielded mixtures of species with the three assayed metal ions.

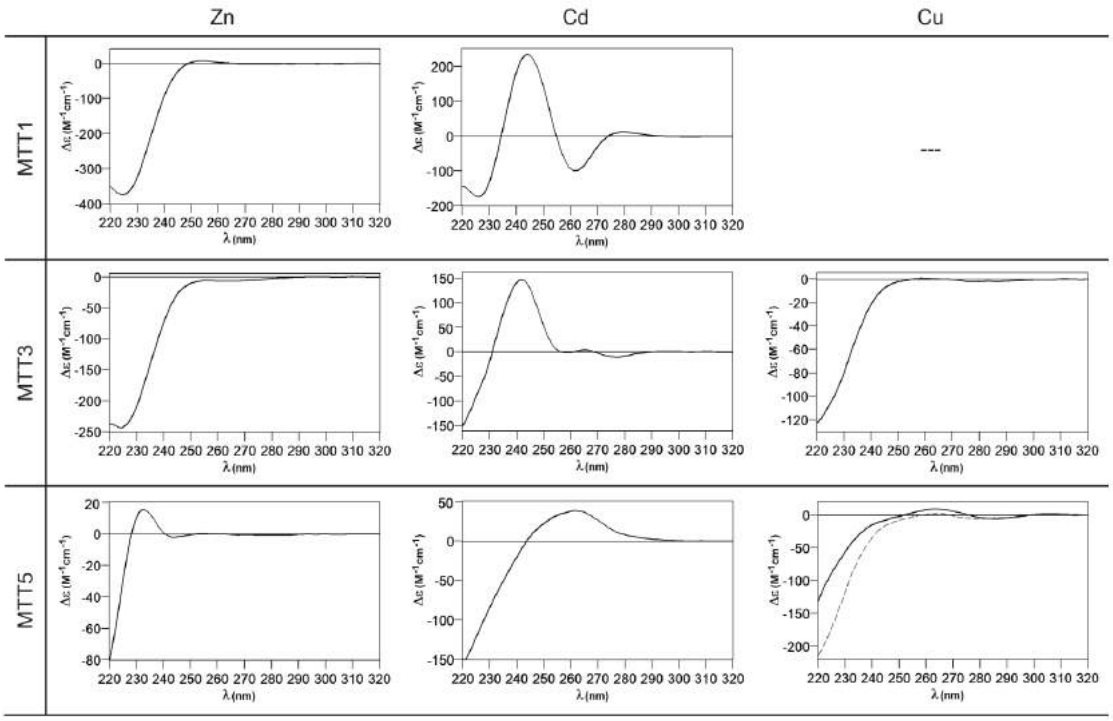

Figure 4. Circular dichroism spectra of the recombinant preparations of MTT1, MTT3 and MTT5. The metal-MTT complexes were synthesized in recombinant cultures supplemented with Zn, Cd, or Cu, and in the case of Cu-enriched media, the synthesis was carried out under regular (solid line) and low aeration (dashed line) conditions.

Finally, MTT5 results were significantly interesting, because it was the unique isoform that yielded stable complexes with the three metal ions analyzed, although the better results for Zn^{2+} and Cd^{2+} than for Cu^{+} confirmed their classification as a 7a-subfamily MT. In view of this special behavior, the *in vitro* Zn/Cd and Zn/Cu replacement reactions were studied for this isoform. The recombinant synthesis of MTT5 in Zn-enriched bacteria yielded two major Zn species (Zn_6- and Zn_5-MTT5, as revealed by ESI-MS (Table 2, Figure 3), together with minor Zn_7-, Zn_8- and Zn_4-, Zn_3-MTT5. The CD spectrum of this preparation exhibited a low intensity Gaussian band centered at 240(+) nm, in correspondence with the typical signals of the Zn-thiolate chromophores. Following a behavior similar to MTT1, MTT5 yielded an almost unique Cd-complex when synthesized in the presence of Cd^{2+}, here Cd_8-MTT5, and only very minor Cd_9-MTT5 species accompanied it (Table 2, Figure 3). However, this Cd_8-MTT5 complex exhibited a CD fingerprint less intense, and different in shape, to those of Cd-MTT1 and Cd-MTT3, with a wide Gaussian band ranging from 240 to 280 nm indicative of the different folding of this Cd_8 complex (Figure 4). For MTT5, the Zn/Cd exchange reaction was followed in detail by CD and UV-Vis spectrophotometry and ESI-MS at discrete steps of the Cd^{2+} addition to the Zn-MTT5 preparation (Figure 5). This reaction demonstrated the progressive incorporation of Cd^{2+} ions into MTT5 (Figure 5A), but this caused the generation of a considerable mixture of Cd_x-MTT5 species, (x = from 3 to 9), even for 10 Cd^{2+} ions added (Figure 5B). Hence, it is clear that the composition of the *in vivo* preparations (*i.e.* an almost unique Cd_8-MTT5 species, Figure 3) could not be reproduced by the Zn^{2+}/Cd^{2+} replacement, which was also highly evident by the comparison of the CD spectra of the respective samples (Figure 5C).

As commented before, the biosynthesis of Cu-loaded MTT5 proved to be feasible in both normal- and low-aerated Cu-supplemented cultures. Under normal Cu conditions, a mixture of M_x-MTT5 (major peaks being, in decreasing order, M_{12}- > M_9- > M_8-MTT5, M=Zn or Cu) was detected by ESI-MS at neutral pH. Since ICP-AES analyses of this sample showed a ratio of 1.6 Zn:11.2 Cu, and acid ESI-MS of the sample revealed a major content of Cu_9- and Cu_8-MTT5, followed by Cu_{12}-MTT5 cores (Table 2, Figure 3), it was reasonable to conclude that some of the recombinant complexes were indeed heterometallic Zn,Cu-MTT5 species. Conversely, cultures grown at high intracellular copper concentrations (*i.e.* low

culture aeration) led to the formation of homonuclear Cu-MTT5 species, which, however, showed an extremely high instability, and only Cu_8- and Cu_4-cores were clearly identified among a myriad of peaks in the corresponding acid ESI-MS analyses (Table 2, Figure 3). The Zn/Cu replacement studies on Zn-MTT5 demonstrated the successive incorporation of Cu^+ into the protein (Figure 5D) and revealed that a mixture of heterometallic species, similar to that yielded *in vivo* when this peptide was synthesized in regular cell copper concentrations, was reached at the interval of 6-to-8 Cu^+ eq added (Figure 5E), despite the fact that the CD fingerprint of this sample was not reproduced at this stage of the Cu^+ addition (Figure 5F). The addition of further Cu^+ ions led to the detection of apo-MTT5, for 12 eq added if the sample was analyzed at neutral ESI-MS conditions, and already at 8 eq added if the sample was subjected to acid (pH 2.4) ESI-MS. This was consistent with a high instability of these complexes, which, logically, was more apparent under the harsh acid ESI-MS conditions.

Metal-binding ability comparison between the three MTT isoforms classically classified as *Tetrahymena* Cd-thioneins (MTT1, MTT3 and MTT5) is not straightforward, because, unlike the Cu-thionein MTT isoforms, they differ either in size and/or in Cys content and patterns (*cf.* Figure 1). However, several of the Zn/Cd- *vs*. Cu-thionein classification criteria coincide in pointing to MTT1 as the isoform with a more pronounced Zn/Cd-thionein character, because, according to these ([5,10]): (i) MTT1 is unable to yield stable Cu-complexes in any of the conditions assayed for Cu-supplemented cultures; (ii) the Zn-MTT1 preparation is a mixture of multiple species, exhibiting an almost silent CD spectrum, and (iii) in contrast with the two preceding points, an almost unique Cd_{17}-MTT1 species, with very particular CD features, is the result of MTT1 folding upon Cd^{2+} ions. Unlike this clearly defined MTT1 behavior, MTT3 and MTT5 somehow present contradictory results. Both isoforms yield several complexes when synthesized under Zn^{2+} surplus, this suggesting a non-optimized polypeptide composition for Zn^{2+} coordination. If considering Cd^{2+}, results clearly indicate the patent ability of MTT5 to fold into a unique, well folded complex, while MTT3 yields a poor mixture of species, the most abundant of which being sulfide-containing complexes, a feature typical of Cu-thioneins ([5,10]). However, the synthesis of MTT3 in Cu-supplemented media was only successful under regular intracellular Cu concentrations, and it only yielded heterometallic species with a high Zn^{2+} content; while MTT5, yielded stable Cu-species also at high Cu concentrations (low aeration of the cultures), with a markedly minimum Zn^{2+} content. All these consideration led us to suggest that MTT5 may be considered as a *second-best* Zn/Cd-thionein, while MTT3 would in fact behave as a MT peptide with patent deficiencies whatever the metal ion considered.

Zn-, Cd- and Cu-binding abilities of the Cu-MTT isoforms (family 7b): MTT2 and MTT4

According to their gene expression profile, the MTT2 and MTT4 isoforms were previously classified as Cu-thioneins (*i.e.* family 7b MTs) ([17]). Following the same approach described above for family 7a MTTs, we studied here the features of their Zn^{2+}-, Cd^{2+}- and Cu^+-complexes, in order to corroborate if the copper responsiveness of their genes was coincident with the metal binding abilities of the encoded peptides and, furthermore, to evaluate if there was any differential behavior between these two *T. thermophila* MT isoforms. First, their divalent metal ion binding abilities were studied. Very significantly, and even after repeated attempts, no MTT2 complexes could be recovered from the Zn- and Cd-supplemented bacterial cells, this indicating the incapacity of MTT2 to fold into stable Zn- or Cd-complexes in an intracellular environment. It is worth commenting that we have commonly encountered this situation the other way round, *i.e.* when attempting to synthesize non-strict Cu-thioneins in copper-enriched host cells ([57,58]), but never in the case of divalent metal ion supplementation. Therefore, it is the first time that we report a Cu-thionein unable to bind Zn^{2+} or Cd^{2+} *in vivo*. Conversely, and for both MTT2 and MTT4, the two types of Cu-supplemented cultures (*i.e.*, low aeration -meaning high cell Cu content-; and regular aeration -meaning normal cell Cu content-), respectively, yielded stable heterometallic and homometallic Cu-containing complexes. Hence, at normal aeration, a major M_{20}-MTT2 complex (M=Zn or Cu) coexisted with minor M_{16}- and M_{17}-MTT2 species, as revealed by ESI-MS at neutral pH (Table 2, Figure 6). Since the major peaks detected at acid ESI-MS were Cu_{20}-, Cu_{16}- and Cu_{12}-MTT2, it is reasonable to deduce that the species present in this sample were homometallic Cu_{20}- and Cu_{16}-MTT2 complexes, together with heterometallic Zn_5Cu_{12}-MTT2, which fits with the ICP-AES-quantification of the total metal in these preparations (3.0 Zn:15.1 Cu per MTT2).

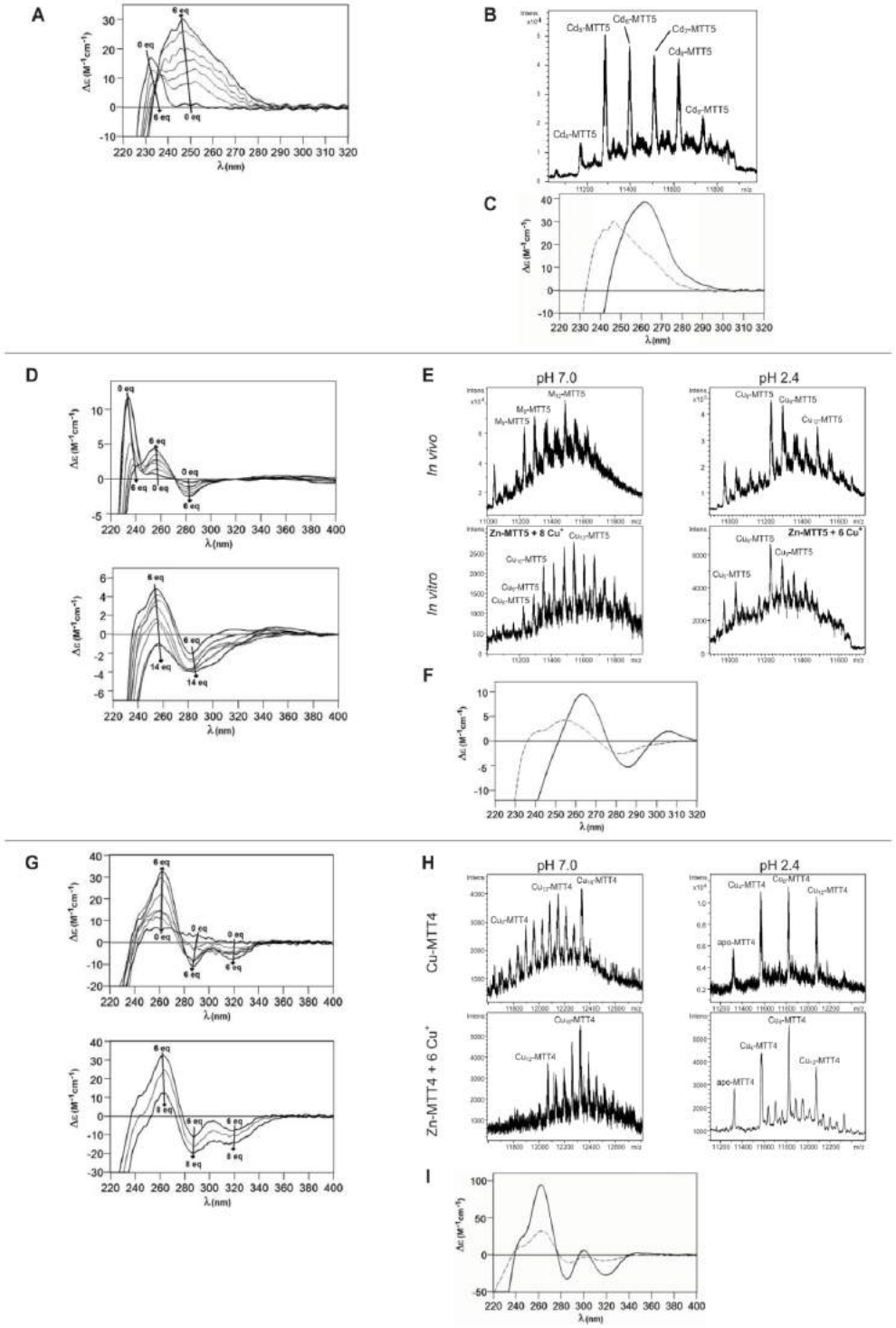

Figure 5. Characterization of *in vitro* prepared metal-MTT5 and metal-MTT4 complexes. (A) Circular dichroism -CD- spectra recorded after the addition of up to 6 Cd^{2+} eq to Zn-MTT5 at pH 7.0. (B) Deconvoluted ESI-MS spectrum recorded after the addition of 10 Cd^{2+} eq to Zn-MTT5. (C) CD spectra corresponding to the Cd-MTT5 preparation (solid line) and that recorded after the addition of 10 Cd^{2+} eq to Zn-MTT5. (D) CD spectra recorded after the addition of up to 14 Cu^{+} eq to Zn-MTT5 at pH 7.0. Comparison of (E) the deconvoluted ESI-MS and (F) the CD spectra of the recombinant Cu-MTT5 preparation (solid line) and those recorded at several stages of the titration of Zn-MTT5 with Cu^{+} (dashed line for the addition of 6 Cu^{+} eq). (G) CD spectra recorded after the addition of up to 8 Cu^{+} eq to Zn-MTT4 at pH 7.0. Comparison of (H) the deconvoluted ESI-MS and (I) the CD spectra of the recombinant Cu-MTT4 preparation (solid line) and those recorded after the addition of 6 Cu^{+} eq to Zn-MTT4 (dashed).

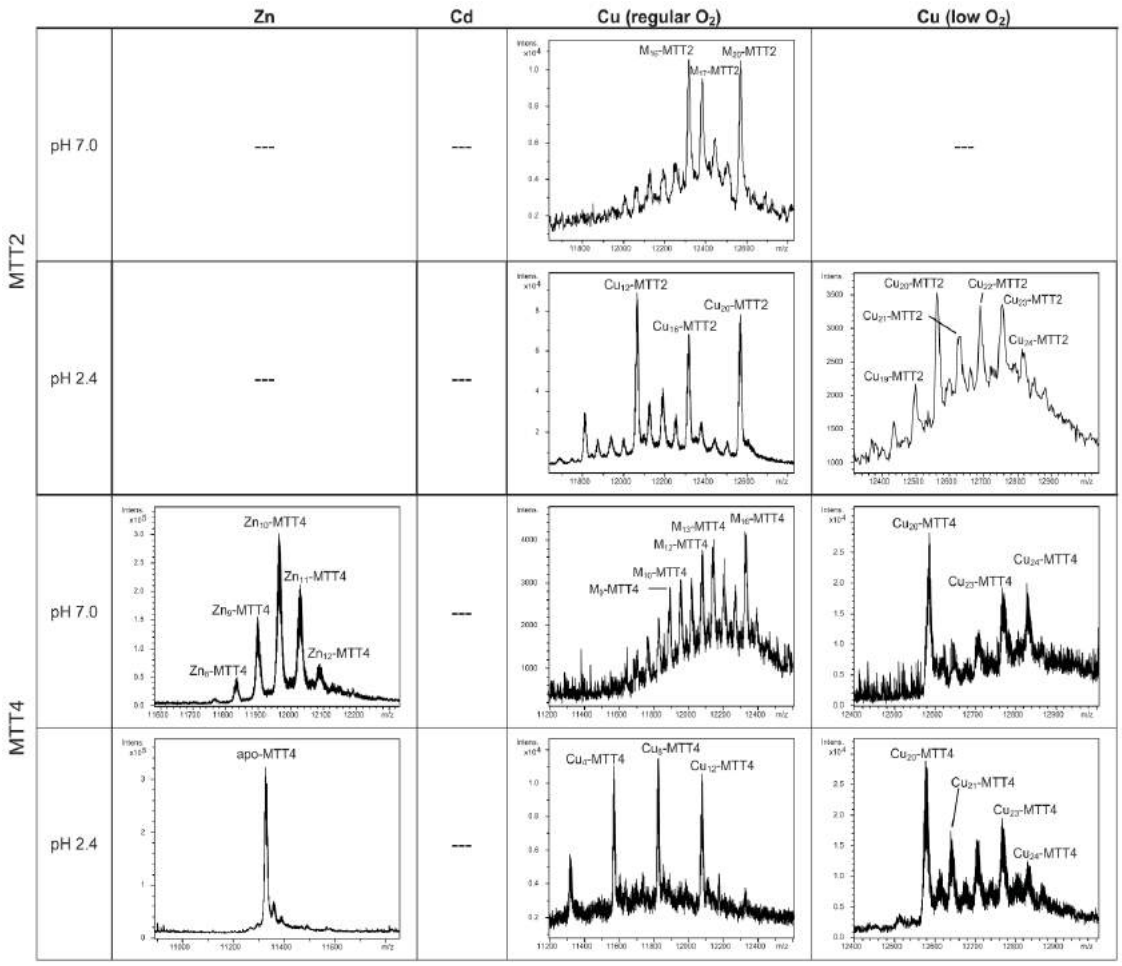

Figure 6. Deconvoluted ESI-MS spectra of the recombinant preparations of MTT2 and MTT4. The metal-MTT complexes were synthesized in recombinant cultures supplemented with Zn, Cd, or Cu, and in the case of Cu-enriched media, the synthesis was carried out under regular and low aeration conditions. ESI-MS was run at pH 7.0 and pH 2.4. (M=Zn or Cu). (---) denotes that no metal-MTT complexes could be purified from the corresponding cultures.

When MTT2 was synthesized by high Cu-enriched cells, the ICP-AES results indicated the total absence of Zn, and therefore all the complexes detected in the acid ESI-MS spectra (Figure 6) were interpreted as homometallic species, major Cu_{20}- and minor Cu_{21}- to Cu_{23}-MTT2. In summary, Cu_{20}-MTT2 was therefore assumed as the principal Cu-containing complex yielded by MTT2, which is also in good agreement with the data estimated in ([18]). The CD spectra of both Cu-MTT2 preparations (regular and normal aerated cultures) showed very similar profiles, with the typical bands at 260(+) and 285(-) nm of tetrahedrally and/or trigonally coordinated Cu^+, as well as absorbances above 300 nm (320-325(-) and 365(+)), which are attributable to digonal Cu^+. The latter are consistently more intense in the *low aeration* sample, which contains homometallic Cu^+ complexes (Figure 7).

MTT4, like MTT2, was unable to fold *in vivo* onto Cd-complexes but, at least it yielded analyzable Zn-MTT4 species, where major Zn_{10}-MTT4 appeared accompanied by several minor species, ranging from Zn_8- to Zn_{12}-MTT4. The multiplicity of peaks in the Zn-preparations (Figure 6) and, as a matter of fact, the impossibility of recovering Cd-MTT4 complexes, was highly concordant with the behavior of a typical Cu-thionein. Conversely, MTT4 folded into stable complexes when coordinating Cu^+ ions. At regular aeration, the producing cells yielded a mixture of Zn,Cu-containing complexes, as revealed by the ICP-AES analyses (9.0 Cu:4.0 Zn per MTT4) and the divergence of the ESI-MS species detected at neutral (major M_{16}- and M_{13}-MTT4, together with significantly intense M_9- to M_{17}-MTT4 peaks) and acid pH (major Cu_8-, and minor Cu_{12}- and Cu_4-MTT4 peaks) (Figure 6). These results are easily interpreted if as-

suming the presence of heterometallic Zn_xCu_4-, Zn_yCu_8-, and Zn_zCu_2-MTT4 species (where x, y, and z are a variable number of Zn^{2+} ions that added to 4, 8 or 12 Cu^+ ions end up in the 9-to-17 metal ion content), and maybe some homometallic Cu_{12}-MTT4 species. Contrarily, with a high Cu, MTT4 yields major homometallic Cu_{20}-MTT4, together with higher nucleation species (Figure 6). The CD spectra of the Cu-MTT4 preparations drew the typical Cu-MT fingerprints already observed for the Cu-MTT2 complexes, and as for MTT2, they were more intense for the homometallic Cu-MTT4 than for the heterometallic Zn,Cu-MTT4 samples (Figure 7). Owing to the availability of Zn-MTT4 preparations, it was possible to perform Zn^{2+}/Cu^+ replacement studies for this isoform, in order to obtain a deeper insight into its *in vitro* Cu^+ binding abilities (Figures 5G to 5I). It is worth noting that, starting from the uninformative Zn-MTT4 CD spectra (marked as 0 in the titration, Figure 5G), a typical Cu-MT CD profile developed, with absorptions at 260(+), 285(-), and 320(-) nm. Remarkably, when 6 Cu^+ equivalents had been added to the initial Zn-MTT4, the CD fingerprint closely resembled that of Cu-MTT4 synthesized in regularly aerated cultures (Figure 5H), also coincident with the composition of the mixture (Figure 5I).

Comparison of the metal binding abilities of MTT2 and MTT4 reveal significant information, because, noteworthy, these two peptides only differ in one amino acid position (#89: Asn in MTT2 and Lys in MTT4, *cf.* Figure 1). Both MTTs bind up to 20 Cu^+, which is consistent with their close similarity and conserved Cys pattern, but several points converge in supporting a more marked Cu-thionein character for MTT2 than for MTT4: i) it was impossible to recover Zn- and Cd-MTT2 complexes, while Zn-MTT4 species are stable; ii) when synthesized under normal Cu, MTT2 is already able to yield Cu_{20}-MTT2 complexes, while this is not the case for MTT4; iii) under these synthesis conditions, MTT2 forms heterometallic species with stable Cu_{12}-cores, while for MTT4, the most stable core is Cu_8, with Cu_4 and Cu_{12} as minor ones; iv) in surplus Cu conditions, MTT2 yields homometallic species with a higher Cu stoichiometry than MTT4. These differential Cu-binding features have to be attributed to the unique amino acid substitution, and therefore it is reasonable to conclude that the presence of Asn89 (MTT2) instead of Lys (MTT4) greatly favors the character of Cu-thionein of the polypeptide. This is in total agreement with the situation found in snail MTs, where the comparative analysis of their homologous and metal-specific CuMT and CdMT protein sequences recently revealed the respective major presence of Asn *vs.* Lys residues in several positions ([59]).

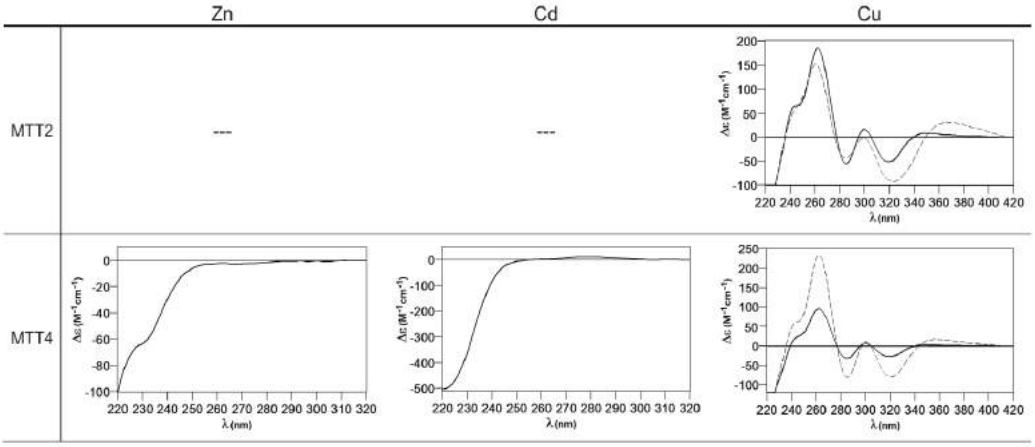

Figure 7. Circular dichroism spectra of the recombinant preparations of MTT2 and MTT4. The metal-MTT complexes were synthesized in recombinant cultures supplemented with Zn, Cd, or Cu, and in the case of Cu-enriched media, the synthesis was carried out under regular (solid line) and low aeration (dashed line) conditions. (---) denotes that no metal-MTT complexes could be purified from the corresponding cultures.

Conclusions

Overall, the results of the current study show the thorough analysis of the Zn^{2+}, Cd^{2+} and Cu^+ binding abilities of each one of the five metallothionein peptides composing the *Tetrahymena thermophila* MT system. These allow the polypeptides to be classified as Zn/Cd- or Cu-thioneins, a metal-binding property that is globally concordant with their specificity previously evaluated from gene response criteria. Hence, in this organism divergence evolution of cysteine-rich sequences and of gene expression regulation has led to the generation of two clear Zn/Cd-thioneins (MTT1 and MTT5), an undefined MT (MTT3), and two

Cu-thioneins (MTT2 and MTT4). The comprehensive comparison of the recombinant complexes yielded by the encoded peptides towards the three metal ions allows their gradual classification from Zn/Cd-thionein to Cu-thionein as follows: MTT1>MTT5>MTT3>MTT4>MTT2; and *vice versa* for the Cu- to Zn/Cd-thionein gradation. Strikingly, the MTT3 isoform is an intermediate isoform, which is not particularly suitable for coordination of any of these three metal ions, if considering the poor features of the corresponding metal complexes. Data in the literature on the type of metal ion inducing expression of the *T. thermophila MTT* genes ([17]) agree with the classification suggested in this work by the features of the metal-MTT complexes. Although MTT3 was then unambiguously considered as a Cd-thionein, a peculiar behavior was already noted for the *MTT3* gene inducibility pattern. Hence, all MTT Cd-thioneins are induced by divalent metal ions, but Cd^{2+} is the best inducer for *MTT1*, and Cd^{2+} is also better than Zn^{2+} for *MTT5*. But for the *undefined* MTT3 isoform, its gene is more responsive to Zn^{2+} at a short inducibility time, while for long treatments, Cd^{2+} is the most effective inducer, so that it is tempting to hypothesize that its lack of a definite metal preference responds to a need of plasticity, allowing it to develop diverse physiological tasks. It is captivating to hypothesize on how evolution may have modulated the amino acid sequences of these paralogous sequences in order to achieve such metal binding preferential behavior, since *T. thermophila* MTs are among the longest MT peptides ever reported. Duplication and subsequent variation of short Cys-rich sequence modules has long been proposed as the basic building mechanism for these long MTs, especially for the three Cd-thioneins, which are far more dissimilar, both in length and in Cys-patterns, than the two Cu-MTTs ([17]). The MTT Zn/Cd-isoforms are also characterized by the high occurrence of Cys doublets and triplets in their sequences (Figure 1B). Although the former are common in MTs, being, for example a signature for the vertebrate α-domains, the Cys-triplet motif is scarcely found among MTs; but here it appears undoubtedly associated to an increased ability for Cd^{2+} coordination. No complex modular structure has been defined for the MTT Cu-thioneins (MTT2 or MTT4) beyond the evidence that they encompass repetitions of a ($CysLysCysX_{2\text{-}5}CysXCys$) motif, and thus the total absence of Cys triplets and doublets appears intrinsically related with an optimal Cu-binding performance. Taking into account that MTT2 and MTT4 only differ in one amino acid position, it can be assumed that they have recently differentiated in evolution. It is relevant how this amino acid change increases the Cu-thionein character of MTT2 (Asn) in relation to MTT4 (Lys), consistently with the respective identification of these amino acids as Cu-thionein and Cd-thionein determinants in snail MTs ([59]). In conclusion, this work confirms how the *Tetrahymena* MT system constitutes an invaluable model for MT evolutionary studies, a subject that is lately revealing extraordinary convergent strategies, even if analyzed in highly distinct organisms. Hence, the need for high-capacity chelating polypeptides seems to have been tackled by tandem repetition of basic building blocks, as we recently described for the pathogenic fungus *Cryptococcus neoformans* Cu-thioneins ([45,46]), and the same amino acids appear to tip the balance in favor of Zn/Cd-thioneins (Lys) or Cu-thioneins (Asn) both in snails ([59]) and ciliates (this work). Therefore, and despite their complete disparity in protein sequence, MTs from the most diverse organisms seem to have adopted common evolutionary trends in order to achieve their functional differentiation and specialization along the tree of life.

Acknowledgements

This work was supported by the Spanish Ministerio de Economía y Competitividad (MINECO), grants BIO2012-39682-C02-01 (to SA), -02 (to MC), and grant CGL2008-00317/BOS (to JCG), which are co-financed by the European Union through the FEDER program. Authors from both Barcelona universities are members of the 2014SGR-423 Grup de Recerca de la Generalitat de Catalunya. AE was the recipient of a predoctoral grant from the MINECO (BES-2010-036553). We thank the Centres Científics i Tecnològics (CCiT) de la Universitat de Barcelona (ICP-AES, DNA sequencing) and the Servei d'Anàlisi Química (SAQ) de la Universitat Autònoma de Barcelona (CD, UV-vis, ESI-MS) for allocating instrument time.

Competing Interests

The authors have declared that no competing interest exists.

References

1. Wolfe KH, Shields DC. Molecular evidence for an ancient duplication of the entire yeast genome. Nature 1997; 387:708-713.
2. Lundin LG. Gene duplications in early metazoan evolution. Semin Cell Dev Biol 1999; 10:523-530.
3. Holland PW, Garcia-Fernandez J, Williams NA, Sidow A. Gene duplications and the origins of vertebrate development. Dev Suppl 1994; 43:125-133.
4. Capdevila M, Bofill R, Palacios O, Atrian S. State-of-the-art of metallothioneins at the beginning of the 21st century. Coord Chem Rev 2012; 256:46–62.
5. Palacios O, Atrian S, Capdevila M. Zn- and Cu-thioneins: a functional classification for metallothioneins? J Biol Inorg Chem 2011; 16:991–1009.
6. Capdevila M, Atrian S. Metallothionein protein evolution: a miniassay. J Biol Inorg Chem 2011; 16: 977–989.
7. Seren N, Glaberman S, Carretero MA, Chiari Y. Molecular evolution and functional divergence of the Metallothioneins gene family in Vertebrates. J Mol Evol 2014; 78:217-233.
8. Palmiter R. The elusive function of metallothioneins. Proc Natl Acad Sci USA 1994; 95:8428-8430.

9. Blindauer CA, Leszczyszyn OI. Metallothioneins: unparalleled diversity in structures and functions for metal ion homeostasis and more. Nat Prod Rep 2010; 27:720-741.
10. Bofill R, Capdevila M, Atrian S. Independent metal-binding features of recombinant metallothioneins convergently draw a step gradation between Zn- and Cu-thioneins. Metallomics 2009; 1:229-234.
11. Waldron JK, Robinson NJ. How do bacterial cells ensure that metalloproteins get the correct metal? Nature Rev Microbiol 2009; 6:25-35.
12. Waldron JK, Rutherford JC, Ford D, Robinson NJ. Metalloproteins and metal sensing. Nature 2009; 460:823-830.
13. Palacios O, Pagani A, Perez-Rafael S, Egg M, Höckner M, Brandstätter A, Capdevila M, Atrian S, Dallinger R. Shaping mechanisms of metal specificity in a family of metazoan metallothioneins: evolutionary differentiation of mollusc metallothioneins. BMC Biology 2011; 9:4.
14. Palacios O, Perez-Rafael S, Pagani A, Dallinger R, Atrian S, Capdevila M. Cognate and noncognate metal ion coordination in metal-specific metallothioneins: the *Helix pomatia* system as a model. J Biol Inorg Chem 2014; 19:923-935.
15. Nemer M, Wilkinson DG, Travaglini EC, Sternberg EJ, Butt TR. Sea urchin metallothionein sequence: key to an evolutionary diversity. Proc Natl Acad Sci USA 1985; 82:4992-4994.
16. [Internet] Metallothioneins: classification and list of entries.www.uniprot.org/docs/metallo.txt
17. Diaz S, Amaro F, Rico D, Campos V, Benitez L, Martin-Gonzalez A, Hamilton EP, Orias E, Gutierrez JC. *Tetrahymena* Metallothioneins Fall into Two Discrete subfamilies. PlosOne 2007; 3:e291.
18. Gutierrez JC, Amaro F, Diaz S, de Francisco P, Cubas LL, Martin-Gonzalez A. Ciliate metallothioneins: unique microbial eukaryotic heavy-metal-binder molecules. J Biol Inorg Chem 2011; 16:1025-1034.
19. Parfrey LW, Lahr DJG, Knoll AH, Katz L. Estimating the timing of early eukaryotic diversification with multigene molecular clocks. Proc Natl Acad Sci USA 2011; 108:13624-13629.
20. Boldrin F, Santovito G, Negrisolo E, Piccinni E. Cloning and Sequencing of Four New Metallothionein Genes from *Tetrahymena thermophila* and *T. pigmentosa*. Evolutionary Relationships in *Tetrahymena* MT Family. Protist 2003; 154:431-442.
21. Boldrin F, Santovito G, Gaerteig J, Wlonga D, Cassidy-Hanley D, Clark TG, Piccinni E. Metallothionein Gene from *Tetrahymena thermophila* with a Copper-Inducible- Repressible Promoter. Eukaryot Cell 2006; 5:422-425.
22. Boldrin F, Santovito G, Formigari A, Bisharyan Y, Cassidy-Hanley D, Clark TG, Piccinni E: MTT2, a copper-inducible metallothionein gene from *Tetrahymena thermophila*. Comp Biochem Physiol C Toxicol Pharmacol 2008; 147:232-240.
23. Santovito G, Formigari A, Boldrin F, Piccinni E. Molecular and functional evolution of *Tetrahymena* metallothioneins: New insights into the gene family of *Tetrahymena thermophila*. Comp Biochem Physiol C Toxicol Pharmacol 2007; 144:391-397.
24. Chang Y, Feng L-F, Xiong J, Miao W. Function comparison and evolution analysis of metallothionein gene MTT2 and MTT4 in *Tetrahymena thermophila*. Zool Res 2011; 32:476-484.
25. Piccinni E, Staudenmann W, Albergoni V, De Gabrieli R, James P. Purification and primary structure of metallothioneins induced by cadmium in the protists *Tetrahymena pigmentosa* and *Tetrahymena pyriformis*. Eur J Biochem 1994; 226:853-859.
26. Santovito G, Irato P, Palermo S, Boldrin F, Sack R, Hunziker P, Piccinni E. Identification, Cloning and Characterisation of a Novel Copper-Metallothionein in *Tetrahymena pigmentosa*. Sequencing of cDNA and Expression. Protist 2001; 152:219-229.
27. Boldrin F, Santovito G, Irato P, Piccinni E. Metal Interaction and Regulation of *Tetrahymena pigmentosa* Metallothionein Genes. Protist 2002; 153:283-291.
28. Guo L, Fu C, Miao W. Cloning characterization, and gene expression analysis of a novel cadmium metallothionein gene in *Tetrahymena pigmentosa*. Gene 2008; 423:29-35.
29. Piccinni E, Irato P, Coppellotti O, Guidolin L. Biochemical and ultrastructural data on *Tetrahymena pyriformis* treated with copper and cadmium. J Cell Sci 1987; 88:283-293.
30. Piccinni E, Bertaggia D, Santovito G, Miceli C, Kraev A. Cadmium metallothionein gene of *Tetrahymena pyriformis*. Gene 1999; 234:51-59.
31. Fu C, Miao W: Cloning and characterization of a New Multi-Stress Inducible Metallothionein Gene in *Tetrahymena pyriformis*. Protist 2006; 157:193-203.
32. Amaro F, de Lucas M, Martin-Gonzalez A, Gutierrez JC. Two new members of the *Tetrahymena* multi-stress-inducible metallothionein family: Characterization and expression analysis of *T. rostrata* Cd/Cu metallothionein genes. Gene 2008, 423:85-91.
33. Shuja RN, Shakoori AR. Identification, cloning and sequencing of a novel stress inducible metallothionein gene from locally isolated *Tetrahymena tropicalis lahorensis*. Gene 2007; 405:19-26.
34. Chaundhry R, Shakoori AR. Isolation and characterization of a novel copper-inducible metallothionein gene of a ciliate, *Tetrahymena tropicalis lahorensis*. J Cell Biochem 2010; 110:630-644.
35. Shuja RN, Taimuri SUA, Shakoori FR, Shakoori AR. Efficient expression of truncated recombinant cadmium-metallothionein gene of a ciliate, *Tetrahymena tropicalis lahorensis* in *Escherichia coli*. Mol Biol Rep 2013; 40:7061-7068.
36. Chang Y, Liu G, Guo L, Liu H, Yuan D, Xiong J, Ning Y, Fu C, Miao W. Cd-Metallothioneins in Three Additional *Tetrahymena* Species: Intragenic Repeat Patterns and Induction by Metal Ions. J Eukaryot Microbiol 2014, 61:333-342.
37. Valls M, Bofill R, Gonzalez-Duarte R, Gonzàlez-Duarte P, Capdevila M, Atrian S. A new insight into Metallothionein (MT) classification and evolution. The *in vivo* and *in vitro* metal binding features of *Homarus americanus* recombinant MT. J Biol Chem 2001; 276:32835-32843.
38. Shang Y, Song X, Bowen J, Corstanje R, Gao Y, Gaertig J, Gorovsky MA. A robust inducible-repressible promoter greatly facilitates gene knockouts, conditional expression, and overexpression of homologous and heterologous genes in *Tetrahymena thermophila*. Proc Natl Acad Sci USA 2002; 99:3734-3739.
39. Dondero F, Cavaletto M, Ghezzi AR, La Terza A, Banni M, Viarengo A. Biochemical Characterization and Quantitative Gene Expression Analysis of the Multi-Stress Inducible Metallothionein from *Tetrahymena thermophila*. Protist 2004; 155:157-168.
40. Gutiérrez JC, Amaro F, Martín-González A. From heavy metal-binders to biosensors: Ciliate metallothioneins discussed. BioEssays 2009; 31:805-816.
41. Amaro F, Turkewitz AP, Martin-Gonzalez A, Gutierrez JC. Whole-cell biosensors for detection of heavy metal ions in environmental samples based on metallothionein promoters from *Tetrahymena thermophila*. Microb Biotechnol 2011; 4:513-522.
42. Amaro F, Turkewitz AP, Martin-Gonzalez A, Gutierrez JC. Functional GFP-metallothionein from *Tetrahymena thermophila*: a potential whole-cell biosensor for monitoring heavy metal pollution and a cell model to study metallothionein overproduction effects. Biometals 2014; 27:195-205.
43. Domenech J, Bofill R, Tinti A, Torreggiani A, Atrian S, Capdevila M. Comparative insight into the Zn(II)-, Cd(II)- and Cu(I)-binding features of the protozoan *Tetrahymena pyriformis* MT1 metallothionein. Biochim Biophys Acta 2008; 1784:693-704.
44. Wang Q, Xu J, Chai B, Liang A, Wang W. Functional comparison of metallothioneins MTT1 and MTT2 from *Tetrahymena thermophila*. Arch Biochem Biophys 2011; 509:170-176.
45. Ding C, Festa RA, Chen YL, Espart A, Palacios O, Espin J, Capdevila M, Atrian S, Heitman J, Thiele D. *Cryptococcus neoformans* copper detoxification machinery is critical for copper virulence. Cell, Host & Microbe 2013; 13:265-276.
46. Palacios O, Espart A, Espin J, Ding C, Thiele D, Atrian S, Capdevila M. Full characterization of the Cu-, Zn-, and Cd-binding properties of CnMT1 and CnMT2, two metallothioneins of the pathogenic fungus *Cryptococcus neoformans* acting as virulence factors. Metallomics 2014; 6:279-291.
47. Fogel S, Welch JW, Cathala G, Karin M. Gene amplification in yeast: CUP1 copy number regulates copper resistance. Curr Genet 1983; 7:347-355.
48. Horowitz S, Gorovsky MA. An unusual genetic code in nuclear genes of *Tetrahymena*. Proc Natl Acad Sci USA 1985; 82:2452-2455.
49. Landt O, Grunert HP, Hahn U. A general method for rapid site-directed mutagenesis using the polymerase chain reaction. Gene 1990; 96:125-128.
50. Pagani A, Villarreal L, Capdevila M, Atrian S. The *Saccharomyces cerevisiae* Crs5 metallothionein metal-binding abilities and its role in the response to zinc overload. Mol Microbiol 2007; 63: 256-269.
51. Cols N, Romero-Isart N, Capdevila M, Oliva B, González-Duarte P, González-Duarte R, Atrian S. Binding of excess cadmium(II) to Cd_7-metallothionein from recombinant mouse Zn_7-metallothionein 1. UV-VIS absorption and circular dichroism studies and theoretical location approach by surface accessibility analysis. J Inorg Biochem 1997; 68:157-166.
52. Capdevila M, Cols N, Romero-Isart N, González-Duarte R, Atrian S, González-Duarte P. Recombinant synthesis of mouse Zn_3-ß and Zn_4-α metallothionein 1 domains and characterization of their cadmium(II) binding capacity. Cell Mol Life Sci 1997; 53:681–688.
53. Bofill R, Palacios O, Capdevila M, Cols N, González-Duarte R, Atrian S, González-Duarte P. A new insight into the Ag^+ and Cu^+ binding sites in the metallothionein β domain. J Inorg Biochem 1999; 73:57–64.
54. Bongers J, Walton CD, Richardson DE, Bell JU. Micromolar protein concentrations and metalloprotein stoichiometries obtained by inductively coupled plasma atomic emission spectrometric determination of sulfur. Anal Chem 1988; 60:2683–2686.
55. Capdevila M, Domenech J, Pagani A, Tio L, Villarreal L, Atrian S. Zn- and Cd-metallothionein recombinant species from the most diverse phyla may contain sulfide (S^{2-}) ligands. Angew Chem Int Ed Engl 2005; 44:4618–4622.
56. Fabris D, Zaia J, Hathout Y, Fenselau C. Retention of Thiol Protons in Two Classes of Protein Zinc Coordination Centers. J Am Chem Soc 1996; 118:12242-12243.
57. Perez-Rafael S, Mezger A, Lieb B, Dallinger R, Capdevila M, Palacios O, Atrian S. The metal binding abilities of Megathura crenulata metallothionein (McMT) in the frame of Gastropoda MTs. J Inorg Biochem 2012; 108:84-90.
58. Perez-Rafael S, Kurz A, Guirola M, Capdevila M, Palacios O, Atrian S. Is MtnE, the fifth Drosophila metallothionein, functionally distinct from the other members of this polymorphic protein family? Metallomics 2012; 4:342-349.
59. Perez-Rafael S, Monteiro F, Dallinger R, Atrian S, Palacios O, Capdevila M. Cantareus aspersus metallothionein metal binding abilities: The unspecific CaCd/CuMT isoform provides hints about the metal preference determinants in Metallothioneins. BBA-Proteins and Proteomics 2014; 1844:1694-1707.

Publication # 2

Cryptococcus neoformans copper detoxification machinery
is critical for fungal virulence.

PUBLICATION #2:

TITLE

"*Cryptococcus neoformans* copper detoxification machinery is critical for fungal virulence"

AUTHORS

Chen Ding, Richard A. Festa, Ying –Lien, **Anna Espart**, Òscar Palacios, Jordi Espín, Mercè Capdevila, Sílvia Atrian, Joseph Heitman, Dennis J. Thiele

REFERENCE

Cell Host Microbe (2013) 13: 265–276 (IF: 13.573)

SUMMARY

Copper has been used for many centuries as an antimicrobial agent in medical and agricultural applications. Although the exact mechanism whereby copper action has antimicrobial activity is not well understood, it is believed that its redox properties, through generation of toxic hydroxyl and hydroxyl anion radicals, damage DNA and cell proteins; and also that the hyperaccumulation of intracellular copper may interfere the Fe-S synthesis pathway.

Cryptococcus neoformans is a pathogenic fungus that causes cryptococcosis in human immunodeficient and immunocompetent individuals. It was known that iron and copper play crucial roles in *C. neoformans* virulence. In this work, it was shown that a high Cu-reporter of *C. neoformans* is significantly induced in fungi during the lung colonization by the pathogen cells, concomitantly with an important induction of their metallothionein genes (*CnMTs*), which would be presumably involved in copper detoxification. Concordantly, high CnMT mRNA levels were detected by RT-PCR in response to copper. Intranasal infection of mice with *C. neoformans* carrying CnMT1-luciferase and CTR4-luciferase reporters, allowed to suggest that *CnMT* genes were induced during the lung infection through directly activation of Cuf1, a copper responding transcription factor. Subsequent deletion of either CnMTs led to

a severely attenuated virulence, whereas a single deletion (cnmt1Δ or cnmt2Δ) did not cause virulence attenuation, so that is was readily concluded that at least one CnMT was required for fungal virulence. To confirm that Cu-chelation by CnMTs plays a crucial role in fungal virulence, a mutated CnMT1 in which cysteines were substituted by alanines (CnMT1ala), and which therefore was unable to bind copper, was shown to confer no virulence or infectivity capacity to the fungus, and therefore mice perfectly survived infection. Taken all the results together, it can be assessed that CnMTs are critical for *C. neoformans* copper resistance and virulence when infecting organisms.

Both CnMTs resulted extremely long when compared with other fungal MTs, like *Neurospora crassa* or *Agaricus bisporus*. CnMT1 contains three cysteine-rich segments separated by three spacer regions, while CnMT2 has five cysteine-rich segments, separated by four spacer regions, this implying a putative evolutionary differentiation emerging from a common fungal ancestor. Finally we showed that in host bronchoalveolar cells, an important increase of the synthesis of the copper importer Ctr1, and a significant decrease of the copper transporter ATP7A, involved in phagosomal copper compartimentalization, occurred in response to *C. neoformans* infection, which is attributed to a complex interplay between the fungal pathogen and the host immune system.

Contribution to this work

This work has been performed in collaboration with the group of Prof. Dennis J. Thiele, in his laboratory at Duke University (Durham, North Carolina, USA), and our regular collaborator group of Dr. Mercè Capdevila, in the department of Chemistry, in the Universitat Autònoma de Barcelona (UAB). My personal contribution to this work was: i) the protein similarity studies of CnMTs, to examine their homology and evolutionary relationships with fungal MTs; ii) the construction of the suitable *E. coli* expression vectors for both CnMT; and iii) the subsequent recombinant synthesis and purification of both CnMTs, as well as the CnMTala mutant, from *E. coli* cultures supplemented with Zn and Cu. All the purified metal-CnMT complexes were then analysed by spectroscopy and spectrometry at the UAB.

Cell Host & Microbe
Article

Cryptococcus neoformans Copper Detoxification Machinery Is Critical for Fungal Virulence

Chen Ding,[1] Richard A. Festa,[1] Ying-Lien Chen,[2,5] Anna Espart,[3] Òscar Palacios,[4] Jordi Espín,[4] Mercè Capdevila,[4] Sílvia Atrian,[3] Joseph Heitman,[1,2] and Dennis J. Thiele[1,*]
[1]Department of Pharmacology and Cancer Biology
[2]Department of Molecular Genetics and Microbiology
Duke University, Durham, NC 27710, USA
[3]Departament de Genètica, Universitat de Barcelona, 08028 Barcelona, Spain
[4]Departament de Química, Universitat Autònoma de Barcelona, 08193 Cerdanyola del Vallès, Barcelona, Spain
[5]Current address: Department of Plant Pathology and Microbiology, National Taiwan University, Taipei 106, Taiwan
*Correspondence: dennis.thiele@duke.edu
http://dx.doi.org/10.1016/j.chom.2013.02.002

SUMMARY

Copper (Cu) is an essential metal that is toxic at high concentrations. Thus, pathogens often rely on host Cu for growth, but host cells can hyperaccumulate Cu to exert antimicrobial effects. The human fungal pathogen *Cryptococcus neoformans* encodes many Cu-responsive genes, but their role in infection is unclear. We determined that pulmonary *C. neoformans* infection results in Cu-specific induction of genes encoding the Cu-detoxifying metallothionein (Cmt) proteins. Mutant strains lacking *CMT*s or expressing Cmt variants defective in Cu-coordination exhibit severely attenuated virulence and reduced pulmonary colonization. Consistent with the upregulation of Cmt proteins, *C. neoformans* pulmonary infection results in increased serum Cu concentrations and increases and decreases alveolar macrophage expression of the Cu importer (Ctr1) and ATP7A, a transporter implicated in phagosomal Cu compartmentalization, respectively. These studies indicate that the host mobilizes Cu as an innate antifungal defense but *C. neoformans* senses and neutralizes toxic Cu to promote infection.

INTRODUCTION

Copper (Cu) has a long history as an antimicrobial agent, employed to sterilize wounds by the ancient Egyptians, to ward off cholera in the 19th century, and as an antifungal agent in Bordeaux mixture in vineyards (Cassat and Skaar, 2012; Hodgkinson and Petris, 2012; Hood and Skaar, 2012; Samanovic et al., 2012). More recently, Cu surfaces are utilized in healthcare settings to reduce nosocomial infections (Schmidt et al., 2012). While the precise mechanisms by which Cu exerts antimicrobial activity are not well understood, the redox properties of this metal foster the generation of toxic hydroxyl radicals (•OH) and hydroxyl anions (OH^-), which can cause DNA and protein damage (Halliwell and Gutteridge, 1985). Furthermore, Cu hyperaccumulation has been shown to interfere with iron-sulfur (Fe-S) clusters that are critical to enzymes involved in a plethora of essential biochemical processes (Chillappagari et al., 2010; Liochev, 1996; Macomber and Imlay, 2009; Macomber et al., 2007).

The phagosomal compartment of innate immune cells presents a hostile environment to invading microbial pathogens via the generation of reactive oxygen and nitrogen species, the elaboration of proteases and other degradative enzymes, acidification of the phagosomal lumen, and by nutritional limitation of metals such as Fe, zinc (Zn), and manganese (Mn) that are essential for microbial growth (Hood and Skaar, 2012; Nathan and Shiloh, 2000). While phagocytic cells sequester these metals from invading pathogens, macrophages infected with *Mycobacterium* species hyperaccumulate Cu within the phagosome (Wagner et al., 2005). Moreover, macrophage cell lines that have been activated with IFN-γ elevate expression of both the plasma membrane Cu^+ importer (Ctr1) and the ATP7A vesicular Cu pump (White et al., 2009). As ATP7A is thought to traffic to the phagosomal membrane in these cells, and ATP7A depletion enhances *E. coli* survival to macrophage killing, these observations suggest that elevated luminal Cu is microbiocidal (White et al., 2009).

Cryptococcus species such as *C. neoformans* are pathogenic fungi that cause cryptococcosis in both immunodeficient and immunocompetent individuals. *C. neoformans* is acquired from the environment through inhalation, disseminates through the bloodstream to the brain, and causes ~600,000 deaths annually from lethal meningitis (Heitman, 2011; Kronstad et al., 2012, 2011). Previous studies demonstrated that the metals Fe and Cu play important roles in *C. neoformans* virulence because they are directly involved in many key biochemical processes (Jung et al., 2009, 2008, 2006; Salas et al., 1996; Walton et al., 2005; Williamson, 1994). In particular, Fe is critical for heme biosynthesis and oxidative phosphorylation and serves as a critical cofactor for dozens of enzymatic reactions. Cu functions in melanin formation, Fe uptake, reactive oxygen detoxification, and respiration (Ding et al., 2011; Jung et al., 2009, 2008, 2006; Kronstad et al., 2012; Samanovic et al., 2012; Williamson, 1994). Melanin, a protective pigment and virulence factor, is synthesized by *C. neoformans* via the secreted Cu-dependent oxidase laccase, using host brain catecholamines as substrate (Williamson, 1994). Accordingly, deletion of the genes encoding laccase,

or the secretory compartment Cu importer Ccc2, severely compromised *C. neoformans* virulence (Salas et al., 1996; Walton et al., 2005). The *C. neoformans* Cu metalloregulatory transcription factor Cuf1 has also been demonstrated to be important for virulence (Waterman et al., 2007). Since Cuf1 plays a critical role in activating expression of the *CTR4* gene (encoding a high-affinity plasma membrane Cu^+ importer), Cu acquisition was proposed to underlie the requirement for Cuf1 for virulence (Waterman et al., 2007). However, additional studies demonstrated that *cuf1Δ* mutants exhibit both Cu sensitivity phenotypes and growth defects under Cu-deficient conditions (Ding et al., 2011; Lin et al., 2006). Accordingly, we demonstrated that Cuf1 activates the transcription of genes encoding the Cu acquisition machinery (*CTR1* and *CTR4*) or genes encoding the Cu detoxification machinery (*CMT1* and *CMT2*) under Cu limitation or Cu excess, respectively (Ding et al., 2011). Given the role of Cuf1 target genes in both Cu acquisition and detoxification, it is important to clarify the specific functions of the Cuf1 regulon in virulence.

In this report, we used live animal imaging studies with specific Cu-activated reporters and demonstrated that the *C. neoformans* high-Cu-sensing reporter is dramatically induced during initial respiratory colonization. We demonstrate that the *C. neoformans* metallothioneins, which are induced in a Cu-specific manner and have a high capacity for Cu binding, play a critical role in virulence. Analysis of host Cu homeostasis proteins in bronchoalveolar lavage (BAL) cells from infected animals showed a dramatic increase in the high-affinity mammalian Cu importer (Ctr1) and decreased abundance of the ATP7A Cu transporter that has been implicated in phagosomal Cu compartmentalization.

RESULTS

C. neoformans Metallothionein Gene Expression Is Activated in Lung Infection

We previously demonstrated that *C. neoformans* genes encoding metallothioneins or Cu transporters are strongly induced under high or low Cu conditions, respectively, in a Cu concentration-dependent manner (Ding et al., 2011). Here, using quantitative RT-PCR (qRT-PCR) as a sensitive and quantitative assay, Cmt1 messenger RNA (mRNA) levels were induced ~800-fold in response to Cu, and Ctr4 mRNA levels were induced ~600-fold in response to the Cu^+-specific chelator bathocuproine disulphonate (BCS) (Figure 1A). To ascertain whether these genes are directly regulated by Cuf1 in response to Cu levels, a FLAG-epitope-tagged Cuf1 allele was generated and expressed in *cuf1Δ* cells for use in chromatin immunoprecipitation (ChIP) experiments. Cuf1 was tagged with two copies of the FLAG sequence at the carboxyl terminus; *cuf1Δ* strains transformed with this expression plasmid are fully complemented with respect to the Cu- and BCS- sensitive phenotype of *cuf1Δ* cells, demonstrating that this is a functional Cuf1-FLAG protein (Figure S1A). ChIP assays followed by quantitative PCR (qPCR) analysis of promoter sequences from the *CMT1/2* and *CTR1/4* genes showed strong Cu-regulated Cuf1 binding to the *CTR1* and *CTR4* promoters under Cu deficiency as compared to high Cu conditions. In contrast, Cuf1 binding to the *CMT1* promoter was induced under high Cu conditions, with binding to *CMT2* observed under both conditions (Figure 1B). These results demonstrate that Cuf1 plays a direct role in the activation of Cu detoxification genes and Cu acquisition genes when cells encounter distinct Cu environments.

To assess the potential Cu environment in host tissue sensed in the initial stages of *C. neoformans* infection through its natural respiratory route of infection, two Cu-responsive reporter plasmids were constructed in which luciferase expression is driven by the *C. neoformans CTR4* promoter (*CTR4*-Luciferase) in response to Cu limiting conditions or the *CMT1* promoter (*CMT1*-Luciferase) in response to elevated Cu. *CMT1*- and *CTR4*- driven luciferase protein expression and activities from each reporter were confirmed by luciferase enzyme assays and immunoblotting (Figures 1C and S1B). In *C. neoformans* cells, luciferase activity from the *CMT1* promoter is induced 17-fold in response to increasing Cu, while activity from the *CTR4* promoter is induced 14-fold in response to BCS treatment; no activity was detected from cells lacking a luciferase reporter (Figure 1C). Intranasal infection of mice was carried out with independent isolates of *C. neoformans* carrying an integrated copy of the *CTR4*-Luciferase or *CMT1*-Luciferase reporter followed by live animal imaging and luciferase activity quantitation (Figures 1D and 1E). After 2 days, weak activity was detected in animals infected with cells harboring the *CMT1* or *CTR4* reporters, but not with control cells. While luciferase activity for the *CTR4*-Luciferase infection remained low and unchanged throughout the subsequent 14 day infection period, there was a time-dependent increase in *CMT1*-driven luciferase activity in lung tissue. To ascertain whether the difference in luciferase activity between the two reporter strains is due to impaired lung colonization by cells harboring the *CTR4*-Luciferase reporter, we performed fungal burden assays and detected no difference in lung fungal cell burden between the two reporter strains (Figure 1F). These results suggest that the Cmt1 gene is induced when *C. neoformans* is acquired by the respiratory route, the natural route of infection in humans.

C. neoformans MTs Are Critical Factors for Lung Colonization and Virulence

Expression from the *C. neoformans CMT1* promoter is activated in pulmonary infection, implying that fungal cells sense elevated Cu in the lung, and Cuf1 directly activates transcription of the *CMT1* and *CMT2* genes, whose encoded proteins are required for Cu detoxification in *C. neoformans* (Figure 1). Consequently, the potential role of *CMT1* and *CMT2* in *C. neoformans* virulence was investigated by infecting mice with wild-type (WT) or isogenic *cmt1Δ*, *cmt2Δ*, or *cmt1Δ cmt2Δ* mutants (Figure 2A). While *CMT1* and *CMT2* are functionally redundant for Cu detoxification (Ding et al., 2011), a *cmt1Δ cmt2Δ* mutant is over 30-fold more Cu-sensitive than WT cells in vitro (half maximal inhibitory concentration (IC_{50}) for WT of 2.3 mM versus 73 μM for *cmt1Δ cmt2Δ*). Deletion of either *CMT1* or *CMT2* did not alter mouse survival compared to the parental strain. However, the *cmt1Δ cmt2Δ* strain was strongly attenuated in virulence (Figure 2A). Two independently generated *cmt1Δ cmt2Δ* strains were evaluated for lung tissue burden 14 days postinfection, with both *cmt1Δ cmt2Δ* strains showing a dramatic decrease in lung tissue fungal burden in comparison to the WT strain (Figure 2B). This observation was validated by staining tissue sections for

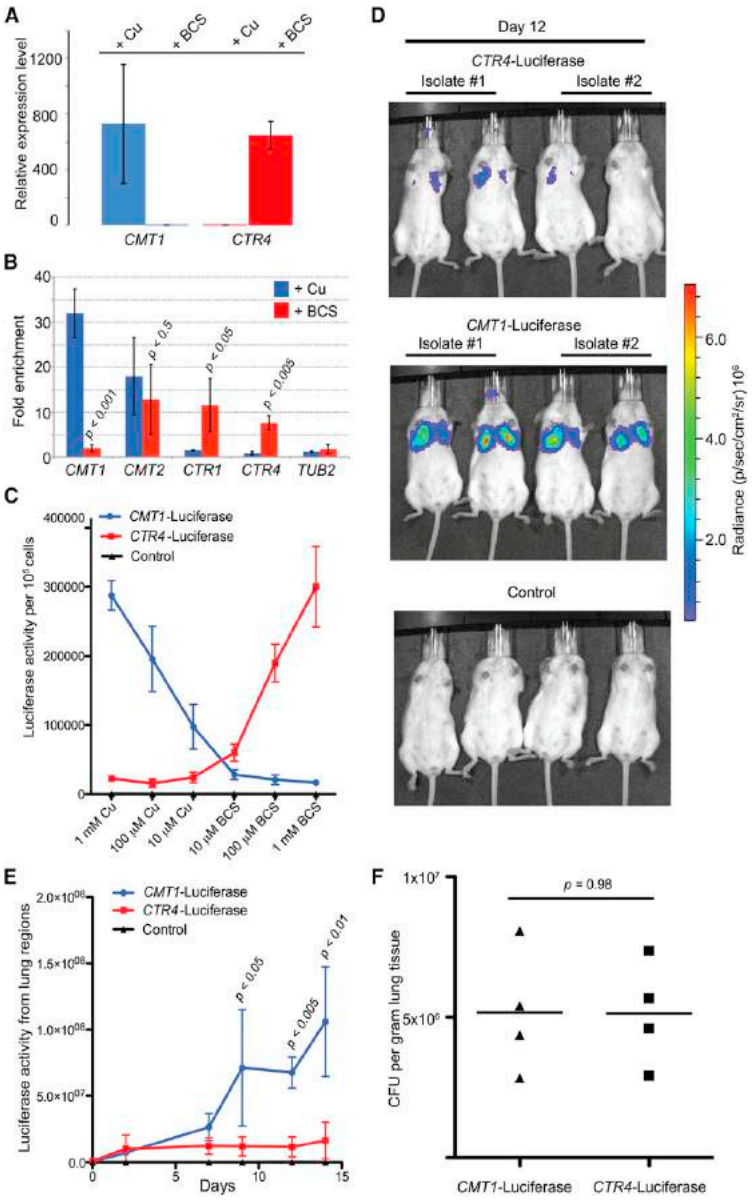

Figure 1. Cu-Sensing Reporter Systems in *C. neoformans*

(A) Expression of *CMT1* and *CTR4* was quantitated using qRT-PCR. Cell cultures were subcultured in SC medium supplemented with 1 mM Cu or BCS and incubated at 37°C for 3 hr. Expression levels were normalized to *ACT1*. Error bars indicate SD.

(B) ChIP was performed in *cuf1Δ/CUF1-2xFLAG* strains after growth in the presence of 1 mM Cu or BCS. qPCR was performed to measure enrichment of promoter sequences from *CMT1*, *CMT2*, *CTR1*, *CTR4*, and *TUB2* (negative control). Statistical analysis was performed using Student's t test. Error bars indicate SD.

(C) Luciferase activities from fungal cells harboring reporter genes for *CMT1*-Luciferase, *CTR4*-Luciferase, or WT (negative control) were quantified. Cells were grown in SC medium supplemented with Cu or BCS at 37°C for 9 hr. Luciferase activities were measured using the Luciferase Reporter Assay (QIAGEN). Error bars indicate SD.

(D) Luciferase activities from four mice each infected with *CMT1*-Luciferase, *CTR4*-Luciferase, or WT were measured using live animal imaging. Two independent isolates carrying *CMT1*-Luciferase or *CTR4*-Luciferase, or control WT cells, were used for intranasal mouse infections and luciferase activity scans performed at days 0, 2, 7, 9, 12, and 14. Day 12 postinfection is shown.

(E) Luciferase activity from the lungs of each mouse (in D) was measured and analyzed using Living Image 4.2 (Caliper, PerkinElmer). Statistical analysis was performed using the Student's t test. Error bars indicate SD.

(F) Fungal cell burden assessed by colony forming units (cfus) from mouse lung homogenates derived from animals in Figure 1D. See also Figure S1 and Table S1.

C. neoformans with the capsule-specific stain mucicarmine, which showed a reduction in *cmt1Δ cmt2Δ* cells as compared to WT cells, with no defect in melanin production, capsule formation, or phagocytosis observed between WT and *cmt1Δ cmt2Δ* cells (Figure S2). Furthermore, a corresponding decrease in host lung tissue damage was evident as determined by hematoxylin and eosin (H&E) staining of lung tissue sections (Figure 2C). Taken together, these results correlate with the strong expression of *CMT1* in lung observed in live animal imaging studies and demonstrate that *C. neoformans* Cmts are required for full fungal virulence when acquired via the respiratory route, the natural route of infection.

C. neoformans MTs Are Atypical Metallothioneins Specifically Activated by Cu

Metallothioneins (MTs) are expressed in organisms from prokaryotes to humans, which bind metals through Cys-thiolate bonds (Butt et al., 1984; Kägi and Hunziker, 1989; Szczypka and Thiele, 1989; Winge and Nielson, 1984; Winge et al., 1985). We previously reported that Cmts from *C. neoformans* possess Cu binding motifs typical of MTs (CxC), yet they are atypical MTs compared with those from other species (Ding et al., 2011). Both Cmt1 and Cmt2 are much larger proteins: Cmt1 and Cmt2 are 122 and 183 amino acids, respectively, compared to human MT1A with 61 amino acids. Multiple sequence alignments demonstrated that metallothioneins from *Cryptococcus* share homology with the MTs from *S. cerevisiae* and humans (Figure S3). Phylogenetic analysis suggests that Cmt1 and Cmt2 share the same evolutionary origin but are distantly related to the Crs5 and Cup1 MTs from *Saccharomyces cerevisiae* and human MT1A and MT2A (Figure 3A). Comparison

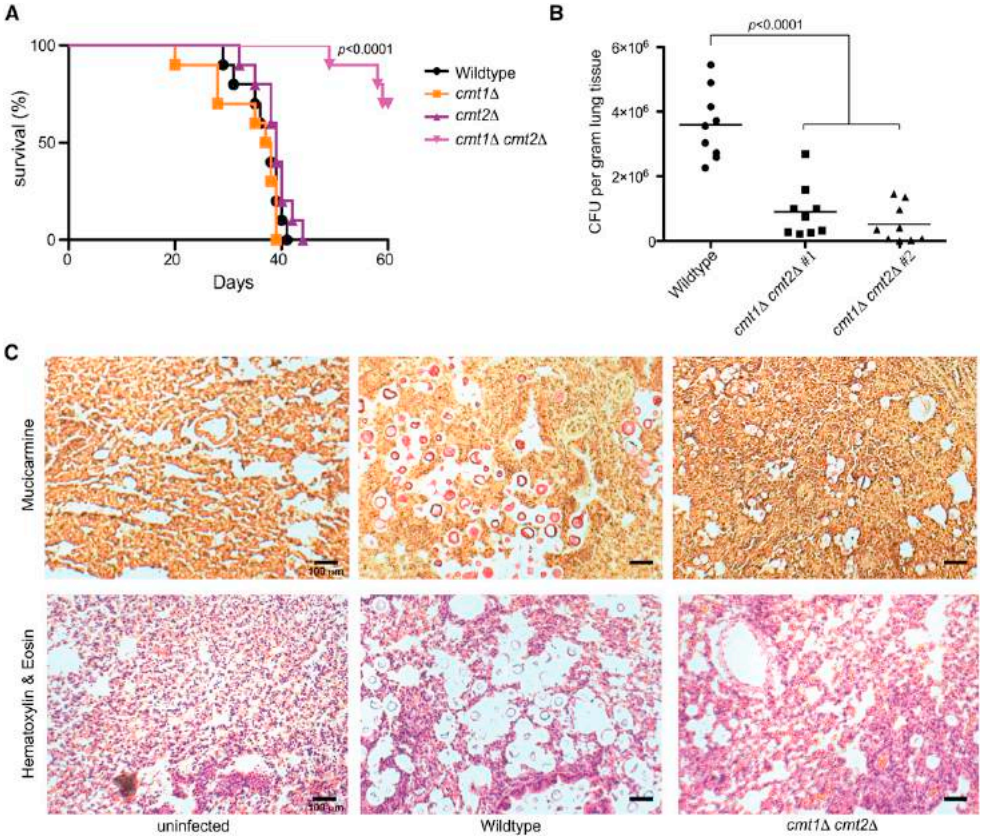

Figure 2. *C. neoformans* Metallothioneins Are Virulence Factors

(A) Ten A/J female mice were infected intranasally with WT, *cmt1Δ*, *cmt2Δ*, or *cmt1Δ cmt2Δ* cells, and animals were monitored for viability over 60 days. Shown is a Kaplan-Meier survival plot.

(B) Mice were infected with WT or two independent *cmt1Δ cmt2Δ* mutants for 14 days, lung tissues were isolated and homogenized, and cfus were quantitated and normalized with respect to tissue weight. Statistical analysis was performed using ANOVA.

(C) Lung tissue from uninfected, WT, or *cmt1Δ cmt2Δ* infected mice were isolated, fixed, and stained with mucicarmine or H&E. See also Figure S2 and Table S1.

of protein sequences between *C. neoformans* MT1 and MT2 reveals that both proteins are divided into multiple Cys-rich sequence segments by spacer sequences termed B1–B4 (Figure 3B), with Cmt1 divided into three segments by three spacer regions and Cmt2 harboring three Cys segments separated by four spacer regions. The spacer regions between Cmt1 and Cmt2 share a high level of similarity for B1 and are identical for B2 and B3. Interestingly, the Cys-rich motif resembles that found in MTs from other fungi, such as *Agaricus* and *Neurospora*, and may imply evolutionary divergence from a common ancestor among these species (Figure 3C).

Mammalian MT genes are transcriptionally induced by metals that include Zn, Cd, Cu, and Ag and protect cells against these and other metals (Durnam and Palmiter, 1984, 1987; Kägi and Hunziker, 1989). To decipher the specificity of metal detoxification with respect to *Cryptococcus* MTs, we measured cell growth in liquid medium supplemented with a range of metal concentrations including Cu, Zn, and Cd. The effect of high and low Fe on cell growth was also tested because Fe acquisition via the Fe permease is directly dependent on a multi-Cu oxidase in *C. neoformans* (Jung and Kronstad, 2008; Kronstad et al., 2012). A potential role for the *C. neoformans* MTs for growth in the presence of reactive oxygen species was also tested using the superoxide generator menadione. We observed a striking growth defect of *cmt1Δ cmt2Δ* cells in the presence of Cu with no significant difference in the presence of Cd, Zn, Fe, the Fe chelator bathophenanthroline disulfonate (BPS), or the superoxide generator menadione (Figure 4A). Agar spotting assays were also performed to confirm the liquid growth experiments, and similar cell growth phenotypes were observed (Figure 4B). Consequently, we determined whether RNA and protein expression of *C. neoformans* MTs are elevated in response to these conditions by qRT-PCR and immunoblot assays. As shown in Figures 4C and 4D, expression of both *CMT1* and *CMT2* mRNA and FLAG-epitope-tagged protein is strongly elevated in response to Cu exposure in a dose-dependent manner, but not in response to any concentration of Zn, Fe, Cd, BPS, or menadione tested. Taken together, these results demonstrate

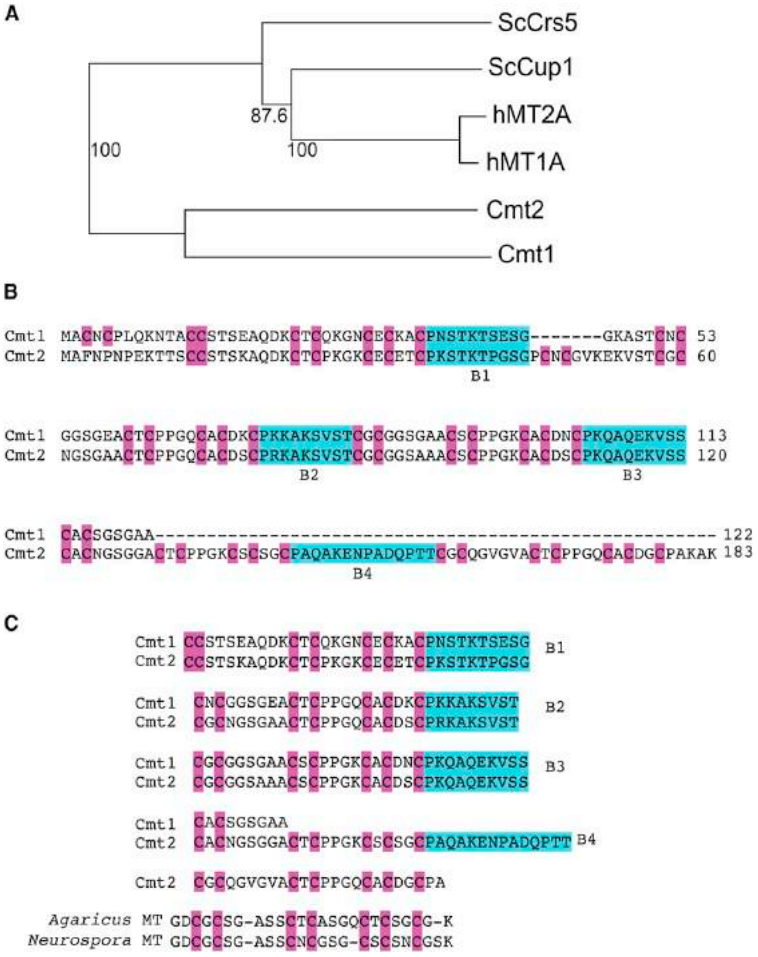

Figure 3. Atypical *C. neoformans* Metallothioneins

(A) A phylogenetic MT tree was generated as described previously (Ding et al., 2011) with percentage of confidence (bootstrap) shown in numbers. Both *C. neoformans* MTs are distantly related to those from *S. cerevisiae* (Sc) and human (h).

(B) Protein sequences from *CMT1* and *CMT2* were aligned. The homologous Cys residues are shaded in purple, and spacer boxes are shaded in green. Both Cmts contain spacer regions (B1–B3 for Cmt1 and B1–B4 for Cmt2). The spacer shares high protein sequence similarity between Cmt1 and Cmt2 and divides each Cmt into multiple Cys-rich segments, resulting in a peculiar architecture of three Cys-rich segments for Cmt1 and five for Cmt2.

(C) Cmt1 and Cmt2 share a common motif (Cys-X-Cys-X_6-Cys-X-Cys-X_4-Cys-X-Cys-X_2-Cys) in their Cys-rich segments. This motif is separated by three spacer regions in Cmt1 and four in Cmt2 and is similar to that found in MTs in other fungi such as *Agaricus* and *Neurospora*. See also Figure S3.

that, of all conditions tested, the *C. neoformans* MT genes are Cu responsive and function specifically in Cu detoxification.

To evaluate the importance of Cu binding by Cmt1 and Cmt2 to Cu detoxification, we tested the importance of the Cmt1 Cys residues in protecting cells from Cu toxicity. A DNA sequence encoding a *CMT1* allele in which all Cys residues were converted to Ala was synthesized, cloned under control of the *CMT1* promoter, and introduced into *cmt1Δ cmt2Δ* cells to generate the Cmt1ala strain. Using qRT-PCR, the expression of *CMT1ala* was confirmed to be robust and Cu responsive, as the fold induction of expression between Cu and bathocuproine disulfonate (BCS) treatment is comparable to that observed for WT *CMT1* (Figure S4A). Cell growth assays demonstrated that the Cmt1 Cu-coordinating Cys residues are essential for Cu resistance (Figure 5A).

To quantify the Cu binding capacity of Cmt1 and Cmt2, the Cmts were synthesized in and purified from *E. coli*, after which spectroscopic analysis of Cmt1, Cmt2, and Cmt1ala was performed. These experiments showed a high, preferential Cu^+ binding capacity yielding major homonuclear Cu_{16}-Cmt1 and Cu_{24}-Cmt2 complexes (Figures 5B and 5C). In vitro Zn/Cu replacement experiments using recombinantly synthesized Zn-Cmt1 and Zn-Cmt2 complexes fully corroborated these stoichiometries (Figures S4B and S4C) and pointed to the progressive and cooperative formation of several Cu_5 ion clusters (three for Cmt1 and five for Cmt2) in accordance with the peculiar protein architecture in the same number of Cys-rich regions (Figure 3). Furthermore, the circular-dichroism (CD) spectra of the complexes and the products of recombinant synthesis were nearly identical (Figures S4D and S4E), indicating equivalent folding. Consistent with the inability of the Cmt1ala mutant to support Cu resistance in *cmt1Δ cmt2Δ* cells (Figure 5A), the Cmt1ala protein was defective in Cu^+ binding and isolated exclusively in the apo form (Figure 5D). These results establish Cu^+ binding to the *C. neoformans* MTs with high stoichiometry that is dependent on Cys-thiolate bonds. To test whether the Cys residues of *CMT1* are required for virulence, mice were infected with WT *C. neoformans* cells, isogenic *cmt1Δ cmt2Δ* cells, or the same mutant strain expressing *CMT1*, *CMT2*, or *CMT1ala*, and fungal burdens were evaluated in host lung tissue. Consistent with the Cu binding results, *C. neoformans* expressing a Cmt1 protein that is incompetent for Cu binding (Cmt1ala) exhibited poor survival as evidenced by decreased fungal burden in lung tissue from infected mice (Figure 5E). These results demonstrate the essential role of the Cmt1 Cys residues, required for Cu^+ coordination, for virulence in mouse lung infection.

Although MTs have been previously localized to the cytosol of fungal and mammalian cells (Banerjee et al., 1982; Hamer, 1986; Winge and Nielson, 1984), the subcellular distribution of Cmt1 and Cmt2 was determined in cells cultured in vitro. The

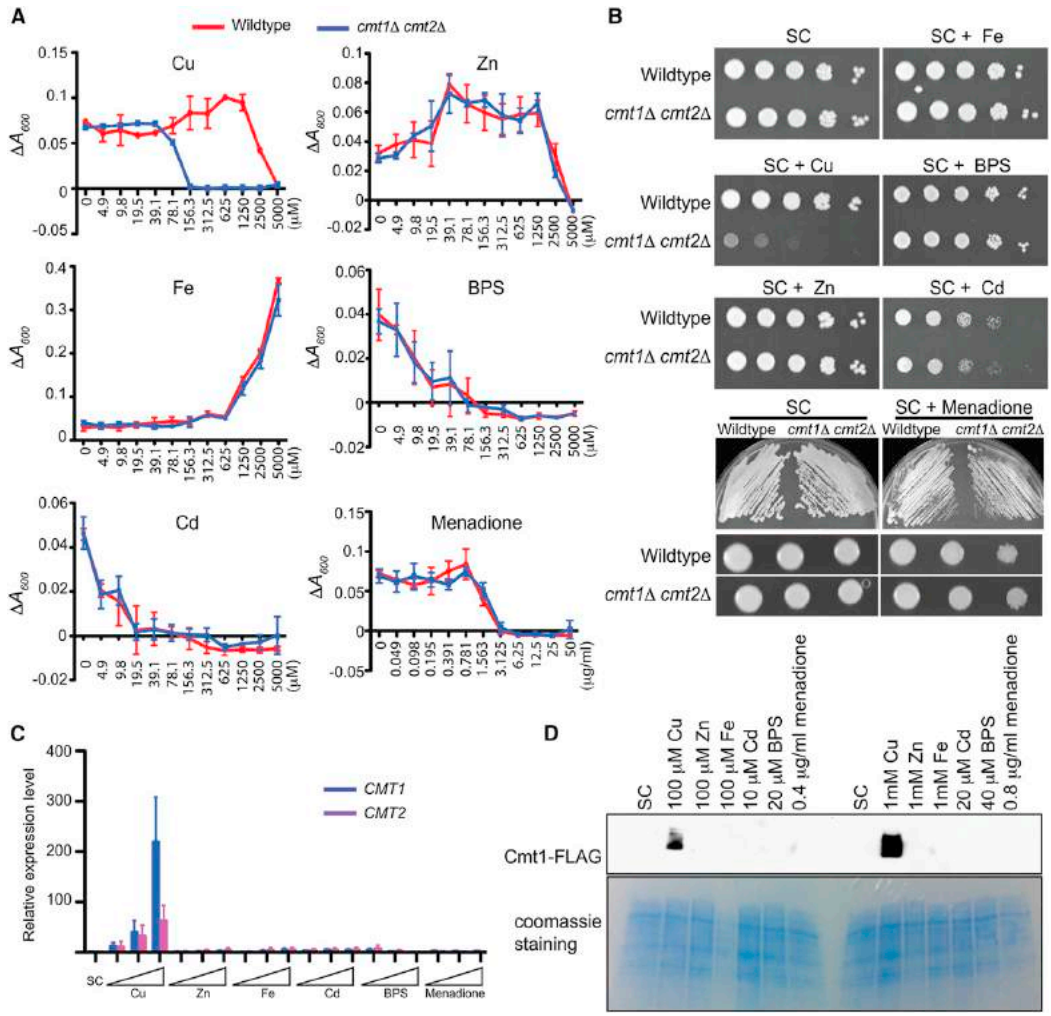

Figure 4. *C. neoformans* MTs Are Cu-Responsive Cu Detoxification Proteins

(A) *C. neoformans* cell growth assays were performed in SC medium in 96 well plates. Cell cultures of WT and *cmt1Δ cmt2Δ* were diluted to an A_{600} of 0.002 supplemented with metals. A_{600} was measured after overnight growth. ΔA_{600} was calculated by subtracting from blank (medium without cells). Graphs show average of three biological replicates. Error bars indicate SD.

(B) *C. neoformans* metal sensitivity assays on agar medium. Cell cultures of WT and *cmt1Δ cmt2Δ* cells were diluted in water to an A_{600} of 1.0. Then, 10-fold serial dilutions cells were spotted onto SC agar or agar supplemented with 400 μM Cu, Zn, Fe, 100 μM Cd, 40 μM BPS, or 10 μg/ml menadione. Plates were incubated for 2 days (6 days for menadione spotting assay) and photographed.

(C) Expression of *CMT1* and *CMT2* was quantitated by qRT-PCR. Cell cultures were diluted to an A_{600} of 0.2 in SC medium at 37°C for 1 hr supplemented with the indicated concentrations (selected according to the results from Figure 4A; 10, 100, and 1000 μM for Cu, Zn, and Fe; 5, 10, and 20 μM for Cd; 10, 20, and 40 μM for BPS; 0.2, 0.4, and 0.8 μg/ml for menadione). Error bars indicate SD.

(D) Protein expression of Cmt1-FLAG was confirmed by immunoblotting. Cells were grown as described in Figure 4C. Protein extracts were treated with TCEP and resolved by SDS-PAGE, and anti-FLAG mouse antibody was used for immunoblotting. Coomassie staining was used as a loading control. See also Table S1.

expression of functional FLAG-epitope-tagged Cmt1 and Cmt2 (Figure 6A) was confirmed by immunoblotting experiments in which an ~20 kDa polypeptide was detected for Cmt1-FLAG and ~37 kDa species for Cmt2-FLAG (Figure 6B). Subcellular localization experiments by indirect immunofluorescence microscopy of Cu-treated *C. neoformans* cell cultures demonstrated that Cmt1-FLAG and Cmt2-FLAG concentrate at the cell periphery (Figure 6C). This observation was recapitulated by immunohistochemistry analysis of lung tissue infected with *C. neoformans* cells expressing either Cmt1-FLAG or Cmt2-FLAG (Figure 6D). Taken together, these experiments demonstrate that a Cu-binding Cmt is critical for both *C. neoformans* Cu resistance in vitro and virulence in mouse infections. Furthermore, distinct from the pancellular localization of Cmts observed

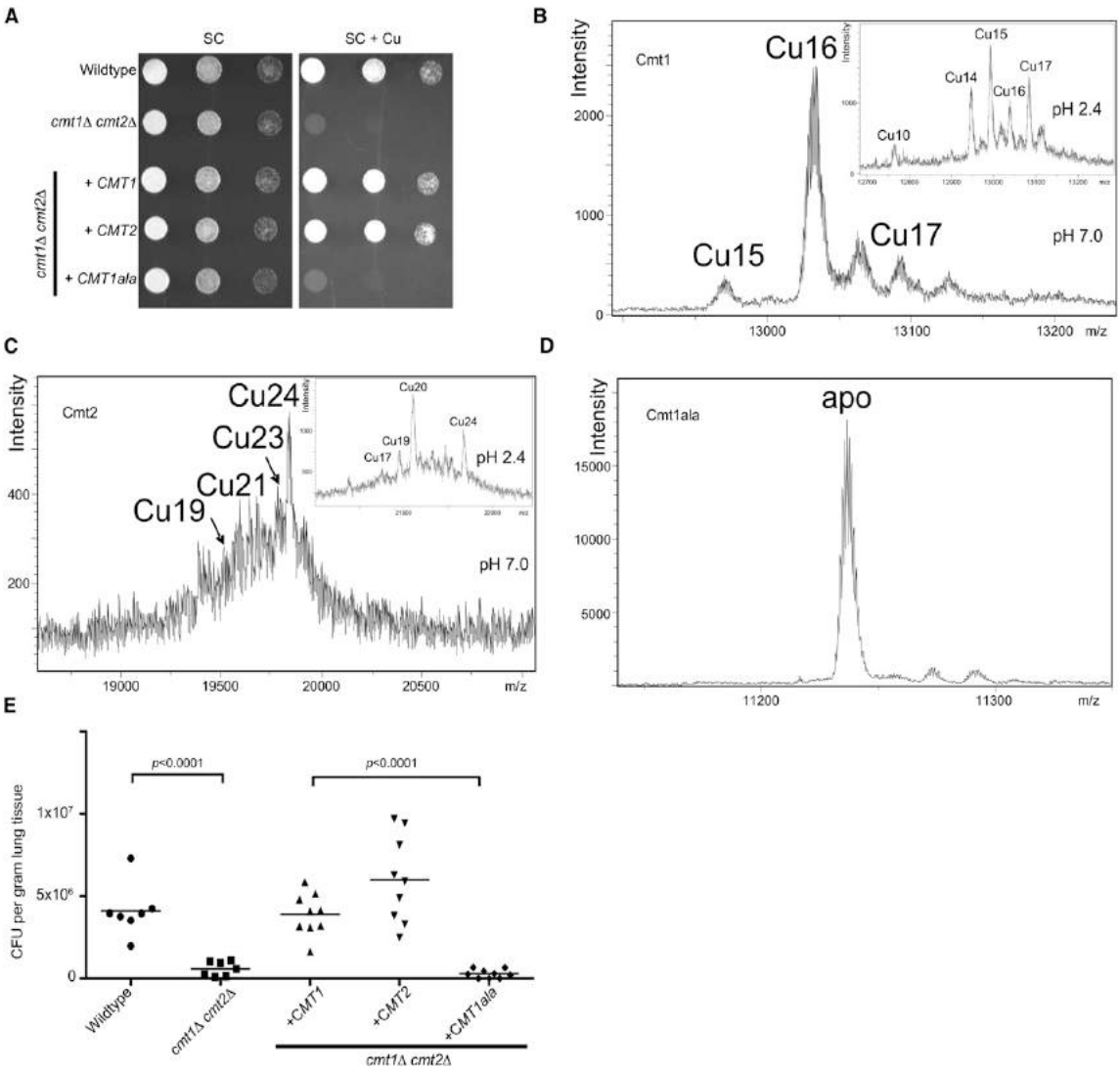

Figure 5. *C. neoformans* MT Cu Binding Capacity Is Critical for Virulence

(A) Cu-resistance growth assays in SC medium supplemented with 1 mM Cu with the *cmt1Δ cmt2Δ* mutant expressing *CMT1*, *CMT2,* or the *CMT1ala* mutant. Growth assays were performed as described in Figure 4B.

(B–D) ESI-MS spectra at pH 7.0 and pH 2.4 (insets) of purified Cmt1 (B), Cmt2 (C), and the Cmt1ala mutant (D).

(E) Lung tissue fungal burden (cfu) from *cmt1Δ cmt2Δ* cells transformed with plasmids expressing *CMT1*, *CMT2*, or *CMT1ala*. Experiments and statistical analysis were performed as described in Figure 2B. See also Figure S4 and Table S1.

in other eukaryotes (Hamer, 1986), the *C. neoformans* atypical MT proteins concentrate at the cellular periphery.

C. neoformans Infection Alters Host Cu Mobilization and Cu Transporter Expression

Bronchial alveolar macrophages are phagocytic cells that provide the first line of defense against *C. neoformans* infection in the lung (Brummer, 1998–1999; Kronstad et al., 2011). Previous in vitro studies demonstrated that macrophage-like cell lines infected with the *Mycobacterium* species accumulate Cu in the phagosomal compartment, and activation of macrophage cell lines with lipopolysaccharide (LPS) induces expression of the ATP7A Cu^+-transporting P-type ATPase and the Ctr1 high-affinity Cu^+ importer (Wagner et al., 2005; White et al., 2009). Macrophage cell lines with reduced expression of ATP7A are deficient in killing *E. coli*, consistent with a potential role for ATP7A in phagosomal microbiocidal Cu^+ loading (White et al., 2009). Because activated macrophages have elevated ATP7A and Ctr1 levels, and we show here that *C. neoformans* senses high Cu and activates the *CMT1* promoter during lung

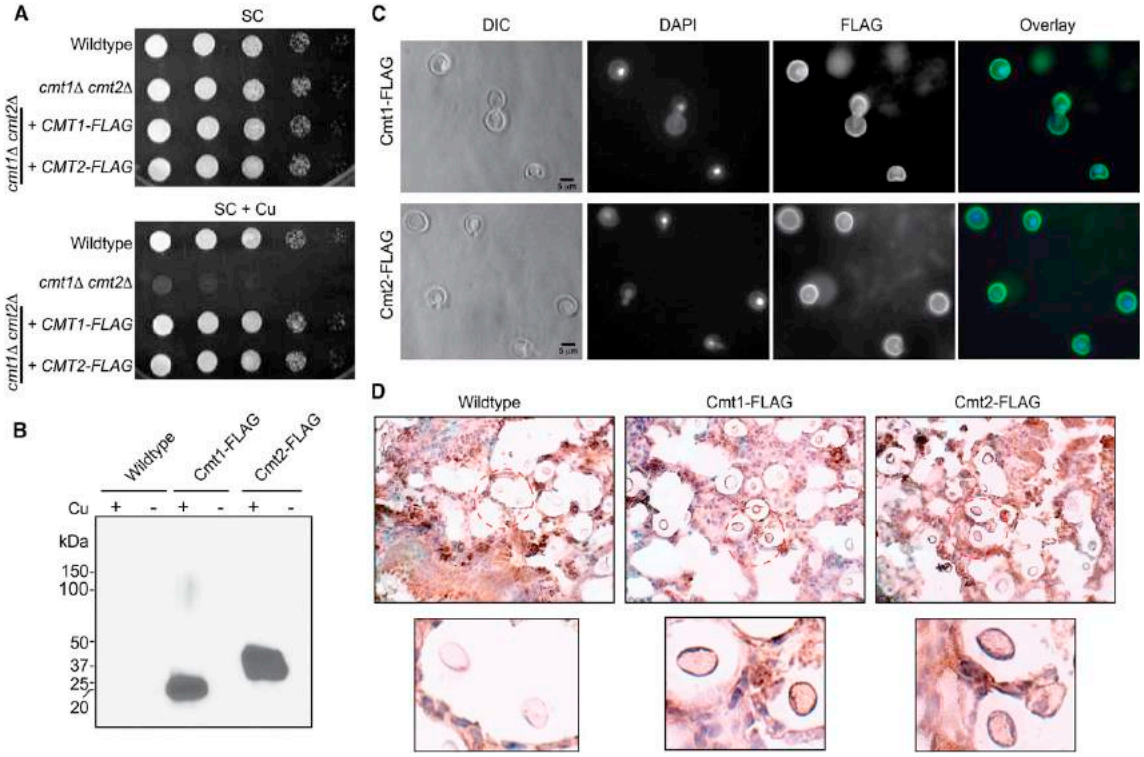

Figure 6. *C. neoformans* MTs Concentrate at the Cell Periphery

(A) *cmt1Δ cmt2Δ CMT1-FLAG* and *cmt1Δ cmt2Δ CMT2-FLAG* cells were generated and Cu-sensitive phenotype assays performed by spotting 10-fold serial dilutions on SC agar or SC agar supplemented with 1 mM Cu.

(B) Immunoblotting confirmed expression of Cmt1-FLAG and Cmt2-FLAG. *C. neoformans* cells (WT, *cmt1Δ cmt2Δ CMT1-FLAG*, and *cmt1Δ cmt2Δ CMT2-FLAG*) were incubated in the presence of 200 μM Cu (+) or BCS (-) in SC medium for 3 hr, and immunoblotting was performed as described in Figure 4D. Ponceau S staining confirmed equal protein loading.

(C) Cmt1-FLAG and Cmt2-FLAG proteins localized by indirect immunofluorescence microscopy with anti-FLAG antibody. DNA stains DAPI for localizing nuclei.

(D) Lung tissue from mice infected (14 days postinfection) with WT, *cmt1Δ cmt2Δ CMT1-FLAG*, or *cmt1Δ cmt2Δ CMT2-FLAG* was analyzed by H&E staining and immunohistochemistry using anti-FLAG antibody. See also Table S1.

infection, we ascertained whether there are changes in host circulating Cu levels and in expression of the host Cu homeostatic machinery in response to *C. neoformans* infection. Serum Cu levels were significantly increased, suggesting a mobilization of host Cu in response to *C. neoformans* infection (Figure 7A). Moreover, cells from mouse BAL 14 days after infection, of which the dominant cell type has been shown to be alveolar macrophages (Giles et al., 2007), displayed a strong decrease in the steady-state levels of ATP7A (Figure 7B) that was observed to a lesser extent 2 days postinfection (Figure 7C). In contrast, infected mice exhibited no apparent change in lung tissue ATP7A levels compared to uninfected controls (Figure 7D). After 14 days of infection, the levels of the Ctr1 high-affinity Cu^+ importer and the COX IV subunit of mitochondrial cytochrome oxidase, whose levels correlate with intracellular Cu availability, were strongly elevated (Figure 7B). Taken together, these observations suggest that in response to *C. neoformans* infection via the respiratory route, hosts mobilize Cu into the circulation, and lung alveolar cells may reorient Cu away from vesicular compartments and toward the mitochondria or other pools.

DISCUSSION

Prokaryotic Cu detoxification mechanisms involving Cu-responsive transcription factors and Cu efflux pumps are emerging as critical virulence factors for organisms such as *M. tuberculosis*, *E. coli*, *S. enterica*, and others (Achard et al., 2010; Osman and Cavet, 2011; Samanovic et al., 2012; Schwan et al., 2005; Wagner et al., 2005; White et al., 2009; Wolschendorf et al., 2011). In line with these observations are studies that demonstrate the compartmentalization of Cu within the macrophage phagosome in response to infection (Wagner et al., 2005; White et al., 2009) in a manner that correlates with elevated expression of the mammalian Ctr1 plasma membrane Cu^+ importer and the ATP7A Cu^+ transporting ATPase (White et al., 2009). As depletion of ATP7A renders macrophages more permissive for *E. coli* survival (White et al., 2009) and mice receiving dietary

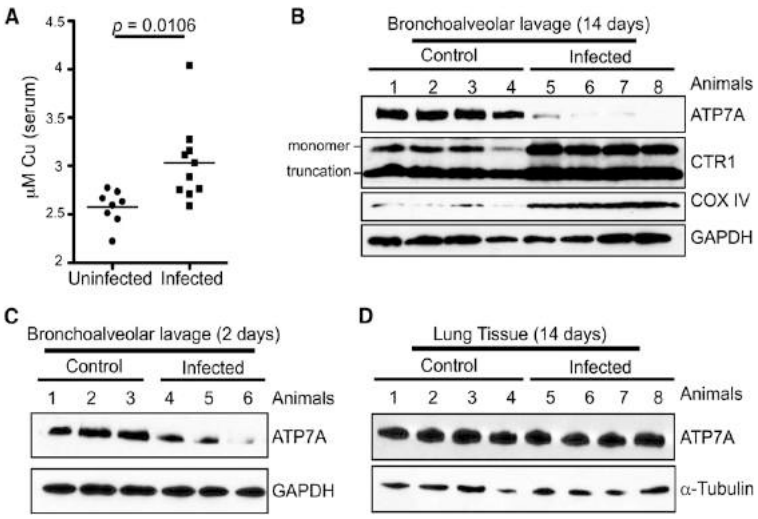

Figure 7. *C. neoformans* Infection Alters Host Cu Transport Machinery

(A) Mice were infected with WT *C. neoformans* cells, and serum was isolated at day 14 post-infection. Cu was measured using inductively coupled plasma mass spectrometry (ICP-MS) and shown for uninfected and *C. neoformans*-infected mice.

(B) BAL cells were isolated from uninfected mice and mice infected with WT cells 14 days post-infection. Protein was extracted from the BAL, and ATP7A, Ctr1, COX IV, and GAPDH levels were analyzed by SDS-PAGE and immunoblotting.

(C) BAL protein extract was analyzed 2 days after infection by immunoblotting for ATP7A and GAPDH.

(D) Lung tissue from mice 14 days after infection was analyzed for ATP7A and tubulin levels by immunoblotting.

Cu supplements more effectively clear *M. tuberculosis* (Wolschendorf et al., 2011), these and other experimental results point to phagosomal Cu compartmentalization, that may involve ATP7A, as a potent antimicrobial weapon against infectious disease (Hodgkinson and Petris, 2012; Rowland and Niederweis, 2012; Samanovic et al., 2012; Wolschendorf et al., 2011).

Pathogenic fungi such as *C. neoformans* and *C. albicans* are quite resistant to Cu levels in vitro (Ding et al., 2011; Weissman et al., 2000), with *C. neoformans* H99 resistant to ~2 mM Cu in liquid medium and clinical isolates of *C. albicans* able to tolerate ~20 mM Cu (Weissman et al., 2000). An important question is why *C. neoformans*, or other pathogenic fungi, are tolerant to such high Cu concentrations; and is this relevant to the concentrations of Cu they encounter during infection? In contrast to Cu detoxification in prokaryotes, Cu acquisition has been implicated in virulence by *C. neoformans* in mouse infection models (Waterman et al., 2007). Cuf1 was previously implicated in virulence by mouse tail vein administration studies, and its known activation of *CTR4* implied a requirement for Cu for virulence (Waterman et al., 2007). More recent studies using *URA5* to disrupt *CTR4* resulted in *C. neoformans* cells with a pleiotropic nutritional deficiency that was not corrected by external Cu and produced a reduction in virulence in mice (Waterman et al., 2012). However, given that such a growth phenotype has not been observed in Cu transporter knockouts of Ctr1 or Ctr4 in *C. neoformans* by us (Ding et al., 2011), or in response to inactivation of other Cu importer genes in *S. cerevisiae*, *S. pombe*, or *C. albicans* in other studies (Beaudoin et al., 2006; Dancis et al., 1994; Marvin et al., 2003; Pena et al., 2000; Zhou and Thiele, 2001), it is not clear why this pleiotropic phenotype was observed. One possibility is that use of the *URA5* marker for gene disruption in *C. neoformans* and the *URA3* marker in *C. albicans* and *C. parapsilosis* has been shown to cause defects in adhesion, colony morphology, and virulence that are unrelated to the target genes of interest (Bain et al., 2001; Ding and Butler, 2007; Kirsch and Whitney, 1991; Kwon-Chung et al., 1992; Lay et al., 1998; Staab and Sundstrom, 2003). While it is possible that the Cu acquisition machinery may contribute to the colonization of lung and brain due to a requirement to activate Cu/Zn SOD (Bermingham-McDonogh et al., 1988; Furukawa et al., 2004), increase activity of Cu-dependent oxidase involved in Fe uptake (Dancis et al., 1994; Jung and Kronstad, 2008), and support the synthesis of melanin from laccase (Walton et al., 2005; Williamson, 1994) using host catecholamine as substrate, the reasons behind these discrepant studies merit further investigation.

A recent study using a *CTR4*-Cherry reporter suggested that *CTR4* is strongly expressed in macrophages in vitro and in lung and brain tissue (Waterman et al., 2012). However, *CTR4*-driven expression of mCherry in this study was compared to that of *C. neoformans* cells harboring an empty vector without the mCherry gene. In this work, we used *C. neoformans* cells harboring high- and low- Cu-responsive reporter plasmids, as well as negative control cells, to quantitatively ascertain, over the course of a 14 day intranasal infection, whether *C. neoformans* is exposed to a high or low Cu environment. While both *CTR4*-Luciferase and *CMT1*-Luciferase are expressed in lung during the initial phase of the infection, the *CMT1*-Luciferase reporter was activated in a time-dependent manner while the *CTR4*-Luciferase remained low and constant. The strong induction of the *CMT1*-Luciferase reporter in lung implies that *C. neoformans* senses elevated Cu levels in the lung. Consistent with this observation, we demonstrated that the *CMT1*, *CMT2*, and a Cu-binding competent Cmt1 protein are required for virulence at the natural site of acquisition: the lungs. Indeed, in contrast to mammalian MTs, the *C. neoformans* MTs and other fungal MTs are transcriptionally activated in response to Cu, rather than to any other metal tested, suggesting a role that is specific under conditions of high Cu. Moreover, we show that the *C. neoformans* MTs are longer and have an exceptionally high Cu binding capacity compared to other MT proteins, perhaps due to evolutionary pressure to evolve by tandem amplification of a basic Cu binding unit similar to that found in well-characterized fungal

metallothioneins. The concentration of Cmt1 and Cmt2 to the cell periphery via currently uncharacterized targeting mechanisms could provide a means to efficiently capture Cu^+ immediately after it enters cells, prior to engaging in redox chemistry, interfering with Fe-S clusters, or targeting other mechanisms for toxicity (Chillappagari et al., 2010; Liochev, 1996; Macomber and Imlay, 2009; Macomber et al., 2007).

The results presented here showing a requirement for *CMT1* and *CMT2* for virulence are consistent with macrophages in the lung and other tissues using Cu as an antimicrobial condition within the lumen of the phagosome. As the expression of ATP7A and Ctr1 was shown to be elevated in activated macrophage cell lines, and a fraction of ATP7A was found in the phagosomal membrane, this Cu^+ pump is implicated as a potential driver of phagosomal compartmentalization of antimicrobial Cu (White et al., 2009). Complementary to the elevation of ATP7A in INF-γ-activated macrophages in vitro, we found that *C. neoformans* infection caused a time-dependent downregulation of ATP7A in lung lavage cells, an environment reported to be composed predominantly of phagocytic cells (Giles et al., 2007). In addition to the Cuf1-dependent Cu detoxification genes, this could provide a survival advantage to *C. neoformans* within the phagosomal compartment that ultimately allows this organism to escape into the cytoplasm by vomocytosis (Nicola et al., 2011). While the mechanism for reducing ATP7A and maintaining Ctr1 levels, is currently unknown, *C. neoformans* infection is known to cause a reduction in host proinflammatory cytokines and an increase in NF-κB activity via glucuronoxylomannan in the outer capsule (Ben-Abdallah et al., 2012; Piccioni et al., 2013), which may reduce ATP7A expression. We speculate that as the Ctr1 promoter, but not that of ATP7A, contains a putative NF-κB binding site (http://genome.ucsc.edu/ENCODE) (Dunham et al., 2012), this could maintain Ctr1 expression while ATP7A levels are tuned down. It is likely that the regulation of Ctr1 and ATP7A expression is due to a complex interplay between *C. neoformans* and the host immune system, which should be explored in more detail. The increased levels of circulating Cu and the high levels of Ctr1 and COX IV in the host could suggest that *C. neoformans* infection results in the downregulation of the host Cu compartmentalization machinery, potentially reorienting available Cu to other intracellular targets such as the mitochondria. The use of *C. neoformans* mutants, in concert with mouse models with altered Cu homeostasis, could help elucidate the detailed mechanisms by which Cu functions at the host-pathogen axis.

EXPERIMENTAL PROCEDURES

Strains and Media

Cryptococcus neoformans H99 strains (Table S1) were routinely grown as previously described (Ding et al., 2011). YPD agar supplemented with 100 mg/L G418 or 200 U/ml hygromycin B was used for colony selection. Mutants were generated as described in Supplemental Experimental Procedures.

Chromatin Immunoprecipitation

Cells expressing Cuf1-FLAG were treated with 1 mM Cu or BCS for 3 hr. Cell fixation and ChIP were performed as described previously (Pondugula et al., 2009), except buffer (50 mM HEPES, 140 mM NaCl, 1% Triton X-100, 1 mM EDTA, protease inhibitors) was used to lyse cells, and M2 beads (Sigma-Aldrich) were used for immunoprecipitation. Promoter sequences from *CMT1*, *CMT2*, *CTR1*, *CTR4*, and *TUB2* were analyzed using qPCR. Primer sequences are described in the Supplemental Experimental Procedures.

Luciferase Assays and Live Animal Imaging

Strains transformed with luciferase reporter genes were diluted to an A_{600} of 0.2 in synthetic complete (SC) medium supplemented with Cu or BCS and incubated at 37°C for 9 hr. Cell cultures were washed and resuspended in PBS. Then, 10 μl of cell suspension was mixed with 100 μl with luciferase reporter reagent (Promega), and activity was measured using a VICTOR bio-illuminator (PerkinElmer). The samples were then measured at A_{600} for cell number.

A/J mice were infected with WT, *CTR4*-Luciferase, or *CMT1*-Luciferase strains intranasally. Mice were anesthetized using 2.5% of isoflurane. Luciferin was introduced intranasally into each animal (no signal was observed when luciferin was administered intraperitoneally). Animals were placed in a Caliper IVIS Spectrum (PerkinElmer) chamber at 37°C. The scan was performed exactly 5 min after introducing luciferin. Scanning was performed on days 0, 2, 7, 9, 12, and 14. Animals were sacrificed on day 14 for colony-forming unit (cfu) analysis. All images were analyzed using Living Image 4.2 (Caliper, PerkinElmer). The lung region from each animal was cropped, and total luciferase signal intensity in the cropped area was extracted using Living Image 4.2. Statistical analysis was performed using Student's t test.

Animal Infection, Fungal Burden Assay, and Histopathology

Animal infections were performed as described previously (Crabtree et al., 2012). Histology of uninfected or infected lung tissue was processed and mucicarmine or H&E staining was performed.

Spectroscopic Analyses and Electrospray Ionization Mass Spectrometry

Cmt proteins were expressed in the *E. coli BL21* strain and purified using GST fusion as described in the Supplemental Experimental Procedures. The S, Zn, and Cu content of the Zn- and Cu-Cmt preparations was analyzed by inductively coupled plasma atomic emission spectroscopy (ICP-AES) as described previously (Bongers et al., 1988; Capdevila et al., 2005).

Molecular weight determinations were performed by electrospray ionization time-of-flight mass spectrometry (ESI-TOF MS). The calibration was attained with 0.2 g NaI dissolved in 100 ml of a 1:1 H_2O:isopropanol mixture. Cmt proteins containing divalent metal ions were analyzed under the following conditions: 20 μl of protein solution was injected through a PEEK (polyether heteroketone) column at 40 μl/min; capillary counter-electrode voltage was 5 kV for Zn and 3.5 kV for Cu; desolvation temperature was 80°C–110°C; dry gas (N_2), 6 L/min; spectra collection range was 800–2,500 m/z. The carrier buffer was a 5:95 mixture of acetonitrile:ammonium acetate (15 mM [pH 7.0]) for Zn and a 10:90 mixture for Cu. Analyses of apo-Cmt and Cu-Cmt at low pH were performed using a 5:95 mixture of acetonitrile:formic acid at pH 2.4. Under all of the conditions assayed, the error associated with the mass measurements was always lower than 0.1%.

Antibodies

ATP7A antibody was a gift from Dr. Michael Petris (University of Missouri). COX IV and luciferase antibodies were purchased from Abcam. GAPDH antibody was purchased from Santa Cruz. FLAG antibody was purchased from Sigma-Aldrich. Immunofluorescence microscopy and immunohistochemistry were performed as previously described (Ding et al., 2011). All microscopy images were taken using a Zeiss Axio Imager widefield fluorescence microscope (ZEISS).

BAL Isolation from Animals

BAL isolation was performed as described previously (Okagaki et al., 2010), except the fluid was centrifuged and resuspended in ACK lysis buffer (NH_4Cl, $KHCO_3$, and EDTA) to lyse red blood cells and then washed three times with PBS.

Ethics Statement

All experiments involving animals were approved by the Institutional Animal Care & Use Program (protocol number A013-13-01) at Duke University.

Cell Host & Microbe
Fungal Defense against Host Copper

SUPPLEMENTAL INFORMATION

Supplemental Information includes four figures, three tables, and Supplemental Experimental Procedures and can be found with this article online at http://dx.doi.org/10.1016/j.chom.2013.02.002.

ACKNOWLEDGMENTS

We thank G. Sempowski and K. Riebe for animal imaging assistance, M.J. Petris for ATP7A antibody, and the Thiele lab for critical comments. C.D. and R.A.F. acknowledge the Duke Scholars in Infectious Disease Training Program. We acknowledge support from the NIH (GM48140-24 to D.J.T., 2P30 AI064518-06 to Y.L.C., and AI50438 to J.H.); Ministerio de Ciencia e Innovación grants BIO2009-12513-C02-01 (to S.A.) and BIO2009-12513-C02-02 (to M.C.); and Serveis Científico-Tècnics and the Servei d'Anàlisi Química and European Union support via FEDER. S.A. and M.C. acknowledge grant 2009SGR-1457 from E1Grup de Recerca de la Generalitat de Catalunya.

Received: November 11, 2012
Revised: January 4, 2013
Accepted: February 1, 2013
Published: March 13, 2013

REFERENCES

Achard, M.E., Tree, J.J., Holden, J.A., Simpfendorfer, K.R., Wijburg, O.L., Strugnell, R.A., Schembri, M.A., Sweet, M.J., Jennings, M.P., and McEwan, A.G. (2010). The multi-copper-ion oxidase CueO of Salmonella enterica serovar Typhimurium is required for systemic virulence. Infect. Immun. *78*, 2312–2319.

Bain, J.M., Stubberfield, C., and Gow, N.A. (2001). Ura-status-dependent adhesion of Candida albicans mutants. FEMS Microbiol. Lett. *204*, 323–328.

Banerjee, D., Onosaka, S., and Cherian, M.G. (1982). Immunohistochemical localization of metallothionein in cell nucleus and cytoplasm of rat liver and kidney. Toxicology *24*, 95–105.

Beaudoin, J., Laliberté, J., and Labbé, S. (2006). Functional dissection of Ctr4 and Ctr5 amino-terminal regions reveals motifs with redundant roles in copper transport. Microbiology *152*, 209–222.

Ben-Abdallah, M., Sturny-Leclère, A., Avé, P., Louise, A., Moyrand, F., Weih, F., Janbon, G., and Mémet, S. (2012). Fungal-induced cell cycle impairment, chromosome instability and apoptosis via differential activation of NF-κB. PLoS Pathog. *8*, e1002555.

Bermingham-McDonogh, O., Gralla, E.B., and Valentine, J.S. (1988). The copper, zinc-superoxide dismutase gene of Saccharomyces cerevisiae: cloning, sequencing, and biological activity. Proc. Natl. Acad. Sci. USA *85*, 4789–4793.

Bongers, J., Walton, C.D., Richardson, D.E., and Bell, J.U. (1988). Micromolar protein concentrations and metalloprotein stoichiometries obtained by inductively coupled plasma atomic emission spectrometric determination of sulfur. Anal. Chem. *60*, 2683–2686.

Brummer, E. (1998–1999). Human defenses against Cryptococcus neoformans: an update. Mycopathologia *143*, 121–125.

Butt, T.R., Sternberg, E.J., Gorman, J.A., Clark, P., Hamer, D., Rosenberg, M., and Crooke, S.T. (1984). Copper metallothionein of yeast, structure of the gene, and regulation of expression. Proc. Natl. Acad. Sci. USA *81*, 3332–3336.

Capdevila, M., Domènech, J., Pagani, A., Tío, L., Villarreal, L., and Atrian, S. (2005). Zn- and Cd-metallothionein recombinant species from the most diverse phyla may contain sulfide (S2-) ligands. Angew. Chem. Int. Ed. Engl. *44*, 4618–4622.

Cassat, J.E., and Skaar, E.P. (2012). Metal ion acquisition in Staphylococcus aureus: overcoming nutritional immunity. Semin. Immunopathol. *34*, 215–235.

Chillappagari, S., Seubert, A., Trip, H., Kuipers, O.P., Marahiel, M.A., and Miethke, M. (2010). Copper stress affects iron homeostasis by destabilizing iron-sulfur cluster formation in Bacillus subtilis. J. Bacteriol. *192*, 2512–2524.

Crabtree, J.N., Okagaki, L.H., Wiesner, D.L., Strain, A.K., Nielsen, J.N., and Nielsen, K. (2012). Titan cell production enhances the virulence of Cryptococcus neoformans. Infect. Immun. *80*, 3776–3785.

Dancis, A., Yuan, D.S., Haile, D., Askwith, C., Eide, D., Moehle, C., Kaplan, J., and Klausner, R.D. (1994). Molecular characterization of a copper transport protein in S. cerevisiae: an unexpected role for copper in iron transport. Cell *76*, 393–402.

Ding, C., and Butler, G. (2007). Development of a gene knockout system in Candida parapsilosis reveals a conserved role for BCR1 in biofilm formation. Eukaryot. Cell *6*, 1310–1319.

Ding, C., Yin, J., Tovar, E.M., Fitzpatrick, D.A., Higgins, D.G., and Thiele, D.J. (2011). The copper regulon of the human fungal pathogen Cryptococcus neoformans H99. Mol. Microbiol. *81*, 1560–1576.

Dunham, I., Kundaje, A., Aldred, S.F., Collins, P.J., Davis, C.A., Doyle, F., Epstein, C.B., Frietze, S., Harrow, J., Kaul, R., et al.; ENCODE Project Consortium. (2012). An integrated encyclopedia of DNA elements in the human genome. Nature *489*, 57–74.

Durnam, D.M., and Palmiter, R.D. (1984). Induction of metallothionein-I mRNA in cultured cells by heavy metals and iodoacetate: evidence for gratuitous inducers. Mol. Cell. Biol. *4*, 484–491.

Durnam, D.M., and Palmiter, R.D. (1987). Analysis of the detoxification of heavy metal ions by mouse metallothionein. Experientia Suppl. *52*, 457–463.

Furukawa, Y., Torres, A.S., and O'Halloran, T.V. (2004). Oxygen-induced maturation of SOD1: a key role for disulfide formation by the copper chaperone CCS. EMBO J. *23*, 2872–2881.

Giles, S.S., Zaas, A.K., Reidy, M.F., Perfect, J.R., and Wright, J.R. (2007). Cryptococcus neoformans is resistant to surfactant protein A mediated host defense mechanisms. PLoS ONE *2*, e1370.

Halliwell, B., and Gutteridge, J.M. (1985). The importance of free radicals and catalytic metal ions in human diseases. Mol. Aspects Med. *8*, 89–193.

Hamer, D.H. (1986). Metallothionein. Annu. Rev. Biochem. *55*, 913–951.

Heitman, J. (2011). Cryptococcus: from human pathogen to model yeast (Washington, DC: ASM press).

Hodgkinson, V., and Petris, M.J. (2012). Copper homeostasis at the host-pathogen interface. J. Biol. Chem. *287*, 13549–13555.

Hood, M.I., and Skaar, E.P. (2012). Nutritional immunity: transition metals at the pathogen-host interface. Nat. Rev. Microbiol. *10*, 525–537.

Jung, W.H., and Kronstad, J.W. (2008). Iron and fungal pathogenesis: a case study with Cryptococcus neoformans. Cell. Microbiol. *10*, 277–284.

Jung, W.H., Sham, A., White, R., and Kronstad, J.W. (2006). Iron regulation of the major virulence factors in the AIDS-associated pathogen Cryptococcus neoformans. PLoS Biol. *4*, e410.

Jung, W.H., Sham, A., Lian, T., Singh, A., Kosman, D.J., and Kronstad, J.W. (2008). Iron source preference and regulation of iron uptake in Cryptococcus neoformans. PLoS Pathog. *4*, e45.

Jung, W.H., Hu, G., Kuo, W., and Kronstad, J.W. (2009). Role of ferroxidases in iron uptake and virulence of Cryptococcus neoformans. Eukaryot. Cell *8*, 1511–1520.

Kägi, J.H., and Hunziker, P. (1989). Mammalian metallothionein. Biol. Trace Elem. Res. *21*, 111–118.

Kirsch, D.R., and Whitney, R.R. (1991). Pathogenicity of Candida albicans auxotrophic mutants in experimental infections. Infect. Immun. *59*, 3297–3300.

Kronstad, J.W., Attarian, R., Cadieux, B., Choi, J., D'Souza, C.A., Griffiths, E.J., Geddes, J.M., Hu, G., Jung, W.H., Kretschmer, M., et al. (2011). Expanding fungal pathogenesis: Cryptococcus breaks out of the opportunistic box. Nat. Rev. Microbiol. *9*, 193–203.

Kronstad, J., Saikia, S., Nielson, E.D., Kretschmer, M., Jung, W., Hu, G., Geddes, J.M., Griffiths, E.J., Choi, J., Cadieux, B., et al. (2012). Adaptation of Cryptococcus neoformans to mammalian hosts: integrated regulation of metabolism and virulence. Eukaryot. Cell *11*, 109–118.

Kwon-Chung, K.J., Varma, A., Edman, J.C., and Bennett, J.E. (1992). Selection of ura5 and ura3 mutants from the two varieties of Cryptococcus neoformans on 5-fluoroorotic acid medium. J. Med. Vet. Mycol. *30*, 61–69.

Lay, J., Henry, L.K., Clifford, J., Koltin, Y., Bulawa, C.E., and Becker, J.M. (1998). Altered expression of selectable marker URA3 in gene-disrupted Candida albicans strains complicates interpretation of virulence studies. Infect. Immun. *66*, 5301–5306.

Lin, X., Huang, J.C., Mitchell, T.G., and Heitman, J. (2006). Virulence attributes and hyphal growth of C. neoformans are quantitative traits and the MATalpha allele enhances filamentation. PLoS Genet. *2*, e187.

Liochev, S.L. (1996). The role of iron-sulfur clusters in in vivo hydroxyl radical production. Free Radic. Res. *25*, 369–384.

Macomber, L., and Imlay, J.A. (2009). The iron-sulfur clusters of dehydratases are primary intracellular targets of copper toxicity. Proc. Natl. Acad. Sci. USA *106*, 8344–8349.

Macomber, L., Rensing, C., and Imlay, J.A. (2007). Intracellular copper does not catalyze the formation of oxidative DNA damage in Escherichia coli. J. Bacteriol. *189*, 1616–1626.

Marvin, M.E., Williams, P.H., and Cashmore, A.M. (2003). The Candida albicans CTR1 gene encodes a functional copper transporter. Microbiology *149*, 1461–1474.

Nathan, C., and Shiloh, M.U. (2000). Reactive oxygen and nitrogen intermediates in the relationship between mammalian hosts and microbial pathogens. Proc. Natl. Acad. Sci. USA *97*, 8841–8848.

Nicola, A.M., Robertson, E.J., Albuquerque, P., Derengowski, Lda.S., and Casadevall, A. (2011). Nonlytic exocytosis of Cryptococcus neoformans from macrophages occurs in vivo and is influenced by phagosomal pH. MBio *2*.

Okagaki, L.H., Strain, A.K., Nielsen, J.N., Charlier, C., Baltes, N.J., Chrétien, F., Heitman, J., Dromer, F., and Nielsen, K. (2010). Cryptococcal cell morphology affects host cell interactions and pathogenicity. PLoS Pathog. *6*, e1000953.

Osman, D., and Cavet, J.S. (2011). Metal sensing in Salmonella: implications for pathogenesis. Adv. Microb. Physiol. *58*, 175–232.

Pena, M.M., Puig, S., and Thiele, D.J. (2000). Characterization of the Saccharomyces cerevisiae high affinity copper transporter Ctr3. J. Biol. Chem. *275*, 33244–33251.

Piccioni, M., Monari, C., Kenno, S., Pericolini, E., Gabrielli, E., Pietrella, D., Perito, S., Bistoni, F., Kozel, T.R., and Vecchiarelli, A. (2013). A purified capsular polysaccharide markedly inhibits inflammatory response during endotoxic shock. Infect. Immun. *81*, 90–98.

Pondugula, S., Neef, D.W., Voth, W.P., Darst, R.P., Dhasarathy, A., Reynolds, M.M., Takahata, S., Stillman, D.J., and Kladde, M.P. (2009). Coupling phosphate homeostasis to cell cycle-specific transcription: mitotic activation of Saccharomyces cerevisiae PHO5 by Mcm1 and Forkhead proteins. Mol. Cell. Biol. *29*, 4891–4905.

Rowland, J.L., and Niederweis, M. (2012). Resistance mechanisms of Mycobacterium tuberculosis against phagosomal copper overload. Tuberculosis (Edinb.) *92*, 202–210.

Salas, S.D., Bennett, J.E., Kwon-Chung, K.J., Perfect, J.R., and Williamson, P.R. (1996). Effect of the laccase gene CNLAC1, on virulence of Cryptococcus neoformans. J. Exp. Med. *184*, 377–386.

Samanovic, M.I., Ding, C., Thiele, D.J., and Darwin, K.H. (2012). Copper in microbial pathogenesis: meddling with the metal. Cell Host Microbe *11*, 106–115.

Schmidt, M.G., Attaway, H.H., Sharpe, P.A., John, J., Jr., Sepkowitz, K.A., Morgan, A., Fairey, S.E., Singh, S., Steed, L.L., Cantey, J.R., et al. (2012). Sustained reduction of microbial burden on common hospital surfaces through introduction of copper. J. Clin. Microbiol. *50*, 2217–2223.

Schwan, W.R., Warrener, P., Keunz, E., Stover, C.K., and Folger, K.R. (2005). Mutations in the cueA gene encoding a copper homeostasis P-type ATPase reduce the pathogenicity of Pseudomonas aeruginosa in mice. Int. J. Med. Microbiol. *295*, 237–242.

Staab, J.F., and Sundstrom, P. (2003). URA3 as a selectable marker for disruption and virulence assessment of Candida albicans genes. Trends Microbiol. *11*, 69–73.

Szczypka, M.S., and Thiele, D.J. (1989). A cysteine-rich nuclear protein activates yeast metallothionein gene transcription. Mol. Cell. Biol. *9*, 421–429.

Wagner, D., Maser, J., Lai, B., Cai, Z., Barry, C.E., 3rd, Höner Zu Bentrup, K., Russell, D.G., and Bermudez, L.E. (2005). Elemental analysis of Mycobacterium avium-, Mycobacterium tuberculosis-, and Mycobacterium smegmatis-containing phagosomes indicates pathogen-induced microenvironments within the host cell's endosomal system. J. Immunol. *174*, 1491–1500.

Walton, F.J., Idnurm, A., and Heitman, J. (2005). Novel gene functions required for melanization of the human pathogen Cryptococcus neoformans. Mol. Microbiol. *57*, 1381–1396.

Waterman, S.R., Hacham, M., Hu, G., Zhu, X., Park, Y.D., Shin, S., Panepinto, J., Valyi-Nagy, T., Beam, C., Husain, S., et al. (2007). Role of a CUF1/CTR4 copper regulatory axis in the virulence of Cryptococcus neoformans. J. Clin. Invest. *117*, 794–802.

Waterman, S.R., Park, Y.D., Raja, M., Qiu, J., Hammoud, D.A., O'Halloran, T.V., and Williamson, P.R. (2012). Role of CTR4 in the Virulence of Cryptococcus neoformans. MBio *3*.

Weissman, Z., Berdicevsky, I., Cavari, B.Z., and Kornitzer, D. (2000). The high copper tolerance of Candida albicans is mediated by a P-type ATPase. Proc. Natl. Acad. Sci. USA *97*, 3520–3525.

White, C., Lee, J., Kambe, T., Fritsche, K., and Petris, M.J. (2009). A role for the ATP7A copper-transporting ATPase in macrophage bactericidal activity. J. Biol. Chem. *284*, 33949–33956.

Williamson, P.R. (1994). Biochemical and molecular characterization of the diphenol oxidase of Cryptococcus neoformans: identification as a laccase. J. Bacteriol. *176*, 656–664.

Winge, D.R., and Nielson, K.B. (1984). Formation of the metal-thiolate clusters of rat liver metallothionein. Environ. Health Perspect. *54*, 129–133.

Winge, D.R., Nielson, K.B., Gray, W.R., and Hamer, D.H. (1985). Yeast metallothionein. Sequence and metal-binding properties. J. Biol. Chem. *260*, 14464–14470.

Wolschendorf, F., Ackart, D., Shrestha, T.B., Hascall-Dove, L., Nolan, S., Lamichhane, G., Wang, Y., Bossmann, S.H., Basaraba, R.J., and Niederweis, M. (2011). Copper resistance is essential for virulence of Mycobacterium tuberculosis. Proc. Natl. Acad. Sci. USA *108*, 1621–1626.

Zhou, H., and Thiele, D.J. (2001). Identification of a novel high affinity copper transport complex in the fission yeast Schizosaccharomyces pombe. J. Biol. Chem. *276*, 20529–20535.

Cell Host & Microbe, Volume *13*

Supplemental Information

Cryptococcus neoformans Copper Detoxification Machinery Is Critical for Fungal Virulence

Chen Ding, Richard A. Festa, Ying-Lien Chen, Anna Espart, Òscar Palacios, Jordi Espín, Mercè Capdevila, Sílvia Atrian, Joseph Heitman, and Dennis J. Thiele

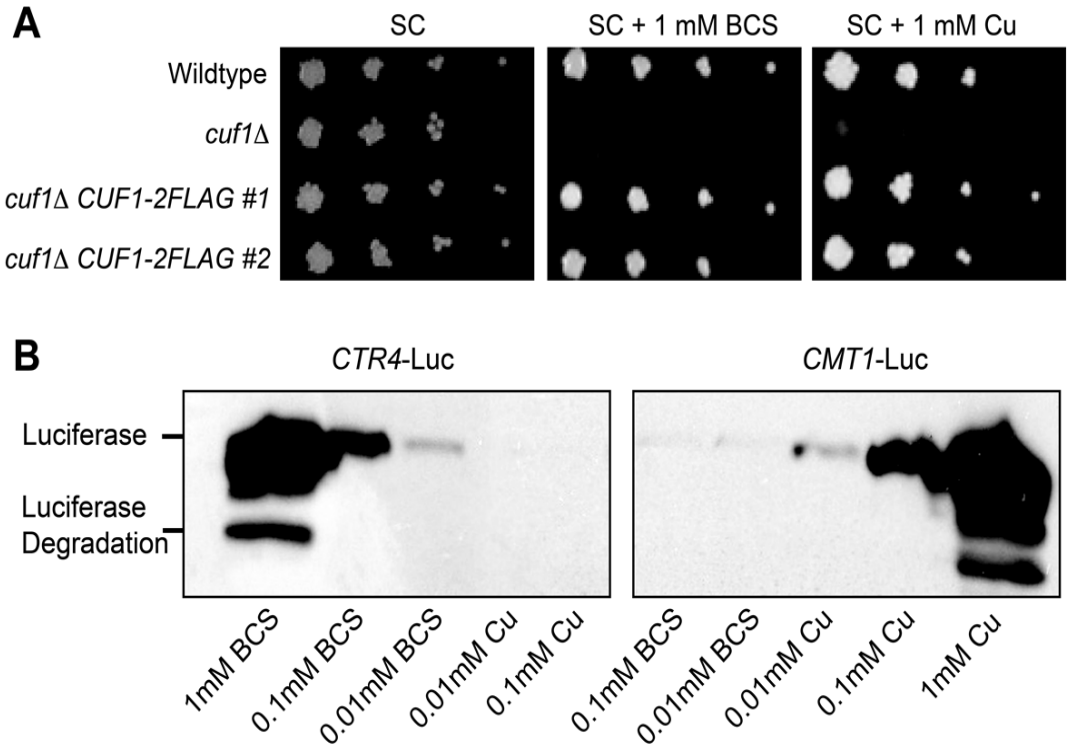

Figure S1. Generation of Carboxyl Terminal Tagged Cuf1 Strains and Immunoblot of Luciferase from *C. neoformans* Wild-Type Cells Transformed with Either the *CMT1*-Luciferase or *CTR4*-Luciferase Reporter Plasmids, Related to Figure 1 and Table S1

A. Carboxyl-terminal 2XFLAG tagged Cuf1 strains were generated. *C. neoformans* growth assays were performed to confirm the complementation by *CUF1-FLAG* in a *cuf1Δ* mutant. Overnight cultures were diluted and spotted onto SC agar, SC agar supplemented with 1 mM BCS, or 1 mM Cu. Plates were incubated at 30°C for 2 days and photographed.

B. Immunoblotting was used to detect luciferase protein from protein extracts from *C. neoformans* cells containing *CMT1*-luciferase or *CTR4*-luciferase reporters.

Overnight cell cultures were sub-cultured in SC medium supplemented with Cu or BCS as indicated. Cell cultures were incubated at 37°C for 9 hrs. Total protein was isolated and quantified using the BCA assay. Equal amounts of protein (50 µg of total protein) were loaded onto SDS-PAGE gels and transferred protein was visualized using Ponceau S staining to confirm equal loading. Antibody against firefly luciferase (Abcam) was used. Experiments were repeated twice with similar results.

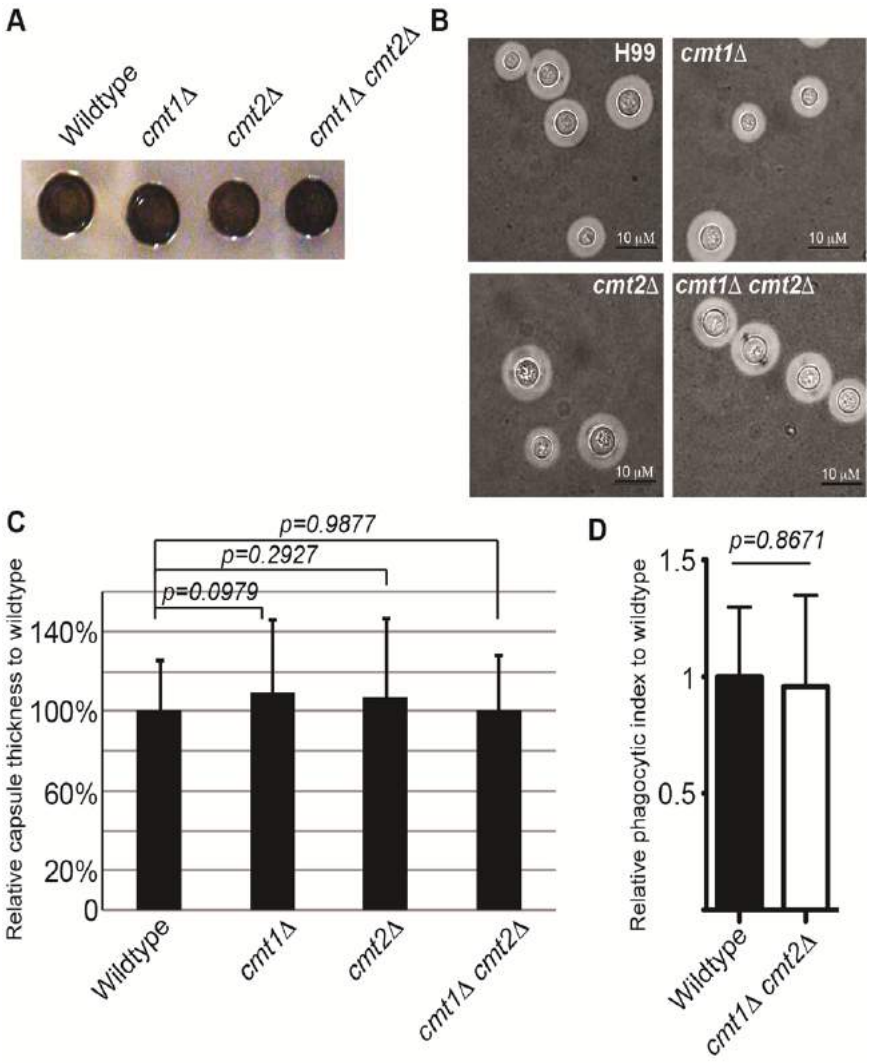

Figure S2. Metallothionein Mutants Exhibit No Defect in Melanin Production, Capsule Formation, or Phagocytosis, Related to Figure 2 and Table S1

A. Melanin formation was qualitatively evaluated in metallothionein mutants, as it is thought to be a virulence factor in *Cryptococcus*. Overnight cell cultures in SC medium were diluted to A_{600} of 1.0, and 5 μl of each culture was spotted onto a melanin inducing plate (agar plates containing L-3,4-dihydroxyphenylalanine). The plate was incubated at 37°C for 3 days until a dark pigment appeared and photographed.

B. Capsule formation was examined in wild type and metallothionein mutants. Cells were incubated in RPMI medium supplemented with serum at 37°C, 5% CO_2 for 3 days to induced capsule formation. Capsule structure was stained with India ink, visualized by a Zeiss Axio microscope and photographed.

C. Capsule thickness of *C. neoformans* wild type and metallothionein mutants was measured and normalized to that of wild type. Photographs from (B) were taken and 60 cells for each strain were measured for capsule thickness. Statistical analysis was performed using the *student t test*. Error bars indicate standard deviation.

D. Phagocytic index was evaluated using bone marrow derived macrophages. Bone marrow cells were isolated from 6 to 8 week old female A/J mice, and differentiated to primary macrophage by GM-CSF at 37°C, 5% CO_2 for 5 days. Before phagocytosis assay, primary macrophages were activated with interferon-γ (5 ng/ml) and lipopolysaccharide (1 μg/ml) for 1 hr. Overnight cultures of wild type and *cmt1Δ cmt2Δ* cells were washed three times with PBS, and incubated with activated BMDM for 3 hrs. Extracellular fungal cells were eliminated by washing 5 times with PBS. The phagocytic index was calculated as previously described (Sano et al., 2003). Cells were visualized and macrophage and internalized fungal cells were counted. The graph represents an average of four replicates; over 200 macrophages were counted for each replicate. The phagocytic index was calculated and normalized to that from wild type. Statistical analysis was performed using the *student t test*. Error bars indicate standard deviation.

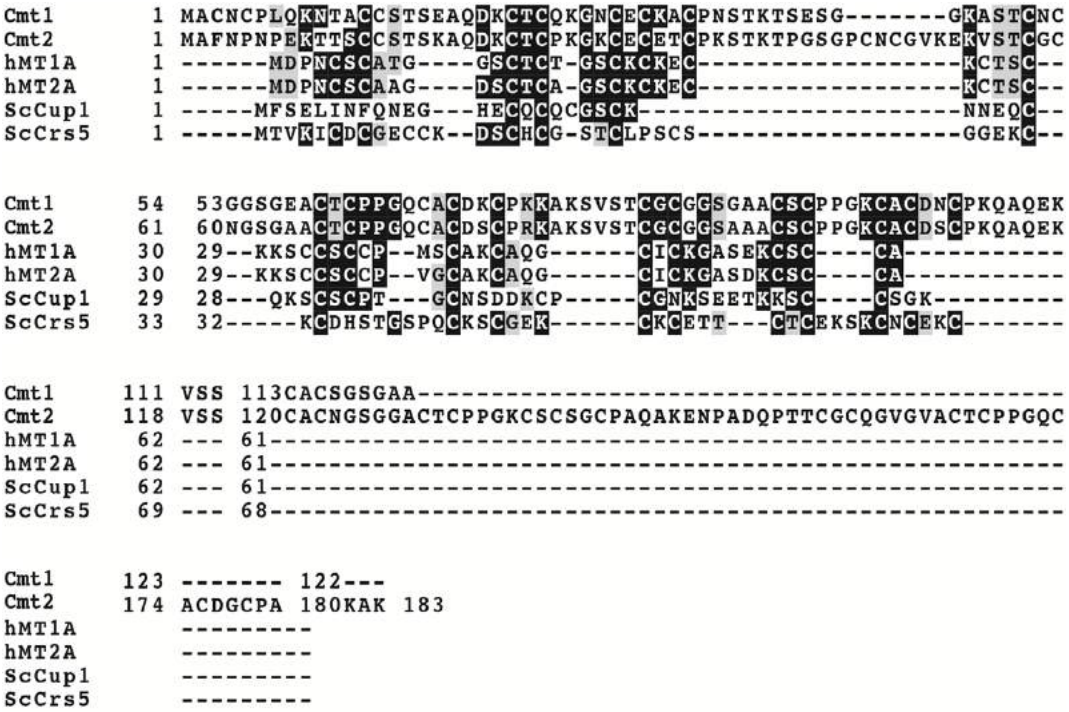

Figure S3. Sequence Analysis of Metallothioneins from *Cryptococcus*, *Saccharomyces*, and Human, Related to Figure 3

Two metallothioneins from each organism were aligned using Clustal W (Larkin et al., 2007). Alignment results are shaded using boxshade (http://www.ch.embnet.org/software/BOX_form.html).

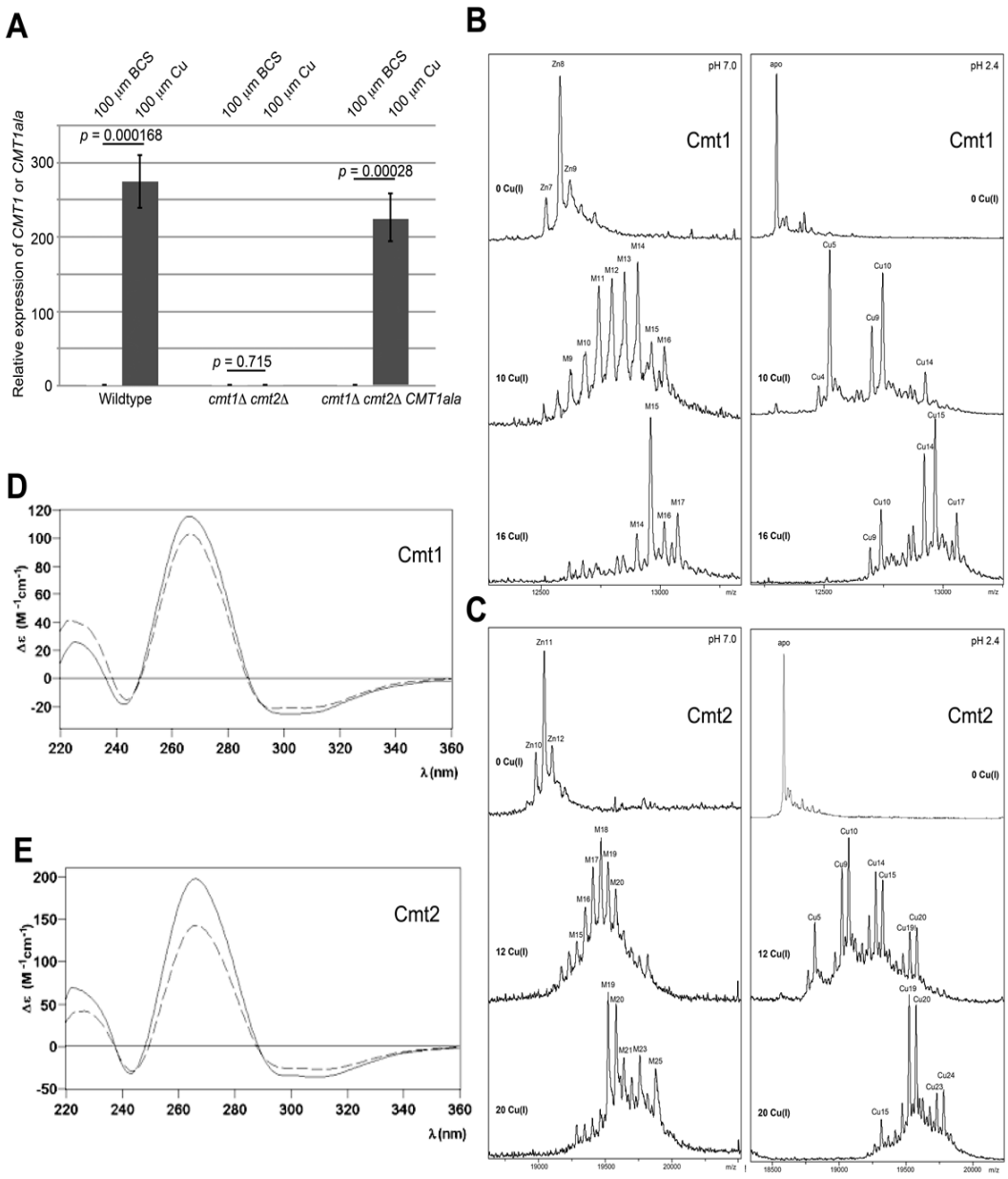

Figure S4. Confirmation of Expression of *CMT1* or *CMT1ala* and the In Vitro Cu^{+} Binding Properties of *C. neoformans* Cmt1 and Cmt2, Related to Figure 5 and Table S1

A. Quantitative RT-PCR was performed to confirm expression of the *CMT1* alanine mutant in *C. neoformans*. Cells were cultured at an initial A_{600} of 0.2 for 3 hrs in

SC medium at 37°C. 100 μM BCS or 100 μM Cu was then added and cultures incubated for 1 hr, since the *cmt1Δ cmt2Δ* strain is Cu sensitive. cDNA was synthesized, and qRT-PCR was performed as previously described (Ding et al., 2011), using primers TACGAGCGAGGCTCAAGACA and CAGGCAGCGCCAGATCCGCT, which recognize both wild type and alanine mutated *CMT1*. Relative expression levels were normalized to *ACT1*. Statistical analysis was performed using *student t test*. Error bars indicate standard deviation.

B. Deconvoluted ESI-MS spectra at pH 7.0 and 2.4 of protein aliquots extracted from the initial Zn-Cmt1 preparation (0 Cu^+) and from solutions at 10 and 16 Cu^+ eq added to Zn-Cmt1.

C. Deconvoluted ESI-MS spectra at pH 7.0 and 2.4 of protein aliquots extracted from the initial Zn-Cmt2 preparation (0 Cu^+) and from solutions at 12 and 20 Cu^+ eq added to Zn-Cmt2.

D. Comparison of the CD spectra of the recombinant Cu-Cmt1 preparation (solid line) and that obtained after the addition of 16 Cu^+ eq to Zn-Cmt1 (dashed line).

E. Comparison of the CD spectra of the recombinant Cu-Cmt2 preparation (solid line) and that obtained after the addition of 20 Cu^+ eq to Zn-Cmt2 (dashed line).

Table S1. Strains Used in this Study

Strain	Genotype	Reference
H99	wild type	(Ding et al., 2011)
cmt1Δ	*cmt1::NAT*	(Ding et al., 2011)
cmt2Δ	*cmt2::NEO*	(Ding et al., 2011)
cmt1Δ cmt2Δ	*cmt1::NAT;cmt2::NEO*	(Ding et al., 2011)
CMT1-Luciferase	*CMT1 promoter*-luciferase-*HYG*	This study
CTR4-Luciferase	*CTR4 promoter*-luciferase-*HYG*	This study
cmt1Δ cmt2Δ CMT1	*cmt1::NAT;cmt2::NEO;CMT1::HYG*	This study
cmt1Δ cmt2Δ CMT2	*cmt1::NAT;cmt2::NEO;CMT2::HYG*	This study
cmt1Δ cmt2Δ CMT1ala	*cmt1::NAT;cmt2::NEO;CMT1ala::HYG*	This study
CMT1-FLAG	*cmt1::NAT;cmt2::NEO;CMT1-FLAG::HYG*	This study
CMT2-FLAG	*cmt1::NAT;cmt2::NEO;CMT2-FLAG::HYG*	This study
CUF1-FLAG	*cuf1::NEO;CUF1-FLAG::HYG*	This study

Supplemental Experimental Procedures

Generation of *Cryptococcus* Mutants and Biolistic Transformation

Cryptococcus Metallothionein (*CMT*) complementation strains were generated as follows: *CMT1* and *CMT2* genomic DNA was amplified and cloned into the pHYG7-KB1 plasmid (a gift from Dr. Jennifer Lodge, Washington University) (Hua et al., 2000). The resulting plasmids were transformed using biolistic methods as previously described (Toffaletti et al., 1993). The *CMT1ala* DNA sequence was synthesized by IDT (Integrated DNA Technologies) with mutation of all cysteine codons to alanine codons. The *CMT1ala* sequence was amplified using primer pair MT1alaKpnI/ClaI (GGGGGGTACCATGGCTGCAAACGCACCTCCC/GGGGATCGATTCAGGCAGCGCC AGATCCGCT), digested with *Kpn*I and *Cla*I, and cloned into a pMT1 plasmid (which is a *CMT1* expression plasmid with *Kpn*I and *Cla*I between *CMT1* promoter and terminator sequences).

The luciferase gene was amplified using primer pair LucCTR4F/R for *CTR4* promoter (TTTACGAAAGGACACCATCCATCATGGAAGATGCCAAAAACATT/CATCCGGTACA TATTATTACTCTTTTACACGGCGATCTTGCCGCCC) or LucMT1F/R for *CMT1* promoter (CAACTCAAACAAACTACAATCATGGAAGATGCCAAAAACATT/AGCATTGGTCTGG AAGACAAGCTTACACGGCGATCTTGCCGCCC). *CTR4*-Luciferase was generated using the *CTR4* promoter, terminator and luciferase gene in an overlapping PCR, whereas the *CTR4* promoter was amplified using primer pair CTR4promoterF/R (GGGGTCTAGATGGATGGTATTCTTCAGTTCCGT/GATGGATGGTGTCCTTTCGTAA

A) and the Cn*CTR4* terminator was amplified using primer pair CTR4terminatorF/R (AAGAGTAATAATATGTACCGGATG/GGGGTCTAGAAGCCTCTGCGACGTTACCGATCA). *CMT1*-Luciferase was generated as described for *CTR4*-Luc using primer pair (GGGGTCTAGATAATCGCTCTCTCGGAGGAA/GATTGTAGTTTGTTTGAGTTG) for *CMT1* promoter, and primer pair GCTTGTCTTCCAGACCAATGCT/GGGGTCTAGAGGAATGTGTATCAAAACTTGGG) for *CMT1* terminator. The resulting overlapping PCR fragments were cloned into the pHYG7-KB1 plasmid. The plasmid was transformed into *Cryptococcus* by biolistic transformation (Toffaletti et al., 1993).

The pHYG-Cuf1-2xFLAG was cloned using the following strategy. Forward Primer, Cuf1-comp-NotI-F (GACGCGGCCGCCAAAGGACCCTTTTGGACCT) and reverse primer Cuf1-comp-FLAG-XbaI-R (GACTCTAGATTTGTCGTCGTCATCTTTATAATCCTCGAGATTACTCCACATCCTAGCCTGATCCC) were used to amplify approximately 1 kb upstream of the Cuf1 translational start site and the entire *CUF1* coding sequence, without the stop codon, with one FLAG tag sequence. A second FLAG tag sequence, including a new stop codon as well as approximately 1 kb of DNA downstream from the *CUF1* open reading frame was amplified using the primers Cuf1-comp-FLAG-XbaI-F (GACTCTAGAGACTACAAGGACGATGATGATAAGTAAGGGCCCTTAAGTAGTAGGGCTGCTGCT) and Cuf1-comp-NheI-R (GACGCTAGCGCTCCTCGACATGTCCTACC). PCR products were digested with NotI/XbaI and XbaI/NheI respectively. Vector pHYG7-KB1 was digested with NotI/SpeI (SpeI and NheI have compatible overhangs). A triple

ligation was performed and transformed into *E. coli* strain DH5α to obtain the vector pHYG-Cuf1-2xFLAG, which was confirmed and biolistically transformed into the *cuf1Δ* strain and resulting transformants were validated and tested for growth on 1 mM $CuSO_4$ and 1 mM BCS.

Chromatin Immunoprecipitation

The following primers were used to amplify approximately 300 bp of their respective promoters: CMT1-CHIP-F (TAAGCTTATGAATGAAAGTCGGC), CMT1-CHIP-R (CAGCTTCTGGATTGCTGTT), CMT2-CHIP-F (GATCGAAAAGCAGTTTCG), CMT2-CHIP-R (CTTGTGTCTGGCGTCTTCCT), CTR1-CHIP-F (AGGATGGCTGAAGGGCTAAT), CTR1-CHIP-R (CAGCCGCTAGTAGGGTTACG), CTR4-CHIP-F (GATTGGCATCAATCTGAGCA), CTR4-CHIP-R (CATCTAGCGGGAAGGTTGTT). The β1-tubulin (*TUB2*) promoter was used as a negative control: TUBULIN-CHIP-F (TGAGTGAAAGTGGCTCATCG) and TUBULIN-CHIP-R (AGCAAGCCAAAAACAACACC).

Metallothionein Expression, Synthesis, and Purification

The *CMT1ala* sequence (Cmt1 cysteine to alanine) was synthesized by Integrated DNA Technologies. The cDNA sequence from *CMT1* or *CMT2* or synthetic DNA sequence from *CMT1ala* was cloned in a pGEX-4T1 expression vector (GE Healthcare). The recombinant plasmids were transformed into the *E. coli MachI* strain for sequence determination. Positive clones were transformed into the *E. coli BL21* protease deficient strain for protein synthesis.

Expression from the pGEX-MT plasmids was performed in 5 L cultures of transformed *E. coli* cells. Expression was induced with isopropyl β-D-thiogalactopyranoside (IPTG) and cultures were supplemented with 300 μM $ZnCl_2$ or 500 μM $CuSO_4$ final concentrations, and allowed to grow for additional 3 hrs. Cu-supplemented cultures were grown either under normal aeration conditions (1 L of media in a 2 L Erlenmayer flask, at 250 rpm) or under low oxygen conditions (1.5 L of media in a 2 L Erlenmayer flask, at 150 rpm), to optimize intracellular Cu availability (Pagani et al., 2007). The total protein extract was prepared from bacterial cultures as previously described (Capdevila et al., 1997). *In vivo*-folded metal-Cmt complexes were recovered from the Cmt-GST fusion constructs by thrombin cleavage and batch-affinity chromatography using Glutathione-Sepharose 4B (GE Healthcare). After concentration using Centriprep Microcon 3 (Amicon), samples were purified through FPLC in a Superdex75 column (GE Healthcare) equilibrated with 50 mM Tris-HCl, pH 7.0. Selected fractions were confirmed by 12% SDS-PAGE and kept at -80^{o}C until further use. All procedures were performed using Ar (pure grade 5.6) saturated buffers, and all syntheses were performed at least twice to ensure reproducibility, as described previously (Capdevila et al., 1997). As a consequence of the cloning requirements, a dipeptide Gly-Ser or penta-peptide Gly-Ser-Pro-Glu-Phe were present at the amino terminus of Cmt1 or Cmt2, respectively; but this had previously been shown not to alter the MT metal-binding features. *In vitro*-substituted Cu(I)-MT complexes were obtained by titration of the Zn(II)-MT preparations with Cu(I) at pH 7, using $[Cu(CH_3CN)_4]ClO_4$ solutions, as previously described (Bofill et al., 1999). During all experiments strict oxygen-free conditions were maintained by saturating all the solutions with Ar.

Supplemental References

Bofill, R., Palacios, O., Capdevila, M., Cols, N., Gonzalez-Duarte, R., Atrian, S., and Gonzalez-Duarte, P. (1999). A new insight into the Ag+ and Cu+ binding sites in the metallothionein beta domain. J Inorg Biochem *73*, 57-64.

Capdevila, M., Cols, N., Romero-Isart, N., Gonzalez-Duarte, R., Atrian, S., and Gonzalez-Duarte, P. (1997). Recombinant synthesis of mouse Zn3-beta and Zn4-alpha metallothionein 1 domains and characterization of their cadmium(II) binding capacity. Cell Mol Life Sci *53*, 681-688.

Ding, C., Yin, J., Tovar, E.M., Fitzpatrick, D.A., Higgins, D.G., and Thiele, D.J. (2011). The copper regulon of the human fungal pathogen Cryptococcus neoformans H99. Mol Microbiol *81*, 1560-1576.

Hua, J., Meyer, J.D., and Lodge, J.K. (2000). Development of positive selectable markers for the fungal pathogen Cryptococcus neoformans. Clin Diagn Lab Immunol *7*, 125-128.

Larkin, M.A., Blackshields, G., Brown, N.P., Chenna, R., McGettigan, P.A., McWilliam, H., Valentin, F., Wallace, I.M., Wilm, A., Lopez, R.*, et al.* (2007). Clustal W and Clustal X version 2.0. Bioinformatics *23*, 2947-2948.

Pagani, A., Villarreal, L., Capdevila, M., and Atrian, S. (2007). The Saccharomyces cerevisiae Crs5 Metallothionein metal-binding abilities and its role in the response to zinc overload. Mol Microbiol *63*, 256-269.

Sano, H., Hsu, D.K., Apgar, J.R., Yu, L., Sharma, B.B., Kuwabara, I., Izui, S., and Liu, F.T. (2003). Critical role of galectin-3 in phagocytosis by macrophages. J Clin Invest *112*, 389-397.

Toffaletti, D.L., Rude, T.H., Johnston, S.A., Durack, D.T., and Perfect, J.R. (1993). Gene transfer in Cryptococcus neoformans by use of biolistic delivery of DNA. J Bacteriol *175*, 1405-1411.

Publication # 3

Full characterization of the Cu-, Zn-, and Cd-binding properties of CnMT1 and CnMT2, two metallothioneins of the pathogenic fungus *Cryptococcus neoformans* acting as virulence factors.

PUBLICATION #3:

TITLE

"Full characterization of the Cu-, Zn-, and Cd-binding properties of CnMT1 and CnMT2, two metallothioneins of the pathogenic fungus *Cryptococcus neoformans* acting as virulence factors"

AUTHORS

Òscar Palacios*, Anna Espart*, Jordi Espín, Chen Ding, Dennis J. Thiele, Sílvia Atrian, Mercè Capdevila

REFERENCE

Metallomics (2014) 6: 279-291 (IF: 4.000)

SUMMARY

The dimorphic basidiomycete *Cryptococcus neoformans,* which is the causing agent of human cryptococcosis in immunodeficient and immunocompetent individuals, encodes two metallothioneins (CnMTs) that were shown to play a critical role in the virulence of the fungus (Ding et al., 2014a). During lung infection, *C. neoformans* finds a hostile environment, with a high copper concentration, which is induced by macrophages to fight against pathogens. Its MTs (CnMT1 and CnMT2) are directly involved in copper detoxification. This specific ability is typical from fungal MTs that are considered Cu-thioneins. CnMT1 and CnMT2 are extremely long compared with other typical fungal MTs being 122 and 183-residue long, respectively. The block distribution of cysteine residues separated by non-cysteine spacer regions, and the hypothetical architecture consisting in several Cu_5Cys_7 clusters, lead to hypothesize a high capacity of CnMT1 and CnMT2 to bind copper through a modular structure. The aim of this study was to characterize by spectroscopic and spectrometric techniques the features of the Zn-, Cd- and Cu-complexes folded *in vivo* (through recombinant synthesis) and *in vitro* (by Zn/Cd and Zn/Cu replacement in Zn-CnMT1 and Zn-CnMT2 species).

The CnMT cDNAs had been previously obtained and sequenced in Prof. Thiele's Lab at Duke University. We used it subsequently *in silico* searches in Broad Institute database, where *C. neoformans var. grubii* H99 genome has its the repository, localizing two

highly similar but not identical genes. A manual revision of the exon-intron boundaries allowed the identification of the correct sequences, this showing that those in the database were wrongly annotated. Synthesis and purification of the CnMT1 and CnMT2 metal complexes showed different behaviour for each metal ion. For Zn, unique, Zn_8-CnMT1 or equimolar Zn_8-CnMT1 and Zn_7-CnMT1 species were obtained; while CnMT2 rendered a mixture of Zn_{11}-CnMT2, Zn_{12}-CnMT2 and Zn_{10}-CnMT2 species. From Cd-supplemented cultures, Cd_8-CnMT1, together with minor Cd_9-CnMT1 and Cd_8S-CnMT1 complexes, were detected; and two major Cd_{13}-CnMT2 and Cd_{15}-CnMT2 species for CnMT2. These results allowed to conclude that CnMTs have a poor preference for divalent metal ion binding. Cu-enriched cultures were grown at two different conditions, regular and low-aeration, the later allowing a higher intracellular content of the producing bacterial cells. CnMT1 synthesized in regularly aerated cultures (i.e. regular *E.coli* Cu content), yielded preparations that neutral ESI-MS resolved as a mixture of equimolar heteronuclear species M_{11}-CnMT1 and M_8-CnMT1, and a minor M_9-CnMT1; in which acid ESI-MS only detected Cu_5-CnMT1 complexes. This suggested a composition of probable $M_{11} = Cu_5Zn_6$, $M_8 = Cu_5Zn_3$ and $M_9 = Cu_5Zn_4$ species. The same type of cultures (regular Cu) rendered a range of heteronuclear CnMT2 complexes, from M_6- to M_{17}-CnMT2, even M_{24}-CnMT2, by analysis at neutral ESI-MS, while Cu_5-, Cu_9- and Cu_{10} cores were identified at acid ESI-MS. Syntheses in low-aerated cultures (*i.e.* Cu-rich environment) rendered significantly different results. Thus, neutral ESI-MS identified a major Cu_{16}-CnMT1, accompanied by very minor Cu_{15}-CnMT1 and Cu_{17}-CnMT1 species for this isoform, while acid ESI-MS rendered almost the same stoichiometries, although with different relative intensities for the detected species. For CnMT2, a major M_{24}-CnMT2 peak in neutral ESI-MS was resolved into Cu_{20}- and minor Cu_{24}-species by acid ESI-MS.

Finally, Zn/Cu displacements in both MTs, revealed a cooperative Cu_5-cluster formation, increasing until Cu_{15}- in CnMT1 and Cu_{20}-species in CnMT2, this being concordant with a basic, stable Cu_5 core that would be amplified three- and five-folds, respectively, according to the CnMTs lengths.

Contribution to this work

This work has been realized in conjunction with our regular collaborator group of Dr. Mercè Capdevila, from the chemical department in the Universitat Autònoma de Barcelona (UAB). As PhD student of this thesis I collaborated doing i) the *in silico* studies of obtained cDNAs and the annotated sequences of CnMTs in database, confirm mis annotated sequences; ii) cloning CnMT1 and CnMT2 in the expression vector pGEX-4T1 and subsequently the cDNAs were expressed in *E. coli* BL21 strains in supplemented media with Zn, Cd or Cu to synthesize the correspondent proteins; iii) purifying them using liquid chromatography. The obtained samples were analysed by spectroscopy and spectrometry by UAB group.

Metallomics

PAPER

View Article Online
View Journal | View Issue

Cite this: *Metallomics*, 2014, **6**, 279

Full characterization of the Cu-, Zn-, and Cd-binding properties of CnMT1 and CnMT2, two metallothioneins of the pathogenic fungus *Cryptococcus neoformans* acting as virulence factors†

Òscar Palacios,‡[a] Anna Espart,‡[b] Jordi Espín,[a] Chen Ding,§[c] Dennis J. Thiele,[c] Sílvia Atrian*[b] and Mercè Capdevila[a]

Received 27th September 2013,
Accepted 18th November 2013

DOI: 10.1039/c3mt00266g

www.rsc.org/metallomics

We report here the full characterization of the metal binding abilities of CnMT1 and CnMT2, two *Cryptococcus neoformans* proteins recently identified as metallothioneins (MTs), which have been shown to play a crucial role in the virulence and pathogenicity of this human-infecting fungus. In this work, we first performed a thorough *in silico* study of the *CnMT1* and *CnMT2* genes, cDNAs and corresponding encoded products. Subsequently, the Zn(II)-, Cd(II)- and Cu(I) binding abilities of both proteins were fully determined through the analysis of the metal-to-protein stoichiometries and the structural features (determined by ESI-MS, CD, ICP-AES and UV-vis spectroscopies) of the corresponding recombinant Zn-, Cd- and Cu-MT preparations synthesized in metal-enriched media. Finally, the analysis of the Zn/Cd and Zn/Cu replacement processes of the respective Zn–MT complexes when allowed to react with Cd(II) or Cu(I) aqueous solutions was performed. Comprehensive consideration of all gathered results allows us to consider both isoforms as genuine copper-thioneins, and led to the identification of unprecedented Cu_5-core clusters in MTs. CnMT1 and CnMT2 polypeptides appear to be evolutionarily related to the small fungal MTs, probably by ancient tandem-duplication events responding to a highly selective pressure to chelate copper, and far from the properties of Zn- and Cd-thioneins. Finally, we propose a modular structure of the Cu–CnMT1 and Cu–CnMT2 complexes on the basis of Cu_5 clusters, concordantly with the modular structure of the sequence of CnMT1 and CnMT2, constituted by three and five Cys-rich units, respectively.

1. Introduction

Metallothioneins (MTs) are a superfamily of ubiquitous small Cys-rich proteins that have been identified in all eukaryotes and most prokaryotes so far analyzed.[1] They constitute polymorphic systems in almost all organisms, so that diversification of MT isoforms may underlie their ability to play versatile biological roles. MTs coordinate closed-shell metal ions, such as Zn(II), Cd(II) or Cu(I) and they have been associated with several physiological processes, among which homeostasis and/or protection against metal ions appear to be the most relevant.[2,3] Recent studies have revealed that metallothioneins of *Cryptococcus neoformans* can be considered as pathogenicity and virulence determinants.[4] *Cryptococcus neoformans* is a dimorphic basidiomicet, responsible for cryptococcosis in both immunodeficient and immunocompetent individuals, establishing a first infection in lungs, and later on developing lethal meningitis.[5] Precisely, it has been shown that the two MTs of *Cryptococcus neoformans* (CnMT1 and CnMT2) play a critical role in the virulence of this opportunistic fungus, as well as in its resistance to the host immune response, because they are directly involved in the detoxification of the high copper concentrations produced by the infection-fighting macrophages.[4] *CnMT1* and *CnMT2* genes are induced in a Cu-specific

[a] *Dept. de Química, Fac. de Ciències, Universitat Autònoma de Barcelona, 08193-Cerdanyola del Vallès, Barcelona, Spain*
[b] *Dept. de Genètica, Fac. de Biologia, Universitat de Barcelona, Av. Diagonal 643, 08028-Barcelona, Spain. E-mail: satrian@ub.edu; Fax: +34 934034420; Tel: +34 934021501*
[c] *Dept. of Pharmacology and Cancer Biology, Duke University School of Medicine, Durham, North Carolina, 27710, USA*

† Electronic supplementary information (ESI) available. See DOI: 10.1039/c3mt00266g

‡ These two authors contributed equally to this work.

§ Current address: College of Life and Health Sciences, Northeastern University, Shenyang, People's Republic of China.

manner, and consequently they are part of the Cu-responsive *C. neoformans* set of genes essential for its virulence known as the *C. neoformans copper regulon*. This regulon is under the transcriptional control of the Cuf1 factor and, besides *CnMT1* and *CnMT2*, it comprises genes encoding for Cu importers (namely Ctr1 and Ctr4). Paradoxically *Ctr1* and *Ctr4* respond to Cu limitation conditions through the same Cuf1 transcription factor, so that both Cu acquisition and Cu detoxification appear to be virulence determinants in *C. neoformans* infections.[6]

Regarding the CnMT1 and CnMT2 proteins, it has been shown that their detoxifying function comes from their high Cu-binding capacity,[4] so that they exhibit all the features to be considered typical Cu-thioneins.[3,7] However, unlike the paradigmatic Cu-thioneins such as the yeast (*Saccharomyces cerevisiae*) Cup1 protein and the fungus *Neurospora crassa* MT,[8] which are very small proteins of 41 and 26 amino acids, respectively, *C. neoformans* MTs are surprisingly longer: CnMT1 is a 122-residue long polypeptide and CnMT2 a 183-residue long polypeptide (*cf.* Fig. 1).[6] The first study of *C. neoformans* CnMT1 and CnMT2 proteins, besides allowing their unambiguous classification as metallothioneins, served to suggest the formation of unusual Cu_5-building blocks,[4] different to the Cu-clusters commonly reported in MTs until the moment. This applies both to taxonomically close yeast and fungal MTs: Cu_8 for *S. cerevisiae* Cup1[9] and Cu_6 for *Neuropora crassa* MT,[10] respectively, and Cu_4- and Cu_6-clusters in the more distant mammalian MTs.[11–13] The presence of several Cu_5Cys_7 clusters in both *C. neoformans* MT isoforms and the high similarity, at the amino acid sequence level, between these two proteins were hypothesized to account for the high specificity and capacity of CnMT1 and CnMT2 for Cu-binding. Strikingly, a modular structure has also been proposed for the five MT isoforms of several species of the ciliate *Tetrahymena* (*T. pigmentosa* and *T. pyriformis*) with lengths ranging between 96 and 181 amino acids.[14] Therefore, unicellular eukaryotes of different taxa (ciliate, fungi) may have followed the same strategy to enhance the metal binding capacity of their MTs, by tandemly repeating a basic, Cys-containing, building block.

In this scenario it was relevant to fully determine the metal binding abilities of the *C. neoformans* MTs. To this end, we characterized the Zn-, Cd- and Cu-species formed *in vivo* (by recombinant synthesis in *E. coli*) and *in vitro* (by Zn/Cd and Zn/Cu replacement in the corresponding recombinant Zn–CnMT species) by spectroscopic and spectrometric techniques. This information confirms a modular organization of the long CnMT1 and CnMT2 peptides regarding metal cluster formation. Furthermore, the correct annotation of their encoding genes and corresponding transcripts in the *C. neoformans* genome highlights the evolutionary relationship that may link these MTs with the other well-studied fungal copper-thioneins (*Neurospora* and *Agaricus*).

2. Experimental

2.1. *In silico* tools for genome, DNA and protein sequence analysis

The last annotated *C. neoformans var. grubii* H99 genome version in the Broad Institute database (www.broadinstitute.org) was used for *in silico* searches of the MT-encoding genes, through the Blast facility accessible in the same site. The *CnMT1* and *CnMT2* cDNAs had been previously obtained and sequenced in D. Thiele's lab,[6] through rtPCR on mRNA isolated from copper induced cells. These *CnMT1* and *CnMT2* cDNA sequences were used as queries for genomic searches. Sequences were aligned with the ClustalW facility available at the EBI website (http://www.ebi.ac.uk/Tools/msa/clustalw2/).

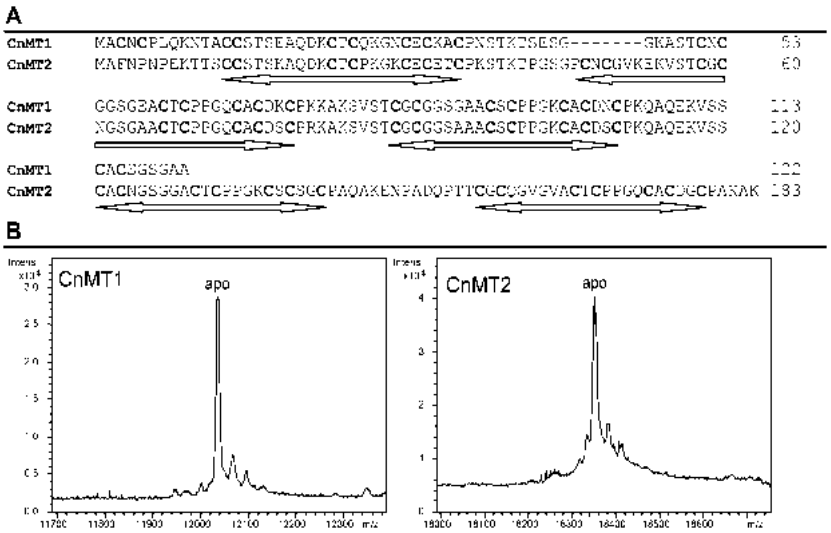

Fig. 1 (A) Alignment of the amino acid sequences of CnMT1 (25 Cys, 122 aa) and CnMT2 (37 Cys, 183 aa). Conserved Cys are in bold and the Cys-rich stretches are underlined. (B) Deconvoluted ESI-MS spectra of the Zn–CnMT1 and Zn–CnMT2 preparations recorded at acidic pH, showing the corresponding recombinant apo-forms. These peptides included the Gly-Ser (CnMT1) and Gly-Ser-Pro-Glu-Phe (CnMT2) residues added at their N-term due to GST-cloning requirements.

2.2. Cloning and recombinant expression of the CnMT1 and CnMT2 cDNAs

The *CnMT1* and *CnMT2* cDNAs were obtained from D.Thiele's lab[6] as p426GPD clones. From there, they were subcloned into the *BamH*I/*Xho*I sites for CnMT1, and *Eco*RI/*Xho*I sites for CnMT2 (owing to the presence of an internal *BamH*I site in *CnMT2*) of the pGEX-4T1 expression vector (GE Healthcare), in order to obtain a GST-MT fusion protein. The two restriction sites were added to the cDNA sequences by PCR amplification, using the following oligonucleotides as primers: 5′-AAAAGGATCCATGGCTTGCAACTGCCCTCCC-CAGA-3′ (forward) and 5′-AAAACTCGAGTCAGGCAGCGCCAG-3′ (reverse) for CnMT1; and 5′-GGGAGAATTCATGGCTTTCAACCC-3′ (forward) and 5′-GGGGCTCGAGTTATTTAGCCTTGGCCG-3′ (reverse) for CnMT2. The 30-cycle amplification reactions were performed with the thermo resistant Hotstar Taq DNA polymerase (Qiagen) under the following conditions: 15 min at 95 °C (activation of the DNA polymerase), 30 s at 94 °C (denaturation), 30 s at 55 °C (annealing) and 1 min at 72 °C (elongation). The final products were analyzed by 0.8% agarose gel electrophoresis and the expected bands were excised (Genelute™ Gel Extraction Kit, Sigma Aldrich). pGEX-4T1 and the amplified inserts were digested with *BamH*I/*Xho*I for CnMT1 and *Eco*RI/*Xho*I for CnMT2, followed, in each case, by a ligation reaction (DNA Ligation Kit 2.1, Takara Bio Inc.). The recombinant plasmids were transformed into the *E. coli* MachI strain for DNA sequencing, using the Big Dye Terminator 3.1 Cycle Sequencing Kit in an ABIPRISM 310 Automatic Sequencer (Applied Biosystems). Positive clones were transformed into the *E. coli* BL21 protease deficient strain for protein synthesis.

2.3. Synthesis and purification of recombinant Zn– and Cu–CnMT complexes and preparation of *in vitro*-substituted complexes

The corresponding GST–CnMT fusion proteins were biosynthesized in 5 L cultures of transformed *E. coli* cells. Expression was induced with 100 μM (final concentration) isopropyl β-D-thiogalactopyranoside (IPTG) and cultures were supplemented with 300 μM $ZnCl_2$, 300 μM $CdCl_2$ or 500 μM $CuSO_4$ (final concentrations), and they were allowed to grow for further 3 h. Cu-supplemented cultures were grown either under normal aeration conditions (1 L of media in a 2 L Erlenmeyer flask, at 250 rpm) or under low oxygen conditions (1.5 L of media in a 2 L Erlenmeyer flask, at 150 rpm), since different results may be achieved depending on the culture aeration conditions owing to the fact that these determine the amount of intracellular copper in the host cells.[15] The total protein extract was prepared from bacterial cultures as fully described before for other MT peptides.[16] Briefly, metal–CnMT complexes were recovered from the CnMT-GST fusion constructs by thrombin cleavage and batch-affinity chromatography using the Glutathione-Sepharose 4B matrix (GE Healthcare). After concentration using Centriprep Microcon 3 (Amicon), samples were finally purified through FPLC in a Superdex75 column (GE Healthcare) equilibrated with 50 mM Tris-HCl, pH 7.0. Selected fractions were confirmed by 12% SDS-PAGE and kept at −80 °C until further use. All procedures were performed using Ar (pure grade 5.6) saturated buffers, and all syntheses were performed at least twice to ensure reproducibility. As a consequence of the cloning requirements, the dipeptide Gly-Ser in the case of CnMT1 and the pentapeptide Gly-Ser-Pro-Glu-Phe in the case of CnMT2 were present at the N-term of the CnMT polypeptides; but this had previously been shown not to alter the MT metal-binding features.[17] *In vitro*-substituted Cd(II)–CnMT and Cu(I)–CnMT complexes were obtained by titration at pH 7 of the corresponding Zn(II)–CnMT preparations with $CdCl_2$ in water (MERCK AAS Cd^{2+} standard of 1000 ppm) or $[Cu(CH_3CN)_4]ClO_4$ solutions as described,[18] respectively. During all the experiments strict oxygen-free conditions were maintained by saturating all the solutions with Ar.

2.4. Spectroscopic analyses (ICP-AES and CD) of the Zn–, Cd– and Cu–CnMT complexes

The S, Zn, Cd and Cu content of the Zn–, Cd– and Cu–CnMT preparations was analyzed by means of Inductively Coupled Plasma Atomic Emission Spectroscopy (ICP-AES) using a Polyscan 61E (Thermo Jarrell Ash) spectrometer, measuring S at 182.040 nm, Zn at 213.856 nm, Cd at 228.802 nm and Cu at 324.803 nm. Samples were routinely treated as reported in ref. 19, but they were also alternatively incubated in 1 M HCl at 65 °C for 15 min prior to measurements in order to eliminate possible traces of labile sulfide ions.[20] Protein concentrations were calculated from the acid ICP-AES sulfur measurements, assuming that all S atoms were contributed by the CnMT peptides. A Jasco spectropolarimeter (Model J-715) interfaced to a computer (J700 software) was used for CD measurements at a constant temperature of 25 °C maintained using a Peltier PTC-351S apparatus. Electronic absorption measurements were performed on an HP-8453 Diode array UV-visible spectrophotometer. All spectra were recorded with 1 cm capped quartz cuvettes, corrected for the dilution effects and processed using the GRAMS 32 program.

2.5. Electrospray ionization time-of-flight mass spectrometry (ESI-TOF MS) of the Zn– and Cu–CnMT complexes

MW determinations were performed by electrospray ionization time-of-flight mass spectrometry (ESI-TOF MS) on a Micro TOF-Q instrument (Bruker) interfaced with a Series 1200 HPLC Agilent pump, equipped with an autosampler, all of which were controlled by the Compass Software. Calibration was attained with ESI-L Low Concentration Tuning Mix (Agilent Technologies). Samples containing CnMT complexes with divalent metal ions were analyzed under the following conditions: 20 μL of protein solution injected through a PEEK (polyether heteroketone) tubing (1.5 m × 0.18 mm i.d.) at 40 μL min^{-1}; capillary counter-electrode voltage 5 kV; desolvation temperature 90–110 °C; dry gas 6 L min^{-1}; spectra collection range 800–2500 *m*/*z*. The carrier buffer was a 5 : 95 mixture of acetonitrile : ammonium acetate (15 mM, pH 7.0). Alternatively, the Cu–CnMT samples were analyzed as follows: 20 μL of protein solution injected at 40 μL min^{-1}; capillary counter-electrode voltage 3.5 kV; lens counter-electrode voltage 4 kV; dry temperature 80 °C; dry gas 6 L min^{-1}. Here, the carrier was a 10 : 90 mixture of acetonitrile:ammonium acetate, 15 mM, pH 7.0. For the analysis

of apo–CnMT and Cu–CnMT preparations at acidic pH, 20 μL of the corresponding sample were injected under the same conditions described previously, but using a 5 : 95 mixture of acetonitrile:formic acid pH 2.4, as a liquid carrier, which caused the complete demetalation of the peptides loaded with Zn(II) but kept the Cu(I) ions bound to the protein. Under all the conditions assayed, the error associated with the mass measurements was always lower than 0.1%. Masses for the holo-species were calculated as previously described.[21]

3. Results and discussion

3.1. *CnMT1* and *CnMT2* gene structure and annotation in *C. neoformans* genome

The Blast search using the *CnMT1* cDNA sequence retrieved CNAG_05449 as the most probable clone containing the desired sequence. However, this exhibited clear sequence differences, also leading to a hypothesized protein 5-residue longer at its C-term end than CnMT1. In order to solve this ambiguity, the genome sequence was searched for the corresponding *CnMT1* gene, which also allowed us to define its exon–intron structure. We were able to assign the *CnMT1* cDNA sequence to a putative *CnMT1* gene, located in *C. neoformans* chromosome 14, between nucleotides 341340 and 342169 at the + strand (Genebank entry CP003833.1). Using the *CnMT1* cDNA sequence as a guide, the possible exon–intron boundaries, according to the GT/AG rule, were manually searched. The result was a perfect match between the *CnMT1* cDNA sequence and the proposed exons of the gene, in number of four (Fig. S1A, ESI†). Therefore, we concluded that the CNAG_05449T0 and CNAG_05449.2 hypothetical protein sequences were incorrectly annotated, and that the reported CnMT1 cDNA and protein sequences represented the real expression products of the *CNAG_05449* gene. When performing a parallel quest for the CnMT2 coding sequences, we also realized that the CNAG_00306 transcript and hypothetical protein, identified through the blast with the *CnMT2* cDNA sequence, were wrongly annotated. Hence, we also defined the correct gene structure (as shown in Fig. S1B, ESI†), and furthermore, we added the final coding stretch by identification in the GenBank AACO02000005.1 entry, since the CNAG_00306 entry appears to be truncated at its 3′ end. The *CnMT2* gene is located between 787948 bp and at 789021 according to the current Genbank entry CP003820.1, at the + strain of *C. neoformans* chromosome 1 and it includes seven intron sequences. No further sequences were retrieved by Blast searches using as a query MT sequences of the following isoforms: human MT1 and MT2, *Mytilus edulis* MT10Ia, *Scylla serrata* MT1, *D. melanogaster* MtnA and MtnD, *Candida glabrata* MT1, *Yarrowia lipolytica* MT1, *Saccharomyces cerevisiae* Cup1 and CRS5, *Neurospora crassa* MT and *Arabidopsis thaliana* MT1A. This strongly suggests that *CnMT1* and *CnMT2* are the only MT encoding genes in the *C. neoformans* genome, although the existence of some highly divergent isoforms cannot be completely ruled out. The cDNAs and genes are, respectively, 86.38% and 79.85% similar (excluding gaps). This clearly suggests that they arose by gene duplication (and further expansion of *CnMT2*, as discussed later) of an ancestral gene, and they may have been subsequently separated to different genome locations by some chromosomal rearrangement events.

3.2. CnMT1 and CnMT2 peptide identity

DNA sequencing confirmed that both CnMT cDNAs were cloned in pGEX in the appropriate frame after the GST encoding moiety and that they included no undesired nucleotide substitutions. Consequently, recombinant syntheses yielded CnMT1 and CnMT2 peptides (Fig. 1A), the identity, purity and integrity of which were confirmed by acid ESI-MS (pH 2.4) of the respective Zn–MT complexes. Hence, for each MT, a unique peak was detected, whose MW was consistent with that calculated for the respective apo-forms (Fig. 1B), including the N-terminal residues derived from the GST-fusion construct prior to the initiator Met. Experimental molecular masses detected were 12034.1 Da for CnMT1 and 18350.29 Da for CnMT2 *vs.* the respective theoretical values of 12034.56 and 18349.91 Da calculated from the amino acid sequence.

3.3. Zn–CnMT1 and Zn–CnMT2 complexes

The repeated synthesis of CnMT1 by Zn(II)-enriched bacteria yielded two types of results regarding the stoichiometry of the recovered Zn–CnMT1 complexes, being always characterized by a rather low protein yield (concentrations *ca.* 0.1 mg L^{-1} of culture). ICP-AES analyses indicated a mean content of 8–9 Zn(II) per MT, which was highly consistent with ESI-MS spectra showing either only major Zn_8–CnMT1 complexes or almost equimolar amounts of Zn_7–CnMT1 and Zn_8–CnMT1, among other minor species (Fig. 2A and B). Despite this disparity, both types of Zn–CnMT1 preparations exhibited identical CD spectra, which can be interpreted as a Gaussian band centered at *ca.* 240 nm, typical of the Zn-SCys chromophores superimposed to the 220–230 nm absorption contributed by the peptidic bonds (Fig. 2D). Contrary to CnMT1, the synthesis of the Zn–CnMT2 complexes yielded invariable results. These consisted of also rather diluted preparations (0.5 mg L^{-1} of culture), including a mixture of major Zn_{11}–CnMT2 and minor Zn_{12}– and Zn_{10}–CnMT2 species (Fig. 2C), nicely matching the average content of 11 Zn(II) per MT shown by ICP-AES. The CD spectrum of this sample (Fig. 2E) was quite similar to that of Zn–CnMT1, but for a more pronounced shoulder at *ca.* 245 nm. In this case, it can be interpreted as resulting from two overlapping Gaussian bands, centered at 225 and 240 nm. At this point of the analysis, it became evident that both isoforms were far from presenting the features typical of MTs optimized for Zn(II) binding (*i.e.* Zn-thioneins),[7] in view of the multiplicity and variability of the recovered species in Zn-supplemented recombinant cultures and the absence of derivative-like curves in their CD fingerprints.

3.4. Cd–CnMT1 and Cd–CnMT2 complexes

The Cd(II) binding abilities of CnMT1 and CnMT2 were studied through the characterization of their recombinant complexes, as well as those obtained by Zn/Cd replacement in Zn–CnMT1 and Zn–CnMT2. The synthesis of CnMT1 and CnMT2 in Cd(II)-supplemented cultures rendered even more diluted (0.010 and

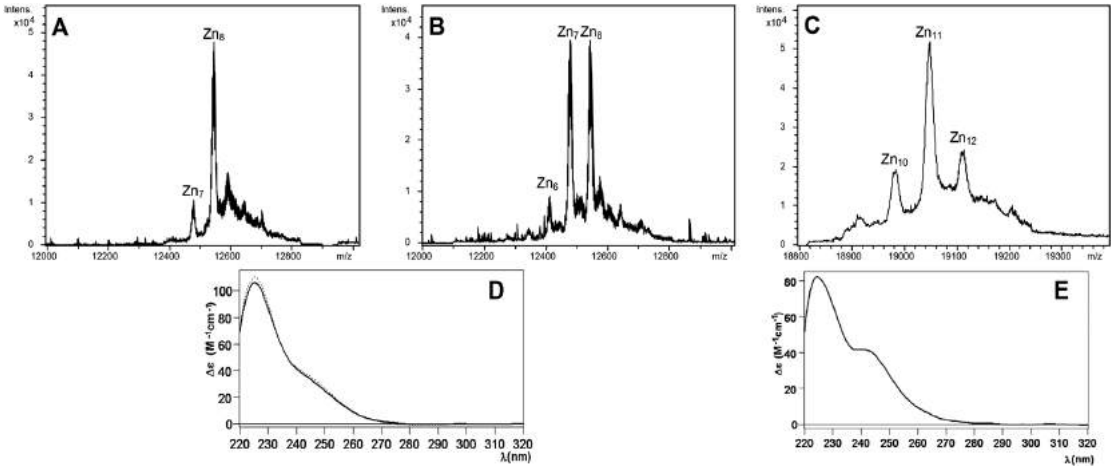

Fig. 2 (A and B) Deconvoluted ESI-MS spectra of two Zn–CnMT1 preparations and (D) the CD fingerprints corresponding to (A), solid line, and (B), dotted line. (C) Deconvoluted ESI-MS spectrum of the Zn–CnMT2 preparation and (E) its corresponding CD spectrum.

0.011 mg L^{-1} of culture, respectively) and more heterogeneous preparations than for Zn(II). Hence, the recovered Cd–CnMT1 complexes contained 8–9 Cd(II) per MT (according to the ICP-AES results), and consisted of major Cd_8–CnMT1 complexes together with minor Cd_9–CnMT1, and significantly Cd_8S_2–CnMT1 (Fig. 3A). The CD fingerprint of this preparation suggests an overlapping of two Gaussian bands, centered at 245 nm (contributed by the Cd-SCys chromophores) and 270 nm (contributed by the Cd-sulfide ligands) (Fig. 3B).[20] The analysis of the Cd(II) titration of Zn–CnMT1 showed that the maximum CD absorbance at 250 nm was reached at 11 Cd(II) eq. added (Fig. S2, ESI†). This point defined also the closest resemblance to the speciation found in the *in vivo* preparation (*cf.* Fig. 3A and Fig. S3B, ESI†), as well as a practical coincidence of the corresponding CD spectra (Fig. 3B). Furthermore, the UV-vis spectra indicated that there was no substantial Cd(II) entry beyond this point. A detailed description of the Cd(II) titration of Zn–CnMT1 can be found as ESI,† including the full set of ESI-MS (Fig. S3, ESI†) and CD and UV-vis spectra (Fig. S2, ESI†) of its successive steps.

Owing to its higher Cys content, the purified Cd–CnMT2 complexes exhibited a mean content of 12–13 Cd(II) per MT, contributed by two major Cd_{13}– and Cd_{15}–CnMT2 complexes, among multiple minor species (Fig. 3C). The CD spectrum of this sample resembled that of Cd–CnMT1, compatible with the presence in the sample of complexes including sulfide ligands (Fig. 3D). The Cd(II) titration of Zn–CnMT2 was analyzed by the same rationale as that of Zn–CnMT1 (full data in ESI,† Fig. S4 and S5). In this case, the maximum similarity with the *in vivo* Cd–CnMT2 preparation was reached for 12 Cd(II) eq. added (Fig. 3C), although this titration caused the generation of a high number of almost inextricable Cd-containing species (Fig. S5, ESI†).

In summary, and as stated before for Zn(II), the results for Cd(II) coordination definitively suggest that both CnMTs are far from exhibiting any binding preference for Cd(II) ions. Precisely, (i) the mixtures of species obtained from the recombinant syntheses, (ii) the variability of the relative intensity of the peaks (relative abundance) of the different species obtained in different productions; and (iii) the presence of sulfide-containing Cd–CnMT1 complexes, indicates a poor ability of both CnMT1 and CnMT2 for divalent metal ion binding.

3.5. Cu–CnMT1 and Cu–CnMT2 complexes

The behavior of CnMTs when binding Cu(I) was studied in great detail, since both our results for divalent metal coordination (explained in the previous sections) and the observed role of these MT isoforms in *C. neoformans* copper metabolism[4] already pointed to their imperative Cu-thionein character. Therefore, Cu(II)-enriched recombinant *E. coli* cultures were grown both under normal and low oxygenation conditions, since low oxygenation leads to higher Cu content in the host cells.[15] Additionally, Cu(I) binding to CnMTs was studied by analyzing the corresponding Zn/Cu displacement reactions in the respective Zn–CnMTs.

3.5.1. Cu(I)-binding by CnMT1: recombinant Cu–CnMT1. *CnMT1* expression in bacteria grown under copper supplementation in normally aerated copper-supplemented cultures rendered 0.4 mg L^{-1} of MT protein, containing both Zn(II) and Cu(I), as indicated by its ICP-AES analysis: average ratio of 4 Zn: 5 Cu per CnMT1 molecule. The neutral ESI-MS spectrum of this sample revealed a mixture of heteronuclear species, with major, almost equimolar, M_{11}– and M_8–CnMT1 followed by M_9–CnMT1 and other minor peaks (M = Zn(II) or Cu(I)) (Fig. 4A). Strikingly, the ESI-MS of the same sample at pH 2.4 yielded a very predominant, almost unique Cu_5–CnMT1 peak (Fig. 4B). This suggests that all the M_x–CnMT1 (x = 5 to 12) complexes are basically constituted by a Cu_5-cluster that completes the observed metal content with Zn(II) ions, *i.e.* $M_{11} = Cu_5Zn_6$, $M_8 = Cu_5Zn_3$, $M_9 = Cu_5Zn_5$. Instead, when CnMT1 was produced in a Cu-richer environment, it yielded homometallic copper complexes, since ICP-AES results ruled out any trace of the Zn presence. The ESI-MS spectrum at neutral pH identified a major Cu_{16}–CnMT1 species, accompanied by very minor Cu_{15}– and Cu_{17}–CnMT1 complexes (Fig. 4C). Interestingly, this preparation

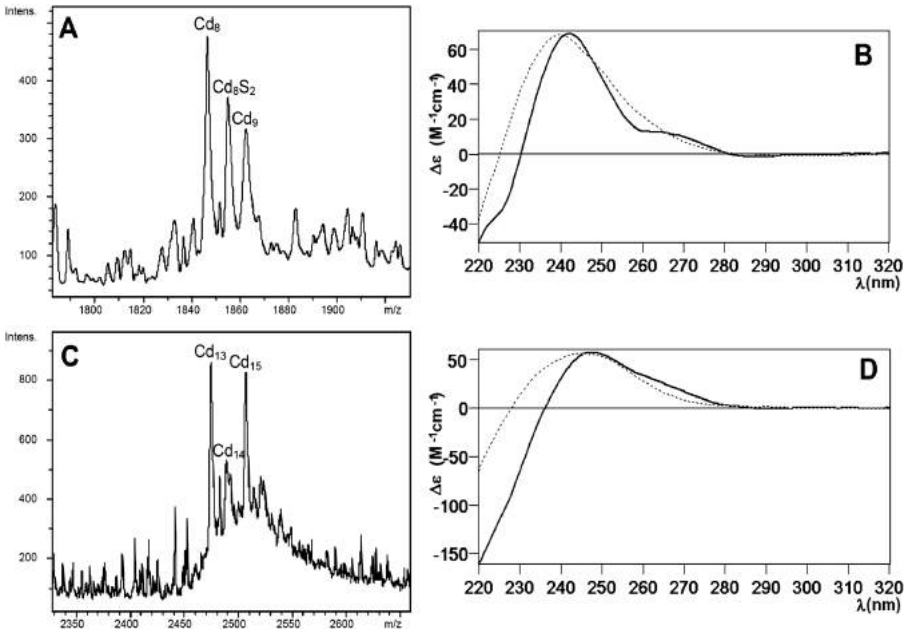

Fig. 3 (A) ESI-MS spectrum corresponding to the recombinant production of CnMT1 in Cd-enriched media, at the +7 charge state. (B) CD spectra of the Cd–CnMT1 preparation (solid line) and that recorded after the addition of 11 Cd(II) eq. to the Zn–CnMT1 preparation (dotted). (C) ESI-MS spectrum corresponding to the recombinant production of CnMT2 in Cd-enriched media, at the +8 charge state. (D) CD spectra of the Cd–CnMT2 preparation (solid line) and that recorded after the addition of 12 Cd(II) eq. to the Zn-CnMT2 preparation (dotted). Full CD and ESI-MS spectra corresponding to the Zn/Cd titration of both isoforms can be found in the ESI.†

was resolved into a different speciation by acidic ESI-MS analysis (Fig. 4D), which indicates that some of the CnMT1-bound Cu(I) would be extremely sensitive to pH changes.

Although the CD spectrum of the Cu–CnMT1 preparation at normal aeration cannot be representative of any species due to the mixture recovered, it clearly shows interesting features, such as the absorptions between 300 and 340 nm that reveal special binding sites for Cu(I) only observed previously for MT isoforms of a prevalent Cu-thionein character.[22] These same CD absorptions, together with the 265 nm centered Gaussian band typical of the fingerprint of Cu–MT complexes, are observed for the Cu–CnMT1 preparation obtained at low oxygenation. In fact, comparison of the normalized spectra of both Cu–CnMT1 preparations highlights their elevated similarity, despite the presence or the absence of Zn(II) ions, which would contribute only to the 220–240 nm region (Fig. 4E).

3.5.2. Cu(I)-binding by CnMT1: Zn/Cu displacement in Zn–CnMT1. Most informative results about the Cu(I) binding abilities of CnMT1 were obtained from the addition of Cu(I) to Zn–CnMT1 (*i.e.* the study of the species constituted *in vitro* by Zn/Cu exchange). The metal-substitution process was followed by CD, UV-vis (Fig. 5A) and ESI-MS analysis (Fig. 5C) of aliquots retrieved every 2 Cu(I) eq., from 0 to 26 Cu(I) equivalents added to Zn-CnMT1. From the start results appeared to be highly promising, since the CD spectra of the full process show very nice isodichroic, although not isosbestic, points, at three different stages: from 0 to 6, from 6 to 16 and from 16 to 26 Cu(I) eq. added (*cf.* Fig. 5A). This strongly suggested a cooperative copper loading and zinc displacement process in CnMT1. In the first step, between 0 and 6 Cu(I) eq. added, two isodichroic points can be clearly observed, which arise by the decrease of the 225 nm band and the increase of the 260 nm CD absorption, owing to the creation of Cu-SCys chromophores, accompanied by the emergence of a new CD absorption at *ca.* 290 nm. For the second step, between 6 and 16 Cu(I) eq. added, the 265(+) and 300–310(−) nm CD absorptions reach their maxima at 16 Cu(I) eq., defining an isodichroic point at 290 nm. At the third step, UV-vis spectra still show Cu(I) entry, although more or less important than for the previous steps, and the Gaussian CD band centered at 265 nm decreases in intensity while the absorption at higher wavelengths shows no significant variation.

It is evident that from the beginning, the addition of Cu(I) increases the complexity of the sample in terms of the number of species present, as the ESI-MS analysis reveals (Fig. 5C). Only after the addition of 12 eq., 16 eq., and an excess of Cu(I), a clear major species is found (respectively, M_{14}–, M_{15}– and M_5–CnMT1). However, the most remarkable features are revealed by the acid ESI-MS spectra, because they made patently clear that CnMT1 builds its copper aggregates on the basis of Cu_5-clusters. Hence, the addition of just 2 Cu(I) eq. at the beginning of the experiment already gave rise to the appearance of a Cu_5 cluster, which remained very abundant while a Cu_{10}-cluster gained in importance. These Cu_5- and Cu_{10}-clusters were predominant until 12 Cu(I) eq. added to Zn–CnMT1, when Cu_{14} and Cu_{15}

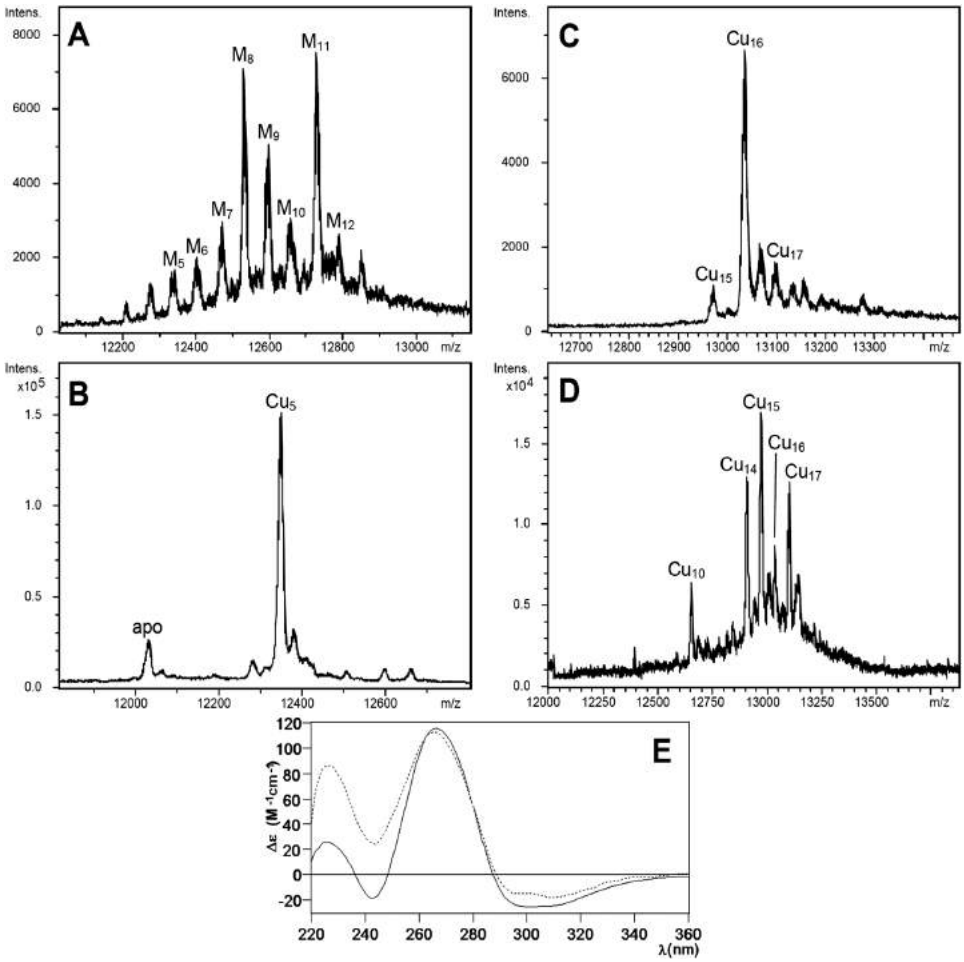

Fig. 4 Deconvoluted ESI-MS spectra corresponding to the production of CnMT1 in Cu-enriched media under (A and B) normal and (C and D) low aeration conditions, recorded at (A and C) neutral and (B and D) acidic pH. (E) CD spectra of the Cu–CnMT1 production under normal (solid line) and low (dotted) aeration conditions.

became the major peaks detected. In the presence of an excess of copper, beyond 16 Cu(I) eq. added, the metal–MT complexes became unstable, so that only highly stable Cu_5-core remained in solution. It is important to note here that apo–CnMT1 is never detected at the end of the reaction (Cu overload conditions), which is an outcome quite common for other MTs.[23,24] It is also highly fascinating that the two landmarks of this Zn(II)/Cu(I) exchange reaction are the addition of 6–8 and 16 Cu(I) eq., because, besides being the spectroscopically crucial steps (Fig. 5A), they are also the moments of predominance of the Cu_5- and Cu_{15}-cores, respectively, as shown by the acidic ESI-MS analysis (Fig. 5C). Most importantly, they also represent the steps when *in vitro* preparations most closely reproduce the results of recombinant CnMT1 synthesis in Cu-enriched cultures (*cf.* Fig. 4B, D and 5C). Hence, precisely, addition of 8 Cu(I) eq. to Zn–CnMT1 yields a sample with spectroscopic (Fig. 5B) and spectrometric features very close to those of the Cu–CnMT1 complexes obtained from normally-aerated cultures (*cf.* Fig. 4A and B *vs.* Fig. 5C at 8 Cu(I) eq.), while those corresponding to the addition of 16 Cu(I) eq. are practically identical to those of the synthesis at low aeration (*i.e.* high intracellular Cu) (*cf.* Fig. 4C and D *vs.* Fig. 5C at 16 Cu(I) eq.), with the unique exception that M_{15} is the major species instead of Cu_{16} at pH 7.0, although both ESI-MS spectra coincide at acid pH, with Cu_{15} as the most abundant complex. Therefore, although a strict cooperative process for the Zn/Cu displacement in Zn–CnMT1 can be ruled out, owing to the many different species coexisting during all the experiment, it is true that it can be assumed for the Cu_5-cores, since Cu(I) is loaded in CnMT1 by sets of 5 Cu(I) ions. The high stability and/or preference for Cu_5-containing clusters were already suggested from the *in vivo* productions (*vide supra*). Besides, the possibility of reproducing the *in vivo* obtained samples at some steps of the Cu(I) addition to Zn–CnMT1 is remarkable, as in fact was the case of the yeast Crs5 MT.[15] It is worth noting that the main peaks representing one or multiple Cu_5-units that emerge

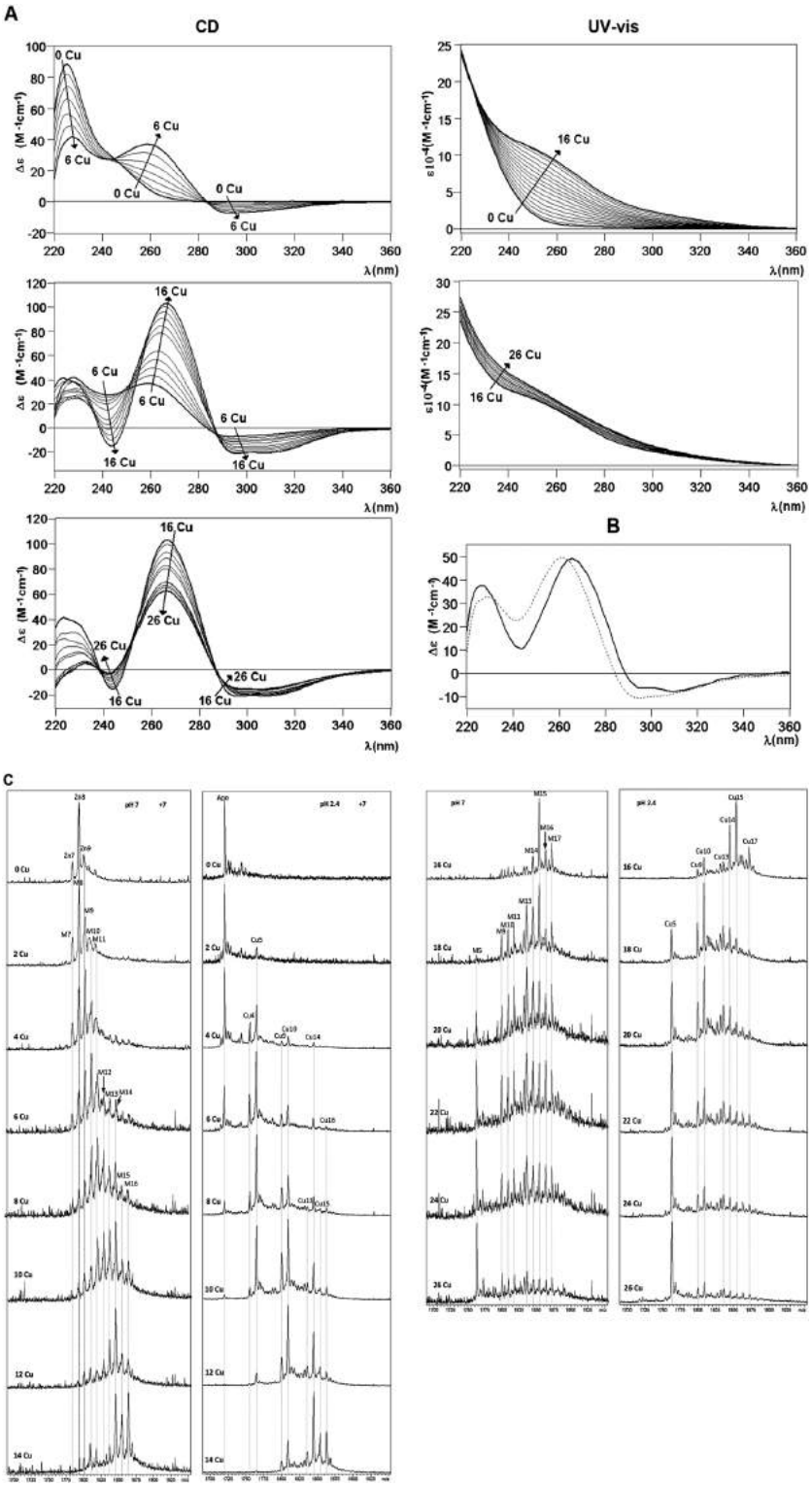

Fig. 5 (A) CD and UV-vis spectra recorded after the addition of Cu(I) to the Zn–CnMT1 preparation. (B) CD spectra corresponding to the Cu–CnMT1 preparation under normal aeration (solid line) and that recorded after the addition of 8 Cu(I) eq. to the Zn–CnMT1 preparation (dotted). (C) ESI-MS spectra recorded after the addition of Cu(I) to the Zn–CnMT1 preparation, recorded at neutral and acidic pH, at the +7 charge state.

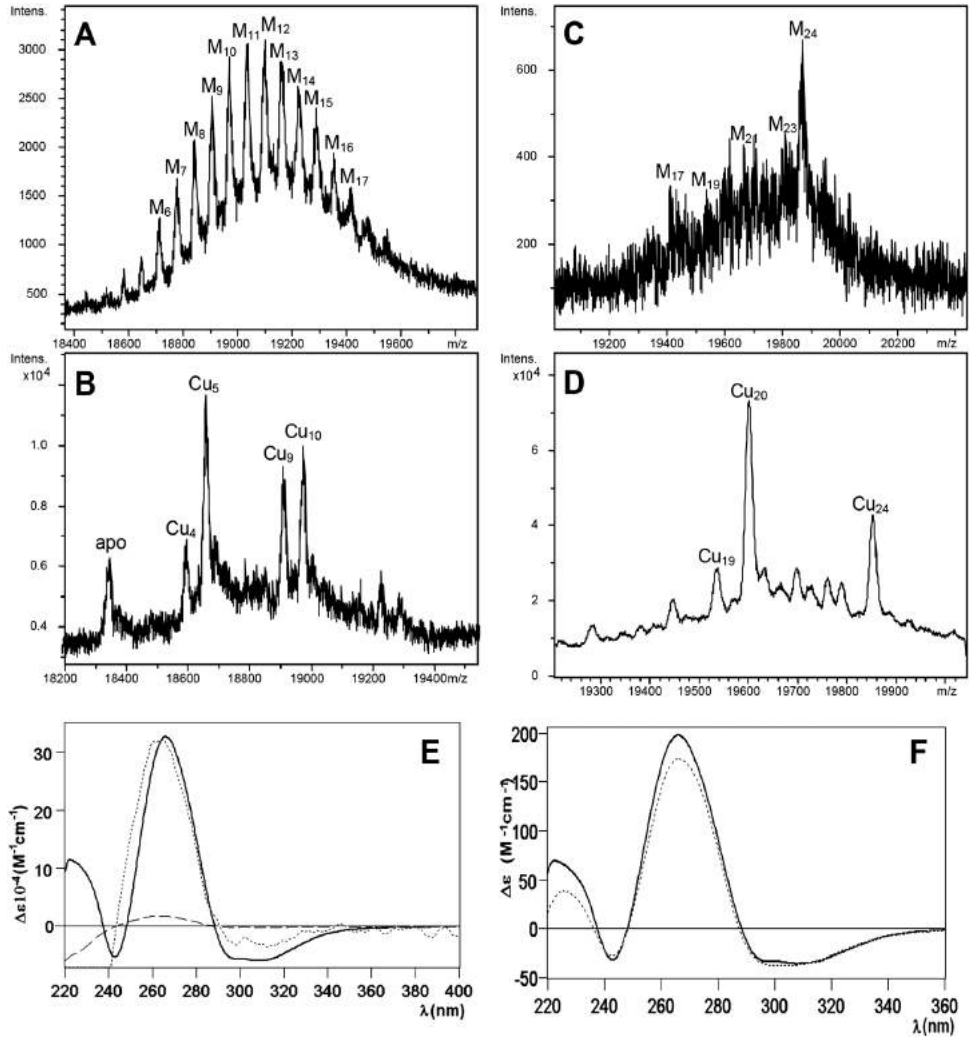

Fig. 6 Deconvoluted ESI-MS spectra corresponding to the production of CnMT2 in Cu-enriched media under (A and B) normal and (C and D) low aeration conditions, recorded at (A and C) neutral and (B and D) acidic pH. CD spectra of (E) the Cu–CnMT2 production under low (solid line) and normal (dashed) aeration conditions – for comparative purpose, the dashed curve has been normalized (dotted); and of (F) Cu–CnMT1 (dotted) and Cu–CnMT2 (solid) productions under low aeration conditions.

during the Zn–CnMT1 titration are always accompanied by a minor peak lacking one of the final numbers of Cu(I) ions (Fig. 5C). Hence, for example, at 4 Cu(I) eq. both the Cu_5/Cu_4 and Cu_{10}/Cu_9 composition added are visible, while at 16 Cu(I) eq., it is the Cu_{15}/Cu_{14} pair the one that becomes predominant. This suggests that at least one Cu_4-cluster has enough stability to persist during this Zn/Cu replacement reaction. Finally, the more than probable involvement in Cu(I) coordination to the N_{term} and C_{term} Cys doublets present in the CnMT1 sequence (*cf.* Fig. 1) would feasibly explain the origin of the Cu–CnMT1 species with more than 15 Cu(I) ions (*i.e.* Cu_{17}– and Cu_{16}–CnMT1), which are not only observable along the corresponding Zn/Cu displacement reaction, but are even the major species resulting from the Cu-MT1 recombinant synthesis in poorly-oxygenated cultures (Fig. 4C and D).

3.5.3. Cu(I)-binding by CnMT2: recombinant Cu–CnMT2. The synthesis of CnMT2 in Cu(II)-enriched cultures was performed both under normal and low oxygenation conditions, repeating the trends described for CnMT1, but obviously with higher metal ion contents, according to its increased size. Thus, normal oxygenation of copper-supplemented cultures rendered a yield of 0.2 mg MT per L, containing 6 Zn: 5 Cu per CnMT2 molecule, according to the ICP results. The ESI-MS spectrum of this preparation reflected a Gaussian-like distribution of heteronuclear complexes ranging from M_6– to M_{17}–CnMT2 (M = Zn(II) or Cu(I)) (Fig. 6A), while its acid ESI-MS analysis revealed that these complexes predominantly contained 5 Cu(I) ions (Cu_5 cores) like the Cu–CnMT1 species, although here the presence of Cu_9- and Cu_{10}-containing CnMT2 complexes was

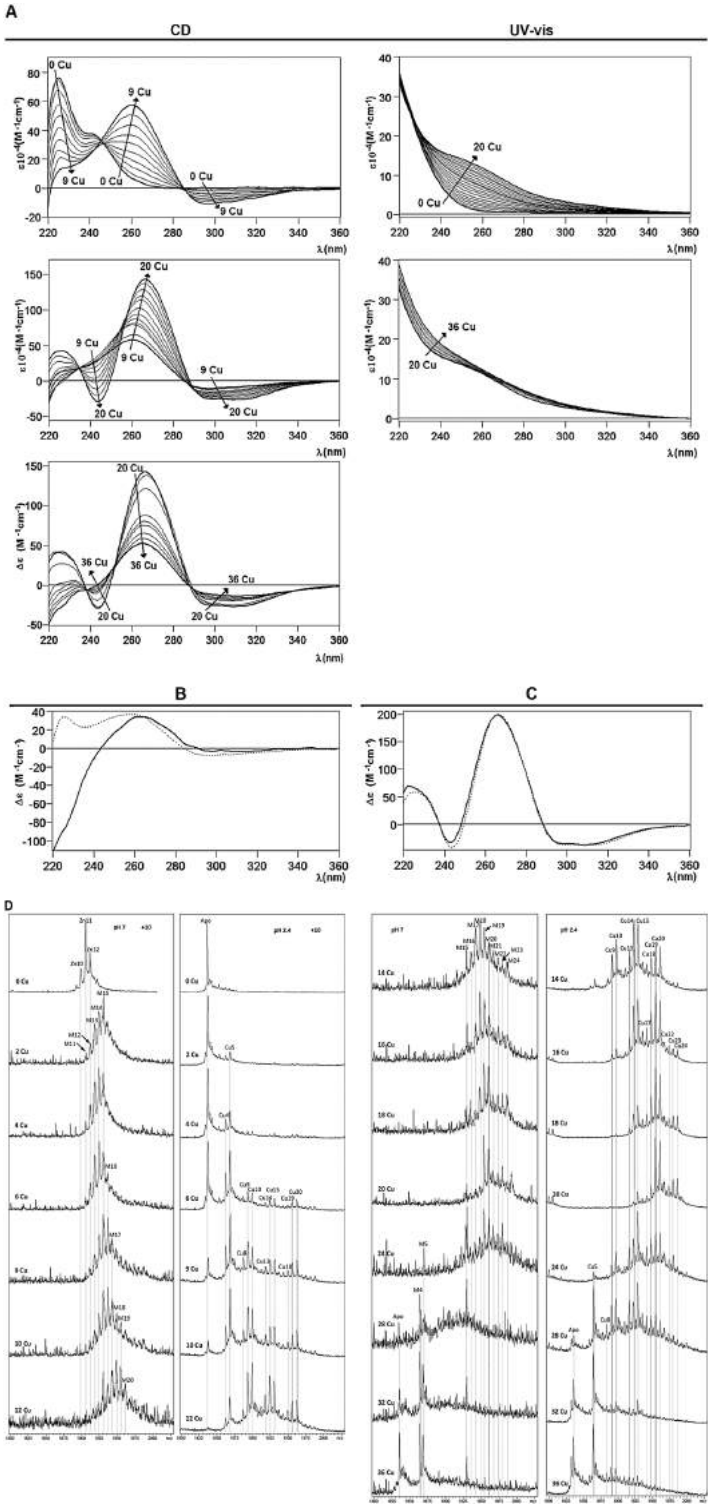

Fig. 7 (A) CD and UV-vis spectra recorded after the addition of Cu(I) to the Zn–CnMT2 preparation. (B) CD spectra corresponding to the Cu–CnMT2 preparation under normal aeration (solid line) and that recorded after the addition of 6 Cu(I) eq. to the Zn–CnMT2 preparation (dotted). (C) CD spectra corresponding to the Cu–CnMT2 preparation under low aeration (solid line) and that recorded after the addition of 20 Cu(I) eq. to the Zn–CnMT2 preparation (dotted). (D) ESI-MS spectra recorded after the addition of Cu(I) to the Zn–CnMT2 preparation, recorded at neutral and acidic pH, at the +10 charge state.

also very important (Fig. 6B). Probably due to the extraordinary length of CnMT2, and differing from CnMT1, the syntheses of this polypeptide under low aeration conditions rendered heteronuclear Zn, Cu-MT preparations (mean content according to ICP-AES results of 2 Zn: 21 Cu per CnMT2), with major M_{24}–CnMT2 and a myriad of minor species (Fig. 6C). Since acid ESI-MS resolved most of these as 20 Cu(I)-, and 24 Cu(I)-containing species, it is likely that most, if not all, M_{24}–CnMT2 complexes could be homonuclear species (Fig. 6D). Regarding the spectroscopic characterization of Cu–CnMT2 preparations, and despite their CD spectra not being obviously representative of unique species, it is clearly shown that the observed fingerprints fully coincide with those of Cu–CnMT1 (Fig. 6E and F). They are contributed by the Cu–MT thiolate absorptions, including the 300–340 nm signals corresponding to the special binding sites for Cu(I) characteristic of the Cu-thioneins.

3.5.4. Cu(I)-binding by CnMT2: Zn/Cu displacement in Zn–CnMT2. As for CnMT1, revealing data for the Cu(I) binding abilities of CnMT2 came from the deep analysis of its Zn/Cu exchange reaction, performed until 36 Cu(I) eq. added to Zn–CnMT2. Hence, analogously, the corresponding CD spectra (Fig. 7) exhibited very nice isodichroic points from 0 to 9, 9 to 20 and 20 to 36 Cu(I) eq. added, which suggested cooperative copper loading and zinc displacement processes. These stages were not isosbestic, and the variation of the CD absorbance at 230 and 260 nm clearly indicated that there are important changes around 9 and 20 Cu(I) eq. added (Fig. 7A). In the first period, two isodichroic points were observed, with a neat increase of the Gaussian band centered at 260 nm, and the negative absorption at *ca.* 300 nm. In the second step, between 9 and 20 Cu(I) eq. added, the spectra follow a similar pattern to that in the first phase, with two nice isodichroic points at 235 and 287 nm and the CD absorption at *ca.* 270 reaching its highest intensity. Finally, in the last titration stage, for more than 20 eq. Cu(I) added, the CD fingerprint decreases its intensity, probably as a result of the MT cluster unfolding (Fig. 7A). ESI-MS monitoring of the process revealed that although no cooperativity can be claimed, Cu_4–Cu_5, Cu_9–Cu_{10}, Cu_{14}–Cu_{15}, Cu_{19}–Cu_{20}, and Cu_{23}–Cu_{24} pairs of complexes were favored when increasing amounts of Cu(I) were added to the sample (Fig. 7D). The addition of Cu(I) increases the complexity of the initial Zn_{11}–CnMT2 sample in terms of the number of species present. But contrasting with this heterogeneity, acid MS spectra revealed that CnMT2 also builds its metallic complexes on the basis of Cu_5-building blocks, here until a total of five Cu_5 clusters. Interestingly, it also seems that just one of the Cu(I) ions in one of the Cu_5 clusters exhibits a certain instability that leads to the observed *perfect series* of doublets of ESI MS peaks. These doublets of mass peaks gain in intensity during all the process until 20 Cu(I) eq. added. Afterwards, their abundance and nuclearity diminish until the end of the reaction (32–36 Cu(I) eq. added) when only the very stable Cu_5-core, and in this case also apo–CnMT2 remain in solution. Also like for CnMT1, two different steps of the titration (here, after 6 and 20 Cu(I) eq. added to Zn–CnMT2) nicely reproduced the features of the *in vivo* samples obtained under normal and low aerated bacterial culture conditions, respectively. The CD spectra at these two points of the titrations also reproduce the CD fingerprints of the normal and low aerated Cu–CnMT2 recombinant preparations (Fig. 7B and C, respectively), as described for CnMT1. Of note, the presence of complexes containing a $(5n - 1)$ number of Cu(I) ions (n being the number of the hypothetical Cu_5-units) accompanying the Cu_{5n}–CnMT2 peaks is also constant during all the Zn/Cu substitution reaction (Fig. 7D), as before commented for CnMT1, so that a parallel interpretation of this result is envisaged. Most significantly, in the case of CnMT2 this applies to the highest Cu(I) stoichiometry detected both *in vivo* and *in vitro* (Cu_{24}–CnMT2) because a Cu_{25}–CnMT2 species has been observed in no case. Finally, the observation that there are no CnMT2 complexes containing supernumerary Cu(I) ions beyond $5n$ values is concordant with the lack of flanking Cys doublets in this isoform, contrary to the case observed for the CnMT1 polypeptide.

4. Conclusions

The *C. neoformans* CnMT1 and CnMT2 metallothioneins exhibit all the coordination features typical of genuine Cu-thioneins, this including an optimal Cu-binding behavior, while suboptimal divalent metal ion binding characteristics.[7] The *C. neoformans* MT system constitutes another outstanding example of how different criteria for considering MT as either divalent-metal-ion thioneins (Zn- or Cd-thioneins) or Cu-thioneins, precisely their gene response pattern or the specificity of their protein function, converge to the same classification. Hence, the detailed study of the metal-binding preferences of both CnMT1 and CnMT2 presented in this work, which attributes to these proteins an unambiguous character of Cu-thioneins perfectly matching the fact of being encoded by genes belonging to the *C. neoformans* copper regulon.[6] This confirms that gene transcription induction by a given effector and optimized function of the corresponding protein towards this effector are strongly correlated in a gene–protein system, as we had previously shown for the *Drosophila melanogaster* Cu-thionein family.[25]

Recombinant synthesis both in Zn(II)- and Cd(II)-enriched *E. coli* cultures rendered a low yield of complexes, exhibiting variable stoichiometries. Besides, the S^{2-}-containing Cd-MT species that are invariably rendered by Cu-thioneins when synthesized in Cd-rich media were clearly identified for both isoforms. Finally, the Zn(II)/Cd(II) displacement process gave rise to a myriad of Zn,Cd-mixed species, present even at the end of the metal replacement reaction, in full agreement with a poor divalent metal ion binding ability. In contrast, the characterization of their Cu(I) coordination properties clearly showed how the CnMT1 and CnMT2 polypeptides are optimized to yield well-folded, high Cu(I)-containing complexes. The nature of these complexes reflects the copper concentration of the surrounding medium, as shown before for the *S. cerevisiae* Crs5 MT,[15] so that under high-Cu conditions both isoforms would exert their maximum detoxification abilities, rendering Cu_{16}–CnMT1 and Cu_{24}–CnMT2 homometallic species. Zn(II)/Cu(I)

replacement reactions proceed by discrete steps of 5 Cu(I) ion incorporations, and in full correspondence with the recombinantly synthesized complexes. This prompted us to propose that the Cu(I)–CnMT species are built on the basis of Cu_5-clusters, a copper–thiolate cluster structure unprecedented in the literature of copper-aggregates in MTs. Significantly, the modular structure of the CnMT1 and CnMT2 polypeptides, constituted by three and five Cys-rich regions separated by spacer stretches, further supports this hypothesis, if assuming that the final stoichiometries (Cu_{16}- and Cu_{24}-) of the homometallic Cu(I)–CnMT species folded *in vivo* at high Cu concentrations represent the respective three- and five-fold amplification of the basic Cu_5-core unit identified in the Cu titration reaction.

Comparison of the CnMT1 and CnMT2 gene and protein sequence features strongly coincide in supporting the emergence of the long *C. neoformans* MTs by ancient tandem repetitions of a primeval fungal MT unit, currently represented by the *Neurospora*[26] and *Agaricus*[27] MT proteins. These are the smallest known MTs (27-amino acid long), characterized by a $-X_3$-[CXC]-X_5-[CXC]-X_3-[CXC]-X_2-CX_3- signature, and encoded by a gene including one single intron.[28] This Cys pattern almost exactly coincides with the Cys-boxes hypothesized in this work to be the building blocks of CnMT1 and CnMT2 (*cf.* Fig. 1), with the only difference that both *Neurospora* and *Agaricus* MTs were described to yield Cu_6-complexes,[29–31] instead of the Cu_5-clusters here reported for the CnMTs. Further work is being carried out in our laboratories to characterize the coordination features of these CnMT building regions and their additive capacity in order to understand how the natural selection pressure to cope with high copper concentrations may have conditioned this amplification of a primeval fungal copper-chelating small peptide.

Conclusively, this study contributes to the characterization of the high Cu(I) binding capacity of *C. neoformans* MTs, which act as a microbial pathogenicity and virulence determinant. The consideration of copper as an active agent used by the immune system (*i.e.* macrophages) of infected organisms against the invading microbes, and the study of the consequent counteracting mechanisms developed by the pathogens to thrive in this adverse surrounding, have lately gathered high research efforts (*cf.* excellent recent reviews[32,33]). Both bacterial (*Enterococcus hirae*, *Salmonella typhimurium* and *Mycobacterium tuberculosis*) and fungal (*Cryptococcus neoformans*) pathogens exhibit either cytoplasmic copper export or/and copper sequestration strategies to tolerate high copper. Therefore, the characterization of the regulation and function of these gene–protein systems attains significant importance in the context of understanding the copper homeostasis at the host–pathogen interface. CnMT1 and CnMT2 play an essential role in *C. neoformans* copper resistance, since MT proteins are the main mechanism of metal homeostasis in eukaryotic cells, in contrast to metal ion export that predominates in prokaryotes. Nevertheless, it is significant that MTs or MT-like proteins such as MymT in *M. tuberculosis*,[34] CusF in *E. coli*,[35] and CueP in *S. typhimurium*[36,37] have been recently identified in bacteria, which promisingly points to a putative role as virulence factors also in pathogenic bacteria.

Abbreviations

MT	Metallothionein
CnMT	*Cryptococcus neoformans* metallothionein

Acknowledgements

This work was supported by the Spanish *Ministerio de Economía y Competitividad*, grants BIO2012-39682-C02-01 (to SA) and 02 (to MC), which are co-financed by the European Union through the FEDER program, and NIH grant GM41840 to DJT. Authors from both Barcelona universities are members of the 2009SGR-1457 *Grup de Recerca de la Generalitat de Catalunya*. We thank the *Centres Científics i Tecnològics (CCiT) de la Universitat de Barcelona* (ICP-AES, DNA sequencing) and the *Servei d'Anàlisi Química (SAQ) de la Universitat Autònoma de Barcelona* (CD, UV-vis, ESI-MS) for allocating instrument time.

References

1 M. Capdevila and S. Atrian, *J. Biol. Inorg. Chem.*, 2011, **16**, 977–989.
2 M. Capdevila, R. Bofill, O. Palacios and S. Atrian, *Coord. Chem. Rev.*, 2012, **256**, 46–62.
3 O. Palacios, S. Atrian and M. Capdevila, *J. Biol. Inorg. Chem.*, 2011, **16**, 991–1009.
4 C. Ding, R. A. Festa, Y. L. Chen, A. Espart, O. Palacios, J. Espin, M. Capdevila, S. Atrian, J. Heitman and D. Thiele, *Cell Host Microbe*, 2013, **13**, 265–276.
5 J. W. Kronstad, R. Attarian, B. Cadieux, J. Choi, C. A. D'Souza, E. J. Griffiths, J. M. Geddes, G. Hu, W. H. Jung, M. Kretschmer, S. Saikia and J. Wang, *Nat. Rev. Microbiol.*, 2011, **9**, 193–203.
6 C. Ding, J. Yin, E. M. Tovar, D. A. Fitzpatrick, D. G. Higgins and D. J. Thiele, *Mol. Microbiol.*, 2011, **81**, 1560–1576.
7 R. Bofill, M. Capdevila and S. Atrian, *Metallomics*, 2009, **1**, 229–234.
8 B. Dolderer, H. J. Hartmann and U. Weser, in *Metal Ions in Life Sciences: Metallothioneins and Related Chelators*, ed. A. Sigel, H. Sigel and R. K. O. Sigel, RSC Publishing, Cambridge, UK, 2009, vol. 5, pp. 83–106.
9 V. Calderone, B. Dolderer, H. J. Hartmann, H. Echner, C. Luchinat, C. del Bianco, S. Mangani and U. Weser, *Proc. Natl. Acad. Sci. U. S. A.*, 2005, **102**, 51–56.
10 P. A. Cobine, R. T. McKay, K. Zangger, C. T. Dameron and I. M. Armitage, *Eur. J. Biochem.*, 2004, **271**, 4213–4221.
11 K. B. Nielson, C. L. Atkin and D. R. Winge, *J. Biol. Chem.*, 1985, **260**, 5342–5350.
12 L. T. Jensen, J. M. Peltier and D. R. Winge, *J. Biol. Inorg. Chem.*, 1998, **3**, 627–631.
13 R. Bofill, O. Palacios, M. Capdevila, N. Cols, R. Gonzalez-Duarte, S. Atrian and P. Gonzalez-Duarte, *J. Inorg. Biochem.*, 1999, **73**, 57–64.
14 S. Díaz, F. Amaro, D. Rico, V. Campos, L. Benítez, A. Martin-Gonzalez, E. P. Hamilton, E. Orías and J. C. Gutierrez, *PLoS One*, 2007, **3**, e291.
15 A. Pagani, L. Villarreal, M. Capdevila and S. Atrian, *Mol. Microbiol.*, 2007, **63**, 256–269.

16 M. Capdevila, N. Cols, N. Romero-Isart, R. Gonzalez-Duarte, S. Atrian and P. Gonzalez-Duarte, *Cell. Mol. Life Sci.*, 1997, **53**, 681–688.
17 N. Cols, N. Romero-Isart, M. Capdevila, B. Oliva, P. Gonzalez-Duarte, R. Gonzalez-Duarte and S. Atrian, *J. Inorg. Biochem.*, 1997, **68**, 157–166.
18 R. Bofill, O. Palacios, M. Capdevila, N. Cols, R. Gonzalez-Duarte, S. Atrian and P. Gonzalez-Duarte, *J. Inorg. Biochem.*, 1999, **73**, 57–64.
19 J. Bongers, C. D. Walton, D. E. Richardson and J. U. Bell, *Anal. Chem.*, 1988, **60**, 2683–2686.
20 M. Capdevila, J. Domenech, A. Pagani, L. Tio, L. Villarreal and S. Atrian, *Angew. Chem., Int. Ed.*, 2005, **44**, 4618–4622.
21 D. Fabris, J. Zaia, Y. Hathout and C. Fenselau, *J. Am. Chem. Soc.*, 1996, **118**, 12242–12243.
22 L. Tío, L. Villarreal, S. Atrian and M. Capdevila, *J. Biol. Chem.*, 2004, **279**, 24403–24413.
23 S. Perez-Rafael, A. Kurz, M. Guirola, M. Capdevila, O. Palacios and S. Atrian, *Metallomics*, 2012, **4**, 342–349.
24 E. Artells, O. Palacios, M. Capdevila and S. Atrian, *Metallomics*, 2013, **5**, 1397–1410.
25 D. Egli, J. Domenech, A. Selvaraj, K. Balamurugan, H. Hua, M. Capdevila, O. Georgiev, W. Schaffner and S. Atrian, *Genes Cells*, 2006, **11**, 647–658.
26 K. Lerch, *Nature*, 1980, **284**, 368–370.
27 K. Münger and K. Lerch, *Biochemistry*, 1985, **24**, 6751–6756.
28 K. Münger, U. A. German and K. Lerch, *EMBO J.*, 1985, **4**, 2665–2668.
29 M. Beltramini and K. Lerch, *Biochemistry*, 1983, **22**, 2043–2048.
30 T. A. Smith, K. Lerch and K. O. Hodgson, *Inorg. Chem.*, 1986, **25**, 4677–4680.
31 M. Beltramini, K. Lerch and M. Vasak, *Biochemistry*, 1984, **23**, 3422–3427.
32 M. I. Samanovic, C. Ding, D. Thiele and H. K. Darwin, *Cell Host Microbe*, 2012, **11**, 106–115.
33 V. Hodgkinson and M. J. Petris, *J. Biol. Chem.*, 2012, **287**, 13549–23555.
34 B. Gold, H. Deng, R. Bryk, D. Vargas, D. Eliezer, J. Roberts, X. Jiang and C. Nathan, *Nat. Chem. Biol.*, 2008, **4**, 609–616.
35 S. Fanke, G. Grass, C. Resing and D. H. Nies, *J. Bacteriol.*, 2003, **185**, 3804–3812.
36 L. B. Pontel and F. C. Soncini, *Mol. Microbiol.*, 2009, **73**, 212–225.
37 D. Osman, K. J. Waldron, H. Denton, C. M. Taylor, A. J. Grant, P. Mastroeni, N. J. Robinson and J. S. Cavet, *J. Biol. Chem.*, 2010, **285**, 25259–25268.

Publication # 4

Understanding the internal architecture of long metallothioneins: 7-Cys building blocks in fungal (*C. neoformans*) MTs.

PUBLICATION #4:

TITLE

"Understanding the internal architecture of long metallothioneins: 7-Cys building blocks in fungal (*C. neoformans*) MTs"

AUTHORS

Anna Espart, Selene Gil-Moreno, Òscar Palacios, Mercè Capdevila, Sílvia Atrian.

REFERENCE

Version 2 submitted for publication in Molecular Microbiology.

SUMMARY

The genome of the opportunistic fungus *Cryptococcus neoformans*, encodes two metallothioneins (MTs), CnMT1 and CnMT2, which are considered genuine Cu-thioneins (Bofill et al., 2009) (Palacios et al., 2011) for their exceptional capacity in Cu-binding. Both are the longest identified MTs in fungi so far, with 122 amino acids in CnMT1 and 183 amino acids in CnMT2, being comparable with those in the ciliate *Tetrahymena* (Espart et al., 2015) which possess also long MTs. Previous studies showed the ability of CnMTs to coordinate high amounts of Cu(I) through 7-Cys segments, separated by spacer regions lacking cysteine residues, those folding into unreported clusters of 5 Cu(I) (Palacios, Espart, et al., 2014a), which accounts for the extraordinary potential for copper detoxification that was showed in the work of Ding et al. (Ding et al., 2013). The collected data aimed us to continue studying these MTs, to comprehend their internal structure hypothetically built by modular blocks.

Seven different segments (S1 to S7) of CnMT1 were designed and the cDNAs encoding each of them were subcloned into the *E.coli* expression vector. *E. coli* transformants were grown to obtain the corresponding recombinant proteins synthesized in Zn- or Cu-supplemented media. The subsequent spectroscopic and spectrometric analysis of the purified complexes illustrated about the ability of the seven fragments to bind each metal ion. S1, S2 and S3 (containing one 7-Cys segment) rendered Zn_2-complexes; S4 (with 9-Cys: one 7-Cys box plus 2 flanking Cys), Zn_3- and minor Zn_4-species; for S6 and S7 (with 2 and 3 blocks of 7-Cys, respectively), the identified species were Zn_4-S6 and major Zn_7- and minor Zn_8- and

Zn_6-complexes in S7. Unfortunately, S5 did not allow recovering any stable complex. Cu-supplementated syntheses yielded Cu_5-complexes for S1, S2, S3 and S4, whereas S6 folded into Cu_9- and Cu_{10}-species; and S7 rendered M_{10}- and M_9- (with minor M_{11}- and M_{13}-complexes; M=Zn or Cu) including Cu_9- and Cu_5-S7 cores according to acid ESI-MS results. Once again, no metal-complexes could be retrieved for S_5.The Zn(II)/Cu(I) replacement analyses, followed by ESI-MS, CD and UV-vis, confirmed the formation of Cu_5-clusters for the S1, S2, and S3 (one 7-Cys box) segments. The presence of different spacers and flanking regions in the CnMT1 fragments, appears to play an interesting role, helping in the stabilisation of the conformed metal-complexes. Finally each CnMT1-Sx (except S5, which showed poor results), as well as CnMT1 and CnMT2, was tested to prove for copper tolerance in the 51.2cΔc5 yeast strain lacking its own two MTs (CUP1 and CRS5). After the required cloning of each cDNA in the suitable yeast expression shuttle vector, the transformed yeast cells were allowed to growth in copper-supplemented liquid and agar media. In conclusion, all the results supported the hypothesis that each 7-Cys block of CnMTs constitute the basic unit responsible of every Cu_5-cluster. Probably the evolution fixed this unusually long repeated structures to increase the Cu binding capacity of these MTs. These results contrast with those of *N. crassa* MT which exhibits a sequence highly similar to one CnMT unit, and yields metal complexes including five Cu(I) ons (unpublished results from our group).

Contribution to this work

This work has been performed in collaboration with the group of Dr. Mercè Capdevila, in the department of Chemistry of the Universitat Autònoma de Barcelona (UAB).

My contribution to this work was: i) the participation in the design of the studied cDNA fragments; ii) the construction of the suitable *E. coli* expression vectors for the seven CnMT1-Sx, and the subsequent recombinant synthesis and purification of CnMT1-Sx mutant, from *E. coli* cultures supplemented with Zn and Cu. Purification of the metal-CnMT1-Sx complexes and spectroscopic analyses; and iii) the performing of the Cu tolerance test by yeast complementation assays.

Understanding the internal architecture of long metallothioneins: 7-Cys building blocks in fungal (*C. neoformans)* MTs

Anna Espart[‡], Selene Gil-Moreno[#], Oscar Palacios[#], Mercè Capdevila[#] and Sílvia Atrian[‡§]

[‡] *Departament de Genètica, Facultat de Biologia, Universitat de Barcelona, 08028 Barcelona, Spain*

[#] *Departament de Química, Facultat de Ciències, Universitat Autònoma de Barcelona, 08193 Cerdanyola de Vallès, Spain*

Running title: Modular Fungal Metallothioneins

[§] For correspondence: E-mail: satrian@ub.edu; Tel (+34) 93 4021501; Fax: (+34) 934034420.

Keywords

Cryptococcus neoformans, Cu-thionein, fungi, metallothionein, modular structure

Abbreviations

CD, circular dichroism;

ESI-MS, electrospray ionization mass spectrometry;

ICP-AES, inductively coupled plasma-atomic emission spectroscopy;

MT(s), Metallothionein(s)

Summary

Cryptococcus neoformans metallothioneins (MTs), CnMT1 and CnMT2, have been identified as essential infectivity and virulence factors of this pathogen. Both MTs are unusually long Cu-thioneins, exhibiting protein architecture and metal-binding abilities compatible with the hypothesis of resulting from three and five tandem repetitions of 7-Cys motives, respectively, each of them folding into Cu_5-clusters. Through the study of the Zn(II)- and Cu(I)-binding capabilities of several CnMT1 truncated mutants, we show that a 7-Cys segment of CnMT1 folds into Cu_5-species, of additive capacity when joined in tandem. This same basic unit forms Zn_2-cores when coordinating Zn(II). All the obtained Cu-complexes share practically similar architectural features, if judging by their almost equivalent CD fingerprints, and they also share their capacity to restore copper tolerance in MT-devoid yeast cells. Besides the analysis of the modular composition of long fungal MTs, we show in this work that the role of the spacer and flanking sequences of Cys-rich stretches, even when encompassing additional Cys residues, is more critical for the stability of the conformed clusters than for increasing their metal ion binding capacity. Overall, we propose an evolution strategy to explain how MTs may have enlarged their original metal coordination capacity under specific selective pressure requirements.

INTRODUCTION

In recent years, metal handling and metabolism have emerged as clear determinants of fungal microbe pathogenicity and virulence (Samanovic *et al.,* 2012; Hodgkinson *et al.,* 2012; Staats *et al.,* 2013; Ding *et al.,* 2014). In this scenario, it has recently been shown that the opportunistic basidiomycete *Cryptococcus neoformans*, responsible for potentially lethal cryptococcosis, senses the Cu ions mobilized by the host macrophages as innate defense and neutralizes their toxic effect, thus allowing the progression of the infection (Ding *et al.,* 2013). The two *C. neoformans* metallothioneins (MTs), CnMT1 and CnMT2, in particular, have been identified as virulence factors required for host pulmonary colonization and spreading, mutant fungi defective in both proteins exhibiting highly reduced virulence (Ding *et al.,* 2013). It has been shown that CnMT1 and CnMT2 Cu-detoxifying function comes from their extraordinary Cu-binding capacity, and that they have all the features to be considered typical Cu-thioneins. Cu-thioneins are a subset of MTs (Bofill *et al.,* 2009; Palacios *et al.*, 2011a), the

heterogeneous superfamily of ubiquitous, small, Cys-rich proteins that have been identified in all eukaryotes and most prokaryotes so far analyzed (latest reviews in Capdevila *et al.,* 2012; Blindauer, 2014). However, unlike the paradigmatic Cu-thioneins (Dolderer *et al.,* 2009) such as the yeast (*Saccharomyces cerevisiae*) CUP1 protein and the fungus *Neurospora crassa* MT, which are very small proteins of 53 and 26 amino acids respectively, *C. neoformans* MTs were characterized as unexpectedly long MTs, CnMT1 consisting of 122 amino acids (*cf*. Fig. 1A) and CnMT2 with 183 amino acids (Ding *et al.,* 2013). Strikingly, the other known "long MTs" are the five isoforms present in several species of another unicellular eukaryote: the ciliate *Tetrahymena* (*T. pigmentosa* and *T. pyriformis*), with lengths ranging between 96 and 181 amino acids (Diaz *et al.,* 2007), the metal binding features of which have been recently comprehensively analyzed (Espart *et al.,* 2015).

Full evaluation of the divalent and monovalent metal ion binding abilities of CnMT1 and CnMT2 (Palacios *et al.,* 2014) clearly showed how these polypeptides are optimized to yield well-folded, high-Cu(I) containing complexes, the nature of which reflects the copper concentration of the surrounding medium, as reported before for the *S. cerevisiae* Crs5 MT (Pagani *et al.,* 2007). This entails that, at high-Cu conditions, both isoforms would exert their maximum detoxification abilities, folding into homometallic copper-species. But most strikingly, we demonstrated how the progression of the Zn/Cu replacement on Zn-CnMT1 and Zn-CnMT2 complexes is a cooperative reaction, proceeding by discrete steps of 5 Cu(I) ion incorporations. This prompted us to suggest the formation of unusual Cu_5-building blocks, different to the Cu-clusters so far reported for any MT. Significantly, the modular structure of the CnMT1 and CnMT2 polypeptide sequences, respectively constituted by three and five 7-Cys regions separated by spacer stretches, further supported this hypothesis, if assuming that the homometallic Cu-CnMT species folded *in vivo* at high Cu concentrations represent the respective three- and five-fold amplification of basic Cu_5-(7-Cys) clusters (Palacios *et al.,* 2014). Comparison of the CnMT1 and CnMT2 gene and protein sequence features strongly supported the emergence of the long *C. neoformans* MTs by ancient tandem repetitions of a primeval fungal MT unit, precisely comprising seven Cys residues. Hence, the Cys pattern of the *Neurospora* and *Agaricus* MTs (X_2-[CXC]-X_5-[CXC]-X_3-[CXC]-X_2-C-X_3) (Lerch, 1980; Münger and Lerch, 1985; respectively) almost coincided with that of the 7-Cys boxes considered as the building blocks of CnMT1 and CnMT2 (Fig. 1B). However, it is worth noting that both *Neurospora* and *Agaricus* MTs were described to yield Cu_6- instead of Cu_5-clusters (Cobine *et al.,* 2004).

In this scenario, we considered it highly relevant to analyze the coordination features of these unprecedented Cu_5-(7-Cys) building regions, their additive capacity and their relation with the reported *Neurospora* MT Cu-binding abilities. This would contribute to understand how the pressure to cope with high copper concentrations may have positively selected the natural amplification of a small primeval fungal copper-chelating peptide, and ultimately, to unveil which are the sequence requirements that allow long MTs to build stable metal-complexes. To this end, we recombinantly synthesized seven CnMT1 truncated mutants, encompassing one, two or three 7-Cys fragments, and exhibiting different combinations of spacer regions and/or flanking amino acids at their N- and C-terminal ends (Fig. 1). On the one hand, their Zn- and Cu-binding abilities were determined through the characterization of their respective Zn- and Cu-species folded *in vivo* in *E. coli*, and *in vitro* (by Zn/Cu replacement on the corresponding recombinant Zn-species), by means of spectroscopic and spectrometric techniques. Furthermore, their Cu-chelating features, as well as those of the full-length CnMT1 polypeptide, were evaluated by their functional competence to detoxify Cu in yeast MT-knockout cells. Our results confirmed the modular origin and organization of CnMT1 and CnMT2 peptides regarding metal cluster formation, and the evolutionary relationship that may link these MTs with the other well-studied fungal copper-thioneins (*Neurospora* and *Agaricus*). But even more interestingly, the data here provided are relevant not only to understand the internal architecture of *C. neoformans* MTs, but also to shed light on the role of the MT regions other than Cys-motifs, *i.e*. spacers and flanking amino acids, which determine the stability of a given metal-MT complex, and therefore the ability of an MT to optimally bind that metal ion.

RESULTS AND DISCUSSION

Cloning and recombinant synthesis of the CnMT1:Sx peptides

For the sake of brevity, the different CnMT1:Sx (x from 1 to 7, *cf*. Fig. 1) segments will be referred to as Sx throughout this work. Once the pGEX constructs coding for the Sx peptides had been confirmed by DNA sequencing, preliminary protein expression assays allowed the identification of their respective apo-forms by electrospray ionization mass spectrometry (ESI-MS) through the acidification to pH 2.4 of the corresponding Zn-Sx

preparations (Table 1). These results confirmed, not only the identity but also the integrity of the obtained peptides.

Table 1. Experimental molecular masses of the recombinant Sx apo-peptides. The corresponding ESI-MS spectra are shown in Supplementary Figures S1 to S7.

Peptide	Experimental MM	Calculated MM[a]
S1	2333	2333.6
S2	3261	3260.8
S3	3191	3191.6
S4	3899	3899.3
S5	3847	3847.4
S6	5349	5350.1
S7	8983	8984.1

[a] Calculated mean molecular mass for neutral species.

Zn(II) binding abilities of the CnMT1:Sx peptides and comparison with the full length CnMT1 protein

The species formed when the *C. neoformans* full-length MTs coordinate Zn(II) were Zn_7- and Zn_8-CnMT1, and Zn_{11}-CnMT2 (Palacios *et al.,* 2014). Taking into account the composition of three 7-Cys boxes for CnMT1 and five for CnMT2, these results suggest that each 7-Cys box would be able to optimally bind 2 Zn(II), while the flanking Cys residues would account for the coordination of the additional Zn(II) ions of the complexes. This assumption was fully corroborated by the behavior of the CnMT1 truncated mutants studied in this work (Table 2). Hence, all the peptides consisting in one 7-Cys box and without extra Cys (*i.e*. S1, S2 and S3) yielded Zn_2-complexes as major products when biosynthesized in Zn-enriched cultures. In the case of the S4 peptide, the Zn(II) content of the recovered complexes was slightly increased up to a major Zn_3 and a very minor Zn_4 species, in good concordance with the presence of two flanking Cys residues at its C-terminal end. It is worth noting that the 3 Zn:9 Cys ratio observed for S4 precisely coincides with the well-know stoichiometry reported for the mammalian MT ß domain, from the first characterization of its metal binding features from native sources (Otvos and Armitage, 1980) and later corroborated by recombinantly prepared complexes (Capdevila *et al*., 1997). This ratio was thereafter corroborated for other 9 Cys MT domains, such as the C-terminal echinodermata (*S.purpuratus*) MT moiety (Wang *et al*., 1995; Tomas *et al*., 2013), or both moieties of the

crustacean (*H.americanus* and other) MTs (Valls *et al.,* 2001). No Zn-complex could be detected by ESI-MS for S5, which is attributable to a marked instability of the Zn-S5 association and not to the lack of protein synthesis -since the apo-S5 peptide was clearly identified (Table 1 and Fig. S5)-, or to the lack of metal -since a comparable amount of Zn(II) to that of S4 was detected by ICP (Table 2)-. In S6, the presence of two 7-Cys blocks automatically doubled the Zn(II) content of the major complexes, resulting in a major Zn_4-S6. Finally, the S7 peptide (three 7-Cys segments) yielded a mixture of major Zn_7-S7 and minor Zn_8-S7 plus Zn_6-S7 complexes, which again is concordant with 2 Zn(II) per 7-Cys box, and some extra Zn(II) possibly contributed by some terminal-to-bridging Zn-SCys bond conversion.

Fig. 1. (A) Sequence alignment of the CnMT1 full-length protein and the corresponding segments (Sx) analyzed in this work. Cys residues are in bold, and the spacer segments between 7-Cys boxes are shadowed in gray. All the Sx segments were expressed in the same GST-fusion system as the entire CnMT1 had been (Palacios et al., 2014) and therefore, the corresponding recombinant peptides exhibit a N-terminal *GS* dipeptide, which has been shown not to alter the MT binding properties (Cols et al., 1997). **(B)** Alignment of the 7-Cys box present in the S1 peptide with the MTs of *Neurospora crassa* and *Agaricus bisporus*.

Table 2. Analytical characterization of the recombinant Zn(II)-Sx complexes. For comparative purposes, data for the full length CnMT1 are included (Palacios *et al.*, 2014).

Peptide	ICP-AES[a]	Neutral ESI-MS[b]	Experimental MM[c]	Calculated MM[d]
S1 (7 Cys)	0.68	**Zn_2-S1**	2460	2460.4
		Zn_1-S1	2396	2397.1
S2 (7 Cys)	1.87	**Zn_2-S2**	3387	3387.5
		Zn_1-S2	3323	3324.2
S3 (7 Cys)	1.19	**Zn_2-S3**	3317	3318.4
		Zn_3-S3	3380	3381.8
		Zn_4-S3	3442	3445.1
		Zn_1-S3	3251	3255.0
		apo-S3	3187	3191.6
S4 (9 Cys)	3.52	**Zn_3-S4**	4088	4089.5
		Zn_4-S4	4150	4152.9
S5 (9 Cys)	3.30	---	---	---
S6 (14 Cys)	3.39	**Zn_4-S6**	5604	5603.7
		Zn_5-S6	5666	5667.1
		Zn_3-S6	5540	5540.0
S7 (21 Cys)	6.09	**Zn_7-S7**	9427	9427.8
		Zn_8-S7	9489	9491.2
		Zn_6-S7	9362	9364.4
CnMT1 (25 Cys)	7.88	**Zn_8-MT1** Zn_7-MT1	(Palacios *et al.*, 2014)	(Palacios *et al.*, 2014)

[a] Zn(II)-to-peptide ratio calculated from S and Zn content (ICP-AES data).
[b] The deduced Zn(II)-species were calculated from the mass difference between the holo- and apo-peptides. The major species are indicated in bold.
[c] Experimental molecular masses corresponding to the detected Zn(II)-Sx complexes. The corresponding ESI-MS spectra are shown in Fig. 4, Fig. 5 and Supplementary Figures S1 to S7
[d] Theoretical molecular masses corresponding to the Zn(II)-Sx complexes.
(---) means non-detected.

Comparison of this collection of Zn-complexes allows some considerations to be made on the role of the Cys residues positioned outside the 7-Cys blocks, and of the spacer and flanking regions devoid of Cys residues. No differences could be detected between S1 and S2, and therefore no significant role has to be assumed for the presence of the N-terminal spacer in S2. Contrarily, the C-terminal spacer of S3 slightly increased the Zn binding capacity of the 7-Cys box, because minor Zn_3- and Zn_4-species were detected, which could be explained by the presence of one glutamic acid in this stretch. Further information is obtained from the comparison between S7 and the full-length CnMT1. Unexpectedly, the fact that CnMT1 has four more Cys than S7 does not considerably enlarge its Zn-binding capacity, since the only

difference is that CnMT1 folds into major Zn_8- and minor Zn_7-complexes, while for S7, the Zn_7-species predominates. This suggests a function of the two flanking spacers plus the two outside Cys-X-Cys pairs (*cf*. Fig. 1) more associated with a stabilizing (or *closing*) role of the metal cluster than to an increase of Zn-coordination capacity.

It is worth noting that the CD fingerprints (Fig. 2) of all the analyzed Zn-Sx preparations are very similar among them, except for those of S4 and S5. Hence, S1, S2, S6 and S7 draw a clear Gaussian band centered at *ca*. 240 nm, characteristic of the absorptions of the $Zn(Cys)_4$ chromophores superimposed to the 220-230 nm absorptions contributed by the peptide bonds, and which are coincident in shape, although far less intense, to that of the entire Zn-CnMT1 complex (Fig. 2). The observed lack of chirality at 240 nm of S3 could be attributed to the mixture of Zn-complexes rendered by this peptide. A poor chirality/degree of folding of the major Zn_3-S4 complex could explain the silent nature of its CD spectrum. Finally, the lack of MS-detectable Zn-S5 species is corroborated by its CD spectrum that resembles that on an apo-peptide

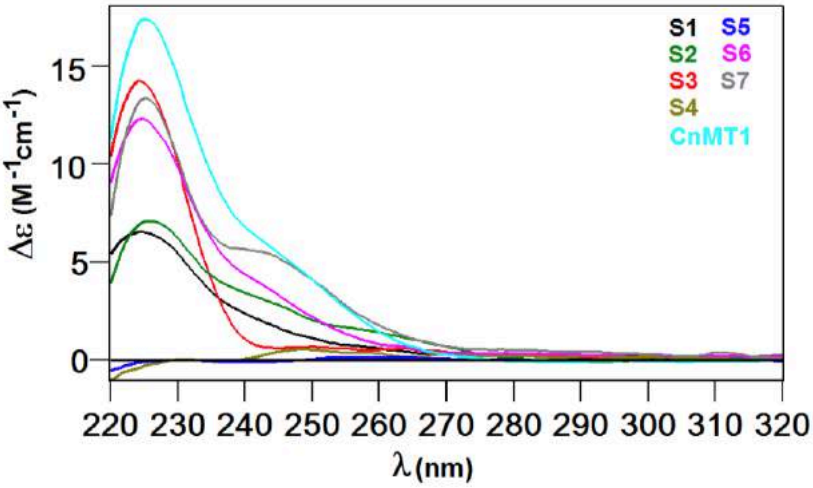

Fig. 2. Comparison of the circular dichroism spectra of the recombinant Zn-Sx preparations as well as that obtained for the CnMT1 protein, which has been normalized to a lower intensity for comparison purposes (Palacios *et al.*, 2014).

Cu(I) binding abilities of the CnMT1:Sx peptides and comparison with the full length CnMT1 protein

A first glance at the results of the syntheses of all the Sx peptides in Cu-enriched bacterial cultures readily showed the extreme Cu-thionein character of the one and two 7-Cys boxes segments –except for S5, *vide infra*-, since all them rendered equivalent results at both culture aeration conditions (Table 3 and Fig. 3), and there were no traces of Zn presence in any of the corresponding Cu-complexes. It is well established that culture oxygenation determine the amount of Cu available in host cells for recombinant MT to form the corresponding complexes; the lower the aeration, the higher the intracellular Cu levels (Pagani *et al*., 2006). Hence, a Cu-thionein will be able to render homometallic Cu-complexes even at regular aeration, when Cu in not specially abundant inside the cell; but at the contrary, a Zn/Cd-thionein will yield heterometallic Zn,Cu-complexes at the same conditions, and only produce homometallic Cu-species when obtained from cells grown under low aeration (*i.e.* high intracellular Cu) (Bofill *et al.*, 2009). Contrarily S7, the three 7-Cys boxes segment, behaved as the full-length CnMT1, because the complexes formed at regular aeration (*i.e.* regular intracellular Cu content) were heterometallic (2.5 Zn:8.7 Cu mean ratio for S7; and 4.2 Zn:5.0 Cu, for CnMT1), but both rendered homometallic Cu-MT complexes when synthesized at low aeration conditions. This indicates that long MTs are more prone than shorter peptides to form Zn,Cu-heterometallic complexes when not synthesized under high Cu concentrations.

All the Sx segments encompassing one 7-Cys box (*i.e*. S1, S2, S3 and S4) yielded major Cu_5-Sx species (Table 3 and Fig. 4), except for S5 for which no Cu-S5 species could be recovered at any culture condition, in agreement with the unsuccessful Zn-S5 synthesis (Tables 2 and 3). Further consideration of the minor species of each synthesis revealed significantly different Cu(I)-binding features of the Sx species. Hence, the presence of an N-term (S2) or a C-term (S3 and S4) flanking spacer (in relation with its absence in S1) conferred stability to the corresponding Cu_5 clusters, as unique Cu_5-Sx (x= 2, 3 and 4) were obtained while a minor Cu_4-S1 was detected for the spacer-devoid S1 peptide. Unexpectedly, the presence of two additional Cys in the final peptide tail of S4 does not apparently enhance the Cu(I)-binding capacity of its 7-Cys core. The results afforded by S6 allowed analyzing the behavior of two 7-Cys-boxes connected by a linker. Significantly, although Cu_5-S6 was the major species produced, Cu_9- and Cu_{10}-S6 could be also detected among the minor species

produced at both aeration conditions (Table 3 and Fig. 5), this indicating that at least a subpopulation of S6 could fill its two 7-Cys boxes with Cu(I). But the fact that Cu_5-, Cu_4-, and even apo-S6, were detected by the acid ESI-MS of the same sample points to a marked instability of Cu_9- and Cu_{10}-S6 if compared with the major Cu_5-S6 complexes. This can be readily explained if assuming that only one of the two 7-Cys boxes of S6 is able to fold into a compact and robust Cu_5-cluster. Finally S7, the three 7-Cys box fragment devoid of N- and C-terminal spacers and adjacent CXC motifs, was the unique CnMT1 truncated mutant that yielded different metal complexes if synthesized in regular or low-aerated Cu-supplemented cultures, as the entire CnMT1 and CnMT2 do (Palacios *et al.,* 2014). Hence, at regular oxygenation, heterometallic Zn,Cu-complexes were recovered, as shown by the ICP-AES results and by the different speciation observed after neutral (major M_{10}- and M_9- and minor M_{11}- and M_{13}-S7, M=Zn or Cu) or acid (major Cu_9- and minor Cu_5- and Cu_{10}-S7) ESI-MS (Table 3 and Fig. 5). Contrarily, only homometallic Cu-complexes were recovered from low-aerated synthesis: major Cu_9- and minor Cu_{14}- and Cu_{12}-S7 according to acidic ESI-MS data (Table 3). These results suggest that when Cu is not particularly high, two of the three 7-Cys boxes in S7 can fold into one or two Cu_{4-5}-clusters (Cu_9-, Cu_{10}-S7 species), which will additionally include some Zn(II) ions. Contrarily, at high copper concentrations, the Cu load of two 7-Cys boxes is completed and accompanied in some cases with a partial load of the third box (up to 14 Cu(I)), although through the formation of complexes of probably very low stability in view of the low yield of the production, the impossibility of recording ESI-MS data at pH 7, and the low intensity of the ESI-MS spectrum at acid pH (data not shown). It is worth remarking here that both S5 and S7, the two peptides that have Cys as their C-termini, exhibit a similarly misbehavior when rendering Cu-complexes, since the only 7-Cys box constituting S5 is totally unable to fold into metallated species, and S7 (three 7-Cys regions) only fills satisfactorily two of them. These results point to a marked unsuitability of Sx peptides with C-terminal Cys to constitute stable Cu-clusters and thus to the need of *closing* residues, as it would be otherwise confirmed by the ability of S6 (with two C-terminal residues after the last Cys), to fully fill its two 7-Cys segments. Comparison with the results of the full-length CnMT1 leads to the hypothesis that in the first case (no Cu surplus), the recovered heterometallic Zn,Cu-CnMT1 complexes exhibit a higher Zn(II) content than the corresponding Zn,Cu-S7, so that it could be assumed that the flanking spacers plus CXC stretches of CnMT1 stabilize the Zn(II) ions coordinated to the Cu-cores. However, in the second case, if Cu is abundant, CnMT1 is also able to fully load its three 7-Cys boxes (major

$Cu_{15\text{-}16}$-CnMT1 species, Table 3), this suggesting that the presence of the flanking regions missing in S7 are necessary to *close* the 3-Cu_5 cluster structure.

Table 3. Analytical characterization of the recombinant Cu(I)-Sx complexes. Normal aeration (na) or low aeration (la) (i.e. high intracellular Cu) is indicated only for those syntheses yielding different results under both conditions. For comparative purposes, data for the full length CnMT1 are included (Palacios *et al.*, 2014).

	ICP-AES[a]	Neutral ESI-MS[b]	MM_{Exp}[c]	MM_{Theor}[d]	Acidic ESI-MS[b]	MM_{Exp}[c]	MM_{Theor}[d]
S1 (7 Cys)	0.0 Zn 3.2 Cu	**Cu_5-S1** Cu_4-S1	2646 2582	2646.4 2583.8	**Cu_5-S1** Cu_4-S1	2646 2582	2646.4 2583.8
S2 (7 Cys)	0.0 Zn 5.7 Cu	**Cu_5-S2**	3573	3573.5	**Cu_5-S2**	3573	3573.5
S3 (7 Cys)	0.0 Zn 4.9 Cu	**Cu_5-S3**	3505	3504.3	**Cu_5-S3**	3504	3504.3
S4 (9 Cys)	0.0 Zn 5.2 Cu	**Cu_5-S4**	4210	4212.1	**Cu_5-S4**	4210	4212.1
S5 (9 Cys)	-----	-----	-----	-----	-----	-----	-----
S6 (14 Cys)	0.0 Zn 4.8 Cu	**Cu_5-S6** Cu_6-S6 Cu_9-S6 Cu_4-S6	5661 5724 5912 5598	5662.9 5725.4 5913.1 5600.3	**Cu_5-S6** apo-S6 Cu_4-S6 Cu_9-S6 Cu_{10}-S6	5660 5348 5597 5911 5974	5662.9 5350.1 5600.3 5913.1 5975.8
$S7_{na}$ (21 Cys)	2.5 Zn 8.7 Cu	**M_{10}-S7** **M_9-S7** M_{11}-S7 M_{13}-S7	9608 9546 9796 9670	9609.6 9547.1 9797.3 9672.2	**Cu_9-S7** Cu_5-S7 Cu_{10}-S7	9546 9294 9610	9547.1 9296.9 9609.6
$S7_{la}$ (21 Cys)	0.0 Zn 11.1 Cu	-----	-----	-----	**Cu_9-S7** Cu_{14}-S7 Cu_{12}-S7	9545 9862 9798	9547.1 9859.1 9796.7
$CnMT1_{na}$ (25 Cys)	4.2 Zn 5.0 Cu	**M_{11}-CnMT1** M_8-CnMT1 M_9-CnMT1	(Palacios *et al.*, 2014)	(Palacios *et al.*, 2014)	**Cu_5-CnMT1**	(Palacios *et al.*, 2014)	(Palacios *et al.*, 2014)
$CnMT1_{la}$ (25 Cys)	0.0 Zn 15.8 Cu	**Cu_{16}-CnMT1**	(Palacios *et al.*, 2014)	(Palacios *et al.*, 2014)	**Cu_{15}-CnMT1** Cu_{16}-CnMT1 Cu_{17}-CnMT1 Cu_{14}-CnMT1	(Palacios *et al.*, 2014)	(Palacios *et al.*, 2014)

[a] Zn(II) and Cu(I)-to-peptide ratio calculated from S, Zn and Cu content (ICP-AES data).[b] The deduced species (M=Zn or Cu) were calculated from the mass difference between the holo- and the respective apo-peptides. The major species are indicated in bold. [c] Experimental molecular masses corresponding to the detected complexes. The corresponding ESI-MS spectra are shown in Fig. 4 and 5. [d] Theoretical molecular masses corresponding to the metal-Sx complexes. (---) means non-detected

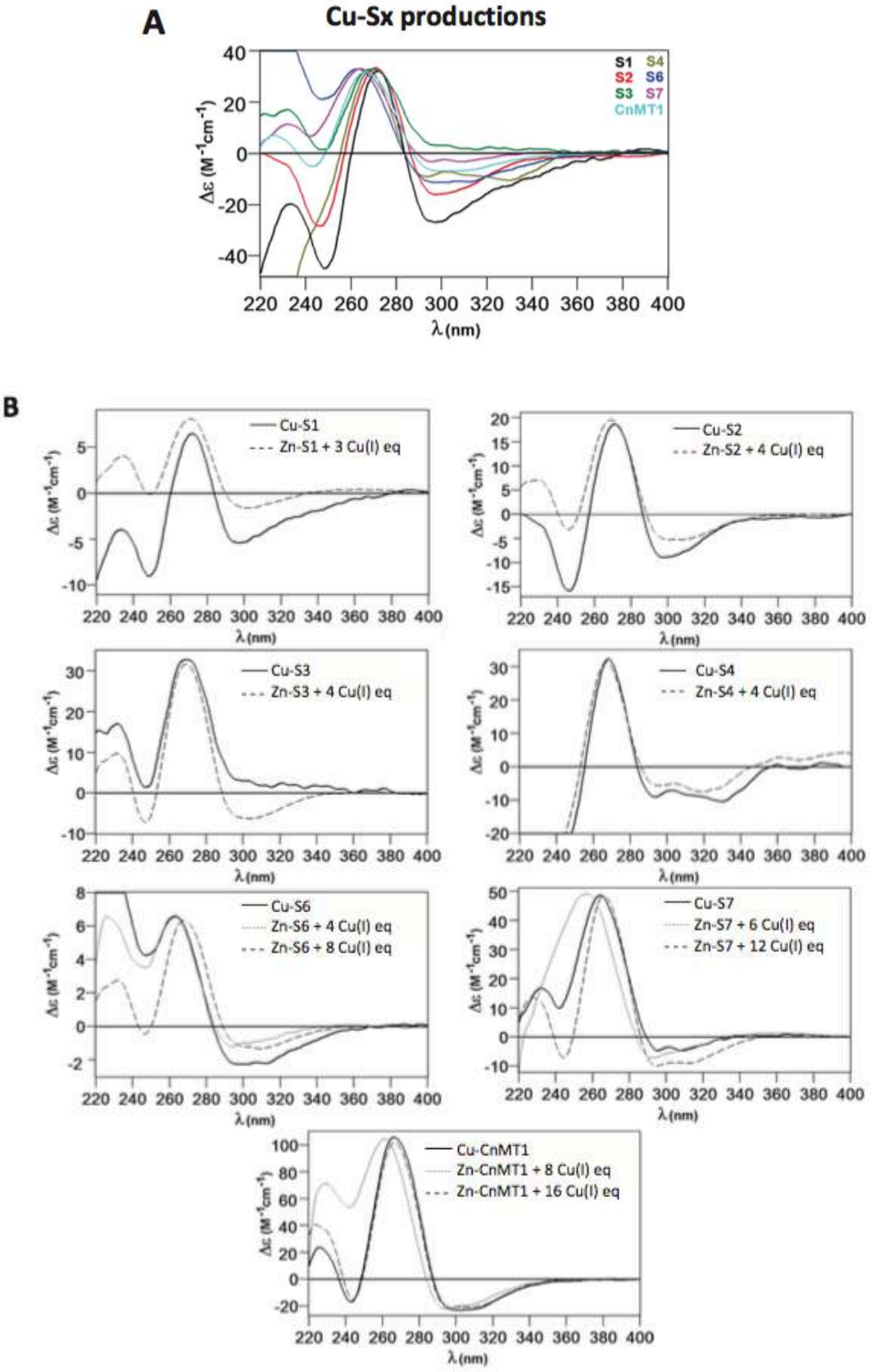
A
Cu-Sx productions
S1
S2
S3
S4
S6
S7
CnMT1
Δε (M⁻¹cm⁻¹)
λ (nm)
B
Cu-S1
Zn-S1 + 3 Cu(I) eq
Cu-S2
Zn-S2 + 4 Cu(I) eq
Cu-S3
Zn-S3 + 4 Cu(I) eq
Cu-S4
Zn-S4 + 4 Cu(I) eq
Cu-S6
Zn-S6 + 4 Cu(I) eq
Zn-S6 + 8 Cu(I) eq
Cu-S7
Zn-S7 + 6 Cu(I) eq
Zn-S7 + 12 Cu(I) eq
Cu-CnMT1
Zn-CnMT1 + 8 Cu(I) eq
Zn-CnMT1 + 16 Cu(I) eq

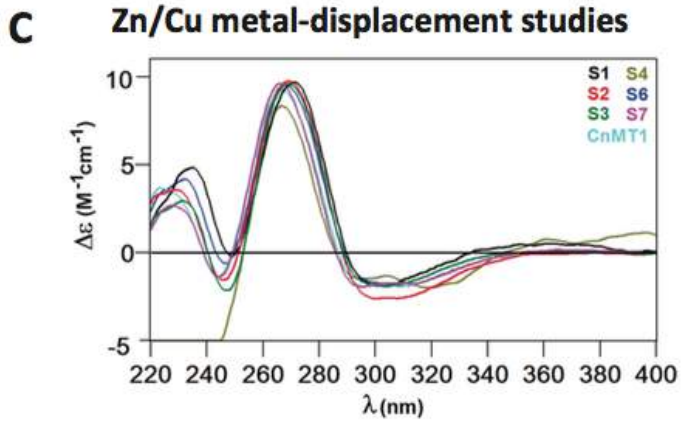

Fig. 3. Comparison of (A) the normalized CD spectra recorded for the recombinant Cu-Sx productions, (B) the circular dichroism spectra corresponding to the recombinant Cu-Sx preparations (solid lines correspond to both types of productions - normal and low aeration conditions-), and those recorded in the corresponding Zn/Cu metal-displacement studies on Zn-Sx (dashed) -when necessary, the spectra in dashed line were normalized in intensity in order to allow comparisons-, and (C) after the *in vitro* addition of several Cu(I) equivalents to the corresponding Zn-Sx preparations. The spectra corresponding to the entire protein, CnMT1, have also been included for comparison.

Globally, the CD spectra of all the Cu-Sx productions except that of S5, which rendered no product, were highly coincident in shape (Fig. 3A), drawing a CD fingerprint with the typical absorptions of the Cu-MT complexes (maximum *ca*. 270 nm and minima at *ca.* 250 and 300 nm), and which are also very similar, although markedly less intense, to that of the entire Cu-CnMT1 complex (included in Fig. 3 for comparative purposes). Further details are discussed in the next section.

Zn(II)/Cu(I) replacement reactions of the CnMT1:Sx peptides and comparison with the full length CnMT1 protein

Very informative results about the Cu(I)-binding abilities of the Sx segments were obtained from the addition of Cu(I) to the respective Zn-Sx recombinant preparations (*i.e*. the study of the species constituted *in vitro* by Zn/Cu exchange). The metal substitution process was followed by ESI-MS analysis, and CD and UV-vis spectrophotometry. For each metal-replacement reaction, the CD spectrum most similar to that of the recombinant Cu-Sx preparation is shown in Fig. 3B and Fig. 3C, and the species detected by ESI-MS at those

titration steps are included in Fig. 4 and Fig. 5; the complete sets of data being available as Supplementary Material (Fig. S1 to S7).

All the Zn-complexes of the peptides containing only one 7-Cys box (S1, S2, and S3) followed a similar behavior when titrated with Cu(I), being those of S2 and S3, the two segments with N- or C-terminal flankers, the more similar among them, while S1 showed higher complexity associated with the already observed lack of stabilization of the Cu_5-S1 complexes. The behavior of the three peptides is clearly suggestive of an almost complete cooperative loading of 5 Cu(I) –a small amount of Cu_4-Sx is also detected- concomitant to the displacement of all the initial Zn(II). This is shown by the isodichroic points observed in the evolution of the corresponding CD spectra, and nicely illustrated by the cooperative formation of M_5-Sx complexes, which are mainly Cu_5-Sx, even for the mixture of Zn_x-S3 species, ranging from the apo-peptide to Zn_4-S3 (Fig. S3). Similarly, the addition of an excess of Cu(I) after the formation of Cu_5-Sx species inevitably provokes a collapse of the CD fingerprints that reveals the unfolding of the complexes, concomitantly to the detection of major peaks corresponding to the apo-peptides by analysis at acidic ESI-MS. The different sequences of S1, S2, and S3 may be associated with the small differences observed in their Zn/Cu exchange processes. Hence, the presence of an N-term spacer in S2 or C-term in S3 (in relation to S1) suggests that the Cu_5-S2 and Cu_5-S3 complexes are almost unique at the step of the titration yielding the species with the highest nuclearity, and before cluster unfolding; while for S1, a clear coexistence of major Cu_5- and minor Cu_4-S1 is detected. These results are fully concordant with those of the corresponding Cu-Sx recombinant syntheses (Fig. 4 and Table 3), and altogether, they indicate that the flanking spacer is essential for the stabilization of the 5^{th} Cu(I) in the cluster.

For the two nine-Cys fragments (7-Cys box plus + 2 adjacent Cys), only the titration of Zn-S4 was somewhat successful, ending in M_5-S4, mainly constituted by a Cu_5-S4 complex, despite the noise of the corresponding ESI-MS spectra. Although no product other than the apo-peptide could be retrieved from the Zn-S5 synthesis, the Cu(I) titration was equally assayed with this preparation. The reaction was clearly unsuccessful, according to the poor CD spectra and the noise of the ESI-MS spectra, data, which is also concordant with the unproductive synthesis of S5 in Cu-supplemented cultures.

The Zn/Cu displacement in Zn-S6 (two 7-Cys boxes) and Zn-S7 (three 7-Cys boxes), both without flanking spacers, clearly differs from that described for S1, S2 and S3, as it takes

place in three successive stages (Fig. 5 and Figs. S6, S7). During the first steps of adding Cu(I) (until 4 and 6 Cu(I) eq, respectively for S6 and S7), a mixture of heterometallic species containing major Cu_5- and minor Cu_4-cores is formed, this process generating clear isodichroic points in the corresponding CD spectra. These species are replaced by major Cu_{10}-S6 and Cu_9-S7 complexes in the second stage of the metal replacement (when 8 or 12 Cu(I) eq had been respectively added), also yielding an isodichroic evolution of the respective CD fingerprints of the mixtures. The third stage in both cases corresponds to the, again, isodichroic unfolding of the formed Cu-complexes into Cu_5-, Cu_4-cores and apo-forms indicating that they do not resist further Cu(I) additions. While this behavior is totally understandable for S6 (two 7-Cys boxes), a further stage corresponding to the filling of its third 7-Cys box would have been expected for S7. This is not observed, although some minor species of higher nuclearity (M_{15}- and Cu_{13}-S7) are detected for 12 Cu(I) eq added. Interestingly, these results nicely reproduce those obtained for the recombinant Cu-S6 and Cu-S7 preparations, those of S6 matching the end of the first stage of the metal replacement pathway, while those of S7 at normal aeration coincide with the results of the second stage of the titration (Fig. 5). It is surprising that while for S6, the Cu(I) filling of its two 7-Cys boxes is achievable (at least *in vitro*, if not *in vivo*) with further Cu(I) additions, for S7 only two of the three 7-Cys boxes are able to fold into Cu_5-cores, and only traces of the loading of the third box are weakly observed at high (12) amounts of Cu(I) added, before unfolding to Cu_5. Hence, the comparison of the S7 and CnMT1 Zn/Cu replacement reactions suggests that the presence of the terminal spacers plus adjacent CXC regions (or at least one of them) may be required to fill up and maintain a third Cu_5-cluster, as occurs for CnMT1, because in this case a clear Cu_{15}-CnMT1 species is detected in the corresponding metal exchange experiment.

Another point worth highlighting, is that there is not only a good concordance between the CD spectra of all the *in vivo* preparations with those recorded after the addition of the number of Cu(I) eq indicated in Fig. 4 and 5 to the corresponding Zn-Sx preparations (Fig. 3B), but also among all the CD fingerprints recorded *in vitro* for the final stages of the Cu(I) additions preceding the unfolding of the complexes and of these with that of Cu-CnMT1 (Fig. 3C). This observation gives support to the modular architecture of the entire protein as well as to that of those mutant peptides that contain more than one 7-Cys box.

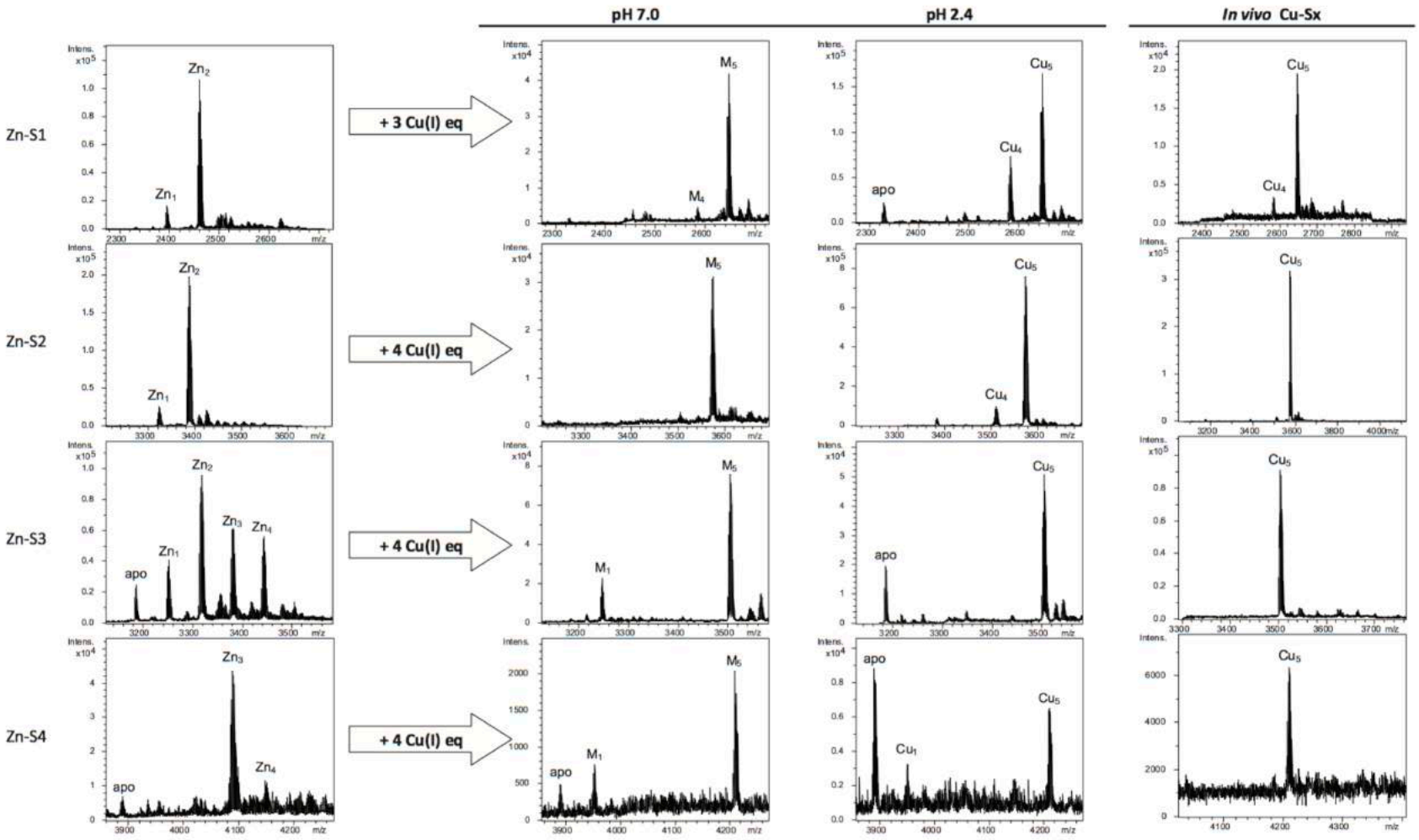

Fig. 4. Deconvoluted ESI-MS spectra recorded, at neutral and acidic pH (central columns), after the addition of the indicated number of Cu(I) equivalents to the corresponding Zn-Sx preparations, x= 1, 2, 3 and 4 (first column). No data are included for S5 due to the lack of metal complexes detected by ESI-MS in all the cases. The ESI-MS spectra of the *in vivo* obtained Cu-Sx preparations are included (last column) for comparison purposes, those at pH 7 and pH 2.4 being identical.

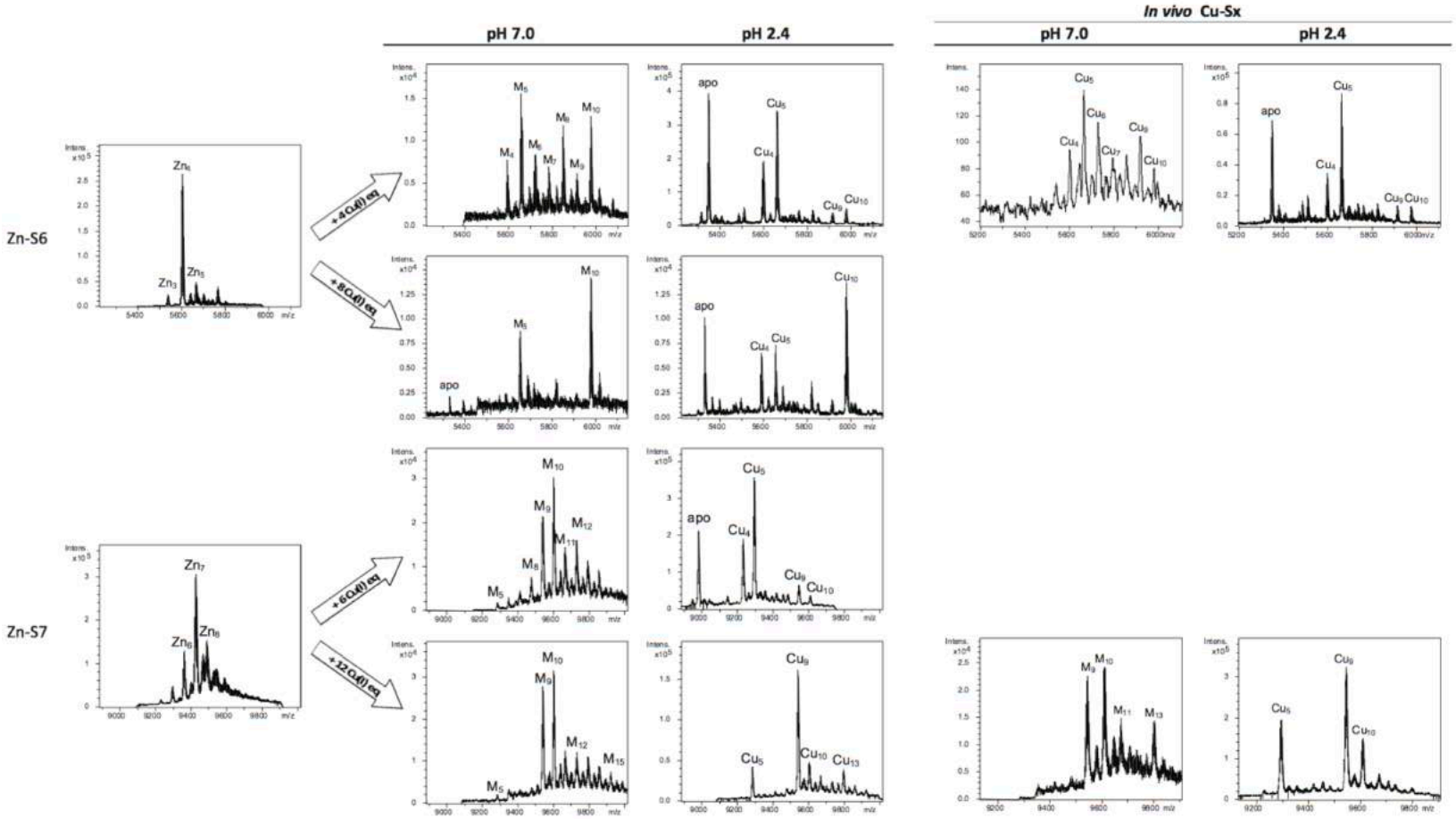

Fig. 5. Deconvoluted ESI-MS spectra recorded, at neutral and acidic pH (central columns), after the addition of the indicated number of Cu(I) equivalents to the corresponding Zn-S6 and Zn-S7 preparations (first column). The ESI-MS spectra at pH 7 and pH 2.4 of the *in vivo* obtained Cu-S6 (regular and low aeration conditions rendering identical spectra) and Cu-S7 (only spectra of the regular aeration conditions shown) preparations are

Cu tolerance tests by a yeast complementation assay

To analyze the effect on Cu tolerance in *S. cerevisiae* of the heterologous expression of all the analyzed Sx peptides, a resistance experiment was performed using a yeast strain devoid of its two MTs (CUP1 and CRS5). Hence, the cDNAs encoding the Sx segments, as well as the *CUP1* cDNA for comparative purposes, were subcloned in the episomic plasmid p424-GDP. 51-2c-Δc5 yeast cells were transformed with either one of these constructs or with non-recombinant p424 as a control. The ability of these transformants to grow in media supplemented with increasing copper concentrations was tested by OD_{600} measurements of liquid cultures (Fig. 6) and by standard dot assays (Fig. 7). The corresponding results clearly show that all the tested peptides are able to restore copper tolerance as efficiently as the yeast CUP1 MT, since growth was impaired beyond the first dilution for the control cells, while those overexpressing CUP1, CnMT1 or any Sx segment yielded colonies even at the fourth dilution range (Fig. 7). Results from the liquid cultures exactly reproduce the similarity of restoring copper tolerance for all the assayed peptides, since they exhibit similar growth rates in Cu-rich cultures, which are equivalent or higher than that of the CUP1-transformed cells, and definitely different to that of the MT-devoid strain. It is worth noting that at 7 μM $CuSO_4$ (the maximum concentration allowing a growth higher than 50 % in liquid cultures, all the Sx segments yield higher resistance than CUP1, an effect that is consistent with the slightly impaired growth of the corresponding transformant in agar plates (*cf.* Fig. 7). The fact that all the Sx constructs appear to be better or as good as the native yeast Cu-thionein in restoring growth at high copper concentrations correlates well with the fact that all of them fold into Cu_5-clusters of similar features (*i.e.* similar CD fingerprints), which suggests that Cu-tolerance would be more related to the capacity of an MT polypeptide to fold into clusters that remain stable inside the cell than to their mere Cu(I) chelating capacity. In fact, such a conclusion was reached some time ago, when showing that different constructs of the *Quercus suber* QsMT2 MT with the same coordination capacity, but different architecture, conferred dissimilar Cd tolerance when assayed in yeast cells (Domenech *et al.,* 2007).

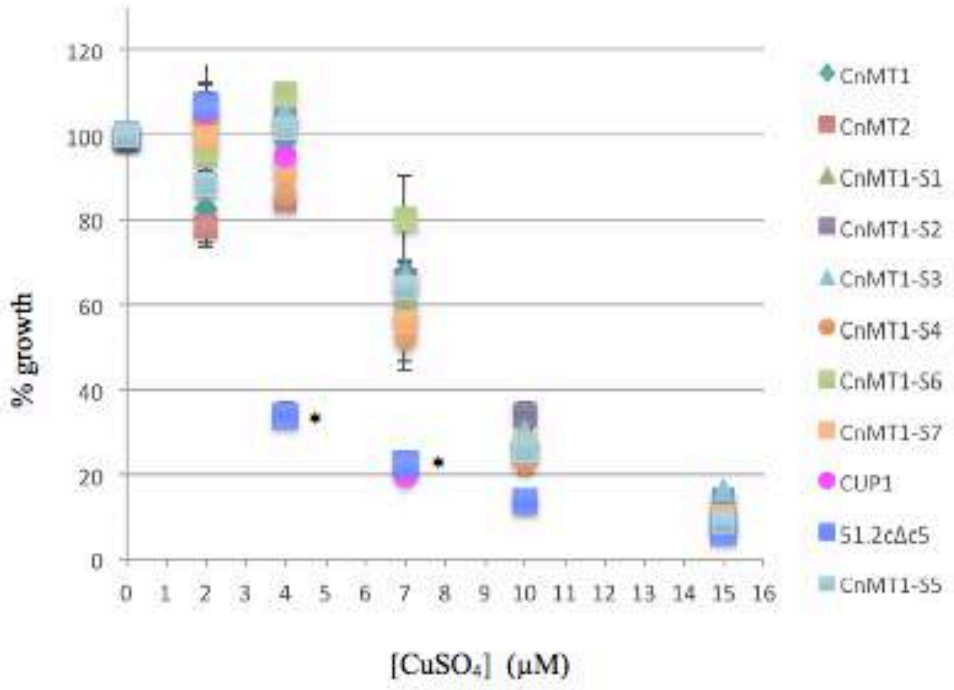

Fig. 6. Scatterplot of the tolerance to copper conferred to *S. cerevisiae* cells by *C. neoformans* MTs and CnMT1 truncated mutants. 51.2cΔc5 (an MT null yeast strain) cells were transformed with the corresponding MT or MT-construct coding regions cloned into the constitutive expression vector p424. Growth was evaluated in liquid cultures and it is represented as the percentage of the growth rate attained in a non-Cu supplemented medium. Controls were the non-transformed yeast strain and the CUP1 (yeast MT) transformants. Each value is the mean of at least two replicates, and vertical lines represent standard deviations. Asterisk show the strains yielding significant different results than the rest at the corresponding Cu concentrations. For more details, see the Experimental Procedures section.

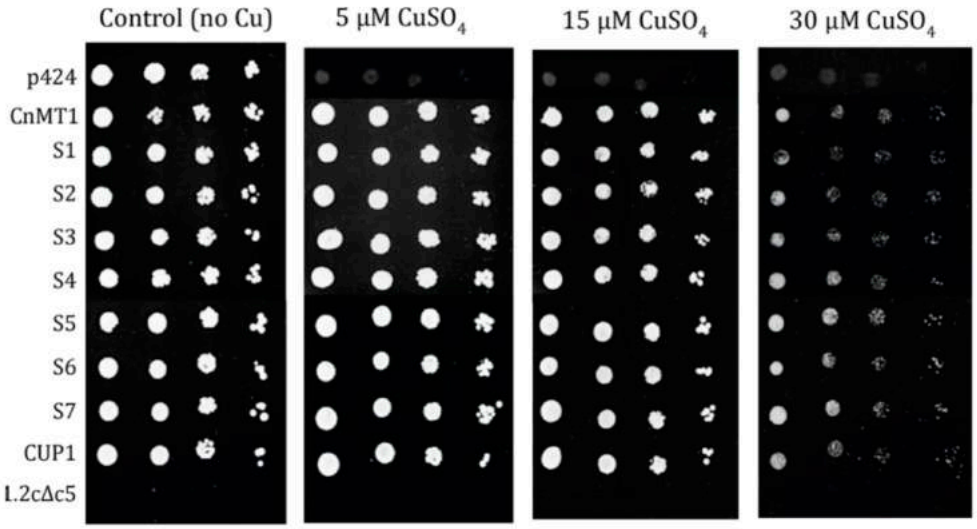

Figure 7. Effect of the heterologous expression of the *C. neoformans* CnMTs and its truncated mutants in *S. cerevisiae* cell growth under Cu supplementation. 51.2cDc5 (an MT null yeast strain) was transformed with the constitutive expression vector p424 (void) or the corresponding MT or MT constructs cloned into p424. Cultures were growth in SC-Trp-Ura-Leu medium overnight at 30 ^{o}C, were diluted to OD_{600} 0.5 and spotted into SC-Trp-Ura-Leu agar plates supplemented with $CuSO_4$ at different concentrations. Plates were allowed to grow at 30 ^{o}C during 3 days. For control growth purposes, non-transformed 51.2cΔc5 cells and cells transformed with the *S. cerevisiae* p424- CUP1 construct were also included in the assay. The results at 50 µM $CuSO_4$ supplementation are not included, because no growth was seen for any transformant.

CONCLUSIONS

After the characterization of the two *C. neoformans* metallothioneins (CnMT1 and CnMT2) as infection and virulence factors (Ding *et al.,* 2013), it has been shown that their increased Cu-binding capacity was derived from their extraordinary length, if compared with the most well-known fungal Cu-thioneins (Palacios *et al.,* 2014). We then proposed that the CnMT proteins had a modular structure built by the repetition of three (CnMT1) or five (CnMT2) 7-Cys unit, separated by spacer regions devoid of Cys residues, plus Cys doublets flanking the whole sequence. This was concordant with each of these 7-Cys boxes forming independent Cu_5-clusters, which would be cooperatively filled with Cu(I) ions. This was an appealing hypothesis, but it remained to be proved, especially because the *N. crassa* MT, with

a sequence completely alignable to the 7-Cys boxes of the *C. neoformans* MTs (Fig. 1), had been shown to form Cu_6-complexes (Cobine *et al.,* 2004). Therefore, a study of the metal-binding behavior of different truncated mutants of CnMT1 was compulsory to shed light on the proposed modular architecture of these MTs, and additionally, to the role of spacers and flanking amino acid sequences when modulating the coordination abilities of the Cys regions in proteins, which are determinant factors for MT preference on monovalent or divalent metal ions (Palacios *et al.,* 2011b).

Consideration of our current results fully supports our previous hypothesis about the modular, independent metal-binding behavior of the *C. neoformans* MT 7-Cys boxes. Strikingly, the influence of elements other than the coordinating Cys is different for Zn(II) and Cu(I) coordination. Hence, each 7-Cys stretch coordinates 2 Zn(II) ions, which is clearly reflected by the Zn_2-complexes yielded by S1, S2 and S3 and the Zn_4-complexes of S6. Noteworthy, the S3 folding about Zn(II) renders a collection of minor species, which is attributable to its C-term spacer. Since Zn_3- and Zn_4-species are detected, it may be possible that the Glu residue, a well-known Zn(II)-coordinating amino acid, contributes to the final complexes. Also, the basic 2 Zn: 7 Cys relationship is enlarged by the presence of two extra flanking Cys (CXC motif) in the S4 C-terminal tail to yield up to Zn_3- and Zn_4-complexes. Finally, the higher Zn(II) binding capacity of S7 (major Zn_7-complex) in relation to the six Zn(II) theoretically bound by the three 7-Cys boxes, is also attributable the glutamic acid present in its N-term spacer region.

In the case of Cu(I) coordination, all the segments consisting of a 7-Cys box invariably render a unique Cu_5-cluster, where one of the Cu(I) ions appears quite unstable if the segment is devoid of a flanking spacer (*i.e.* S1). No effect is seen for the two extra Cys in S4. When several 7-Cys boxes are tandemly combined (two in S6 and three in S7), always one of them seems unable to remain filled with Cu(I), although the presence of high Cu(I) (*i.e.* in low aeration Cu-synthesis or Zn/Cu replacement experiments) enhances its capability to render higher nuclearity Cu-complexes. Therefore, the presence of flanking amino acids is revealed necessary to endow the Cu_5-clusters with enough stability in cell environments. Finally, it can be observed that the higher the number of 7-Cys boxes in these modular MTs, the higher the difference between the species rendered when synthesized in normal or high Cu cultures. The trend is that at normal aeration (regular Cu cell content), heterometallic Zn,Cu-complexes are recovered, while from poorly aerated cultures, homometallic Cu-species are purified, as

occurs for S7 and the full-length CnMTs. A comparison between S7 and CnMT1 suggests that the two CXC motives present in CnMT1 and absent in S7 favor the coordination of Zn(II), if Cu(I) is not specially high. Therefore, if the main influence of spacer and flanking regions for Zn(II) coordination is the increase in the metal content of the afforded complexes, for Cu(I) coordination, it would be the stabilization of the final Cu_5-clusters, this sometimes contributed by additional Zn(II) coordination.

Overall, all the data presented in this study fully supports the initial hypothesis that each 7-Cys segment constituting the basic unit of *C. neoformans* MTs folds into very favored Cu_5-clusters. The interest of deepening in the architecture of these novel Cu(I)-MT clusters promoted a revision of the model structures reported for inorganic Cu(I) thiolates (Dance 1986; Henkel and Krebs, 2004), as well as of the unique X-ray diffraction-solved Cu-MT structure (Cu_8-Cup1) (Calderone et al. 2005). According to all the knowledge gathered for inorganic metal thiolates, there is a unique model structure for a $Cu_5(SR)_7$ complex, which can be considered an extension of the $Cu_4(SR)_6$ complexes. It contains four metal ions in trigonal-planar and one in linear coordination, and was first observed in $[Cu_5(SPh)_7]^{2-}$ (Dance, 1978). Interestingly this is the model structure that has been quoted in bioinorganic studies related to Cu-proteins, such as precisely MTs (Maiti *et al.,* 2007) and Cu-chaperones (Pushie *et al.*, 2012) illustrating the flexibility of the Cu(I) thiolates and the facile interconversion of Cu_4-, Cu_5- and Cu_6 clusters as features explaining their biological function. Finally, a modification of the structure of Cu_8-Cup1 consisting in the deletion of three Cys residues and three Cu(I) ions has rendered a "biological model" that exactly matches the inorganic model, which is shown in Fig. 8.

Furthermore, the sequence, and significantly the Cys motifs of the 7-Cys boxes are, as stated in the Introduction, fully alignable with those of *N. crassa MT* (Fig. 1), which has been reported to yield Cu_6-NcMT complexes. To tackle this apparent paradox, we have already performed experiments consisting of the recombinant synthesis of NcMT in Cu-supplemented media, by following the same rationale used in this work. They have unambiguously shown formation of a unique Cu_5-NcMT species (manuscript in preparation). Hence, we are readily aiming at solving the 3D structure and the corresponding Cu-thiolate connectivities of these until nowadays unreported Cu-MT clusters, the significance of which, not only in the MT universe, but for the global knowledge on metalloproteins, where a limited number of metal cluster structures is known, is patently clear.

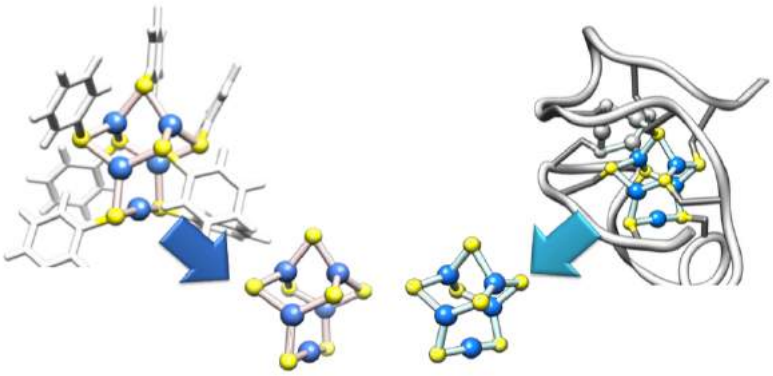

Fig. 8. Comparison of the 3D crystal structures of the [Cu5(SPh)7]2- complex (left) and the Cu8-Cup1 species (right) in which the Cu5S7 clusters have been coloured and represented separately (centre) to illustrate their high similarity (i.e. same metal and sulfur coordination environments). The inorganic complex data have been retrieved from the Cambridge Structural Database (entry MITWAO) and those for the protein from the Protein Data Bank (entry 1rju). They have been both treated with the Chimera software (Pettersen *et al*., 2004).

EXPERIMENTAL PROCEDURES

Construction of CnMT1 fragments and E. coli expression vectors

The cDNAs encoding the seven Sx segments of CnMT1 analyzed in this work (Fig. 1) were obtained by specific PCR amplification using as template, the complete CnMT1 cDNA sequence (GenBank: AFR98878.2) subcloned in the pGEX-4T-1 (GE Healthcare) *E. coli* expression vector (Palacios *et al.,* 2014), and as primers the oligonucleotides shown in Table S1 (Supplementary material). These oligonucleotides served to introduce the *BamH*I/*Xho*I sites for pGEX-4T-1 insertion, as well as a translation stop codon at the end of each coding sequence. 30-cycle PCR amplification reactions were performed with thermo-resistant Taq DNA polymerase (Expand High Fidelity PCR System, Roche) under the following conditions: 2 min at 94ºC (initial denaturation), 15 s at 94ºC (denaturation), 30 s at 57ºC (annealing) and 30 s at 72ºC (elongation). The final products were analyzed in 2% agarose gel and the expected bands were excised (Genelute ^{TM} Gel Extraction Kit, Sigma Aldrich). pGEX-4T-1 and the amplified inserts were digested with *BamH*I/*Xho*I and subsequently

ligated (DNA Ligation Kit 2.1, Takara Bio Inc.). The recombinant plasmids were transformed into the *E. coli* MachI strain for DNA sequencing, using the Big Dye Terminator 3.1 Cycle Sequencing Kit in an ABIPRISM 310 Automatic Sequencer (Applied Biosystems). Positive clones were transformed into the *E. coli* BL21 protease deficient strain for protein synthesis.

Synthesis and purification of the recombinant Zn- and Cu-complexes of the CnMT1:Sx peptides

The GST-Sx fusion proteins were biosynthesized in 5-l Luria Bertani (LB) cultures of transformed *E. coli* BL21 cells. Gene expression was induced with 100 μM (final concentration) of isopropyl β-D-thiogalactopyranoside (IPTG); after 30 min of induction, cultures were supplemented with 300 μM $ZnCl_2$ or 500 μM $CuSO_4$ (final concentration), and they were allowed to grow for a further 2.5 h for the synthesis of the respective metal complexes. In the case of Cu-supplementation, cultures were grown either under normal aeration conditions (1-l medium in a 2-l Erlenmeyer flask, at 250 rpm), or under low oxygen conditions (1.5-l medium in a 2-l Erlenmeyer flask at 150 rpm), since culture aeration determine the amount of intracellular copper available for recombinant MTs in the host cells (Pagani *et al.,* 2006).

After growth, cells were harvested by centrifugation, resuspended in ice-cold PBS (1.4 M NaCl, 27 mM KCl, 101 mM Na_2HPO_4, 18 mM KH_2PO_4) with 0.5% v/v β-mercaptoethanol, and subsequently disrupted by sonication (20 s pulses for 5 min). To prevent metal-MT complex oxidation pure grade argon was invariably bubbled in all the steps of the purification, and also in the PBS buffer stock. The sample was the centrifuged at 12 000 *g* for 30 min, and the recovered supernatant was incubated (gentle agitation for 60 min at room temperature) with Glutathione-Sepharone 4B (GE Healthcare) to allow batch affinity purification of the GST-Sx polypeptides. After three PBS washes of the Glutathione-Sepharone matrix, the Sx portion was recovered by thrombin cleavage (10 u per mg of fusion protein at 17^{o}C over-night), so that the cleaved metal-Sx complexes remained in solution. This was concentrated by Centriprep Microcon 3 (Amicon, cut-off of 3 kDa) centrifugation, and the metal complexes were finally purified through FPLC in a Superdex75 column (GE Healthcare) equilibrated with 50 mM Tris-HCl, pH 7.0 and run at 0.8 ml min^{-1}. Fractions were collected and analyzed

for protein content by their absorbance at 254 and 280 nm. Further details of the synthesis and purification steps are described in Cols *et al.,* 1997 and Capdevila *et al.,* 1997.

Zn(II)/Cu(I) replacement reactions on the CnMT1:Sx peptides

The *in vitro*-constituted Cu(I)-Sx complexes were prepared *via* metal replacement by adding a Cu(I) standard solution to each recombinant Zn-Sx preparation. These reactions were performed at pH 7.0 following the procedure previously reported for mammalian MTs (Bofill et al., 1999). Characterization of the *in vitro* complexes was performed by UV–Vis and CD spectroscopies, as well as ESI-MS analysis, as explained below. All assays were carried out in an argon atmosphere, and the pH remained constant throughout all the experiments, without the addition of any other reagent, such as buffers or reductants.

Spectroscopic analyses (ICP-AES and CD) of the Zn- and Cu-complexes rendered by the CnMT1:Sx peptides

The S, Zn and Cu content of all the Sx preparations was analyzed by means of Inductively Coupled Plasma Atomic Emission Spectroscopy (ICP-AES) in a Polyscan 61E (Thermo Jarrel Ash) spectrometer, measuring S at 182.040 nm, Zn at 213.856 nm and Cu at 324.803. Samples were treated as in Bongers *et al.* (1988), but they were alternatively incubated in 1 M HNO_3 at 65ºC for 10 min prior to measurements in order to eliminate possible traces of labile sulfide ions (Capdevila *et al.,* 2005). Protein concentrations were calculated from the acid ICP-AES sulfur measurements, assuming that all S atoms were contributed by the Sx peptides.

A Jasco spectropolarimeter (Model J-715) interfaced to a computer (J700 software) was used for CD measurements at a constant temperature of 25ºC maintained using a Peltier PTC-351S equipment. Electronic absorption measurements were performed on an HP-8453 Diode array UV-visible spectrophotometer. All spectra were recorded with 1-cm capped quartz cuvettes, corrected for the dilution effects and processed using the GRAMS 32 software.

Electrospray Ionization Time-of-Flight Mass Spectrometry (ESI-TOF MS) of the Zn- and Cu-Sx complexes

MW determinations were performed by electrospray ionization time-of-flight mass spectrometry (ESI-TOF MS) on a Micro TOF-Q instrument (Bruker) interfaced with a Series 1200 HPLC Agilent pump, equipped with an autosampler, all of which were controlled by the Compass Software. Calibration was attained with ESI-L Low Concentration Tuning Mix (Agilent Technologies). Samples containing Zn-Sx complexes were analyzed under the following conditions: 20 µl of protein solution injected through a PEEK (polyether heteroketone) tubing (1.5 m x 0.18 mm i.d.) at 40 µl min^{-1}; capillary counter-electrode voltage 5 kV; desolvation temperature 90-110ºC; dry gas 6 l min^{-1}; spectra collection range 800-2500 m/z. The carrier buffer was a 5:95 mixture of acetonitrile:ammonium acetate (15 mM, pH 7.0). Alternatively, the corresponding Cu-complexes were analyzed as follows: 20 µl of protein solution injected at 40 µl min^{-1}; capillary counter-electrode voltage 3.5 kV; lens counter-electrode voltage 4 kV; dry temperature 80ºC; dry gas 6 l min^{-1}. Here, the carrier was a 10:90 mixture of acetonitrile:ammonium acetate, 15 mM, pH 7.0. For the analysis of the apo-peptides and Cu-Sx complexes at acidic pH, 20 µl of the corresponding sample were injected under the same conditions described previously, but using a 5:95 mixture of acetonitrile:formic acid pH 2.4, as liquid carrier, which caused the complete demetalation of the peptides loaded with Zn, but kept the Cu ions bound to the peptide. Under all the conditions assayed, the error associated with the mass measurements was always lower than 0.1%. Masses for the holo-species were calculated as previously described (Fabris *et al.,* 1996)

Metal tolerance complementation assays in transformed yeast MT-knockout cells

The *Saccharomyces cerevisiae* 51.2cΔc5 strain (*MAT*a, *trp*1-1, *ura*3-52, *ade*-, *his*-, CAN^R, *gal*1, *leu2-3*, *112 met13*, *cup1*Δ::*URA*3 *crs5*Δ::*LEU2*), derived from VC-sp6 (Culotta *et al.,* 1994) was used for copper tolerance complementation assays. The cDNAs coding for the full size CnMT1 and its derived constructed segments (Sx) were ligated into the *BamH*I/*Xho*I sites of the yeast vector p424-GPD (ATCC), while the CnMT2 cDNA had to be cloned into its *Eco*RI/*Xho*I sites due to an internal *BamH*I restriction site. ATG and STOP codons were suitably inserted into the coding sequences for proper translation when amplified

by PCR using the oligonucleotides shown in Table S2. The p424-GPD vector contains TRP1 as a selection marker, the constitutive glyceraldehyde-3-phosphate dehydrogenase (GPD) promoter for gene expression, and the cytochrome-c-oxidase (CYC1) transcriptional terminator (Mumberg *et al.,* 1995). The recombinant p424 plasmids were introduced into the 51.2cΔc5 cells using the LiAc/SS-DNA/PEG procedure (Gietz and Woods, 2002). Transformed cells were selected according to their capacity to grow in synthetic complete medium (SC) without Trp, Leu and Ura. The construction p424-CUP1, encoding for the yeast Cu-thionein CUP1, was used as control. For copper tolerance tests, transformed yeast cells were initially grown in selective SC-Trp-Ura medium at 30ºC and 220 rpm until saturation. These cells were then diluted to OD_{600} 0.01 and used to re-inoculate tubes with 3 ml of fresh medium supplemented with $CuSO_4$ added at 0, 2, 4, 7, 10 and 15 μM final concentrations. These cultures were allowed to grow for 18 h, and the final OD_{600} was recorded and plotted as a percentage of the OD_{600} reached by the culture grown without metal supplement. Two replicates were run for each concentration, and each kind of transformation. Data were analyzed by a Principal Component algorithm, due to the complexity of including 11 strains and 4 Cu concentrations.

Alternatively, cell cultures were grown in SC-Trp-Ura liquid medium at 30°C until an OD600 of 0.5, and from them, three or four 10-fold dilutions were performed, so that 3 μl of each dilution were spotted on SC plates and on SC supplemented with copper at 0, 5, 15, 30 and 50 μM final concentrations. Plates were incubated for 3 days at 30°C and then photographed.

ACKNOWLEDGEMENTS

This work was supported by the Spanish *Ministerio de Economía y Competitividad* (MINECO), grants BIO2012-39682-C02-01 (to SA) and -02 (to MC), which are co-financed by the European Union through the FEDER program. Authors are members of the 2014SGR-423 *Grup de Recerca de la Generalitat de Catalunya*. AE was the recipient of a predoctoral grant from the MINECO (BES-2010-036553). SGM received a predoctoral fellowship from the *Departament de Química, Universitat Autònoma de Barcelona*. We thank Jordi Espín and Nerea Rovellada, who performed some experimental work, and the *Centres Científics i Tecnològics (CCiT) de la Universitat de Barcelona* (ICP-AES, DNA sequencing) and the *Servei d'Anàlisi Química (SAQ) de la Universitat Autònoma de Barcelona* (CD, UV-vis, ESI-MS) for allocating instrument time. Finally, we are deeply

indebted to Prof. D. Thiele (Duke University, NC, USA) for introducing us to the fascinating world of fungal MTs and for his continuous support.

REFERENCES

Blindauer, C.A. (2014) Metallothioneins. In *RSC Metallobiology Series No.2: Binding, Transport and Storage of Metal Ions in Biological Cells.* Maret, W. and Wedd, A. (eds). Cambridge U.K., RSC Publishing, pp. 594-653.

Bofill, R., Palacios, O., Capdevila, M., Cols, N., González-Duarte, R., Atrian, S., and González-Duarte, P. (1999) A new insight into the Ag^{+} and Cu^{+} binding sites in the metallothionein β domain. *J Inorg Biochem* **73**: 57–64.

Bofill, R., Capdevila, M., and Atrian, S. (2009) Independent metal-binding features of recombinant metallothioneins convergently draw a step gradation between Zn- and Cu-thioneins. *Metallomics* **1**: 229-234.

Bongers, J., Walton, C.D., Richardson, D.E., and Bell, J.U. (1988) Micromolar protein concentrations and metalloprotein stoichiometries obtained by inductively coupled plasma. Atomic emission spectrometric determination of sulfur. *Anal Chem* **60**: 2683-2686.

Calderone, V., Dolderer, B., Hartmann H-J., Echner, H., Luchinat, C., Del Bianco, C., Mangani, S., and Weser, U. (2005) The crystal structure of yeast copper thioneins: the solution of a long-lasting enigma. *Proc Natl Acad Sci USA* **102**: 51-56.

Capdevila, M., Bofill, R., Palacios, O., and Atrian, S. (2012) State-of-the-art of metallothioneins at the beginning of the 21st century. *Coord Chem Rev* **256**: 46–62.

Capdevila, M., Cols, N., Romero-Isart, N., Gonzalez-Duarte, R., Atrian, S., and Gonzalez-Duarte, P. (1997) Recombinant synthesis of mouse Zn_3-β and Zn_4-α metallothionein 1 domains and characterization of their cadmium(II) binding capacity. *Cell Mol Life Sci* **53**: 681–688.

Capdevila, M., Domenech, J., Pagani, A., Tio, L., Villarreal, L., and Atrian, S. (2005) Zn- and Cd-metallothionein recombinant species from the most diverse phyla may contain sulfide (S^{2-}) ligands. *Angew Chem Int Ed Engl* **44**: 4618–4622.

Cobine, P., McKay, R.T., Zangger, K., Dameron, C., and Armitage, I.M. (2004) Solution structure of Cu_6 metallothionein from the fungus *Neurospora crassa. Eur J Biochem* **271**: 4213-4221.

Cols, N., Romero-Isart, N., Capdevila, M., Oliva, B., Gonzalez-Duarte, P., Gonzalez-Duarte, R., and Atrian, S. (1997) Binding of excess cadmium(II) to Cd_7-metallothionein from recombinant mouse Zn_7-metallothionein 1. UV-VIS absorption and circular dichroism studies and theoretical location approach by surface accessibility analysis. *J Inorg Biochem* **68**: 157-166.

Culotta, V.C., Howard, W.R., and Liu X.F. (1994) CRS5 encodes a metallothionein-like protein in *Saccharomyces cerevisiae*. *J Biol Chem* **269**: 25295-25302.

Dance, I.G. (1978) The hepta(μ-benzenethiolato)pentametallate(I) dianions of copper and silver: formation and crystal structures. *Aust J Chem* **31**: 2195-2206.

Dance, I.G. (1986) The structural chemistry of metal thiolate complexes. *Polyhedron* **5**: 1037-1104.

Díaz, S., Amaro, F., Rico, D., Campos, V., Benítez, L., Martin-Gonzalez, A., Hamilton, E.P., Orias, E., and Gutierrez, J.C. (2007) *Tetrahymena* metallothioneins fall into two discrete subfamilies. *PLoS One* **3**: e291.

Ding, C., Festa, R.A., Chen, Y-L., Espart, A., Palacios, O., Espín, J., Capdevila, M., Atrian, S., Heitman, J., and Thiele, D. (2013) *Cryptococcus neoformans* copper detoxification machinery is critical for fungal virulence. *Cell Host Microbe* **13**: 265-276.

Ding, C., Festa, R.A., Sun, T.-S., and Wang, Z.-Y. (2014) Iron and copper as virulence modulators in human fungal pathogens. *Mol Microbiol* **93**: 10-23.

Dolderer, B., Hartmann H.J., and Weser, U. (2009) In *Metal Ions in Life Sciences, vol. 5: Metallothioneins and Related Chelators: Metallothioneins in Yeasts and Fungi*. Sigel, A., Sigel, H., and Sigel, R.K.O. (eds). Cambridge U.K., RSC Publishing, pp. 83-106.

Domenech, J., Orihuela, R., Mir, G., Molinas, M., Atrian, S., and Capdevila, M. (2007) The Cd^{II}-binding abilities of recombinant *Quercus suber* metallothionein: bridging the gap between phytochelatins and metallothioneins. *J Biol Inorg Chem* **12**: 867-882.

Espart, A., Marín, M., Gil-Moreno, S., Palacios, P., Amaro F., Martín-González, A., Gutierrez, J.C., Capdevila, M., and Atrian, S. (2015) Hints for Metal-Preference Protein Sequence Determinants: Different Metal Binding Features of the Five *Tetrahymena thermophila* Metallothioneins. *Int J Biol Sci* **11**: 456-71.

Fabris, D., Zaia, J., Hathout, Y., and Fenselau, C. (1996) Retention of thiol protons in two classes of protein zinc ion coordination centers. *J Am Chem Soc* **118**: 12242–12243.

Gietz, R.D., and Woods, R.A. (2002) Transformation of yeast by lithium acetate/single-stranded carrier DNA/polyethylene glycol method. Methods Enzymol **350**: 87-96.

Henkel, G., and Krebs, B. (2004) Metallothioneins: Zinc, Cadmium, Mercury, and Copper thiolates and selenolates mimicking protein active site features- Strcutural aspects and biological implications. *Chem Rev* **104**: 801-824.

Hodgkinson, V., and Petris, M. (2012) Copper homeostasis at the host-pathogen interface. *J Biol Chem* **287**: 13549-13555.

Lerch, K. (1980) Copper metallothionein, a copper-binding protein from *Neurospora crassa. Nature* **284**: 368-370.

Maiti, B.K., Pal, K., and Sabyasachi, S. (2007) Flexible Cu^{I}-thiolate clusters with relevance to metallothioneins. *Eur J Inorg Chem* **2007**: 5548-5555.

Mumberg, D., Müller, R., and Funk, M. (1995) Yeast vectors for the controlled expression of heterologous proteins in different genetic backgrounds. *Gene* **156:** 119-122.

Münger, K., and Lerch, K. (1985) Copper metallothionein from the fungus *Agaricus bisporus*: chemical and spectroscopic properties, *Biochemistry* **24**: 6751-6756.

Otvos, J.D., and Armitage I.M. (1980) Structure of the metal clusters in rabbit liver metallothionein. *Proc Natl Acad Sci USA* **77**: 7094-7098.

Pagani, A., Villarreal, L., Capdevila, M., and Atrian, S. (2007) The *Saccharomyces cerevisiae* Crs5 metallothionein metal-binding abilities and its role in the response to zinc overload. *Mol Microbiol* **63**: 256-269.

Palacios, O., Atrian, S., and Capdevila, M. (2011a) Zn- and Cu-thioneins: a functional classification for metallothioneins? *J Biol Inorg Chem* **16**: 991–1009.
Palacios, O., Espart, A., Espín, J., Ding, C., Thiele, D.J., Atrian, S., and Capdevila, M. (2014) Full characterization of the Cu-, Zn- and Cd-binding properties of CnMT1 and CnMT2, two metallothioneins of the pathogenic fungus *Cryptococcus neoformans* acting as virulence factors. *Metallomics* **6**: 279-291.

Palacios, O., Pagani, A., Perez-Rafael, S., Egg, M., Höckner, M., Brandstätter, A., Capdevila, M., Atrian, S., and Dallinger, R. (2011b) Shaping mechanisms of metal specificity in a family of metazoan metallothioneins: evolutionary differentiation of mollusc metallothioneins. *BMC Biology* **9**: 4.

Pettersen, E.F., Goddard, T.D., Huang, C.C., Couch, G.S., Greenblatt, D.M., Meng, E.C., and Ferrin, T.E. (2004) UCSF Chimera- a visualization system for exploratory research and analysis. *J Comput Chem.* **25**: 1605-12.

Pushie, M.J., Zhang, L., Pickering, I.J., and George, G.N. (2012) The fictile coordination chemistry of cuprous-thiolate sites in copper chaperones. *Biochim Biophys Acta* **1817**: 938-947.

Samanovic, M.I., Ding, C., Thiele, D.J., and Darwin, H. (2012) Copper in microbial pathogenesis: meddling with the metal. *Cell Host Microbe* **11**: 106-115.

Staats, C.C., Kmetzsch, L., Schrank, A., and Vainstein, M. H. (2013) Fungal zinc metabolism and its connections to virulence. *Front Cell Infect Microbiol* **3**: 1-7.

Tomas, M., Domenech, J., Capdevila, M., Bofill, R., and Atrian, S. (2013) The sea urchin metallothionein system: Comparative evaluation of the SpMTA and SpMTB metal-bindig preferences. *FEBS Open Bio* **3**: 89-100.

Valls, M., Bofill, R., Gonzalez-Duarte, R., Gonzalez-Duarte, P., Capdevila, M., and Atrian, S. (2001) A new insight into metallothionein (MT) classification and evolution. The *in vivo* and *in vitro* metal binding features of *Homarus americanus* recombinant MT. *J Biol Chem* **276**: 32835-32843.

Wang, Y., Mackay, E.A., Zerbe, O., Hess, D., Hunziker, P.E., Vašák, M., and Kägi, J.H.R. (1995) Characterization and sequential localization of the metal clusters in sea urchin metallothionein. *Biochemistry* **34:** 7460-7467.

Staats, C.C., Kmetzsch, L., Schrank, A., and Vainstein, M. H. (2013) Fungal zinc metabolism and its connections to virulence. *Front Cell Infect Microbiol* **3**: 1-7.

SUPPLEMENTARY MATERIAL

Segment	Forward (5'-3')	Reverse (5'-3')
CnMT1-S1	AAAAGGATCCTGCGGGTGCGGT	AAGGCTCGAG**TCA**CTTGGGGCA
CnMT1-S2	AGGGGGATCCCCTAAAAAGGCG	AAGGCTCGAG**TCA**CTTGGGGCA
CnMT1-S3	AAAAGGATCCTGCGGGTGCGGT	GGGGCTCGAG**TCA**GGAGCTGACTT
CnMT1-S4	AAAAGGATCCTGCGGGTGCGGT	AAAACTCGAG**TCA**GGCAGCGCC
CnMT1-S5	GGAAGGATCCATGGCTTGCAAC	AGGGCTCGAG**TCA**GCAGGCTTT
CnMT1-S6	AAAAGGATCCTGCAACTGCGGT	AAAACTCGAG**TCA**CTTGGGGCA
CnMT1-S7	AAAAGGATCCTGCTGCTCTACG	GGAACTCGAG**TCA**GCAGTTGTCA

Table S1. The underlined nucleotides correspond to the restriction sites for the *BamH*I (forward-oligonucleotides) and *Xho*I (reverse-oligonucleotides), used for subsequent cloning of the PCR fragments into the pGEX-4T1 expression vector. In bold, the corresponding stop codons.

Segment	Forward (5'-3')	Reverse (5'-3')
CnMT1	AAAAGGATCC**ATG**GCTTGCAACTGC	AAAACTCGAG**TCA**GGCAGCGCCAG
CnMT2	GGGGGAATTC**ATG**GCTTTCAACCCC	GGGGCTCGAG**TTA**TTTAGCCTT
CnMT1-S1	AAAAGGATCC**ATG**TGCGGGTGCGGT	AAGGCTCGAG**TCA**CTTGGGGCA
CnMT1-S2	AGGGGGATCC**ATG**CCTAAAAAGGCG	AAGGCTCGAG**TCA**CTTGGGGCA
CnMT1-S3	AAAAGGATCC**ATG**TGCGGGTGCGGT	GGGGCTCGAG**TCA**GGAGCTGACTT
CnMT1-S4	AAAAGGATCC**ATG**TGCGGGTGCGGT	AAAACTCGAG**TCA**GGCAGCGCC
CnMT1-S5	GGAAGGATCC**ATG**ATGGCTTGCAAC	AGGGCTCGAG**TCA**GCAGGCTTT
CnMT1-S6	AAAAGGATCC**ATG**TGCAACTGCGGT	AAAACTCGAG**TCA**CTTGGGGCA
CnMT1-S7	AAAAGGATCC**ATG**TGCTGCTCTACG	GGAACTCGAG**TCA**GCAGTTGTCA

Table S2. The underlined nucleotides correspond to the restriction sites for the *BamH*I or *Eco*RI (forward- oligonucleotides) and *Xho*I (reverse-oligonucleotides), used for subsequent cloning of the PCR fragments into the p424 yeast plasmid. In bold, the corresponding translation start and stop codons.

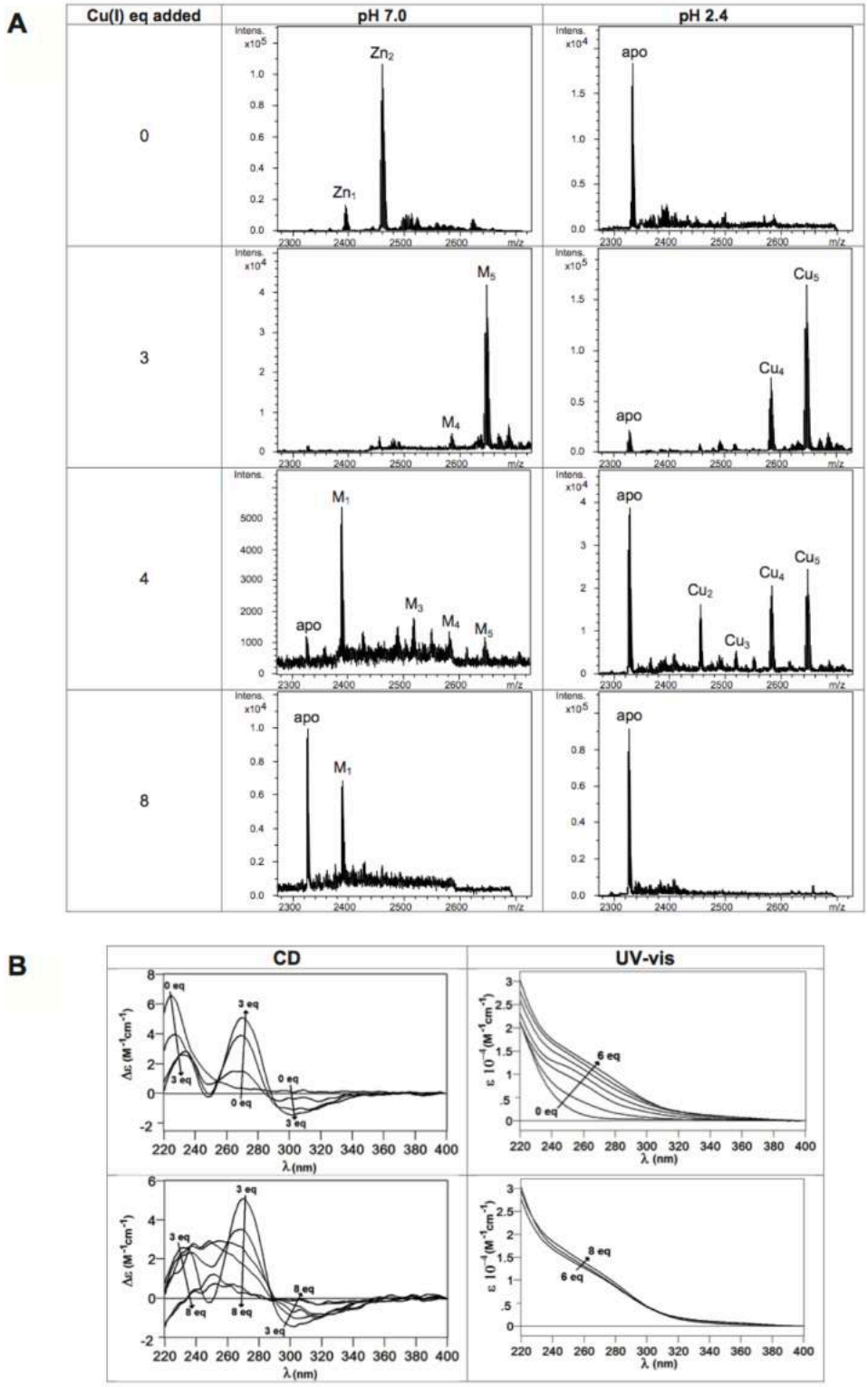

Figure S1. *In vitro* characterization of S1: (A) Deconvoluted ESI-MS and (B) circular dichroism spectra recorded during the addition of several Cu(I) eq to a 10 μM preparation of Zn-S1 at pH 7.0.

A

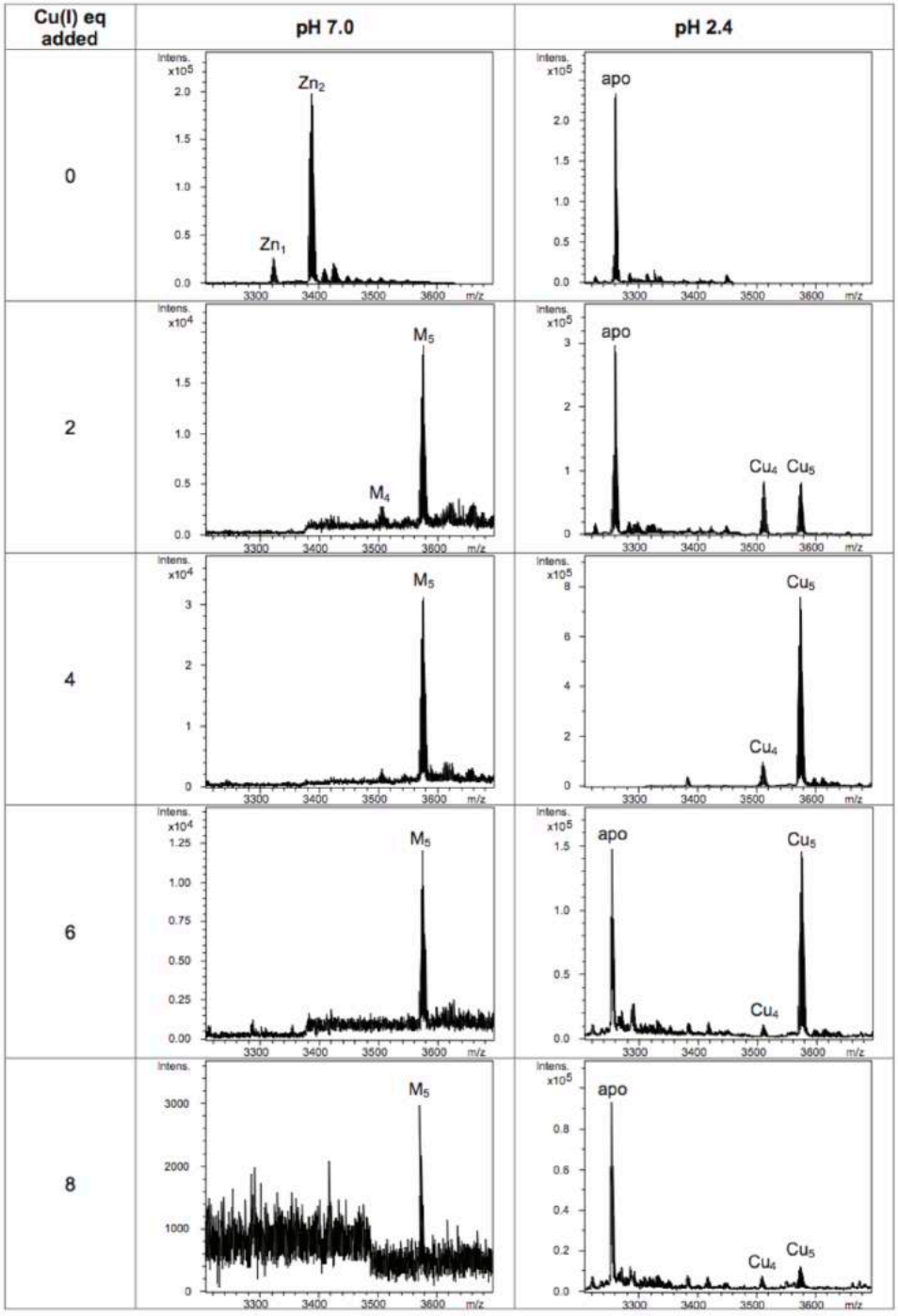
Cu(I) eq added
pH 7.0
pH 2.4
0
2
4
6
8
Zn1
Zn2
M4
M5
apo
Cu4
Cu5
Intens.
m/z

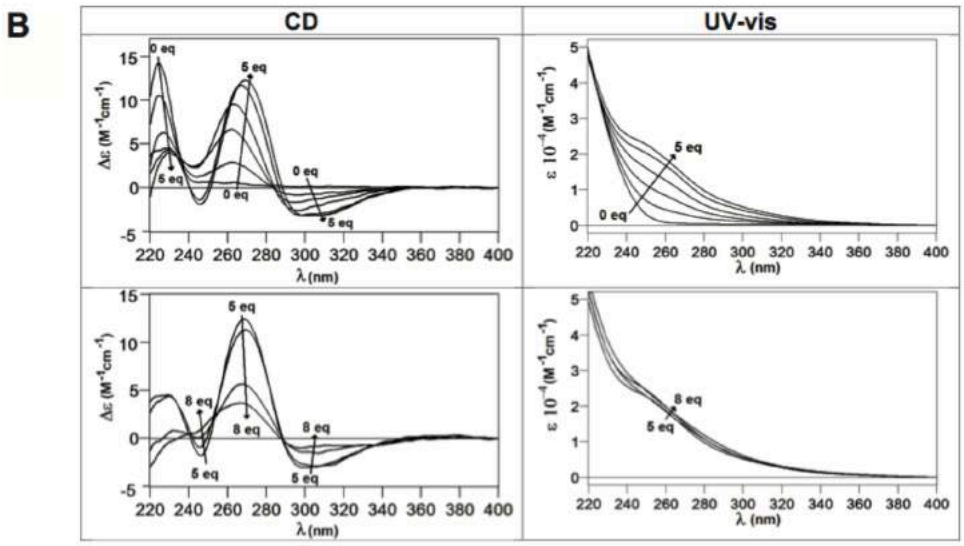

Figure S2. *In vitro* characterization of S2: (A) Deconvoluted ESI-MS and (B) circular dichroism spectra recorded during the addition of several Cu(I) eq to a 10 μM preparation of Zn-S2 at pH 7.0.

A

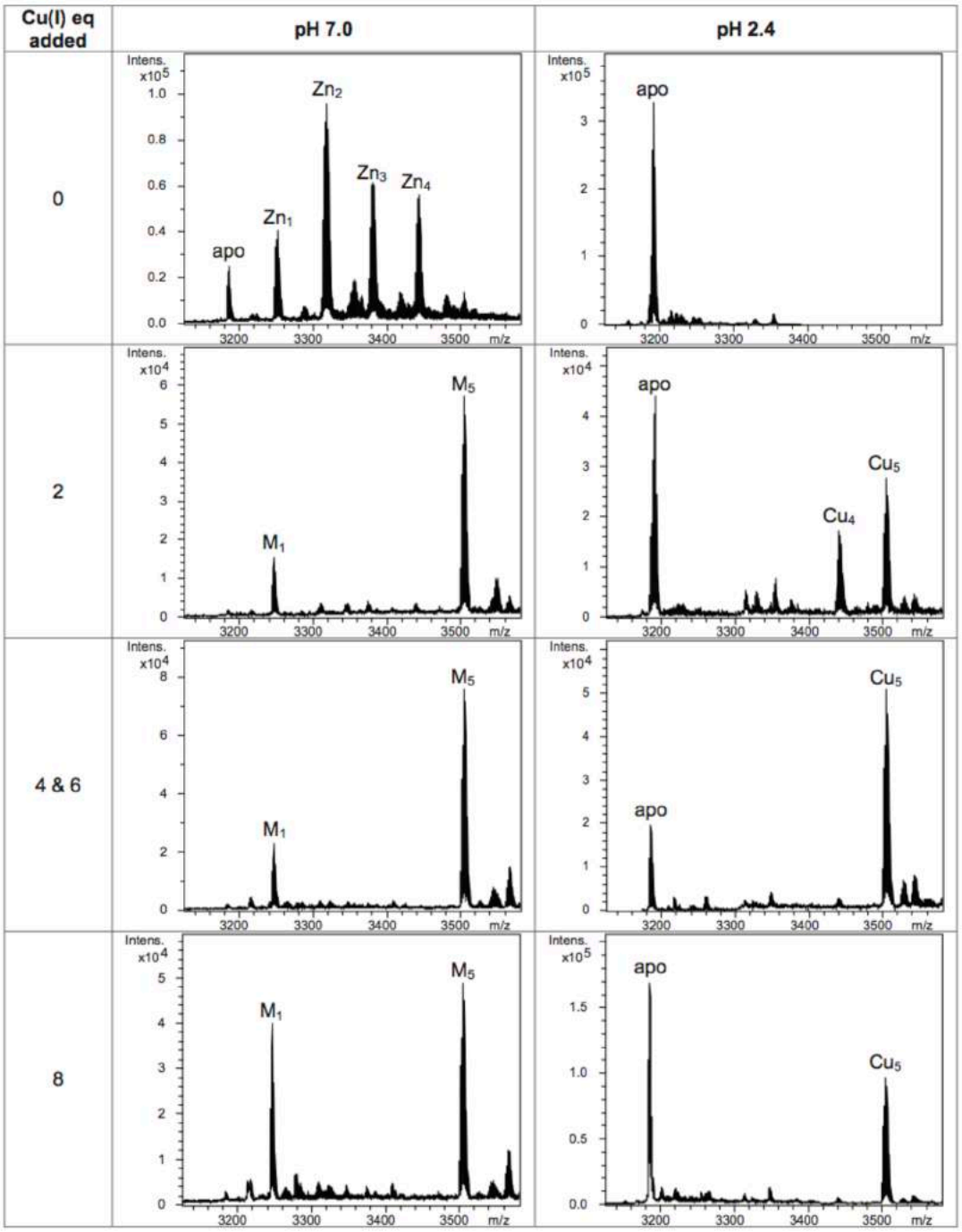
Cu(I) eq added
pH 7.0
pH 2.4
0
2
4 & 6
8
Intens.
x10^5
x10^4
m/z
3200
3300
3400
3500
apo
Zn1
Zn2
Zn3
Zn4
M1
M5
Cu4
Cu5

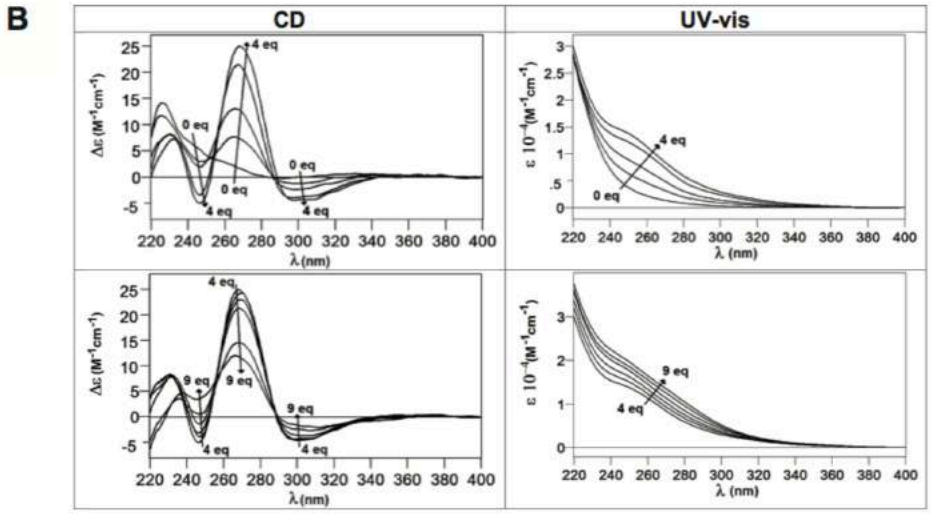

Figure S3. *In vitro* characterization of S3: (A) Deconvoluted ESI-MS and (B) circular dichroism spectra recorded during the addition of several Cu(I) eq to a 10 μM preparation of Zn-S3 at pH 7.0.

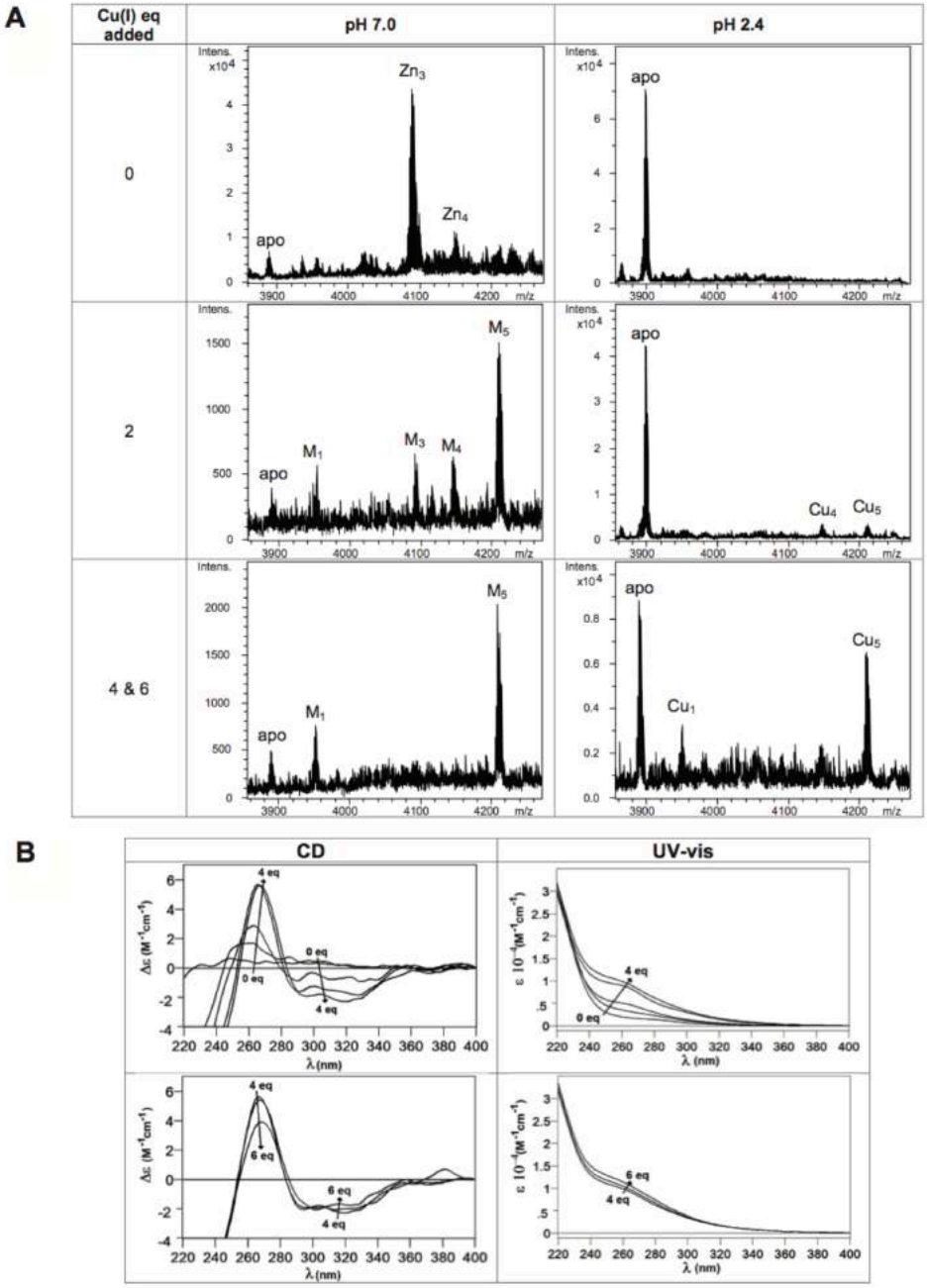

Figure S4. *In vitro* characterization of S4: Deconvoluted ESI-MS and circular dichroism spectra recorded during the addition of several Cu(I) equivalents to a 10 µM preparation of Zn-S4 at pH 7.0.

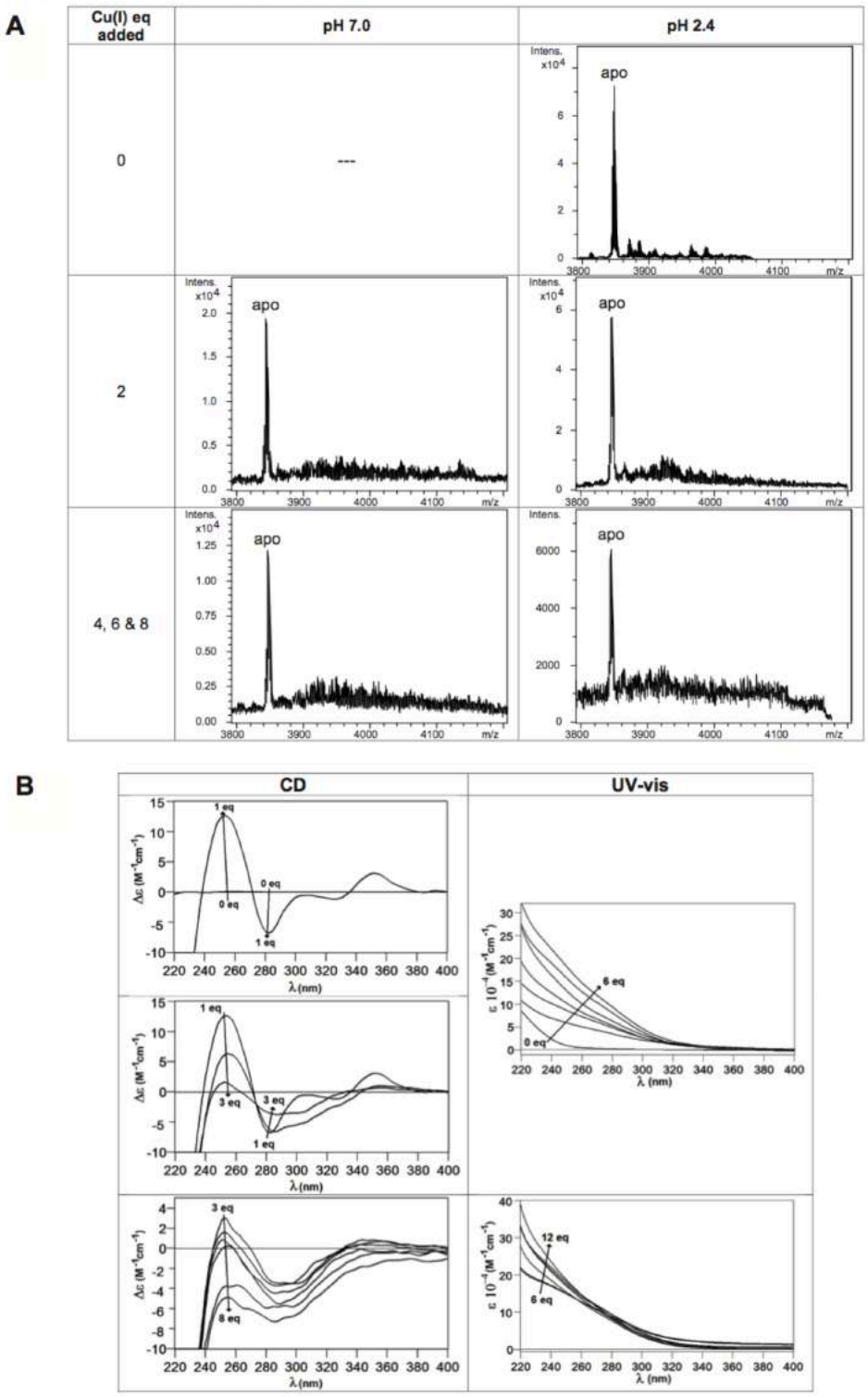

Figure S5. *In vitro* characterization of S5: (A) Deconvoluted ESI-MS and (B) circular dichroism spectra recorded during the addition of several Cu(I) eq. to a 10 μM preparation of Zn-S5 at pH 7.0.

A

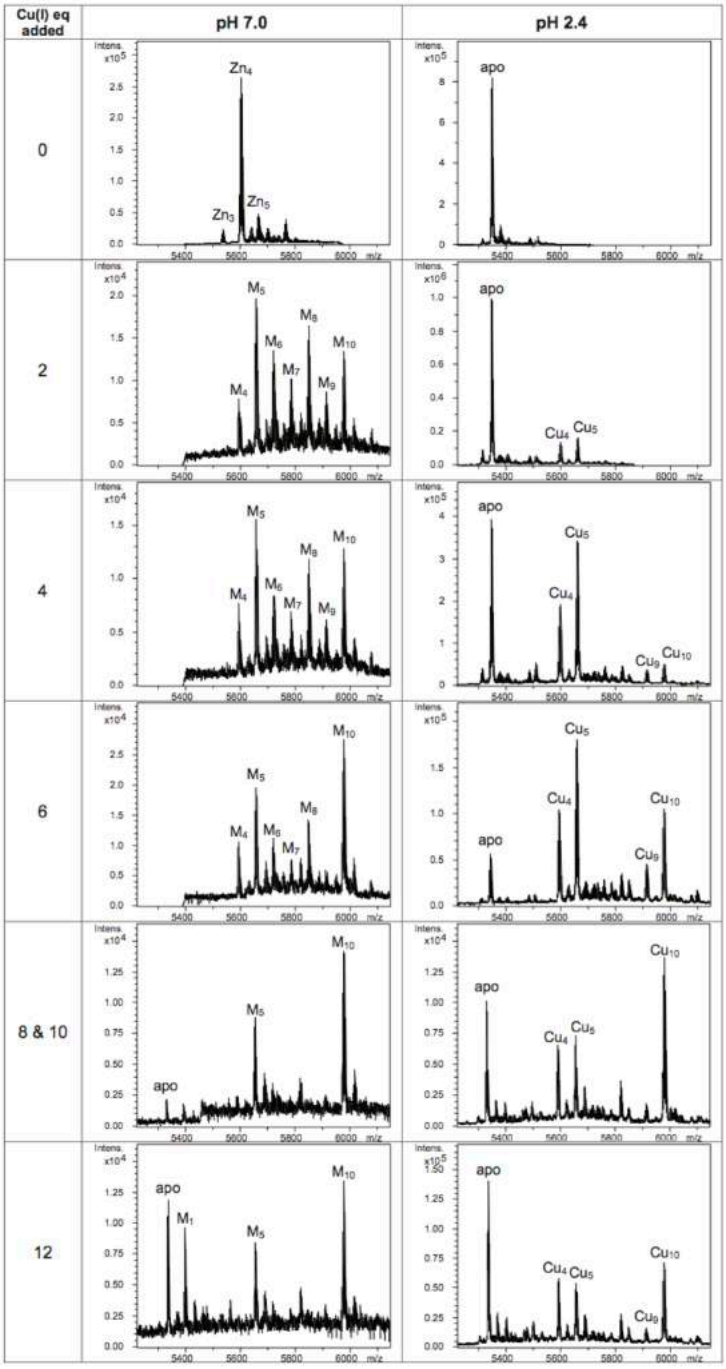
Cu(I) eq added
pH 7.0
pH 2.4
0
2
4
6
8 & 10
12
Zn4
Zn3
Zn5
apo
M4
M5
M6
M7
M8
M9
M10
M1
Cu4
Cu5
Cu9
Cu10
m/z

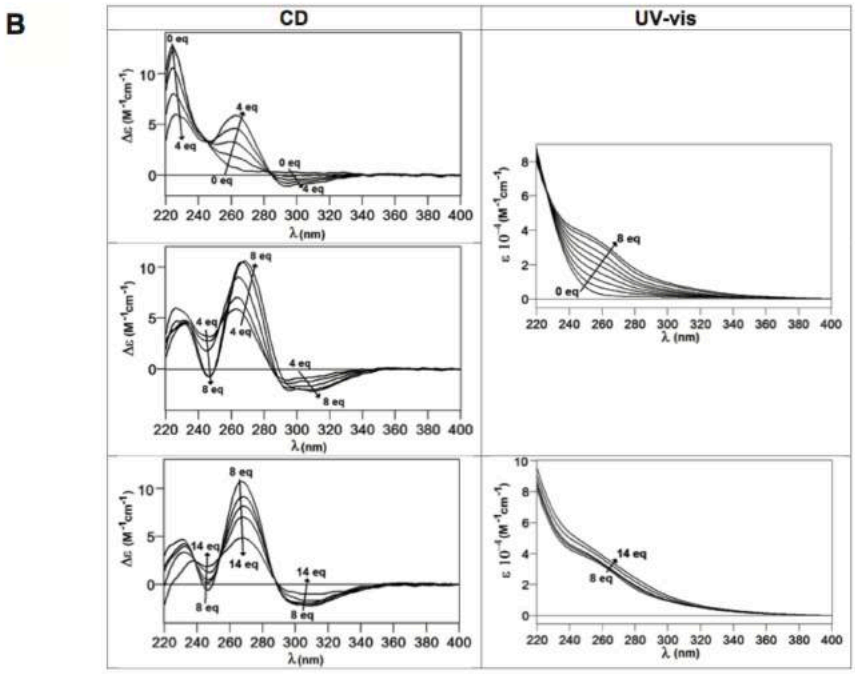

Figure S6. *In vitro* characterization of S6: (A) Deconvoluted ESI-MS and (B) circular dichroism spectra recorded during the addition of several Cu(I) eq to a 10 μM preparation of Zn-S6 at pH 7.0.

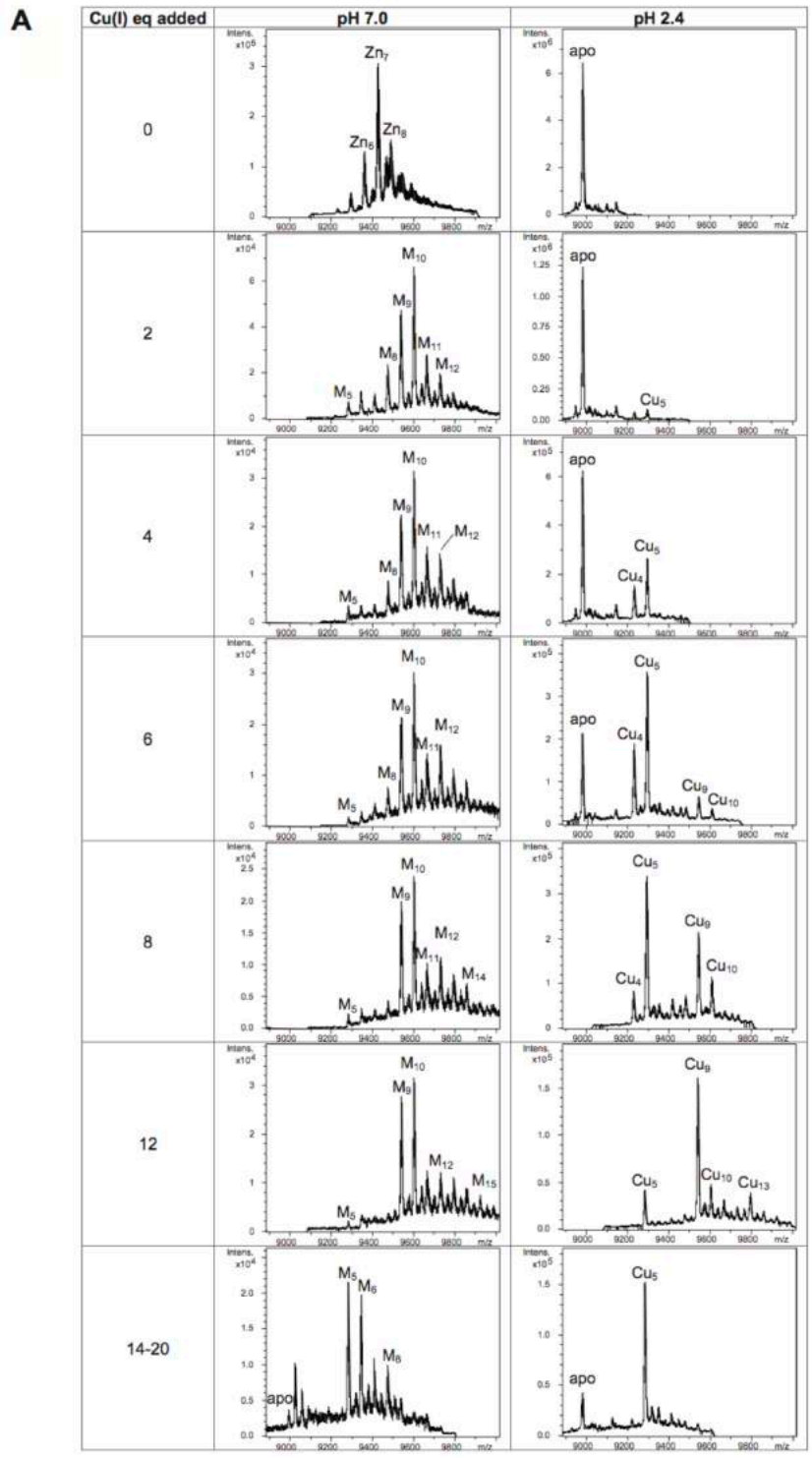
A
Cu(I) eq added
pH 7.0
pH 2.4
0
2
4
6
8
12
14-20
Zn7
Zn6
Zn8
apo
M10
M9
M8
M11
M12
M5
Cu5
Cu4
Cu9
Cu10
M14
M15
M6
Cu13
Intens.
m/z

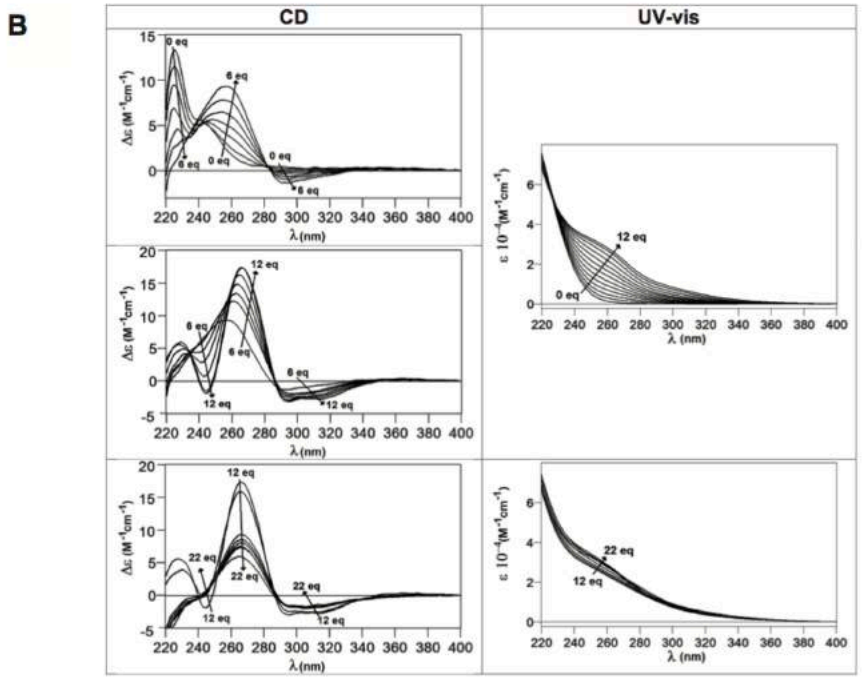

Figure S7. *In vitro* characterization of S7: Deconvoluted ESI-MS and circular dichroism spectra recorded during the addition of several Cu(I) equivalents to a 10 µM preparation of Zn-S7 at pH 7.0

Manuscript

The unexplored universe of fungal MTs: review and new data.

MANUSCRIPT:

TITLE

"The unexplored universe of fungal MTs: review and new data"

AUTHORS

Anna Espart et al.

REFERENCE

Publication in preparation.

SUMMARY

This document gathers the current available information about fungal MTs. From the first fungal MT reported to the most recent, the manuscript aims to review for the first time, what is known about these metalloproteins. The sequence features, the metal-binding abilities exhibit by some fungal models, or the role of MTs in some pathogenic fungi are discussed. Evenly, new identified MTs of human opportunistic pathogenic fungi and plant pathogenic fungi are described taking into account the frequent mis annotated sequences found in databases. Finally, a new classification into four subfamilies in accordance with the number of cysteine residues and the MT length is proposed.

THE UNEXPLORED UNIVERSE OF FUNGAL MTS: REVIEW AND NEW DATA

Fungi are eukaryotic unicellular, multicellular or syncytial spore-producing organisms, ubiquitously present in a wide range of environments, both terrestrial and aquatic. As heterotrophic systems, they obtain carbon and energy from external sources, either sugars, complex carbohydrates or polypeptides. All the required nutrients are absorbed through their cell wall, and once inside the cell, they are directly metabolized or transformed into other organic molecules, using the vast range of enzyme that fungi possess (Alexopoulos & Blackwell, 1996). The structure body of most of them is composed by hyphae that can specialize (haustoria in plant-parasitic or arbuscules in mycorrhizal fungi) for nutrient uptake from other living organisms. When hyphae accumulate in mass, they conform the mycelium if the fungus continues growing. Alternatively, other fungi, such as the generally called *yeasts*, are only composed by single cells and lack the ability to form hyphae. Fungal reproduction can adopt multiple strategies, reflecting the differences in structure and genetic divergence inside this kingdom. Asexual and sexual reproduction is found to coexist in almost all species, this leading to alternate haploid and diploid life cycles. Asexual reproduction happens via vegetative spores, mycelial fragmentation or yeast budding; whereas sexual reproduction, through meiotic generation of haploid cells, can be extremely divergent between species depending on its mating preferences; and hence heterothallic fungi spores mate with different type, while homothallic mate with itself. Either way, asexual and asexual spores are very efficiently spread in order to ensure reproduction success (Ni et al., 2011) (Cole & Hoch, 1991).

RELATIONSHIP WITH HUMAN LIFE

Fungi are reported to have been present in different aspects in human life since many centuries ago. Egyptian culture already used yeasts to elaborate bread, wine and beer (Dugan, 2008). Fungi have also been present for similar purposes in many other cultures, until nowadays. They are present in a wide range of human ecosystems; from food, to crops or livestock, they have been acting through improving or harming human life broadly. Currently they are also used for human benefit, as food biocatalyst (*e.g.* cheese, beer, wine, cured meat,

etc.), source of medical drugs (*e.g.* antibiotic or immune suppressants), in advantageous partnerships for plants (*i.e.* mycorrhizal fungi), to obtain fertilizer from organic matter decay, or even also as biocontrol for some pests. The scientific advances in fungus knowledge are speeding up new uses that ensure profitable applications: uses of new natural fungal metabolites, specific chemical biocatalysts, plastic degraders, or as new biocontrols (Schueffler & Anke, 2014). Nevertheless, food spoilage, or plant and animal diseases, represents the dark side of this kingdom. Two of the most impacting fungal diseases are those affecting crops and those causing opportunistic human infections, mainly among immunocompromised individuals (Pitt & Hocking, 2009) (Taylor, 2014).

CLASSIFICATION

According to Hawksworth (Hawksworth, 2004) there exist no less than 1.5 million fungal species living in the Earth, in a mutualistic, symbiotic or parasitic/pathogenic relationship. The particular features of each species hinder a single and schematized classification, although the advances in DNA technologies facilitate new fungal species identification and their re-classification. Two of the most employed taxonomic classifications are based on fungal morphological characteristics or their belonging to a specific phylum. In morphological classification, fungi are divided in yeast and moulds and subdivided into: *aseptate hyphae* and *septate hyphae* fungi. In the phylum classification, a new relationship between phyla have been established in the last years, classifying fungi in seven groups: *Ascomycota*, *Basidiomycota*, *Glomeromycota*, *Zygomycota*, *Chytridiomycota*, *Microsporidia* and *Neocallimastigomycota* (Figure 1) (Guarro et al., 1999). Some phyla share similar features, although it is worth noting that species and phyla are rearranged often according to new ways of understanding and describing them (Table 1).

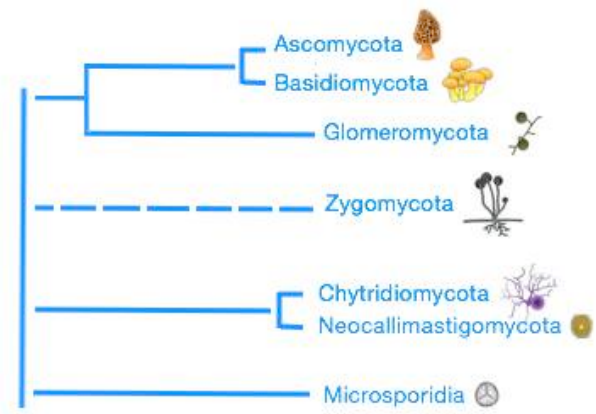

Figure 1. Fungi phyla. The dashed line indicates non-monophyletic groups. Adapted from Blackwell (2011) and Hibbett (2007)

PHYLUM	GENERAL FEATURES	RELATION WITH HUMANKIND	SIGNIFICANT EXAMPLES
Ascomycota	-Sexual reproduction through spores	-Source of antibiotics -Important in food tech (bread, alcoholic beverages, cheese). -Human and plant pathogens	-*Saccharomyces* spp -*Aspergillus* spp -*Fusarium* spp -Lichens (symbiosis)
Basidiomycota	-Production of basidiospores -Most are saprophytes	-Edible -Human and plant pathogen (rust, must)	-*Agaricus bisporus.* -*Lentinula edodes* -*Cryptococcus neoformans*
Glomeromycota	-Multinuclear cells with exclusively asexual reproduction through spores	-Arbuscular mycorrhiza	-*Gigaspora margarita* -*Glomus intraradices*
Zygomycota	-Production of zygospores and reproduction through two compatible hyphae	-Common bread moulds -Some are plant and animal parasites	-*Rhizopus* spp
Chytridiomycota	-Saprophytes -Form zoospores with flagelli -Present in terrestrial and aquatic media	-Some are plant and animal parasite	-*Synchytrium endobioticum* -*Batrachochytrium dendrobatidis*
Neocallimastigomycota	-Anaerobic -Form zoospores without flagelli	-Present in digestive tracts of herbivores degrading fiber	-*Neocallimastix patriciarum*
Microsporidia	-Unicellular	-All are animal parasites	-*Trachipleistophora hominis*

Table 1. Fungal classification according to the phylum and general features.

FUNGAL INTERACTION WITH OTHER ORGANISMS

In general terms, all living organisms interact with other in heterogeneous and complex relationships; these interactions will depend on temporary or permanent features of the organisms and their requirements. Interactions may be beneficial for both involved organisms, *i.e.* symbiosis/mutualism, or for only one of them, *i.e.* parasitic/pathogenic associations. The relationship they establish with plants, animals or other microbes are permanent, diverse and particular, in each case. In some cases they require a host to complete their biological cycle, involving a complex life cycle in which different fungal structures and stages (infective, vegetative and reproductive) are present (González-Fernández & Jorrin-Novo, 2012). Due to their economical and sociological importance, the most well studied fungal interactions are fungal-plants (pathogenic or not) and fungal-human pathogens (Perotto et al., 2013) (Gauthier & Keller, 2013). But fungi maintain associations not only with plants or animals, but also with bacteria, in a kind of symbiosis, in which they establish an indirect beneficial relationship, living in a specific environmental niche where both can take advantages. Bacterial-fungal interactions have been poorly understood so far, due to the limited scientific works on this issue. In last years references considering these interactions have increased, principally owing to they are considered an excellent model system to understand the fundamentals of host-pathogen relationship that can be involved in fungal-plant or fungal-human pathology, besides they can be interesting in other scientific applications (Kobayashi & Crouch, 2009).

Plants and fungi

Interactions between plants and fungi are extremely common, because fungi live generally in mutualistic or parasitic symbiosis with plants (Bonfante & Genre, 2010). Two examples of mutualistic relationship are lichens, a successful symbiosis between fungi and algae, and mycorrhizal fungi (ectomycorrhizal and arbuscular mycorrhizal), in which the plant benefits of the fungal metabolism, and the fungus obtain nutrients from the plant. On the other hand, parasitic and pathogenic fungi take advantage of the plant to obtain nutrients, regardless of the damage they can cause. Even so, fungal parasitism does not imply pathogenicity in all cases; endophytes are an example of how they can obtain nutrients without hurting plants.

Fungi are responsible of the major plant diseases, although only 10% (about 8,000 species) becomes harmful. Rust, anthracnose, mildew or black moulds are some examples of plant infections in which seeds, seedlings or adult plants are affected by fungi and cause significant economic losses in infected crops (Brown et al., 2012). The number of pathogenic plant fungi is very large and can vary depending on the latitude, being the most significant those affecting cereal or legume crops, as well as beans such as cacao or coffee (Table 2). The increasing number of fungal plant pest episodes (mainly caused by changes in agricultural procedures, such as monocultures and climate change) has produced an increase in the scientific research in this field (Dean et al., 2012) (González-Fernández & Jorrin-Novo, 2012).

FUNGAL PATHOGEN	CLASSIFICATION	HOST	MAIN DISEASE
Aspergillus spp.	*Ascomycete*	Corn, peanuts, cotton	Bread mould, seed decay
Blumeria graminis	*Ascomycete*	Wheat, barley	Corn mildew
Botrytis cinerea	*Ascomycete*	Grape, tomato, strawberry	Grey mould
Colletotrichum spp.	*Ascomycete*	Broad-range	Anthracnose
Fusarium graminearum	*Ascomycete*	Grain	*Fusarium* head blight
Fusarium oxysporum	*Ascomycete*	Tomato, tobacco, banana, legumes, sweet potatoes	Panama disease
Hemileia vastatrix	*Basidiomycete*	Coffee	Coffee rust
Magnaporthe grisea	*Ascomycete*	Rice	Rice blast
Melampsora lini	*Basidiomycete*	Flax	Flax rust
Moniliophthora perniciosa	*Basidiomycete*	Cacao	Witches' broom
Mycosphaerella graminicola	*Ascomycete*	Wheat	Wheat septoria leaf
Puccinia spp.	*Basidiomycete*	Asparagus, guava, eucalyptus, wheat…	Rust disease
Sclerotinia sclerotiorum	*Ascomycete*	Canola, rice	White mould
Uromyces appendiculatus	*Basidiomycete*	Beans	Rust
Ustilago maydis	*Basidiomycete*	Corn	Corn smut
Verticillium dhaliae	*Ascomycete*	Tomato, olive	Vascular wilt

Table 2. Examples fungal pathogens in plants, classification, host and caused disease. Adapted from R. Dean et al. (2012) and R. González-Fernández et al. (2012).

Animals and fungi

Relationships between animals and fungi are also complex and diverse. Mutualism is not as abundant as with plants, but there are also significant examples. Hence, fungi are part of the microbiota of cattle guts; and there is a close relationship between leaf-cutter ants (*Acromyrmex* and *Atta* genus) and the basidiomycete *Leucocoprinus* spp, in which ants feed the fungal *garden* as source of own food, these being the most clear examples of animal fungal mutualism. But in animals and more particularly in humans, fungi are known to be the causal agent of several diseases, although the number of reported pathogens for animals is lower than for plants (around 400 species, of which less than 50 species cause the 90% of

mammalian infections) (Sigler, 2003). Most of them are superficial pathogens (mainly dermatophytes), causing minor symptoms in skin or nails in 25% of population worldwide. Mucosal infections (oral and genital) caused by *Candida* species, are also common in infants and women in fertile stages, affecting until 75% of this population. All these fungi, mostly *Ascomycetes* and *Basidiomycetes*, are well studied and their pathophysiology is well established (Brown et al., 2012). Additionally, a small number of fungi are opportunistic, causing invasive fungal infections (IFIs) that affect especially immunocompromised, but also immunocompetent individuals. The immune state of the affected person may contribute to the severity of the infection, being HIV/AIDS patients, solid organ transplanted people and patients under chemotherapy treatments, the principal affected groups. *Ascomycetes* and *Basidiomycetes* along with *Zygomycetes* and *Microsporidia* are predominant as IFI agents. Despite their low incidence, mortality rates caused by these infections are not negligible (Table 3), reaching and even exceeding the 50%, despite attempted treatments. Unlike plant pathogenic and animal/human epidermal pathogenic fungi, opportunistic fungi are not well known by science and poorly recognized by health institutions.

According to Brown, the *Aspergillus*, *Candida*, *Cryptococcus* and *Pneumocystis* species are responsible of more than 90% of IFIs; however it has to be taken into account that infections caused by these species are normally underdiagnosed, resulting in loss of valuable information by misleading data (Brown et al., 2012). Besides *Aspergillus* spp and *Candida* spp which represent the principal hospital fungal infections, *Cryptococcus neoformans* (the main pathogenic species in the *Cryptococcus* genus) has a great impact globally, according to the CDC, due to its high mortality rate, reaching around 600,000 deaths per year, principally concentrated in Sub-Saharan Africa (Hope et al., 2013). Other important fungal infections due to their severity, are those caused by *Fusarium* spp, whose pathogenic forms can infect both superficially or sistemically; in this last case, the mortality rates reach almost to 100% of the cases without treatment (Nucci & Anaissie, 2007).

One of the current major challenges involves the development of new antifungal drugs able to fight against these infections. Current antifungal techniques are limited, as well as they present drug-related toxicity and interactions with other drugs (Hope et al., 2013); it is why that a better understanding of these organisms is required at different levels.

FUNGAL PATHOGEN	CLASSIFICATION	MORTALITY RATES (INFECTED POPULATIONS)
Aspergillus fumigatus	*Ascomycete*	30-95%
Blastomyces dermatitidis	*Ascomycete*	<2-68%
Candida albicans	*Ascomycete*	46-75%
Coccidiodes immitis	*Ascomycete*	<1-70%
Cryptococcus neoformans	*Basidiomycete*	20-70%
Histoplasma capsulatum	*Ascomycete*	28-50%
Paracoccidioides brasiliensis	*Ascomycete*	5-27%
Penicillium marnefeei	*Ascomycete*	2-75%
Pneumocystis jirovencii	*Ascomycete*	20-80%
Rhizopus oryzae	*Zygomycete*	30-90%

Table 3. IFI in humans, classification and mortality rates. Adapted from Brown et al. (2012).

FUNGI, METAL METABOLISM & METALLOTHIONEINS

All living organisms depend on transition metals. Heavy metal ions, such as iron, copper, zinc or manganese are required in low concentrations as cofactors or structural elements of several proteins; by contrast, higher amounts of these metals produce toxicity in cells. Furthermore, other non-physiological metals as cadmium, mercury or lead, and even some physiological metal ions such as copper, when they are not ligand-bound, may cause irreparable cell damage through reactive oxygen species (ROS) production. An imbalance of required metals can drive the organism to death, either by an insufficient concentration or high amounts of it. Therefore, all living organisms have developed homeostasis and detoxification mechanisms that ensure the sufficient level, of the essential metals. Among these, iron, copper and zinc play an important role, acting as cofactors of various enzymes, and being crucial in electron transfer reactions (Sacky et al., 2014). Intracellular sequestration of zinc, cadmium and silver in *Hebeloma mesophaeum* and characterization of its metallothionein genes. Globally, metal metabolism and handling is similar in all eukaryotic organisms, although there are significant differences related to particularities of each kingdom, reason why a global outline of metal metabolism in fungi follows below.

Physiological metal and metabolism in fungi

In fungi, the yeast *Saccharomyces cerevisiae* is accepted as the model organism to study and to understand how metal ions, precisely iron, copper and zinc, enter into the cell, are stored, mobilized and/or metabolized. Uptake, storage and metabolism are the three main steps of metal ion homeostasis, so that when required, they will be integrated into protein structures and participate in different cell/organism functions (Table 4) (Hosiner et al., 2014).

Iron homeostasis in S. cerevisiae

Regarding iron uptake, genes responsible for import and storage are similarly regulated. Depending on the situation in which *S. cerevisiae* grows (aerobic or anaerobic), iron can be differently available, and therefore the requirements of specific proteins may be different. Before entering the cell, two metalloreductases, Fre1 and Fre2, reduce Fe(III) ions that act as substrate for high-affinity transporters. The resulting Fe(II) is bound, re-oxidized and transported through the plasma membrane by the complex Fet3/Fet1. Paradoxically, Fet3 requires copper as a cofactor; which is why the synthesis of the chaperones Atx1 and Ccc2 that transfer cellular copper to Fet3, are ultimately regulated by iron. Fet4 and Smf1 are other low-affinity metal transporters, able to incorporate Fe(II), as well as other metals (copper and zinc, and manganese, respectively) into the cytoplasm. Iron can be also captured through siderophores; however *S. cerevisiae* is not able to synthesize them and use xenosiderophores from other organisms. To this end, it synthesizes siderophore receptors and transporters, such as the proteins Arn1, Arn4 and Fit1 to Fit3, as well as Fit1, Fit2 and Fit3 which are cell wall mannoproteins that retain xenosiderophores (De Silva et al., 1996) (Bleackley & MacGillivray, 2011). Two transcriptions factors, Aft1 ad Aft2, are responsible of iron-regulated gene expression, and Aft1 is also able to respond to zinc (Pagani et al., 2007) and cobalt (Stadler & Schweyen, 2002).

Under iron scarcity, Aft1 translocates into the nucleus to induce the expression of the iron regulon, if not it remains into the cytoplasm. Evenly, Aft2 acts similarly to Aft1, although Aft2 is involved in the expression of iron-dependent vacuolar and mitochondrial genes (Rutherford et al., 2001) (Bleackley & MacGillivray, 2011) (Courel et al., 2005). Once inside the cell, mitochondria are the major site of iron metabolism, being Mrs3 and Mrs4 the membrane proteins responsible of mitochondrial iron uptake (Mühlenhoff et al., 2003). Likewise Yfh1, which is a yeast frataxin homolog, acts as a mitochondrial iron-chaperone and

decreases the ROS production at the same time that delivers iron where it is needed (Bulteau et al., 2004). Vacuoles, which act as iron storage among other metals and molecules, possess the membrane transport protein Ccc1 that imports iron, as well as manganese from the cytosol (Li et al., 2001). When the cell requires iron, the Fre6 reductase, the Smf3 (a metal divalent transporter) and the complex Fth1/Fet5 are responsible to efflux iron to the cytosol. Iron intracellular transport from the uptake to the delivery point is not still well understood in yeast. Some proteins have been identified in mammalian cells as responsible for this iron mobilization, and some preliminary experiments suggest the existence of potential homologs in *S. cerevisiae* (Jo et al., 2008) (Bleackley et al., 2011).

Copper homeostasis in S. cerevisiae

The environmental Cu(II) ions are reduced to Cu(I) by the membrane reductases Fre1 and Fre2 to enter the cell through the high-affinity transporters Ctr1 and Ctr3. The expression of the corresponding genes is controlled by Mac1, which is a copper sensing transcription factor and acts binding copper responsive elements to the specific Cu-related genes (Labbé et al., 1997). After copper import, the metal can be delivered to three main pathways, thanks to different chaperones: i) copper can be bound to the chaperone Cox17 and be transported to the mitochondrial membrane; there it will be delivered to Sco1 and Cox11 which will transfer the metal ions to cytochrome *c* oxidase, the electron transport chain responsible to reduce molecular oxygen and translocate four protons across the mitochondrial membrane (Horng at el., 2004); ii) copper can be also bound to the cytosolic chaperone Atx1, that will transfer the metal ion to Ccc2 in the Golgi, for the subsequent copper incorporation to the high-affinity Fet3 (Lin et al., 1997); iii) Ccc1 is the metallochaperone responsible to insert copper into the Cu,Zn superoxide dismutase (SOD) Sod1, that contributes to protect the cell against oxidative stress induced by Cu^{+} and transforming superoxide into O_2 and H_2O_2 (Bermingham-McDonogh, et al., 1988) (Ding et al., 2014b) .

S. cerevisiae also possesses two metallothioneins (MTs), which are low-weight cysteine-rich proteins, that in fungal organisms show a high affinity for Cu^{+}. *S. cerevisiae* MTs are discussed in subsequent section.

Zinc homeostasis in S. cerevisiae

In yeasts, there is a close relationship between zinc and copper homeostasis. Proteins related with zinc metabolism are extremely conserved in different eukaryotic kingdoms. In *S. cerevisiae*, two specific zinc transporters Zrt1 (high-affinity) and Zrt2 (low-affinity) are the responsible of zinc uptake into the cell. Also the transporter Fet4, which is a low-affinity transporter that can be regulated by other metals is a relevant zinc transporter (Waters & Eide, 2002). In zinc scarcity, the nuclear transcription factor Zap1 binds to the zinc responsive elements in the promoters of the genes involved in the metal uptake (Zhao et al., 1998). When its requirements are covered, the remaining zinc is stored into vacuoles; Zrc1 and Cot1 are the vacuolar membrane transporters for the corresponding zinc uptake, whereas Zrt3 will export it to the cytosol, when the cellular concentrations decrease (MacDiarmid et al., 2002). Regarding to zinc trafficking, the presence of specific chaperones supposes a controversial idea in different groups, some of them defend the presence of zinc-chaperones similar to those in copper transport, while others support the dependence of protein-protein interactions to deliver zinc to target proteins is the regular scenario (Outten & O'Halloran, 2001) (Bleackley et al., 2011). Either way, other cell proteins have been shown to play a role in zinc homeostasis in specific situations. For instance Crs5, besides binding copper ions would yield homometallic Zn-Crs5 or heterometallic Zn,Cu-Crs5 complexes in high zinc stress conditions (Pagani et al., 2007) Another zinc-related protein that is involved in zinc homeostasis is the mitochondrial aconitase (Aco1). Although Aco1 harbours a Fe-S cluster, it has been shown that the absence of its enzymatic activity results in an increased zinc tolerance in *S. cerevesiae* (Guirola et al., 2014).

Metal detoxification

It has been already mentioned that the presence of metal ions is crucial for living organisms, although at the same time they may be harmful, and ultimately driving cells and/or organisms to death. When high concentrations of free physiologic or xenobiotic metal ions are present, they jeopardize the correct cell functioning mainly by metal substitution in active proteins or by genesis of oxidative stress, in which reactive oxygen species (ROS) are involved. This can affect proteins, lipids, DNA and other cell components (Wysocki & Tamás 2010). Fortunately cells are provided with complex systems to avoid metal ion accumulation.

To this end, three strategies are used: metal export, vacuolar metal sequestration and metal chelation.

Metal export proteins mediate the export of metals outside the cell; in *S. cerevisiae* there are two well characterized exporters: Acr3 for arsenic and Pca1 for cadmium. However, and in relation to the abundance or known export strategies in other organisms like bacteria, this mechanism has a minor importance in eukaryotic (and thus fungal) cells. Much more significant in fungi is vacuolar metal sequestration. In this case, metals are compartmentalized into membrane-bound organelles: in yeast, the ATP-binding cassette (ABC) transporter Ycf1, transports GSH-conjugated and xenobiotic metals to compartments; although the mechanism and transporter proteins involved, either for storage or mobilization in and out the vacuoles, are poorly known and understood (Perego & Howell, 1997). Finally, phytochelatins (PCs) and MTs play an important role in detoxification through metal chelation. PCs are glutathione oligomers that contribute to heavy metal (mainly cadmium) chelation and consequently to metal detoxification; and despite they are not identified in *S. cerevisiae*, are present in other fungal organisms such as *Schizosaccharomyces pombe* (Clemens, 2006b). Regarding *S. cerevisiae* MTs, Cup1 and Crs5 act sequestering copper efficiently, avoiding cell damaging, caused for high copper concentrations (Culotta et al., 1994) (Winge et al., 1985). As the subject of this paper, they will be further described in a special section (see below).

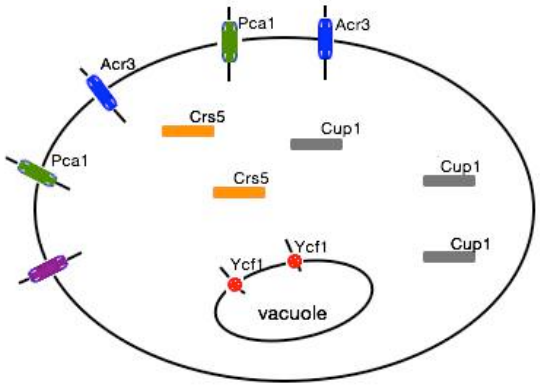

Figure 2. Proteins involved in metal chelation or export for detoxification purposes in *S. cerevisiae*. Adapted from Wysocki et al. (2010).

METAL METABOLISM IN PATHOGEN MICROORGANISMS

Pathogenic fungi and bacteria species have evolved to acquire metals from different sources, significantly from the infected hosts. Here, metal ions are not only required for physiological maintenance, but they may be involved in the infection strategy, thus conferring virulence to the pathogen. For this reason, a suitable handling of metal balance inputs and outputs is essential to accomplish both tasks. Precisely, the best-known metals participating in pathogenicity are iron, copper and zinc, being iron that for which more data have been gathered (Fones & Preston, 2013) (Ding et al., 2014b) (Porcheron et al., 2013). Despite common features, the iron metabolism of typical human pathogens (*C. albicans*, *C. neoformans* and *A. fumigatus*) differs from that of *S. cerevisiae*, because they obtain iron from ferritin, haemoglobin and siderophores. For instance, in *C. albicans*, Ftr1 is an important protein for iron acquisition, but Fet3, which requires copper at the same time through Ccc2 loading, is not, and its virulence is independent of Fet3 (Ding et al., 2014b). On the other hand, *C. neoformans* uses the melanin complex and 3-hydroxyanthranilic acid (3HAA), as well as the Fre family of proteins to reduce iron and import iron (Nyhus et al., 1997). Significantly, in this fungus, a close relationship has been demonstrated between melanin formation and an important number of Fe-importers and related proteins (such as Lac1, Atx1, Ccc2, and Fre4), the Cir1 transcriptional regulator and Sit1, a siderophore importer (Ding et al., 2014b). Every fungal pathogen contains Fre-orthologous proteins that has been related to virulence. Hence, Cfl1 of *C. albicans* regulates iron reduction, oxidative stress protection and virulence; whereas in *C. neoformans*, a big Fre protein family has been identified, in which two of the eight members, Fre2 and Fre4, are responsible for iron uptake from heme groups and melanin pathway, respectively. Other proteins, such as the Cft1 and Cft2 ferropermeases and the Cfo1 ferroxidase, have been shown to play an important role in virulence (Jung et al., 2009). Finally, in *A. fumigatus* also Fre proteins are responsible for high-affinity iron uptake, but contrarily, the FtrA permease seems to have no role in determining fungal virulence.

Copper is required for different functions and is closely related with iron metabolism; then it is sensible to hypothesize an important role of copper as virulence determinant. CTR transporters are highly conserved proteins in fungi, although they are absent in some organisms. In *C. neoformans*, low copper concentrations induce the expression of Ctr4 gene to offset the consequences of copper scarcity. On the other hand, members of the also highly conserved Ccc2 family of proteins act differently in virulence depending on the species: in *C.*

albicans, the disruption of CCC2 gene is not directly related with pathogenicity, whereas in *C. neoformans* either the disruption of ATX1 or CCC2 affect melanin formation and by extension, influence the fungal virulence (Walton et al., 2005). Cu/Zn SOD proteins are also relevant for fungal virulence; the disruption of SOD1 results in a decrease of virulence factors such as laccase, urease and phospholipase (Cox et al., 2003). Finally, also MT have been shown to play a definite role in fungal virulence, as will be explained below (Ding et al., 2014a).

Zinc is needed for SODs activity, as well as for Zap1, the transcription factor that controls zinc metabolism. These are also related to cellular matrix regulation in some pathogenic fungi as *C. albicans*, in which a reduction of virulence when Zap1 is mutated has been shown (Moreno et al., 2007) (Kim et al., 2001).

DEFINITION AND FEATURES OF METALLOTHIONEINS

Metallothioneins (MTs) are a ubiquitous cysteine-rich (about 30% of their content) superfamily of metal-binding proteins of low molecular weight, which have been identified from prokaryotes to higher eukaryotes. They constitute an heterogeneous polymorphic group in most of the organisms, being able to coordinate, though metal-thiolate bonds, different heavy metal ions, as divalent Zn(II) or Cd(II), or monovalent as Cu(I). The main function of MTs remains unclear, although it is known they participate in physiologic metal homeostasis, detoxification of xenobiotic metals, protection against oxidative stress and even cellular control of the redox status (Coyle et al., 2002). Margoshes and Vallee identified the first MT characterized in the horse kidney, in 1957; and from then, a wide range of MTs has been described in animals, plants, fungi and some bacteria, proposing a polyphyletic origin and evolution that would be related to their functional diversity (Capdevila & Atrian, 2011) (Blindauer, 2014) (Palacios et al., 2011). In fungi, the first MTs described were those of *Neurospora crassa* (NcMT), *Agaricus bisporus* (AbMT) and the yeast *S. cerevisiae* (Cup1), which were isolated and characterized during the early eighties (Münger et al., 1985) (Münger & Lerch, 1985a) (Winge et al., 1985) respectively. The vast majority of fungal MTs reported up to date exhibit a clear preference for Cu(I) binding, so that the character of Cu-thionein is accepted as one of the main features of the MTs of this kingdom (Bofill et al., 2009). However, a preference for divalent metal ions (Zn(II) or Cd(II)) has been described for some

MTs of different fungi, such as *Heliscus lugdunensis*, *Hebeloma mesophaeum* or *Russula atropurpurea* (Loebus et al., 2013) (Leonhardt et al., 2014).

Fungal MTs in Metallothionein Classification

Since the horse kidney MT identification in 1957, many others have been described in a broad range of organisms, so that a clear requirement of classification emerged. Until now, three classification criteria have been used. First, Kägi & Kojima proposed in 1987, a classification based on sequence homology to the horse MT, so that MTs were divided into three classes: similar to mammalian MTs (Class I), non-similar to mammalian MTs (Class II) and cysteine-rich, enzymatically-synthesized peptides, such as PCs or cadystins (Class III). A second classification proposed in 1999 by Binz & Kägi divided MTs in 15 families according their taxonomic origin. In this classification, MTs from one taxonomical group of organisms are commonly represented inside only one family, although others, due to the diversity of their MT sequences, are split among several families (Binz & Kägi, 1999). Finally in our research group, Valls et al. proposed in 2001 a third classification criteria, based on the metal-binding preferences of MTs, so that they are divided in Zn-thionein, those for a divalent metal ion preference (Zn(II) or Cd(II)) or Cu-thionein with monovalent (Cu(I)) metal ion preference, assuming that between these two big groups there is a gradation wherein different MTs should be placed (Valls et al., 2001) (Bofill et al., 2009) (Palacios et al. 2011).

Fungal MTs are classified in 6 different families according to Binz & Kägi's, owing to the divergence of their Cys patterns and their polypeptide lengths (Table 4).

FAMILY	NAME	EXAMPLE	CYS. PATTERN
8	Fungi 1	*Neurospora crassa* MT	-CXC- -CXCXXC-
9	Fungi 2	*Candida glabrata* MT1	-CXC- -CXCXXC- -CXXXCXC-
10	Fungi 3	*Candida glabrata* MT2	-CXC- -CXCC- -CXXXCXC-
11	Fungi 4	*Yarrowia lipolitica* MT3	-CXC- -CCC-
12	Fungi 5	*Saccharomyces cerevisiae* CUP1	-CC- -CXC- -CXCXCXXC- -CXXXCXCXXXC-
13	Fungi 6	*Saccharomyces cerevisiae* CRS5	-CC- -CXC- -CXXC- -CXXXC- -CXCXXC-

Table 4. Binz & Kägi fungal MT classification.

Finally, according to our functional classification (Valls et al., 2001), virtually all-fungal MTs can be considered as Cu-thioneins, although in last years some fungal MTs are identified as Zn-thioneins, as mentioned before.

FUNGAL MTS

YEAST MTS

As illustrated in Table 4, five out of six families of fungal MTs in Kägi's classification include the MTs of yeast species: *S. cerevisiae*, *C. glabrata, Y. lipolytica* and *S. pombe*. Among all of these, *S. cerevisiae* is adopted as a model organism among unicellular eukaryotes, and also its Cup1 MT is the Cu-thionein more characterized up to now.

Saccharomyces cerevisiae MTs

In 1984, D.R. Winge identified an MT in *S. cerevisiae*. The protein, which conferred clear Cu-resistance to cells, was called Cup1, and consisted of 61 amino acid with 12 Cys, which means a nearly 20 % of its total residues. However, the mature form of Cup1, as natively isolated, has only 54 residues, so that a proteolytic cleavage is supposed to occur. Cup1 is encoded by an intronless gene, mapping in chromosome 8, which has the capacity of

undergoing natural tandem amplification under high copper pressure (Winge et al., 1985). Most of the *S. cerevisiae* strains contain from 5 to 15 copies of CUP1, although strains with a single CUP1 copy have also been isolated, this leading to cell copper sensitivity (Karin et al., 1984). Ten years later, in 1994, Culotta identified a new *S. cerevisiae MT* gene, called CRS5. Crs5 is a 69-amino acid protein containing 19 Cys, which represents a 27.5% of its total residues (Figure 3). Contrarily to CUP1, CRS5 is always a single copy gene, mapping in chromosome 15 (Culotta et al. 1994).

```
Cup1      MFSELINFQNEGHECQCQCGSCKNNEQCQKSCSCPTGCNSDDKCPCGNKSEETKKSCCSG
Crs5      MTV---------KICDCEGECCKDSCHC--GSTCLPSCSGGEKCKCDHSTGSPQCKSCGE

Cup1      K------------------- 61
Crs5      KCKCETTCTCEKSKCNCEKC 69
```

Figure 3. CUP1 & CRS5 protein sequences alignments. Cysteines are marked in red. The N-term portion cleaved in the native Cup1 is in italics.

Both proteins bind preferentially copper ions. They are classified in two different families in Binz & Kägi classification: Cup1 belongs to family 12 (Fungi 5) and Crs5 to family 13 (Fungi 6). Concerning to our classification, Cup1 is considered as an extreme Cu-thionein, whereas Crs5 presents an improved capacity for zinc binding, so that it was considered intermediate between Cu-thioneins and Zn-thioneins (Pagani et al., 2007). This was in agreement with several studies that sustain the dominance of Cup1 over Crs5 in terms of copper tolerance. The advantages of the CUP1 system upon CRS5 for copper tolerance are: i) the tandem amplification of CUP1 genes in the CUP1 locus, as opposed to CRS5, which only has a single copy (Culotta et al., 1994) (Fogel & Welch, 1982); ii) the higher response of CUP1 promoter to copper ions; and iii) the stability of the Cu-Cup1 in relation to Cu-Crs5 complexes (Jensen et al., 1996). Cup1 has been reported to bind from 6 to 8 Cu(I), depending on the origin and of the analyzed Cu-complexes (Jensen et al., 1996) (Calderone et al., 2005); whereas Crs5 is able to bind 11 or 12 Cu(I) (Jensen et al., 1996). Both MTs bind other metal ions, such as Zn(II), Cd(II) or Ag(I), so that the corresponding complexes has been also analyzed. Hence, we have reported that, Cup1 is able to coordinate from 3 to 5 Zn(II) when recombinantly synthesized in Zn-supplemented cultures, while it renders homometallic Cd_5-Cup1 and tertiary Cd_6S-Cup1, Cd_6S_4-Cup1 or Cd_7S_7-Cup1 complexes when synthesized by Cd-enriched bacteria (Orihuela et al., 2010). Significantly, these sulfide-containing species are also present in native Cd-Cup1complexes (Orihuela et al., 2010).

Moreover, the crystal structure of Cu_8-Cup1 has been solved, being this the unique Cu-MT cluster whose structure is known up to now (Calderone et al., 2005) (Figure 4). The obtained structure suggested an active role of Cup1 in the delivery of copper to metal-free chaperones, in addition to its Cu-chelation function (Calderone et al., 2005).

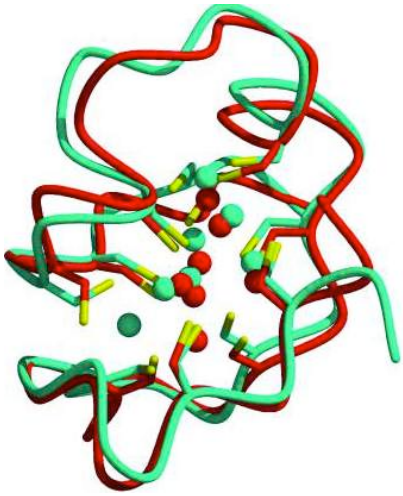

Figure 4. Superposition of the Cu_8-Cup1 crystal structure obtained from X-ray diffraction (cyan line) compared to the NMR model of the polypeptide chain fold in a Cu_7-Cup1 complex (red line) . The cysteine side chains are indicated (yellow lines), as well as Cu_8-atoms (cyan spheres) and Cu_7-atoms (red spheres). Adapted from Calderone (2005).

The induction of *S. cerevisiae* MT genes by copper is mediated by the activation of ACE1, a specific metalloregulatory transcription factor. Furthermore, the presence of four Cu-responsive upstream activation sequences (UAS) in each copy of CUP1 result in higher activity of CUP1 promoter in front a one single UAS copy in CRS5 promoter (Thiele 1988) (Culotta et al., 1994) (Strain & Culotta, 1996).

Candida glabrata MTs

MTs have also been well characterized in the human pathogen *Candida glabrata*. Hence, two Cu-induced MTs were identified and named MT-1 and MT-2 (Mehra et al., 1988). MT-1 is a 63 amino acid protein, with 18 Cys (28.6 % of total residues), and MT-2 contains 52 amino acids, with 16 Cys (30 % of total residues) (Figure 5). Their respective genes are both intronless and map in different chromosomes: *MT-1* in chromosome D, and *MT-2* in

chromosome H of the fungus. Their sequence similarity is limited; and thus MT-1 is classified in family 9 (Fungal 2) and MT-2 in family 10 (Fungal 3) (Mehra et al., 1990) (Mehra et al., 1989).

```
MT-1        MANDCKCPNGCSCPNCAN---------GGCQCG----DKCECKKQSCHGCGEQCKCGSHG
MT-2        MPEQVNCQYDCHCSNCACENTCNCCAKPACACTNSASNECSCQTCKCQT----CKC----

MT-1        SSCHGSCGCGDKCECK 63
MT-2        ---------------- 52
```

Figure 5. *C. glabrata* MT-1 & MT-2 protein sequences.
Cysteines are marked in red

C. glabrata MT genes are only induced by copper presence in the medium (Mehra et al. 1989). MT-2 is considered as equivalent to Cup1 in regard its major role in copper tolerance than MT-1, which can be compared to Crs5, which confers limited copper tolerance. This approach in *S. cerevisiae* and *C. glabrata* MTs follows the same strategy that it is found in higher vertebrates, in which one of the two MT genes is localized in multiple forms (Mehra et al., 1989). Evenly MT-1 and MT-2 are able to bind 11 or 12, and 10 Cu(I) ions, respectively, being involved in copper detoxification (Mehra et al., 1989) (Lachke et al., 2000). The metal-dependent transcription factor protein AMT1 of *C. glabrata* is the analogous ACE1 in *S. cerevisiae*. Thus, they are considered as a "copper handling" transcription factor, sharing strong similarities on their N-terminus and a weak similarity in C-terminus, confirming the importance of that region for DNA binding. ACE1 is constitutively expressed, whereas AMT1 is self-regulated, allowing the accumulation of copper when it is needed or in detoxifying processes if necessary (Zhou & Thiele, 1991).

Yarrowia lipolytica MTs

The genome of the dimorphic heterothallic yeast *Yarrowia lipolytica*, encodes four high similar MTs (MTP1 to 4) (García et al., 2002). They have 55 (MTP1 and 3) and 54 (MTP2 and 4) amino acids, and 9 Cys (~16.5% of total residues). They all contain triplets of Cys, which is an atypical Cys arrangement in fungal MTs (Figure 6).

```
MTP1      MEFTTAMFGTSLIFTT-STQSKHNLVNNCCCSSSTSESSMPASCACTKCGCKTCKC 55
MTP3      MEFTTAMLGASLISTT-STQSKHNLVNNCCCSSSTSESSMPASCACTKCGCKTCKC 55
MTP2      MEFTSALFGASLVQSKHKTTKKHNLVDSCCCSKPTEK--PTNSCTCSKCACDSCKC 54
MTP4      MEFLNANFGASLIQSKHKTTKKHNLVNSCCCSKPAEK--PTNSCTCSKCACDSCKC 54
```

Figure 6. Alignment between *Yarrowia lipolytica* MTs.
Cysteine residures are marked in red

MTPs are grouped as "Fungi 4" in the family 11 in Binz & Kägi classification, presenting an identity of 42% and respectively, a 96 and 90% of homology between MTP1-3 and MTP2-4. According to García et al., the expression of *MTPs* genes, which are located contiguously in the chromosome, is copper dependent, MTP1 and 2 showing a significantly increased expression in relation to MTP3 and 4 (García et al., 2002).

Schizosaccharomyces pombe MT

In 2002, Borrelly et al. (Borrelly et al., 2002), identified a 50 amino acids long MT in *S. pombe*. This protein, named Zym1, contains 12 Cys (24% of total residues) and confers a clear Zn-tolerance to cells. Its sequence bears limited similarity to Cup1 and Crs5 from *S. cerevisiae*, but contrarily, it shows a higher identity with mouse MT-1, in which 9 of 12 cysteine residues can be well aligned (Figure 7).

```
Zym1      MEHTTQCKSKQGKPCDCQSKCGCQDCKESCGCKSSAVDNCKCSSCKCASK 50
MT-1      --MDPNCSCSTGGSCTCTSSCACKNCKCT---------SCKKSCCSCCPV 61
```

Figure 7. Alignment between Zym1 and mouse MT-1.
Cysteines are marked in red.

The expression of *zym1* is induced by zinc and not by copper. Also H_2O_2 induces the synthesis of Zym1 (ref). However, at elevated zinc concentrations only a small tolerance decrease was observed for Zym1-null cells, suggesting that the main role of Zym1 is not zinc detoxification. This scenario is also found in mammalian cells, where zinc transporters are the primary detoxifying mechanisms (Palmiter, 1995). Furthermore, phytochelatins, and not the Zym1 MT, have been identified as the principal Cd defense mechanisms of *S. pombe* cells.

The alignment of all described here yeast MTs, allows us to compare the sequence similarities as well as the Cys-distribution (Figure 8).

```
Cup1      ------MFSELINFQNEGHE---------CQCQCGSCKNNEQCQKSCSCPT----GCNSD
MT-1      ------------------------MANDCKCPNGC-----------SCPNCANGGCQCG
Csr5      ------------------------MTVKICDCEGECC------KDSCHCGSTCLPSCSGG
MT-2      --------------MPEQVNCQYDCHCSNCACENTCNC--C-AKPACACTNS------AS
Zym1      --------------MEHTTQCK-SKQGKPCDCQSKCGC--QDCKESCGCKSS------AV
MTP1      MEFTTAMFGTSLIFTT-STQSK-HNLVNNCCCSSSTSE--SSMPASCACT----------
MTP3      MEFTTAMLGASLISTT-STQSK-HNLVNNCCCSSSTSE--SSMPASCACT----------
MTP2      MEFTSALFGASLVQSKHKTTKK-HNLVDSCCCSKPTEK----PTNSCTCS----------
MTP4      MEFLNANFGASLIQSKHKTTKK-HNLVNSCCCSKPAEK----PTNSCTCS----------

Cup1      DKCPCGNKSEETKKS-------------CCSG------K------ 61
MT-1      DKCECKK----QSCHGCGEQCKCGSHGSSCHGSCGCGDKCECK-- 63
Csr5      EKCKCDHSTGSPQCKSCGEKCKCETTCTCEKS------KCNCEKC 69
MT-2      NE------------------------CSCQTC------KCQTCKC 52
Zym1      DN------------------------CKCSSC------KCASK-- 50
MTP1      -K------------------------CGCKTC------KC----- 55
MTP3      -K------------------------CGCKTC------KC----- 55
MTP2      -K------------------------CACDSC------KC----- 54
MTP4      -K------------------------CACDSC------KC----- 54
```

Figure 8. Yeast MTs alignment between *S. cerevisiae* (Cup1 & Crs5), *C. glabrata* (MT-1 & MT-2), *Y. lipolytica* (MTP1-4) and *S. pombe* (Zym1) MTs.

NON-YEAST MTS

Among MTs of non-yeast fungi, those of *Neurospora crassa* (NcMT) and *Agaricus bisporus* (AbMT) are considered the traditional, archetypical fungal MTs, first identified by Kägi in 1979 and Münger in 1985 respectively (Kägi et al., 1979) (Münger & Lerch, 1985b). Both sequences are highly similar, even though *N. crassa* belongs to the *Ascomycota* phylum and *A. bisporus* to the *Basidiomycota*. This shows that their respective MTs have been conserved although the evolution.

NcMT is considered as the classic model for non-yeast fungal MTs. Its encoding gene is located on the chromosome 5 of the fungus; its coding region is interrupted by a short intron and the resulting protein is a 26-amino acid sequence (25 in its N-term processed form) with seven cysteines, this representing a 27 % of their residues. Evenly, AbMT possess also 7 Cys in its sequence. The cysteine pattern, as well as many other residues, are exactly the same in both sequences, which share a 80% of similarity (Figure 9). Both are included in family 8

(Fugal 1) in Binz & Kägi's classification and should be considered as genuine Cu-thionein according to Valls' classification.

```
NcMT MGDCGCSGASSCNCGSG-CSCSNCGSK 26
AbMT -GDCGCSGASSCTCASGQCTCSGCG-K 25
```

Figure 9. Alignment between NcMT and AbMT.
Cysteines are marked in red.

It was concluded that NcMT folds into a homometallic complex after binding 6 Cu (I) ions (Cu_6-NcMT). A polypeptide fold strcuture for the Cu_6-NcMT complex was solved by NMR, into which the Cu(I) ions were subsequently modelled (Figure 10) (Beltramini & Lerch, 1986) (Cobine et al., 2004a). Although NcMT synthesis is only induced *in vivo* by copper, *in vitro* NcMT, as all other MTs, can also bind divalent metal ions, like Zn(II), Cd(II), Co(II) and Ni (II) (Münger et al., 1987).

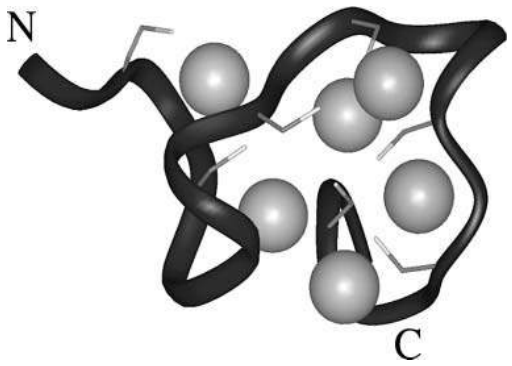

Figure 10. Diagram of the NcMT NMR structure,
including six modeled Cu(I) ions. Cobine et al. (2004).

Unlike other fungal MTs, the distribution of cysteine residues in NcMT exactly matches that of the first seven cysteines of the mammalian MT-2 and MT-1 isoforms (Figure 11), which led to suggest a relation between NcMT and a primordial MT gene in vertebrates (Cobine et al., 2004).

```
NcMT        M-GDCGCSGASSCNCGSGCSCSNCGSK----------    26
MT2         MDPNCSCAAGDSCTCAGSCKCKECKCTSCKKSCCSCCP... 61
MT1         MDPNCSCSTGGSCTCTSSCACKNCKCTSCKKSCCSCCP... 61
```

Figure 11. Alignment between NcMT, *Mus musculus* MT-2 and *Homo sapiens* MT-1 ß-domains. Cysteines are marked in red.

FUNGAL MTS IN 21ST CENTURY

Almost sixty years after the first MT identification, the scientific interest for these cysteine-rich proteins has not stopped to increase. From more than 300 scientific works published in the decade of 70s, there are now to more than 600 articles in 2010 (Capdevila et al., 2012) showing the importance of elucidate the structural and biochemical characterization of MTs, as well as their putative functions. Currently 30% of the studies concern mammalian MTs, while the other 70% comprise the rest of phyla and kingdoms, proving a less attention to other interesting MTs. Among the described MTs, those concerning fungi have been poorly investigated over the times. Fortunately, their interest has increased in last decades, attending the number of published scientific research devoted to fungal MTs. Currently, about 80 published works respond to "fungal MTs" query in PubMed database (www.ncbi.nlm.nih.gov/pubmed). Their heterogeneity among phyla, but at the same time their similarities between some MTs from different groups or with MTs from other kingdoms, their characteristic short sequences or their high affinity for copper, that contributes to cell copper detoxification, make them an exceptional MTs. Among all the fungal MTs, probably those related with mycorrhizal fungi and pathogenic fungi are most interesting. Mycorrhizal fungi have shown to alleviate heavy metal stress of plants in increasingly polluted soils (Hildebrandt et al., 2007), whereas pathogenic fungi are becoming an important challenge worldwide not only for crop care (by plant pathogenic fungi), but also in relation to human diseases that affect basically immunocompromised people. A better understanding of all these MTs should allow us to develop new biotechnological and biomedical tools to solve specific modern problems related to these issues. In this manuscript, pathogenic fungal MTs are discussed more deeply (Capdevila et al., 2012).

MTs IN PATHOGENIC FUNGI

Two of the most significant and representative pathogenic fungi where MTs have been analysed are *Magnaporthe grisea* (MMT1), the causing agent of rice blast fungus disease (Tucker, 2004), and *Cryptococcus neoformans* (CnMT1 and CnMT2) (Figure 12), the pathogenic fungus responsible of human cryptococcosis (Ding et al., 2011). In *M. grisea,* MMT1, its unique MT, can be considered the smallest MT reported in all kingdoms: it has 22 amino acids and 6 Cys and it is 40% similar to NcMT. It has been reported that MMT1 is essential for fungal pathogenicity (Tucker, 2004), it exhibits a high preference for zinc binding, resulting in a great ability to play an antioxidant role by release of these metal ions when ROS are present. However, its gene expression is not upregulated by any metal ion, but it is often induced through environmental stresses and specifically by hyperosmotic conditions, showing an unusual behaviour among fungal MTs (Tucker, 2004). Thus, during *M. grisea* infection, two possible roles of MMT1 have been proposed that would explain its requirement for virulence independently of its metal chelation function. First, MMT1 may be required as a potent antioxidant to confront plant defense mechanisms that can involve a rapid oxidative burst, localized in the infection point. Second, MMT1 may be required for cell wall differentiation in the appressorium, being necessary in the developmental biology of plant pathogenic fungi. It has been shown that *mmt1* mutants are not affected in metal tolerance but in reducing drastically the conidiogenesis, affecting hyphal growth and therefore, their pathogenicity (Tucker, 2004).

MMT1 22 aa
MCGDNCTCGASCSCSSCGTHGK

CnMT1 122 aa

MACNCPPQKNTACCSTSEAQDKCTCQKGNCECKACPNSTKTSESGGKASTCNCGGSGEACTCPPGQCACDKCPKK
AKSVSTCGCGGSGAACSCPPGKCACDNCPKQAQEKVSSCACSGSGAA

CnMT2 183 aa

MAFNPNPEKTTSCCSTSKAQDKCTCPKGKCECETCPKSTKTPGSGPCNCGVKEKVSTCGCNGSGAACTCPPGQCA
CDSCPRKAKSVSTCGCGGSAAACSCPPGKCACDSCPKQAQEKVSSCACNGSGGACTCPPGKCSCSGCPAQAKENP
ADQPTTCGCQGVGVACTCPPGQCACDGCPAKAK

Figure 12. *M. grisea* and *C. neoformans* MTs. Cys-residues (in red) and spacer regions with no Cys (in grey) are marked.

In *C. neoformans*, two unusually long MTs were identified (Ding et al., 2014a) (Festa et al., 2012). CnMT1 is a 122 amino acids long polypeptide, with 25 Cys, whereas CnMT2 comprises 183 amino acids, with 37 Cys. Both MTs are formed by Cys-rich segments separated by portions with no Cys residues or spacers (Figure 10). The cysteine segments are characterized by a cysteine doublet at the beginning, followed by "spacer-CXC-X_6-CXC-X_4-CXCXXC-spacer" pattern. The cysteine pattern in each Cys-rich segment is highly similar to the NcMT sequence, this indicating a probable evolutionary common origin from the same ancestor (Ding et al., 2014a) (Palacios, Espart et al., 2014a). Following the identification of both CnMTs, it was shown that they exhibited an extraordinary capacity to bind copper, not observed before. In high Cu-concentrations, CnMT1 is able to bind until 16 Cu(I) ions per molecule, and CnMT2 up to 24 Cu(I) ions, producing homometallic species. Both CnMTs bind Cu(I) through the cooperative construction of Cu_5-clusters, which allow to obtain the complete Cu_{16}-CnMT1 and Cu_{24}-CnMT2 complexes, so that each Cys-rich fragment is responsible to bind 5 Cu(I) in a cluster. Although additional experiments have shown that, like all MTs, they can also bind Zn(II) and Cd(II) if exposed to them; the metal-CnMTs complexes obtained from the respective recombinant synthesis in Zn(II) or Cd(II) metal enriched media are not stable and the obtained yield is poor, differently that occur with copper ions. The role of CnMTs during *C. neoformans* infection is closely related with its Cu detoxification machinery. In the infection process, the phagosomal compartment of innate immune cells creates an adverse environment to fight against the invader through: generation of reactive oxygen and nitrogen species, acidification of the paghosomal lumen, nutritional limitation or synthesis of proteases and degradative enzymes (Nathan & Shiloh, 2000) (Hood & Skaar, 2012), whereas macrophages hyperaccumulate copper inside the paghosome (Wagner et al., 2005). Meanwhile Cuf1, the metalloregulatory transcription factor induces the CTR4 gene expression that will import Cu^+ (which is also required for the well functioning of Cuf1), and also activates the transcription of CnMTs under copper excess conditions to chelate the metal ions, indicating the importance of Cuf1 and the activated genes as virulence factors. Ding et al., conducted *in vitro* and mice experiments, where they showed that during pulmonary infection, the CnMT1 promoter was activated at the same time that Cuf1 induced the CnMTs gene expression (Ding et al., 2014a). These data support the idea of the requirement of CnMTs for virulence, when macrophages use Cu^+ within the lumen of the phagosome as antimicrobial agent. This, was also corroborate in fungal cells expressing CnMT1ala, being incompetent for Cu-binding and exhibiting poor survival in lung infection (Ding et al., 2014a).

OTHER REPORTED FUNGAL MTS

In the last years, and as a consequence of the outburst of Genome projects, an increasing number of fungal MTs are being reported, and some of them are being also functionally characterized. Studies on mycorrhizal and plant and animal/human pathogenic fungal MTs are not negligible. Understanding the implications that MTs can have in plant metabolism or how they are involved in virulence, is crucial to know the fungal behaviour in high metal concentration environments, as well as how they use metal ions in their favour. Table 5 summarizes an important number of MTs, belonging to mycorrhizal fungi or plant/human pathogens.

Although fungal MTs are mainly Cu-thioneins, not all the MTs listed in Table 5 respond exclusively to Cu and even a small group of them are induced by another different metals. Hence, among mycorrhizal fungi, characterized by their high capacity to accumulate heavy metals from the soil, MT genes inducible by Zn, Cu, Cd, or even Ag have been identified. For instance, the three *Hebeloma mesophaeum* MTs bind Zn, Cd and Ag differently; HmMT1 binds specifically Zn and Cd, whereas HmMT2 and HmMT3 bind Ag (Sacky et al., 2014). On the contrary, the MTs of *Hebeloma cylindrosporum*, confer cell tolerance only to Cu and Cd; and the corresponding HcMT1 gene is induced by Cu while HcMT2 is also induced by Cd, besides Cu, suggesting a diversification in their heavy metal detoxifying contribution (Ramesh et al., 2009). This situation is also repeated for *Paxillus involutus* and *Gigaspora margarita*, whose *MT* genes (*Pimt1* and *Gmarmt1*, respectively) are induced by Cu and Cd conferring cellular tolerance against both metals (Bellion et al., 2007) (Lanfranco, 2002). Contrarily to that, other mycorrhizal fungi show a single preference, as *Russula atropurpurea*, whose two MTs bind specifically Zn^{2+} ions accumulated in the cytoplasm (Leonhardt et al., 2014). This is also observed for *Amanita strobiliformis* MTs (AsMTs), but with Ag instead of Zn; all three AsMTs sequester Ag in fruit bodies and mycelia, hyperaccumulating this metal (Osobová et al., 2011) or *Glomus intraradices* MT, which as a typical fungal MT that confers Cu-tolerance to cell, its gene being induced by Cu (González-Guerrero et al., 2007).

This scenario is not exclusive of mycorrhizal fungi; also other fungal MTs are known to be induced by different metal ions. Thus, the arthropod parasite *Beauveria bassiana* (BbMT) or the plant pathogenic fungus *Colletotrichum gloeosporioides* MTs (*Cap3* and *Cap5*) genes are both induced by Cu and Cd, showing their potential function in heavy metal

resistance (Kameo et al., 2000) (Osobová et al., 2011). Moreover, the MT of the aquatic fungi *Heliscus lugdunensis* is Cd-induced, being the Cd detoxification its primarily function (Loebus et al., 2013a). Other known fungal MTs listed in Table 5, such as *Uromyces fabae*, *Phaeosphaeria nodorum* or *Laccaria bicolor*, are not fully characterized and no metal preferences have been determined so far.

FUNGUS & MT NAME	PHYLUM	LENGTH (AA)	CYS. NUMBER	PATHOGENICITY	REPORT
***H. lugdunensis* MT**	*Ascomycota*	24	8	No	Jaeckel, P. (2005)
***U. fabae* MT**	*Basidiomycota*	24	6	Yes	Hahn, M. (1996)
***P. nodorum* MT**	*Ascomycota*	25	7	Yes	Hane, J.K. (2006)
***C. gloeosporioides* Cap3**	*Ascomycota*	26	7	Yes	Hwang, C.S. (1995)
***C. gloeosporioides* Cap5**	*Ascomycota*	27	8	Yes	Hwang, C.S. (1995)
***P. anserina* PaMT1**	*Ascomycota*	26	7	No	Averbeck, NB. (2001)
***C. albicans* CUP1**	*Ascomycota*	33	6	Yes	Weissman, Z. (1999)
***C. albicans* CRD2**	*Ascomycota*	76	12	Yes	Riggle, P.J. (1999)
***A. strobiliformis* MT1a**	*Basidiomycota*	34	6	No	Osobova, M. (2011)
***A. strobiliformis* MT1b**	*Basidiomycota*	34	7	No	Osobova, M. (2011)
***A. strobiliformis* MT1c**	*Basidiomycota*	34	6	No	Osobova, M. (2011)
***H. mesophaeum* HmMT1**	*Basidiomycota*	59	13	No	Sacky, J. (2013)
***H. mesophaeum* HmMT2**	*Basidiomycota*	58	13	No	Sacky, J. (2013)

***H. mesophaeum* HmMT3**	*Basidiomycota*	52	13	No	Sacky, J. (2013)
***H. cylindrosporum* HcMT1**	*Basidiomycota*	59	13	No	Bellion, M. (2007)
***H. cylindrosporum* HcMT2**	*Basidiomycota*	57	13	No	Bellion, M. (2007)
***G. margarita* GmarMT1**	*Glomeromycota*	65	13	No	Lafranco, L. (2002)
***S. pombe* Zym1**	*Ascomycota*	50	12	No	Borrelly, GPM. (2002)
***G. intraradices* ntMT**	*Glomeromycota*	71	12	No	González-Guerrero, M. (2005)
***B. bassiana* MT**	*Ascomycota*	?	?	Yes	Kameo, S. (2002)
***P. tinctoricus* MT**	*Basidiomycota*	35	7	No	Voiblet, C. (2001)
***P. involutus* PiMT1**	*Basidiomycota*	34	7	No	Courbot, M. (2004)
***L. edodes* MT**	*Basidiomycota*	34	7	No	Kwan, HS. (2005)
***R. atropurpurea* RaZBP1**	*Basidiomycota*	53	6	No	Sacky, J. (2013)
***R. atropurpurea* RaZBP2**	*Basidiomycota*	53	6	No	Sacky, J. (2013)
***L. bicolor* MT1**	*Basidiomycota*	37	8	No	Reddy, MS. (2014)
***L. bicolor* MT2**	*Basidiomycota*	58	14	No	Reddy, MS. (2014)

Table 5. Other fungal MTs described in the literature.

OUR WORK. *IN SILICO*, *IN VIVO* AND *IN VITRO* APPROACHES

In recent years, our laboratory has focused part of its efforts to identify and characterize fungal MTs, principally from plant or mammalian pathogenic fungi. Our approach goes through three main rationales: *in silico*, *in vivo* and *in vitro*, which allow us to screen a hypothetical fungal MT and characterize it, to better understand some steps of fungal metal metabolism and the MT role in infection and virulence.

The previous results obtained for *C. neoformans* MTs led us to suspect the existence of more mis annotated putative fungal MTs, or even of many fungal MTs that were merely non annotated in the corresponding genomes. Consequently, we decided to explore by *in silico* screening and BLAST searches (NCBI, www.ncbi.nlm.nih.gov), fungal genomes in search of MT ORFs and check them manually. If existing, the corresponding ESTs were analyzed, to confirm the correct or incorrect associated hypothetical protein. During these analyses, other well annotated sequences, but not identified as fungal MTs, were localized and subsequently checked through their existing ESTs. In some other cases, the hypothetical cDNA was obtained by rtPCR of isolated mRNA preparations, to be able to identify the ORF as a real gene. For the most appealing MTs, we proceeded to characterize their metal-binding abilities through recombinant synthesis of their Zn-, Cd-, and Cu-complexes.

NEWLY IDENTIFIED FUNGAL MTS

The database analysis strategy allowed us to identify an interesting group of MTs from plant and human pathogenic and non-pathogenic fungi. Their sequences and cysteine residues are diverse, following the trend of the different fungal MTs in the Binz & Kägi fungal classification. Some identified sequences are similar to NcMT (*e.g. Blastomyces dermatitidis* MT2), while others are more similar to *C. glabrata* MTs (*e.g. Sporothrix brasiliensis* MT) or presumably have a modular structure, as *C. neoformans* MTs (*e.g. Tremella mesenterica* MT). It is worth noting that the existence of a large number of long MTs (longer than the short MTs considered until now as models for this kingdom) is clearly evidenced, breaking the dogma that most commonly, fungal MTs are small size peptides. Also, it seems evident that the length of an MT would not be related with the pathogenicity of the corresponding fungus, because, pathogenic species as *Coccidioides posadasii*, the causing agent of coccidioidomycosis, and *C. neoformans* possess MTs of very dissimilar size (32 amino acids

C. posadassi and 122 and 183 amino acids *C. neoformans*), although in the first case no relationship between MT and virulence has been yet demonstrated.

IN SILICO OVERVIEW OF THE FUNGAL MTS

A comprehensive compilation of existing and newly-identified fungal MTs facilitates their classification according different criteria, and also allows hypothesizing on their functional features, and their possible role in metal metabolism and in infectivity processes. Table 6 includes a significant number of them, with sequence and pathogenicity data, whereas Table 7 classifies taxonomically all fungi of which MTs have been reported.

Table 6. Fungal MTs newly identified in this work

FUNGUS & MT NAME	PHYLUM	LENGTH (AA)	CYS. NUMBER	PATHOGENICITY	SEQUENCE
***Aspergillus flavus* / *oryzae* MT**	*Ascomycota*	23	8	*A. flavus*: Plant/Human A. *oryzae*: No	MSPCSCNCCSGNCNSCSCSDCKH
***Aspergillus nidulans* MT**	*Ascomycota*	23	8	No	MSPCTCNCCSGECNSCSCSSCKH
***Aspergillus niger* MT**	*Ascomycota*	23	8	Plant/Human	MAPCECKCCSGSCNSCSCSNCKH
***Uncinocarpus reesi* MT**	*Ascomycota*	23	8	No	MSPCSCNCCSGNCNSCSCSNCSH
***Coccidioides posadasii* MT1**	*Ascomycota*	23	8	Human	MNPCSCNCCSGNCNNCSCGSCGH
***Coccidioides posadasii* / *immitis* MT2**	*Ascomycota*	32	9	Human	MGCGCGTGSCSCNGPQNCSCPSDTCHCTTCGK
***Blastomyces dermatitidis* MT1**	*Ascomycota*	24	8	Human	MSPCNCNCCAGDCNSCSCTSCSVP
***Blastomyces dermatitidis* MT2**	*Ascomycota*	33	9	Human	MGCGCGDDKCPCEGPKTCSCSSSGTCGCTTCGK
***Histoplasma capsulatum* MT**	*Ascomycota*	34	9	Human	MACGCGNNSCPCDGPQSCTCSSGGGSSCGCTTCK
***Paracoccidioides brasiliensis* MT**	*Ascomycota*	36	9	Human	MGCGCGSECSCSGPQNCVCGTSGGGSTCHCTSCTVS
***Yarrowia lypolitica* MT5**	*Ascomycota*	59	20	No	MACSTNCSCPKPCTNCACEKACTCSPCSCESCKCAKACECEKSTTCKCESCKCEGSCKC
***Fusarium oxysporum* / *graminearum* MT**	*Ascomycota*	26	7	Plant/Human	MAGDCGCSGASSCNCGSSCSCSGCGK

***Moniliophthora perniciosa* MT1**	*Basidiomycota*	33	7	Plant	MIATEFTVVNAHCGSSTCNCGENCACKPGECKC
***Moniliophthora perniciosa* MT2**	*Basidiomycota*	36	7	Plant	MLFVTAIPVDQACGSNSCNCTSSCDCKTGTCNCGSK
***Moniliophthora perniciosa* MT3**	*Basidiomycota*	36	7	Plant	MQFVAAVPVNQACGSNSCNCTSSCDCKAGTCGCGSK
***Sporothrix brasiliensis* MT**	*Ascomycota*	79	12	Human	MVSSTCCGKGGAECVCAQNATCSCGKQSALHCNCDRAATENNTAGDRCSCGQRPAGACTCATNPSEVNTANETDFTTRK
***Scedosporium apiospermum* MT**	*Ascomycota*	101	16	Human	MSPADTCCRKGEGACVCAQQATCSCGKQSALHCTCDKAAVENTISGPSCSCGSRPVGQCTCENATVENQKPTGATCGCGARPAGSCTCNNSANETDFTTKK
***Neurospora crassa* MT2**	*Ascomycota*	112	16	No	MSAPVAKASTCCGKSAECICAKQATCSCGKQSALHCTCDKANSENAVEGPRCSCRARPAGQCTCDRASTENQKPTGNACACGTR PADACTCEKAADGGFKPTDLETDFTTKN
***Tremella mesenterica* MT**	*Basidiomycota*	257	57	No	MSAPVETKEKSCGCQPAPAVQSCNCSNEGNCTCAPGKCACSSCSSDSIKKTGKCGGSEGCTCEAGKCDCASCPGSSGQVKACTCGTSCSCPPGECTCAGCPNNKGKEKAKDEKAGECSCGPSCSCPPGECSCAGCSNVKSTGKEKAPAKACECGEECSCPPGQCSCANCPAKEKKDACSCSEGCSCPPGQCACANCPHKDEAKGCSCGESCSCPPGECKCANCPKKTEPAKACACGDECSCPPGQCGCADCPGKTSS

PHYLUM	ORDER	ORGANISMS
Basidiomycota	Tremellales	*C. neoformans* *T. mesenterica*
	Agaricales	*H. mesophaeum/cylindrosporum* *A. strobiliformis* *P. involutus* *G. lucidum* *A. bisporus* *M. perniciosa*
	Urodinales	*U. fabae*
Ascomycota	Eurotiales	*A. flavus*/niger*/oryzae/fumigatus/nidulans*
	Onygenales	*C. posadasii/immitis* *P. brasiliensis* *H. capsulatum* *B. dermatitidis* *U. reesii*
	Saccharomycetales	*C. albicans/glabrata* *S. cerevisiae*
	Hypocreales	*F. verticillioides*/oxysporum/graminearum* *H. lugdunensis*
	Sordariales	*P. anserina* *N. crassa*
	Microascales	*S. apiospermum*
	Magnaporthales	*M. grisea*
	Pleosporales	*P. nodorum*
	Ophiostomatales Glomerellales	*S. brasiliensis*
	Glomerellales	*C. gloeosporioides*
Glomeromycota	Glomerales	*G. margarita* *G. intraradices*

Table 7. Fungus taxons in which new fungal MTs have been identified.
In red: Human pathogenic fungi. In green: Plant pathogenic fungi.
*: Human & plant pathogenic fungi.

The most appealing conclusion when analysing the miscellanea of fungal MTs presented in Table 6, is the existence of MTs of different lengths, and with different Cys motifs (*i.e.* Cys distribution). Taking into account these two features, four subfamilies emerged when all the newly identified sequences were aligned using the Clustal Omega tool (www.ebi.ac.uk/Tools/msa/clustalo). Identified MTs of the four subfamilies are grouped below (in bold, newly identified fungal MTs).

Subfamily 1: short MTs (XX amino acids, 6-7 Cys).

This subfamily is characterized by the -CXC-, -CC- and -CXCXXC- patterns.

```
U.fabae_MT                ----------MNPCSSNC---SCGASC---TCSGCSSHKK 24
H.lugdunensis_MT          ----------SPCTCSTC--NCAGACNSCSCTSCSH--- 24
P.nodorum_MT              ----------MSPCNCQTC--SCSGDCSGCSCSSCSH--- 25
C.gloeosporioides_Cap5    ----------MAPCSCKSCGTSCAGSCTSCSCGSCSH--- 27
B.dermatitidis_MT1        ----------MSPCNCNC----CAGDCNSCSCTSCSVP-- 24
C.posadasii_MT1           ----------MNPCSCNC----CSGNCNNCSCGSCGH--- 23
A.nidulans_MT             ----------MSPCTCNC----CSGECNSCSCSSCKH--- 23
A.oryzae/flavus_MT        ----------MSPCSCNC----CSGNCNSCSCSDCKH--- 23
U.reesi_MT                ----------MSPCSCNC----CSGNCNSCSCSNCSH--- 23
M.perniciosa_MT1          MIATEFTVVNAHCGSSTCNCG-ENCACKPGECKC-------- 33
A.niger_MT                ----------MAPCECKC----CSGSCNSCSCSNCKH--- 23
C.gloeosporioides_Cap3    ----------MSGCGCASTG-TCHCGKD-CTCAGCPHK-- 26
A.bisporus_MT             ----------GDCGCSGAS-SCTCASGQCTCSGCGK--- 25
N.crassa_MT               ----------MGDCGCSGAS-SCNCGSG-CSCSNCGSK-- 26
F.oxysporum_MT            ----------MAGDCGCSGAS-SCNCGSS-CSCSGCG-K-- 26
```

Subfamily 2: medium MTs (XX amino acids, 9 Cys).

This subfamily exhibits only the -CXC- and -CXCXXC- patterns.

```
P.brasiliensis_MT         MGCGCGS-ECSCSGPQNCVCGTSGGGSTCHCTSCTVS 36
H.capsulatum_MT           MACGCGNNSCPCDGPQSCTCSS-GGGSSCGCTTCK-- 34
C.posadasii/immitis_MT2   MGCGCGTGSCSCNGPQNCSCPS--D--TCHCTTCGK- 32
B.dermatitidis_MT2        MGCGCGDDKCPCEGPKTCSCSS-SG--TCGCTTCGK- 33
```

Subfamily 3: long MTs (XX amino acids, 12-18 Cys).

Different Cys patterns: -CXC-, -CC-, -CXCXXC-, -CX_{2-3}CXC-, and also -CX_{2-3}CXCXXXC-

```
S.cerevisiae_CUP1   ----------MFSELINFQNEGHECQCQCGSCKNNEQC--QKSCSCPT------------
C.albicans_CRD2     ------------------------MACS------AAQCVCAQKSTCSCGKQPALKCNCSK
N.crassa_MT2        ------MSAPVAK-------ASTCCGK-------SAECICAKQATCSCGKQSALHCTCDK
S.brasiliensis_MT   ----------MV-------SSTCCGKG------GAECVCAQNATCSCGKQSALHCNCDR
S.apiospermum_MT    ----------MSP-------ADTCCRKG------EGACVCAQQATCSCGKQSALHCTCDK
Y.lypolitica_MT5    MACSTNCSCPKPCTNCACEKACTCSPCSCESCKCAKACECEKSTTCKC------------
C.glabrata_MT2      MPEQVNCQYDCHCSNCACENTCNCCAKPACACTNSASNEC-SCQTCKC------------

S.cerevisiae_CUP1   ----------------GCNSDDKCPCGNKSEETKKS----CCSGK---------------
C.albicans_CRD2     ASVENVVPSSNDACACGKRNKSSCTCGANAICDGT----------------------R---
N.crassa_MT2        ANSENAVEG--PRCSCRARPAGQCTCDRASTENQKPTGNACACGTRPADACTCEKAADGG
S.brasiliensis_MT   AATENNTAG--DRCSCGQRPAGACTCATNPSEV----------------------NTAN--
S.apiospermum_MT    AAVENTISG--PSCSCGSRPVGQCTCENATVENQKPTGATCGCGARPAGSCTCNNSAN--
Y.lypolitica_MT5    -------E--------SCKCEGSCKC-----------------------------------
C.glabrata_MT2      -------Q--------TCKC-------------------------

S.cerevisiae_CUP1   -------------- 61
C.albicans_CRD2     ----DGETDFTNLK 76
N.crassa_MT2        FKPTDLETDFTTKN 112
S.brasiliensis_MT   ------ETDFTTRK 79
S.apiospermum_MT    ------ETDFTTKK 101
Y.lypolitica_MT5    -------------- 59
C.glabrata_MT2      -------------- 52
```

Subfamily 4: extramely long MTs (XX amino acids, >22 Cys).

Different Cys are identified: -CXC-, -CC-, -CXCXXC-, -CXCXXC- and -$CX_{3\text{-}5}$CXC-.

```
T.mesenterica_MT     MSAPVETKEKSCGCQPAPAVQSCNCSNEGNCTCAPGKCACSSCSSDSIKKTGKCGGSEGC
C.neoformans_MT1     ---------MACNCPPQKNTACC----------------------------STSEAQDKC
C.neoformans_MT2     ---------MAFNPNPEKTTSCC----------------------------STSKAQDKC

T.mesenterica_MT     TCEAGKCDCASCPGSSGQVKACTCGTSCSCPPGECTCAGCPNNKGKEKAKDEKAGECSCG
C.neoformans_MT1     TCQKGNCECKACPNSTKTSE---------------------------------SG-----
C.neoformans_MT2     TCPKGKCECETCPKSTKTPG---------------------------------SGPCNCG

T.mesenterica_MT     PSCSCPPGECSCAGCSNVKSTGKEKAPAKACECGEECSCPPGQCSCANCPAKEKKDA-CS
C.neoformans_MT1     --GK--------------------ASTCNCGGSGEACTCPPGQCACDKCPKKAKSVSTCG
C.neoformans_MT2     VKEK--------------------VSTCGCNGSGAACTCPPGQCACDSCPRKAKSVSTCG

T.mesenterica_MT     ---CSEGCSCPPGQCACANCPHKDEAKGCSC-----GESCSCPPGECKCANCPKKTEPAK
C.neoformans_MT1     CGGSGAACSCPPGKCACDNCPKQAQEKVSSCACSGSGAA---------------------
C.neoformans_MT2     CGGSAAACSCPPGKCACDSCPKQAQEKVSSCACNGSGGACTCPPGKCSCSGCPAQAKENP

T.mesenterica_MT     --------ACACGDECSCPPGQCGCADCPGKTSS 257
C.neoformans_MT1     ---------------------------------- 122
C.neoformans_MT2     ADQPTTCGCQGVGVACTCPPGQCACDGCPAKAK- 183
```

With the newly characterized sequences, four interesting groups can be proposed. Subfamily 1 comprise the shortest fungal MTs, which contain between 6 and 7 cysteines arranged in three different patterns; *N. crassa* MT and homologous fungal MTs are placed in this group. Subfamily 2 are medium-length MTs, which contain 9 cysteines and only 2 Cys distributions are present; so far, only human opportunistic fungal MTs represent this group. Subfamily 3 comprises not only yeast MTs, but also moulds and dimorphic fungi. All these sequences show high similarity with *C. albicans* CRD2, retrieved from *C. albicans* genome searches, as well as other CRD2 as *C. dubliniensis*, *C. orthopsilosis* (data not shown) and also *C. glabrata* MT2. Newly identified putative *Sporothrix brasiliensis* and *Scedosporium apiospermum* MTs, as well as a new *Y. lipolytica* MT, possess a high similarity to all these described MTs, so far. It is remarkable to note that *N. crassa* MT (MT1 hereinafter) has been considered as the fungal MT model par excellence, in contraposition to the yeast MT model represented by *Candida* spp and *S. cerevisiae* MTs. Regarding to subfamily 4, it is constituted by extremely long fungal MTs, in which *Tremella mesenterica* posses the longest MT described so far in all kingdoms; together with the *C. neoformans* MTs, they comprise an unusual group of extremely large MT whose potential abilities binding metal ions outweigh the described to date, opening a new horizon in studying the features of MTs.

CURRENT CHARACTERIZATION OF FUNGAL MTs

Recently, different human opportunistic fungal MTs have been our focus of work, and several of the mentioned cases are being currently analysed by different member of our research group. Among them, we concentrated the studies on *Fusarium verticillioides* and *Aspergillus fumigatus* MTs. Unfortunately, the work with *A. fumigatus* MT, presented several technical inconveniences, yielding so far, no plausible results. Contrarily, the work in *F. verticillioides* allowed characterizing its corresponding MT.

Fusarium verticillioides MT

Introduction

Fusarium is a genus of filamentous fungi belonging to the *Ascomycota* phylum; most of them living in soils and associated with plants (Nucci & Anaissie, 2007). Within the large number of *Fusarium* species conforming this group, an important number of them, are toxin-producers that can affect plants, human and animals, inducing acute and chronic toxic effects, as well as susceptibility to infectious diseases (Antonissen et al., 2014). Besides producing multiple toxins, a non-negligible amount of *Fusarium* species are plant pathogen, affecting different crops. Furthermore, some of them may also cause specific superficial or disseminated infections in animals; until twelve species are related with fusariosis in humans, among them *F. solani* is responsible of ~50% of fusariosis, followed by *F. oxysporum* (~20%) and *F. verticillioides* (~10%) (Nucci & Anaissie, 2007).

The sexual, heterothallic *F. verticillioides* species, also known as *F. moniliforme* or *Gibberella fujikuroi*, is a dual pathogen, causing infections in plants and animals. In plants, it affects rice crops causing the bakanae disease, and also maize causing ear rot and kernel diseases. In humans, *F. verticillioides* can infect immunocompromised people at superficial or disseminated level, even compromising human life in some cases; and also the *F. verticillioides* toxins have been related with health problems as esophageal cancer and neural tube defects (Kriek et al., 1981) (Seefelder et al., 2003). Previous studies in *Cryptococcus neoformans*, another opportunistic human pathogenic fungus, revealed the importance of different agents involved in pathogenicity, among which MTs are identified. They have been shown to play a critical role in virulence, thanks to their extraordinary capacity to detoxify

copper (Ding et al., 2014a) (Palacios, Espart et al., 2014a). With this information in mind, it seemed interesting to characterize the putative MTs of *F. verticillioides*.

In the Broad Institute (www.broadinstitute.org), a *Fusarium* comparative genomics database is available in which *F. verticillioides*, *F. graminearum* and *F. oxysporum* genomes are present. No identified *Fusarium* MTs are annotated in the Broad Institute or other databases so far, although according Ebbole et al. an homolog of *N. crassa* MT and an homolog of the putative *H. capsulatum* MT, were described for *F. graminearum* (Ebbole et al., 2004). No other homolog proteins have been described in other *Fusarium* species, this showing the scarce information available about *Fusarium* MTs. Therefore, we include here the identification and characterization of the shortest (26 amino acids) *Fusarium verticillioides* MT (FvMT).

Experimental procedures

The main steps to characterize a fungal MT are shown in Scheme 1. The FvMT identification and characterization steps are detailed below.

In silico search of *F. verticillioides* MTs. The *F. graminearum* MT and the *N. crassa* MT cDNA sequences were used for *in silico* BLAST searches of a putative MT in *F. verticillioides*, in the Broad Institute (www.broadinstitute.org) and in NCBI (www.ncbi.nlm.nih.gov). The retrieved sequences were analyzed and used to deduce the corresponding cDNA sequences, which were manually analysed .

Culture, mRNA isolation, total cDNA synthesis and specific amplification of the FvMTcDNA. *F. verticillioides* cultures were kindly donated by Dr. Xavier Capilla from the MICOLOGI group (Faculty of Medicine, University Rovira i Virgili, Tarragona-Reus, Spain). They were grown in PDA agar plates at 25 ^{o}C during 4-5 days and subsequent mRNA isolation was conducted using an adaptation of Sherman's protocol (Sherman et al., 1994); the resulting mRNA was analyzed by 1% agarose gel electrophoresis with TAE buffer and quantified using NanoQuant® (TECAN) spectrophotometer. A succeeding rtPCR was carried out using the Phusion RT-PCR Kit (Thermo Scientific) to obtain the total cDNA of *F. verticillioides.* To amplify the cDNA of the hypothetical FvMT. PCR amplification was carried out using the following oligonucleotides as primers: 5'-AAAAGGATCCATGGCTGGCGACTGTGGCTG-3' (forward) and the degenerated 5'-GGAACTCGAGTTATTTGCCGCAGCCTGAGC-3' (reverse), which were designed from

related *Fusarium* EST MTs (*F. graminearum* and *F. oxysporum*). Additionally, two restriction sites were added to the cDNA sequence for cloning purposes. The 30-cycle amplification reaction were performed with the thermo-resistant Taq DNA polymerase (Expand High Fidelity PCR System, Roche) under the conditions: 2 min at 94 ^{o}C (initial denaturation), 15 s at 94^{o}C (denaturation), 30 s at 57 ^{o}C (annealing) and 30 s at 72 ^{o}C (elongation). The final product was analyzed by 2% agarose gel electrophoresis and the expected band was excised (Genelute™ Gel Extraction Kit, Sigma Aldrich).

Cloning and recombinant expression of the FvMT cDNA. The FvMT cDNA was cloned into the *BamH*I/*Xho*I sites of the pGEX-4T1 expression vector (GE Healthcare), in order to synthesize a GST-MT fusion protein. pGEX-4T1 and the amplified insert was digested with *BamH*I/*Xho*I followed, in each case, by a ligation reaction (DNA Ligation Kit 2.1., Takara Bio Inc.). The recombinant plasmid was transformed into the *E. coli* MachI strain for DNA sequencing, using the Big Dye Terminator 3.1 Cycle Sequencing Kit in an ABIPRISM 310 Automatic Sequencer (Applied Biosystems). Positive clones were transformed into *E. coli* BL21 protease deficient strain for protein synthesis.

Synthesis and purification of recombinant Zn-, Cd- and Cu-FvMT complexes and preparation of *in vitro*-substituted complexes. The corresponding GST-MT fusion proteins were biosynthesized in 5-L cultures of transformed *E. coli* cells. Expression was induced by 100 μM (final concentration) isopropyl β-D-thiogalactopyranoside (IPTG) in cultures supplemented with 300 μM $ZnCl_2$, 300 μM $CdCl_2$ or 500 μM $CuSO_4$ (final concentrations), which were allowed to grow for further 3h. Cu-supplemented cultures were grown either under normal aeration conditions (1-L media in a 2-L Erlenmeyer flask, at 250 rpm) or under low oxygen conditions (1.5 L of media in a 2-L Erlenmeyer flask, at 150 rpm), since different results may be achieved depending on the culture aeration conditions owing to the fact that this determine the amount of intracellular copper in the host cells. The total protein extract was prepared from bacterial cultures as fully described before for other MT peptides (Capdevila et al., 1997). Briefly, metal-FvMT complexes were recovered from the FvMT-GST fusion constructs by thrombin cleavage and batch-affinity chromatography using the Glutathione-Sepharose 4B matrix (GE Healthcare). After concentration using Centriprep Microcon 3 (Amicon), samples were finally purified through FPLC in a Superdex75 column (GE Healthcare) equilibrated with 50 mM Tris-HCl, pH 7.0. Selected fractions were confirmed by 12% SDS-PAGE and kept at -80 ^{o}C until further use. All procedures were

performed using Ar (pure grade 5.6) saturated buffers, and all syntheses were performed at least twice to ensure reproducibility. As consequence of the cloning requirements, the dipeptide Gly-Ser was present at the N-term of the FvMT polypeptides; but this had previously been shown not to alter the MT metal-binding features (Cols et al., 1997). *In vitro*-substituted Cd(II)-FvMT and Cu(I)-FvMT complexes were obtained by titration at pH 7 of the corresponding Zn(II)-FvMT preparations with $CdCl_2$ in water (MERCK AAS Cd^{2+} standard of 1000 ppm) or $[Cu(CH_3CN_4]ClO_4$ solutions as described (Bofill et al., 1999), respectively. During all the experiments strict oxygen-free conditions were maintained by saturating all the solutions with Ar.

Spectroscopic analyses (ICP-AES and CD) of the Zn-, Cd-, and Cu-FvMT complexes. The S, Zn, Cd and Cu content of all the metal-FvMT preparations was analyzed by Inductively Coupled Plasma Atomic Emission Spectroscopy (ICP-AES), using a Polyscan 61E (Thermo Jarrell Ash) spectrometer, measuring S at 182.040 nm, Zn at 213.856 nm, Cd at 228.802 nm, and Cu at 324.803 nm. Samples were routinely treated as reported in (Bongers, Walton, Richardson, & Bell, 1988). Alternatively their incubation in 1 M HCl at 65 °C for 15 min prior to analyses allowed the elimination of labile sulfide ions (Capdevila et al., 2005). Protein concentrations were calculated from the ICP-AES sulfur measurement, assuming that all S atoms were contributed by the FvMT peptides. CD spectra were recorded in a Jasco spectropolarimeter (Model J-715) interfaced to a computer (J700 software), where a 25 °C temperature was maintained constant by a Peltier PTC-351S equipment. Electronic absorptions measurements were performed on an HP-8453 Diode array UV-visible spectrophotometer. 1-cm capped quartz cuvettes were used to record all the spectra, which were corrected for the dilution effects and processed using the GRAMS 32 program.

Electrospray ionization time-of-flight mass spectrometry (ESI-TOF MS) of the metal-FvMT complexes. Electrospray ionization time-of-flight mass spectrometry (ESI-TOF MS) was performed on a Micro TOF-Q instrument (Bruker) interfaced with a Series 1200 HPLC Agilent pump, equipped with an autosampler, all of which controlled by the Compass Software. The ESI-L Low Concentration Tuning Mix (Agilent Technologies) was used for equipment calibration. For the analysis of Zn- and Cd-FvMT complexes, samples were run under the following conditions: 20 µl of protein solution injected through a PEEK (polyether heteroketone) tubing (1.5 m x 0.18 mm i.d.) at 40 µl min^{-1}; capillary counter-electrode voltage 5 kV; desolvation temperature 90-110 °C; dry gas 6 l min^{-1}; spectra collection range 800-2500

m/z. The carrier buffer was a 5:95 mixture of acetonitrile:ammonium acetate (15 mM, pH 7.0). Instead, the Cu-FvMT samples were analyzed as follows: 20 µl of protein solution injected at 40 µl min^{-1}; capillary counter-electrode voltage 3.5 kV; lens counter-electrode voltage 4 kV; dry temperature 80 °C; dry gas 6 l min^{-1}. Here, the carrier was a 10:90 mixture of acetonitrile:ammonium acetate, 15 mM, pH 7.0. Acidic-MS conditions, which causes the demetalation of the peptides loaded with divalent metal ions, but keeps the Cu^{+} ions bound to the protein, were used to generate the apo-FvMT forms and to analyze the Cu-containing FvMT samples. For it, 20 µl of the preparation were injected under the same conditions described previously, but using a 5:95 mixture of acetonitrile:formic acid, pH 2.4, as liquid carrier. For all the ESI-MS results, the error associated with the mass measurements was always inferior to 0.1%. Masses for the holo-species were calculated according the rationale previously described (Fabris et al., 1996).

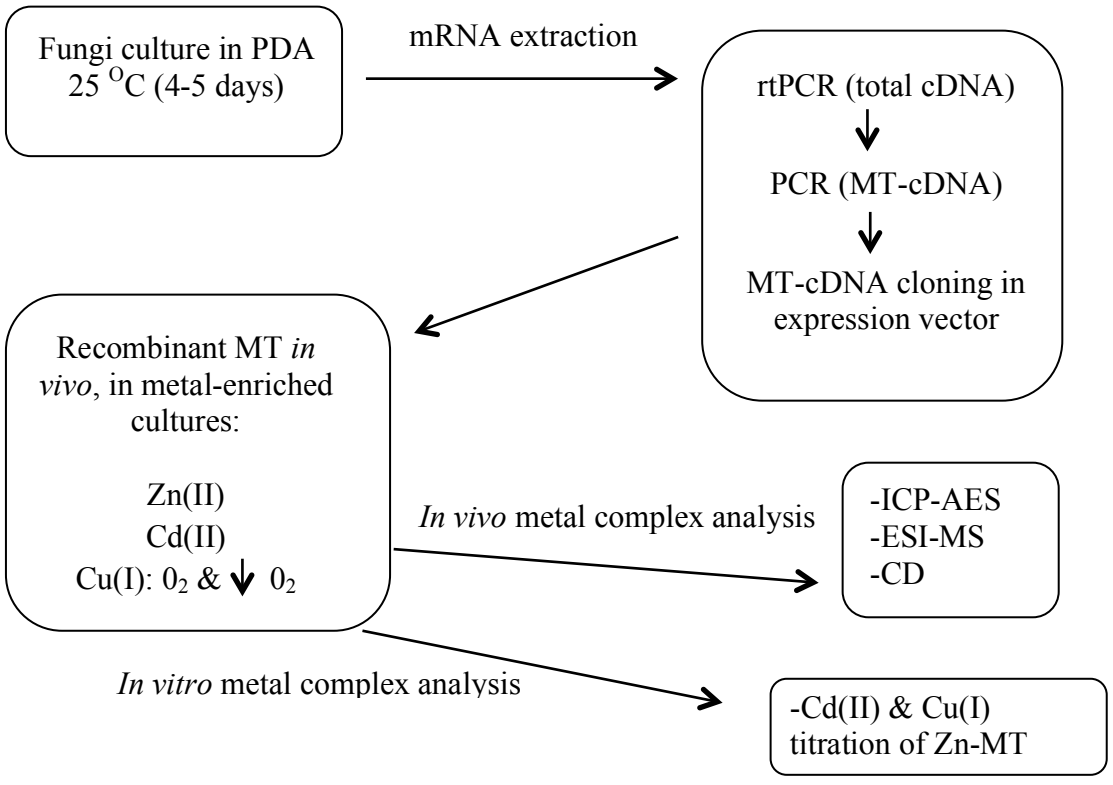

Scheme 1. Schematic process of obtaining and characterizing fungal MTs: from fungus cultures to metal-MT physico-chemical characterization.

Results and discussion

In silico search of FvMT. Not putative MT sequences were retrieved for *F. verticillioides* from the Broad Institute neither the NCBI databases, but hypothetical sequences were recovered for *F. graminearum* (already described by Ebbole et al. (Ebbole et al., 2004)) and *F. oxysporum* in NCBI. The analysis of the hypothetical protein sequences revealed an identical short sequence of 26 amino acids for *F. graminearum* (XP_009260356.1) and *F. oxysporum* (EGU76845.1), in which six cysteines were distributed in the same CXC pattern. Subsequent EST sequence analyses allowed identifying two nucleotide changes (position 65 C/T and position 75 A/C) that are silent in the translated protein sequences. The impossibility of identifying a hypothetical MT encoded in the *F. verticillioides* genome, and the 97.5% of similarity of the identified hypothetical *Fusarium* MT, suggested a putative *F. verticillioides* MT cDNA virtually similar to those localized, and therefore they were used to design oligonucleotides to amplify the putative *F. verticillioides* MT.

FvMT peptide identity. DNA sequencing confirmed that the isolated FvMT cDNA possesses the same coding sequence than the hypothetical *F. oxysporum* MT (Figure 13A) and is translated to the same protein sequence as *F. oxysporum* and *F. graminearum* MTs (Figure 13B). Therefore, the FvMT cDNA was cloned into pGEX in the appropriate frame after the GST encoding moiety. Consequently, recombinant synthesis yielded an FvMT peptide, the identity, purity and integrity of which was confirmed by acid ESI-MS (pH 2.4) of the purified Zn-complexes. Hence, a unique peak was detected, with a MW consistent with that calculated for the apo-form (Figure 13C), including the two N-terminal residues derived from the GST-fusion construct prior to the initiator Met. Experimental molecular masses detected were 2593.47 Da for FvMT, while the respective theoretical value of 2592.6 Da was calculated from the amino acid sequence.

A

```
FvMT    ATGGCTGGCGACTGTGGCTGCTCTGGTGCCTCTTCTTGCAACTGCGGCTCTAGCTGCTCT
FoMT    ATGGCTGGCGACTGTGGCTGCTCTGGTGCCTCTTCTTGCAACTGCGGCTCTAGCTGCTCT

FvMT    TGCTCCGGCTGCGGAAAATAA 81
FvoT    TGCTCCGGCTGCGGAAAATAA 81
```

B

```
FvMT        MAGDCGCSGASSCNCGSSCSCSGCGK 26
FgMT        MAGDCGCSGASSCNCGSSCSCSGCGK 26
FoMT        MAGDCGCSGASSCNCGSSCSCSGCGK 26
```

C

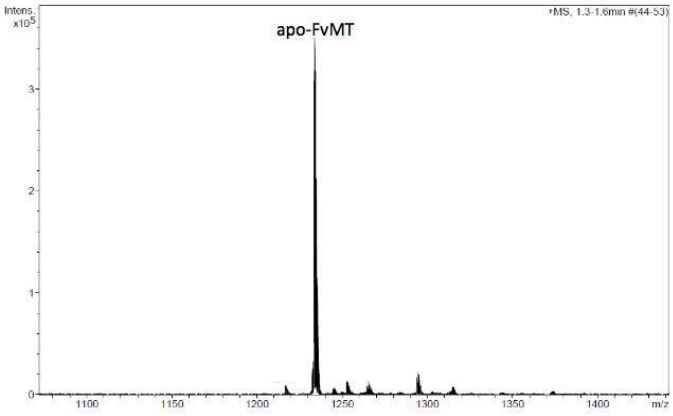

Figure 13. A Alignment of the cDNA sequences of confirmed FvMT and hypothetical *F. oxysporum* MT (FoMT) **B** *In silico* identified *F. graminearum* (FgMT) and *F. oxysporum* (FoMT) MTs. **C** Deconvoluted ESI-MS spectra of the Zn-FvMT preparation recorded at acidic pH, showing the recombinant apo-form. This peptide included the Gly-Ser residues added at its N-term due to GST-cloning requirements.

Zn-, Cd- and Cu-FvMT complexes. The synthesis of FvMT by Zn(II)-enriched bacteria, yielded low amounts of protein (concentration *ca*. 0.12 mg L^{-1} of culture); the Zn-complexes recovered were almost equimolar amounts of Zn_2-FvMT and Zn_3-FvMT. ICP-AES analyses indicated a mean on content of 2.25 Zn(II) per MT, which is highly consistent with ESI-MS spectra (Figure 14A). Conversely, only a low amount of the Cd_3S_2-FvMT species was recovered from Cd-supplemented cultures. Contrarily, FvMT folded into unique, well-folded complexes when coordinating Cu(I). At normal oxygenation, the producing cells yielded homometallic species, as revealed by the ICP-AES analyses (5 Cu(I) per FvMT) and the ESI-MS spectra, which at neutral pH revelaed a unique Cu_5-FvMT; exactly the same results were were obtained at acidic ESI-MS. In low oxygenation culture conditions, Fv-MT yields also the same homometallic Cu_5-complex; and the ESI-MS spectra are exactly the same as in normal oxygenation (Figure 14B). These results, are comparable with those find for other

short fungal MTs, such as the published by Cobine et al. for *N. crassa* MT (Cobine et al., 2004), although in *N. crassa* the complex is Cu_6-MT instead of Cu_5-MT, and the obtained in our work with the *C. neoformans* CnMT1 fragments (Espart et al. 2015) in which every Cys-building block that forms the full-lenght CnMT1 is able to form Zn_2- and Cu_5-complexes.

A

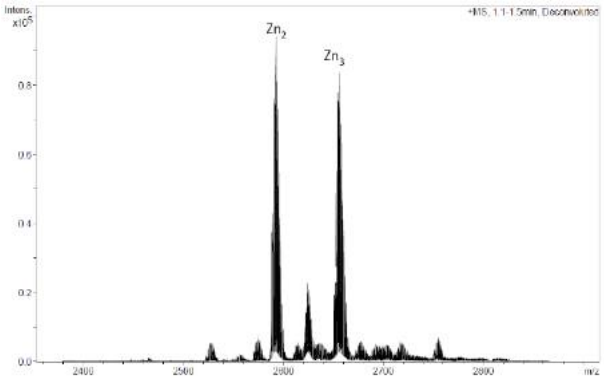

B

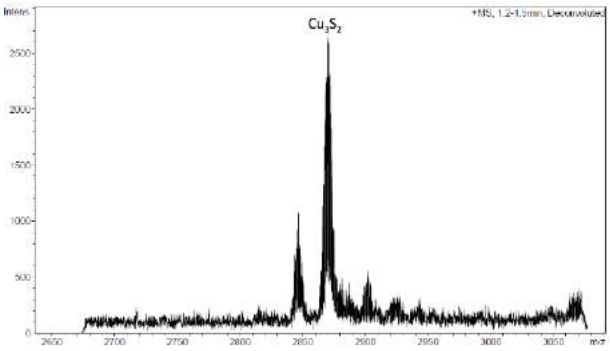

C

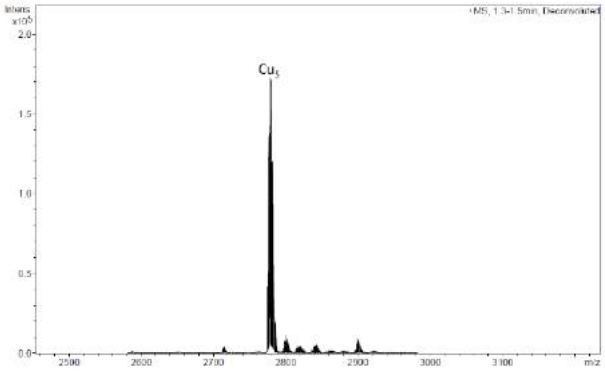

Figure 14. Deconvoluted ESI-MS spectra of the recombinant FvMT preparations (A) in Zn-supplemented cultures, showing two major species: Zn_2- and Zn_3-FvMT; (B) in Cd-supplemented cultures: Cd_3S_2-FvMT complex; (C) in Cu-supplemented cultures: homometallic Cu_5-FvMT complex.

Zn/Cu displacement reactions in Zn-FvMT. To complete the data about the Cu^+ binding abilities of FvMT, Zn/Cu exchange reactions in Zn-FvMT were conducted. Globally, a Gaussian bands at *ca.* 260 nm developed in the CD spectra corresponding to successive Cu^+ additions, reaching a maximum when 5 Cu^+ eq had been added (data not shown). Further addition of Cu^+ brought about the unfolding of the complex. ESI-MS analyses of the products of the stepwise Cu^+ addition confirmed the formation of the Cu_5-FvMT species, this confirming that this is the most energy-favoured Cu-FvMT complex.

In summary, *F. verticillioides* MT cDNA sequencing revealed that the sequence is identical to those identified in *F. oxysporum* and *F. graminearum,* and its functional characterization exhibited its Cu-thionein character. Thus, in Zn^{2+}-enriched recombinant cultures, the recovered metal-complexes were a major Zn_2- with almost as important Zn_3-FvMT species, while for Cd(II), only a low yield Cd_3S_2-FvMT was recovered. Contrarily, in Cu(I)-enriched cultures at both oxygenations, the complexes retrieved were always unique Cu_5-FvMT. These results indicate that *Fusarium* MTs can be considered as genuine Cu-thioneins, according to Bofill et al., in view of the variable stoichiometry of the complexes produced in Zn(II)- and Cd(II)-enriched cultures, the formation of ternary metal-S^{2-}-MT species when coordinating Cd(II), and the unique homometallic Cu-species recovered from Cu-enriched cultures (Bofill et al., 2009).

Conclusions

The newly identified *F. verticillioides* FvMT exhibits the features of a genuine Cu-thionein, as a typical fungal MT, this including an optimum Cu-binding behaviour, as well as suboptimal divalent metal ion binding abilities. The classification developed and proposed by Bofill et al., and Valls et al., seems to be the most practical to establish not only the preferences of the MT for a specific metal, but also to know what behaviour it shows against other metals with different chemical features (Bofill et al., 2009) (Valls et al., 2001).

The hypothetical coding cDNAs annotated for *F. oxysporum* and *F. verticillioides* MTs allowed to identify the *F. verticillioides* MT, whose sequence is not available in public genome databases. It is expected that the results here exposed, will be exactly the same for *F. oxysporum* and *F. graminearum* hypothetical MTs. The homology that these sequences exhibit with the *N. crassa* MT, the basic unit of Cys-building blocks in *C. neoformans* CnMTs and with other fungal MTs belonging to the Subfamily 1 (previously discussed in this PhD thesis), led to consider that with a high probability, the metal binding abilities with divalent and monovalent metal ions, will be the same. Evenly, since both *C. neoformans* as *F. verticilliiodes* (but also *F. oxysporum* and *F. graminearum*) are fungal pathogens, is reasonable to think that most likely, *Fusarium* MTs will be also involved in pathogenicity acting as virulence factors.

As said at the beginning, two putative *F. graminearum* were described; in this work, only the shortest homolog MT was characterized but not the longest. Identification and characterization of the longest hypothetical FvMT is necessary, as well as the identification of other putative MTs. A complete study of the *F. verticillioides* MT system will help to understand the metal metabolism of this fungus, which is able to live in soils (usually polluted with xenobiotic metals as Cd) infecting crops, but also is able to infect immunocompromised people.

FUTURE DIRECTIONS IN FUNGAL MTS

Currently, the work performed in our group aims at characterizing the metal binding abilities of some of the newly identified MTs, specifically: *S. brasiliensis* MT, *S. apiospermum* MT and *C. posadasii* MTs belonging to opportunistic fungi; *Uncinocarpus reesii* MT for being a non-pathogenic model of *Coccidioides* spp MTs; *N. crassa* MT2 for the implications of discovering new MT peptides in this model fungus; and *Tremella mesenterica* MT for its similarity to modular CnMTs and because it is the most long MT identified so far. At the same time, it will be of high relevance to understand the metal binding abilities of different MT isoforms in the same fungus, and their implication in virulence and pathogenicity processes. Finally, the localization and characterization of polymorphic fungal MT of plant pathogens can provide valuable information for phytopathology studies and agricultural applications. It is possible that in the near future, a new vision of MTs will provide valuable information able to establish novel implications of these proteins in cell metabolism.

SUMMARY AND GENERAL DISCUSSION

4. SUMMARY AND GENERAL DISCUSSION

The role of metal ions in living organisms is crucial. They carry out a set of specific cell functions, which can be classified into three main categories: structural, metabolic and catalytic. The required metals vary depending on the function in which they are involved in. Transition metals such as Fe, Cu, Zn, Mn, Mo, Ni or Co are required for many enzymes to perform catalytic functions, being essential a good metal balance to maintain an optimal cell metabolism and avoid the toxicity that metals can produce (Kleczkowski & Garncarz, 2012) (Bleackley & MacGillivray, 2011). Organisms have evolved to preserve this balance through an optimal uptake, intracellular transport, storage and elimination, in case of metal excess. Furthermore, some of these transition metals, such as Cu and Fe participate in free radical reactions thanks to their unpaired electrons, being the substrate for the formation of highly reactive hydroxyl radicals that can damage cellular structures (Kleczkowski & Garncarz, 2012). The presence of some enzymatic mechanisms acting as antioxidants (*i.e.* superoxide dismutase or glutathione S-transferase, among others), avoids this potential cell damage; but also some non-enzymatic mechanisms such as metallothioneins (MTs), sequestrated metals, transferrin or polyamides, are involved in the mitigation of ROS formation (Kleczkowski & Garncarz, 2012). However, cell damage may be also induced by other non physiological metals such as Cd, Hg or Ag, that can be present in the cell.

Zn, Cu and Cd are three heavy metals with different cellular implications. While Zn^{2+} and Cu^{+} are essential in a wide range of functions, Cd^{2+}, which is considered as highly toxic, can displace Zn^{2+} disturbing the zinc homeostasis in mammalian cells. Although the cadmium toxicity mechanisms are not well understood, zinc and cadmium share a range of physico-chemical properties facilitating the Cd-binding to some Zn-proteins and the subsequent toxicity (Vilahur et al., 2015) (Martelli et al., 2006). Although cadmium is considered a xenobiotic heavy metal, in general, all cells are able to manage small cadmium concentration. Unlike mammalian and yeast, plants are able to tolerate certain higher Cd concentrations, thanks to some molecules and proteins like phytochelatins or MTs. MTs possess a high Cys-content resulting in a specific capacity to bind physiological and non-physiological heavy metals through the thiol groups from cysteines. The almost universal presence of MTs along with this particular binding metals ability, convert these metalloproteins in a valuable molecule involved in metal detoxification homeostasis.

This thesis work aimed to enlarge the knowledge about the characterization of different MTs, specifically five MT isoforms present in the protozoan model *Tetrahymena thermophila* and two isoforms in the human pathogenic fungus *Cryptococcus neoformans*. Furthermore, the fungal MT from *Fusarium verticillioides* was also characterized, and as well as other interesting fungal MTs were *in silico* identified. The obtained results, contribute to interpret the molecular evolution of unicellular eukaryote MTs, precisely of their differential protein features and function in polymorphic systems, and of the selection forces that can have modelled these features, such as acting as virulence factors.

Different tools have been used to succeed in our aims; the use of Bioinformatic resources allowed examining the published or unpublished genomic MT sequences in the principal databases, not forgetting the presence of mis annotated sequences, quite common in fungal MTs. The Recombinant DNA, as well as the Molecular Biology, techniques were used to originate different expression plasmids able to yield recombinant MTs fused to the glutathione S-transferase (GST), to produce a GST-MT in *E. coli*; the resultant proteins were purified to obtain metal-MT complexes following the strategy as Cols et al., and Capdevila et al., developed in our group (Cols et al., 1997) (Capdevila et al., 1997). Finally, spectroscopic (ICP-AES, CD and UV-Vis) and spectrometric (ESI-MS) tecnhiques were used to characterize the metal-MT complexes formed when they were synthesized in Zn^{2+}, Cd^{2+} or Cu^{+}, supplemented media.

4.1. METAL-BINDING ABILITIES OF THE FIVE MT ISOFORMS IN *Tetrahymena thermophila*.

The ciliate *T. thermophila* presents an unusual MT system, consisting of five MT isoforms with longer sequences than those identified in higher eukaryotes such as mammals or plants, even being a unicellular eukaryote organism. Divided into two subfamilies, the five *T. thermophila* MTs had been previously classified according to different features: the presence or absence of modular cysteine clusters, the location of Lys relative to Cys residues or the gene induction by Cd or Cu (Díaz et al., 2007). Nevertheless, no metal preferences and/or abilities to conform metal-MT complexes, were deciphered yet, and therefore no particular functions could be suggested for these MTs, besides those attributed generally to all MTs. Although the gene expression inducibility and the protein sequence similarity were the

object of other works (Gutiérrez et al., 2011) (Díaz et al., 2007), no results about metal-binding abilities were available. Hence, to fill the gap of protein functional studies on *Tetrahymena* MTs, the full characterization of their Zn-, Cd- and Cu-complexes were characterized and communicated in publication 1. On the basis that MTT1, MTT3 and MTT5 were classified as subfamily 7a and MTT2 and MTT4 as subfamily 7b, we conducted the metal-MTTs characterization. The multiple sequence alignment using Clustal Omega tool, have revealed similarities and divergences among the isoform sequences (Figure 1), that would correspond to the metal-binding ability behaviour.

```
MTT2       MDT-----------------------------------QTQTKVTVGCSCNPC---KCQ
MTT4       MDT-----------------------------------QTQTKVTVGCSCNPC---KCQ
MTT5       MDKI----SGESTKICSKTEEKWCCCPSETQNCCNSDDKQCCVGSGEGCIYVCCKCCKVQ
MTT1       MDKVNSCCCGVNAKPCCTDPNSGCCCVSKTDNCCKSDTKECCTGTGEGCKCVNCKCCKPQ
MTT3       MEKINNSCCGENTKICCTDLNRQCNCACKTDNCCKPETNECCTDTLEGCKCVDCKCCKSH

MTT2       PLCKCGTTAACNCQPCEN----------CDPCSCNPCKCGVTESCGCNPCKCAE-----C
MTT4       PLCKCGTTAACNCQPCEN----------CDPCSCNPCKCGVTESCGCNPCKCAE-----C
MTT5       AECKCGPNAKYCCIDPNTGNCCVCKTKFCSKSDSKECCPGGSC-----------------
MTT1       ANCCCGVNAKPCCFDPNSGCCCVSKTNNCCKSDTKECCTGTGEGCKCTSCQCCKPVQQGC
MTT3       VTCCHGVNVKSSCLDPNSGYQCASKTDNCCKSDTKECCTGTQEGCKCTNCQCYKQAQQGC

MTT2       KCGSHTE-----KTSACKCNPCACNPCNCGSTSNCKCNPCKCAECKC 108
MTT4       KCGSHTE-----KTSACKCNPCACNPCKCGSTSNCKCNPCKCAECKC 108
MTT5       -------------------------------------------------  99
MTT1       CCGDKAKACCTDPNSGCCCSNKANK--CCDATSKQECQTCQCCK--- 162
MTT3       CCGDKAKACCTDPNSGCCCSNKANK--CCDATSKKECQVCQCCK--- 162
```

Figure 1. Sequence alignment (Clustal Omega) of the five *T. thermophila* MTs. Cys residues are marked in red; doublets and triplets of Cys residues are highlighted in grey.

MTT1, MTT3 and MTT5 sequences possess doublets and triplets of Cys residues not identified in MTT2 and MTT4. The initial greatest similarity between MTT1 and MTT3 seemed to suggest *a priori*, a closest comparable behaviour than to MTT5. Described previously as Cd-thioneins, in our study these three isoforms exhibited a particular capacity to bind Zn^{2+} and Cd^{2+}. Thus, among the different metal-complexes detected in these three isoforms, the major Zn species identified were: Zn_{17}-MTT1, Zn_{12}-, Zn_{11}- and Zn_{13}-MTT3, and Zn_6- and Zn_5-MTT5; whereas in Cd-complexes: Cd_{17}-MTT1, $Cd_{15}S$-, $Cd_{16}S$- and Cd_{18}-MTT3 and Cd_8-MTT5, were the major species characterized. No Cu-species were retrieved from the MTT1 productions in Cu-supplemented media; only a few heterometallic (Zn,Cu) species were recovered for MTT3 in which a mixture of $Zn_x(Cu_8, Cu_4, Cu_{12})$ were detected; and finally, heterometallic (Zn,Cu) species were detected in normal oxygenation culture

conditions for MTT5 with a major M_{12}-MTT5 (M=Zn or Cu), but also homometallic Cu_8-MTT5 complexes were recovered at low oxygenation conditions. The CD spectra show, in turn, a practically featureless envelope in Zn-MTT1, but an intensive spectrum in Cd-MTT1. Evenly, the spectrum obtained in Zn- and Cu-MTT3, exhibit similar characteristics to that expected for an apo-MT, which is the result of a mixture of species, whereas the Cd-MTT3 have a similar profile to the observed in Cd-MTT1. Finally, in Zn-MTT5 the CD spectrum shows a low intensity, a major intensity for Cd-MTT5 (although less than in Cd-MTT1 and Cd-MTT3) and a very poor profile in Cu-MTT5. These results together with those obtained in the CD spectra, show a significant ability of MTT1, MTT3 and MTT5 to bind divalent metal ions against monovalent metal ions. MTT1 could be considered the isoform with a strongest Zn/Cd-thionein behaviour according to Bofill et al., and Valls et al. criteria (Bofill et al., 2009) (Valls et al., 2001); its limited number of folded Zn-, Cd-complexes, which are able to bind high amounts of divalent metal ions and their incapability to render Cu-containing species makes this MT as a genuine example of Zn/Cd-thionein character. Following to MTT1, MTT5 is able to conform metal-complexes under all the metal-supplementation culture conditions; although the amount of bound metal ions for MTT5 is lower due to its shorter sequence. Definite Zn- and Cd-MTT5 complexes were identified, in contraposition to some heterometallic Zn_xCu_y-MTT5 species (also recovered in *in vitro* Zn/Cu replacement studies), as well as the presence of minor homometallic Cu-MTT5 at low oxygenation culture conditions, which confers a significant Zn/Cd-thionein character to MTT5. Finally MTT3 can be considered an undefined isoform, due to its mixed features of Zn/Cd- and Cu-thionein. Hence, the number of multiple Zn-MTT3 species detected, contrasted with the presence of ternary CdS-complexes, are in agreement with a poor ability to bind Cd^{2+} ions, which is typical of Cu-thionein behaviour; but at the same time, heterometallic Zn,Cu-MTT3 species in Cu-supplemented cultures without homometallic complexes were recovered, even at low oxygenation conditions, which is typical from Zn/Cd-thionein behaviour. Therefore, it becomes difficult to attribute a specific divalent- or monovalent-thionein character to MTT3.

Contrarily, MTT2 and MTT4 showed a clear Cu-thionein character. It was impossible to recover Zn- and Cd-MTT2 species from the respective recombinant MTT2 syntheses. Contrarily, major homometallic Cu-MTT2 complexes resulted from Cu-supplemented cultures, being Cu_{20}-MTT2 the major species obtained in normal oxygenation conditions, among other minor homo- and heterometallic (Cu_{16}- and Zn_5Cu_{12}-MTT2, respectively) species; at low oxygenation conditions, again the major species was Cu_{20}-MTT2, although

other minor homometallic species with higher nuclearity (Cu_{21}-, Cu_{22}- and Cu_{23}-MTT2) were also observed. In a similar way, no Cd-MTT4 could be obtained, but Zn-MTT4 complexes could be purified, among which Zn_{10}-MTT4 was the major species. Heterometallic species (M_{16}- and M_{13}-MTT4) were obtained from Cu-supplemented cultures grown at normal oxygenation, with Cu_{20}-MTT4 as major complex and other minor complexes, reaching a 24 Cu content (Cu_{24}-MTT4) at low oxygenation conditions. The *in vitro* Zn/Cu replacement studies on MTT4 corroborated the results obtained for the *in vivo* folded Cu-MTT4 species. In summary, the absence of Cd-complexes for MTT2 and MTT4, the presence of some Zn-MTT4 species with only 10 to 12 Zn^{2+} as maximum, are bound to the 32 Cys residues present MTT4, and the ability to yield well-folded, homometallic Cu-complexes render these MTs a marked Cu-thionein character. The CD spectra observed in Cu-MTT2 and Cu-MTT4, exhibit a very typical Cu-thioneins fingerprints, whereas in Zn-MTT4 a similar profile to Cu-MTT4, but with low intensity was identified.

The presence of both metal-binding preferences in the *T. thermophila* MT system allows to classify all the isoforms into a gradation from Zn/Cd-thionein to Cu-thionein character as follows: MTT1>MTT5>MTT3>MTT4>MTT2. The revealed genuine Zn/Cd- and Cu-thionein properties of MTT1, MTT5 and MTT2, MTT4, respectively, match with the exposed by other authors (Díaz et al., 2007) (Gutiérrez et al., 2011) (Santovito et al., 2007) (Boldrin et al., 2008). By contrast, little is know about MTT3. The undefined metal-binding preferences observed for MTT3 in our study are in concordance with the differences detected in the *MTT3* gene induction pattern, because whereas *MTT1* and *MTT5* are always induced stronger by Cd than by Zn, Zn is the principal *MTT3* inducer at short time exposure, whereas Cd is only a more potent inducer in prolonged exposures (Díaz et al., 2007).

When taking all this data together, we concluded that the five MT isoforms present in *T. thermophila* covers the whole spectrum of divalent- and monovalent-binding abilities that MTs can exhibit. The modular structure of MTT1, MTT3 and MTT5, as well as the unusually long sequences of all the isoforms, already discussed in other works (Díaz et al., 2007) (Santovito et al., 2007), could respond to evolutionary events. According to literature, Ciliates appeared in the early stages of Earth life, even before other important kingdoms, like Fungi (Parfrey et al., 2011), whose MTs were characterized to be very short Cu-MTs, as those identified in *Neurospora crassa* or *Agaricus bisporus* (Kägi et al., 1979) (Münger & Lerch, 1985c). Thus, only different evolutionary episodes could explain the presence of the

differentiated behaviour in the *T. thermophila* MT isoforms. Based on the assumption that initially only short Cu-MTs were present, MTT2 and MTT4 may have evolved by tandem duplication of the CXCXPC pattern (Figure 1), in which this module is present until seven times in both sequences, being CXCNPC the most frequent. This phenomenon would explain the extraordinary ability to bind high amounts of Cu ions that both MTs exhibit. Furthermore, a single substitution in one amino acid (Asn in MTT2 by Lys in MTT4, in position 89) would confer a stronger Cu-thionein behaviour to MTT2 regarding MTT4. Contrarily, the evolutionary footprint in MTT1, MTT3 and MTT5 would have been several episodes of duplications of both single cysteine residues and complete modules, which would explain the presence of Cys doublets and triplets that are likely linked to divalent metal ion preferences. Nevertheless, it is clear that this scenario is not applicable to MTT3, whose undefined character could explained by a hypothetical need of an ambivalent MT isoform in the cell, which could play a dual role depending on metal detoxification or other stress requirements (*i.e.* oxidative stress).

Be that as it may, *T. thermophila* MT system is a very valuable model to understand how MTs have evolved to meet the needs of metal homeostasis and avoid the potential damage that a high metal concentration can cause. The presence of two genuine Zn/Cd-thioneins, two genuine Cu-thioneins and an intermediate MT, turn *T. thermophila* into an extraordinary organism, able to cope with multiple stresses simultaneously. An analogous strategy, as is discussed below, is also used by other organisms to deal with adverse scenarios in which the presence of a specific metal causes a high cell toxicity.

4.2. *Cryptococcus neoformans* MT SYSTEM, METAL-BINDING ABILITIES, BUILDING BLOCKS ARCHITECTURE AND ROLE AS VIRULENCE DETERMINANTS.

The MT system of the opportunistic human pathogenic fungus *C. neoformans*, comprises two recently described MTs, which are the longest MT sequences characterized in fungi so far, in contrast with the paradigmatic short Cu-MTs identified in this kingdom. The expression of *CnMT1* and *CnMT2* genes, under cellular copper excess (Figure 2) (Ding et al., 2011), suggested a Cu-thionein character for conditions both peptides, similar to that observed for other fungi; however no metal-binding studies had been conducted, before those here

presented. The obtained results, which have been communicated in three different publications (publications 2, 3 and 4 of this PhD thesis), provide extensive information about the metal-binding behaviour of these atypical MTs.

```
CnMT1       MACNCPPQKNTACCSTSEAQDKCTCQKGNCECKACPNSTKTSESG-------GKASTCNC
CnMT2       MAFNPNPEKTTSCCSTSKAQDKCTCPKGKCECETCPKSTKTPGSGPCNCGVKEKVSTCGC

CnMT1       GGSGEACTCPPGQCACDKCPKKAKSVSTCGCGGSGAACSCPPGKCACDNCPKQAQEKVSS
CnMT2       NGSGAACTCPPGQCACDSCPRKAKSVSTCGCGGSAAACSCPPGKCACDSCPKQAQEKVSS

CnMT1       CACSGSGAA----------------------------------------------------
CnMT2       CACNGSGGACTCPPGKCSCSGCPAQAKENPADQPTTCGCQGVGVACTCPPGQCACDGCPA

CnMT1       --- 122
CnMT2       KAK 183
```

Figure 2. Sequence alignment (Clustal Omega) of CnMT1 and CnMT2. Cys residues are marked in red; spacer regions without cysteines are marked in grey.

First, the protein sequence features, together with the general Cu-binding abilities exhibited by CnMT1 and CnMT2 were analysed (publication 2). The CnMTs protein sequences previously reported, were aligned and compared with other eukaryotic MTs, such as mammalian, yeast and other fungal MTs. The best results were those obtained with the *N. crassa* and *A. bisporus* peptides. Hence, it was surprisingly evident that both CnMTs were organized in cysteine-rich units, separated with spacer regions lacking Cys-residues (Figure 2). CnMT1 and CnMT2 share a 7-Cys motif ($CXCX_6CXCX_4CXCXXC$) that is repeated three and five times respectively, in which the cysteine number and positions totally match with those found in *N. crassa* and *A. bisporus* MTs. This cysteine pattern, also present in other fungal MTs, gave us a first clue to understand a possible CnMTs evolutionary origin from a common one-unit fungal MT ancestor. Indirectly, these preliminary data, allowed us to suggest a highly probable genuine Cu-thionein behaviour for CnMTs.

The metal-binding ability of CnMTs was analyzed following the same strategy mentioned before. The recombinant CnMTs yielded peculiar Cu-MT complexes not described so far. From Cu-supplemented cultures at normal oxygenation conditions, homometallic Cu_{16}-CnMT1 and Cu_{24}-CnMT2 species, accompanied with few minor species, were recovered. These results were corroborated in low-oxygenated cultures, from which Cu_{15}-CnMT1 and Cu_{24}-, and Cu_{20}-CnMT2 complexes were purified. The Zn/Cu replacement studies in Zn-

CnMT1 and Zn-CnMT2 confirmed these stoichiometries, evidencing an extraordinary capacity of CnMTs to coordinate high amounts of Cu ions. Furthermore, the unmetalated complexes produced by the mutant CnMT1ala, in which all the cysteines has been replaced by alanines, confirmed the requirement of the thiol groups provided by cysteines, for metal-MT coordination.

Using *in silico* tools to compare the information available in genome databases and the CnMT cDNAs that had been isolated in Prof. Thiele's lab, it was readily seen there were serious discrepancies. A deeper analysis of the genomic sequences allowed us to detect mis annotation problems for both sequences, in which exon-intron boundaries did not match the universal GT-AG rule, probably due to the automatic analysis of the genome. Therefore, both cDNA sequences were manually analyzed and finally corrected regarding the genomic annotation.

To confirm the genuine Cu-thionein properties of CnMTs and complete their full analysis, the synthesis and purification of recombinant Zn- and Cd-CnMTs complexes were performed. From Zn-supplemented cultures, a major Zn_8-CnMT1 and Zn_{11}-CnMT2, together with other minor species, were respectively recovered. Cd-supplemented cultures yielded a major Cd_8-CnMT1, with minor complexes, significantly Cd_8S-CnMT1 species, and two major Cd_{13}- and Cd_{15}-CnMT2 species. Thus, all the evidences reaffirmed the Cu-thionein character of CnMTs. New recombinant metal-CnMTs complexes retrieved in Cu-supplemented cultures, yielded the same results, already discussed before. The CD spectra of the Zn, Cd, and Cu-CnMTs recombinant complexes, as well as the Zn/Cu replacement studies of Zn-CnMTs preparations, corroborated again the Cu-thionein character shown of this fungal MT system. It is worth to note the cooperative Cu loading in sets of 5 Cu^+ ions during the Zn/Cu reopalcement reaction in Zn-CnMT1 and Zn-CnMT2, until 15-16 and 23-24 Cu^+ ions respectively, in full concordance with the stoichiometry observed for the *in vivo* Cu-CnMTs folded complexes.

It remained evident that the extraordinary ability and specificity of CnMTs to bind Cu^+ ions could be related to their unusual length, so that the number of Cys-residues was determinant. This ability endows them a useful advantage when binding of Cu^+ ions, and consequently it supposes an optimum detoxification mechanism, necessary during the infection process conducted by *C. neoformans* to evade the host immune system (Ding et al., 2011) (Ding et al., 2014b). The genuine Cu-thionein behaviour corroborated by our

experiments, according to the exposed by Bofill et al., match with the expected in typical fungal Cu-MTs, but with the particularity of unusual long sequences (Bofill et al., 2009). The peculiar architecture of CnMTs, based on the repetitions of well defined Cys-rich blocks, is crucial to understand CnMT properties. The pattern and distribution of the cysteines in 7-Cys building blocks, is presumably the structure allowing to bind 5 Cu^{+}, until the complete load of the different blocks. This is similarly found in *N. crassa*, whose unique seven Cys are able to bind in this case, up to 6 Cu^{+} ions, according to the literature (Cobine et al., 2004). So, it is possible to hypothesize that under the selection pressure to bing high Cu amounts, a single MT unit, as found in *N. crassa*, *A. bisporus* and other fungi, may have been the primeval structure in virtually all fungal MTs; and it would have undergone several duplication processes. In summary, what probably happened in *C. neoformans* were tandem duplications of the complete 7-Cys unit linked by Cys-free segments, together with single cysteine duplications at the sequence ends, to yield long MTs, with exceptional Cu-binding capacity, this turning them into virulence determinants, crucial in the Cu detoxification machinery of the fungus.

Despite all the evidences shown until this point, it remained to be experimentally shown that each 7-Cys building block could bind 5 Cu^{+} ions in independent clusters. To elucidate this subject, a set of new experiments was performed, in which several segments of CnMT1 were designed and recombinantly synthesized in Zn- and Cu- enriched cultures, following the strategy used for the entire CnMTs. The results (publication 4) provided the answer to this question and also additional information to characterize the *C. neoformans* MT metal binding properties. The designed segments (CnMT1Sx) corresponded to diverse combinations of 7-Cys units, with the presence or absence of a spacer segment at the end of each fragment (Figure 3). The constructed fragments yielded different metal-MT complexes depending on the number of 7-Cys building units and adjacent sequences. Hence, S1, S2 and S3, which contain one 7-Cys unit, rendered the same Zn_2- and Cu_5-complexes, showing that the absence of the spacer region in N-terminus, as well as the incomplete spacer at the C-terminus, does not greatly affect the metal-complexes retrieved. Contrarily, unequal results were observed for S4 and S5, composed by 7+2 and 2+7 cysteine residues, respectively: whereas for S4, Zn_3- and Cu_5-complexes were recovered; S5 was to fold into metal complexes, this showing that the number of cysteines in the N- or C-terminus affects somehow the stability of the metal-complexes. Finally, the presence of two (S6) or three (S7) 7-Cys building blocks was translated to a higher capacity to coordinate metal ions. Thus for S6, Zn_4-

and Cu_9- and Cu_{10}-S6 complexes were purified from the respective metal-supplemented cultures; while for S7, Zn_7- and equimolar heterometallic M_{10}- and M_9-S7 (M= Zn or Cu), containing Cu_9- and Cu_5-S7 cores (as revealed by ESI-MS analyses) were recovered. The Zn(II)/Cu(I) replacement reactions resulted in very informative data. S2 and S3 showed a similar behaviour in which a cooperative loading of 5 Cu(I) was retrieved, whereas S1 exhibited a higher complexity that correlates with the lack of stabilization observed in Cu5-S1. On the other hand, the progressive replacement in the 7+2 Cys-fragment S4, yielded a M5-S4 (M= Zn or Cu) mainly constituted by Cu5-S4, but no Zn(II)/Cu(I) displacement were observed in S5, corroborating one more time the unproductive synthesis of S5 in Cu-supplemented cultures. Finally, in S6 and S7, similar results to the obtained Cu-supplementation cultures were observed. In S6, the two Cys-building blocks divided by a spacer region, are able to load 10 Cu(I) in the second metal replacement agent; whereas S7, with three Cys-building blocks, is able to load only 9 Cu(I) and not 15 Cu(I), as it would expected, knowing what happens in the 7-Cys, 7+2-Cys and 7+7-Cys fragments; these last results suggest an important role of the CXC flanking regions in S7, to stabilize the loading of a third Cu5-cluster.

The interpretation of all these results confirms that each 7-Cys building unit is able to cooperatively coordinate 5 Cu^+ ions, forming independent Cu_5-clusters. This last result raises the possibility that the NMR structure of the *N. crassa* MT peptide, which was solved ten years ago as folded around 6 Cu^+ ions, (Cobine et al., 2004), has to be reconsidered in terms of the amount of coordinated Cu^+ ions.

Finally, our results indicate that the N- and C-terminal flanking regions (containing a CXC motif each) may play a stabilizing role in the Cu_5-cluster complexes, so that their absence in S7 may impair the formation of a stable Cu_{15}-complex, as expected taking into account the presence of three 7-Cys blocks.

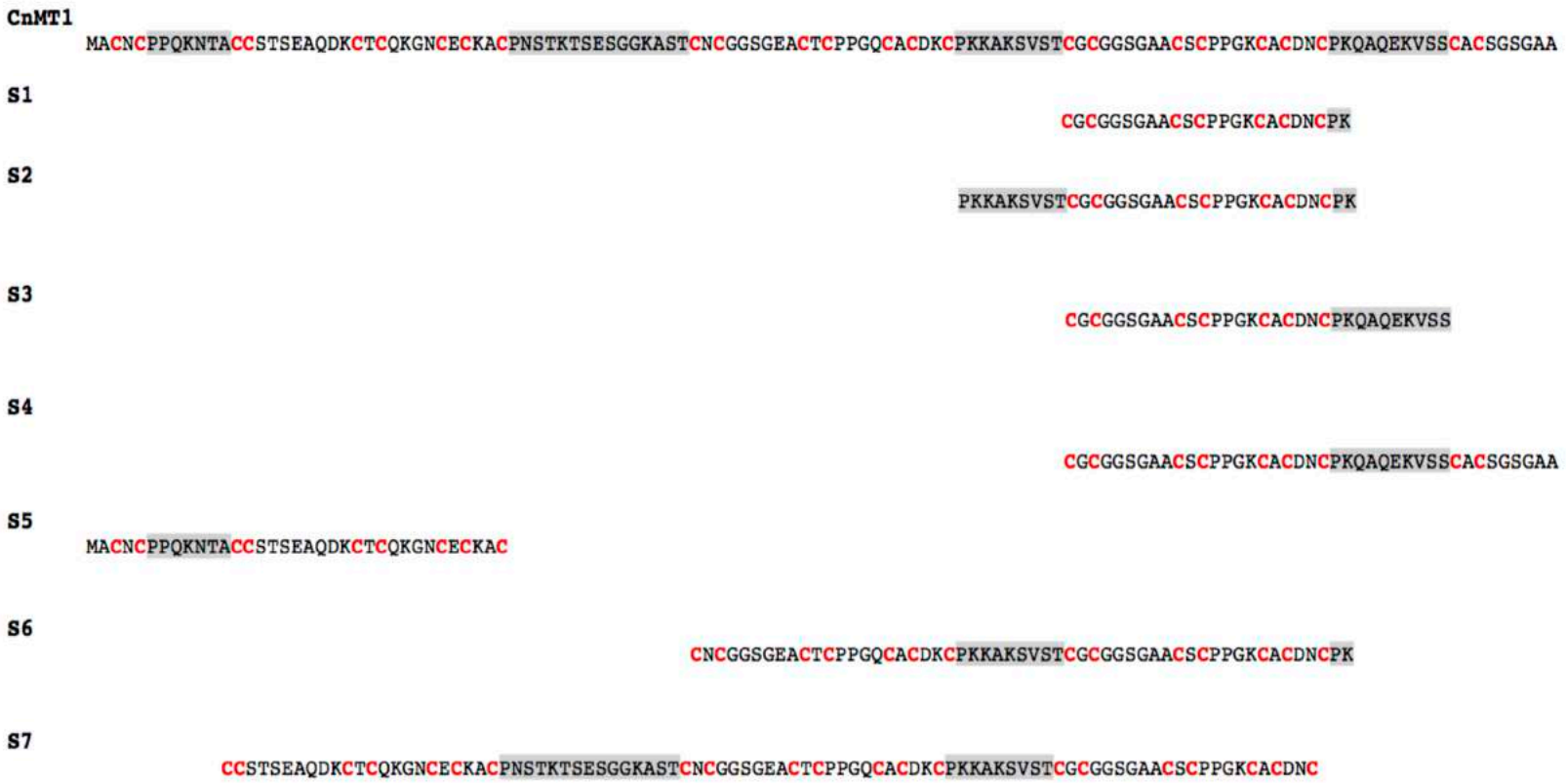

Figure 3. Sequence alignment of the CnMT1 full-length protein and the corresponding designed fragments (from S1 to S7). Cys residues are in marked in red, and the spacer segments are highlighted in grey.

In a final experiment, the contribution to Cu tolerance of these Sx peptides, as well as of the entire CnMTs, in a *S. cerevisiae* MT-knockout strain (51.2cΔc5) was analysed. The growth rate in Cu-rich media of different yeast transformants (with each Sx peptide and the entire CnMTs) and the wild-type yeast cells, was comparable, contrasting with the poor growth rate observed in the non-transformed yeast MT-knockout, indicating that both whole CnMTs as Sx peptides restore the Cu tolerance lost in other organisms.

In conclusion, all the information gathered about how *CnMT* genes are induced by Cu excess (Ding et al., 2011), together with all the metal-binding features here exposed, provide invaluable data to understand the way how this and probably other opportunistic pathogenic fungi overcome host defense mechanisms, based on Cu toxicity, in their infective process. These conclusions open a new scenario in which the study of a wide range of fungal MTs would give more clues to understand the need of some pathogenic but also non-pathogenic, fungi, to induce phenomena of duplication and expansion of their MT peptide sequences.

4.3. PAST, PRESENT AND FUTURE OF FUNGAL MTS

Finally, and as a consequence of the research in the *C. neoformans* MT system, a review of fungal MT features has been included in this thesis. The first identified MTs corresponding to yeasts: *Saccharomyces cerevisiae* (Cup1 and Crs5) and *Candida glabrata* (MT-1 and MT-2); and fungi: *N. crassa* MT and *A. bisporus* MT, established the idea of an exclusive Cu-thionein character for fungal MTs, as well as a short and medium protein sequence length (up to 69 amino acids) (Winge et al., 1985) (Mehra et al., 1988) (Kägi et al., 1979) (Münger & Lerch, 1985c). From then on, other MTs, with new unreported features, have been described; for instance, new metal-binding abilities and new cysteine arrangements not previously identified among fungal MTs. *E.g.* the description of Zym1 (*Schiziosaccharomyces pombe*) revealed that it was a Zn-thionein rather than a typical fungal Cu-thionein, who induces this *MT* gene (Borrelly et al., 2002); or the identification of four MTs (MTP1-4) from *Yarrowia lipolytica*, which revealed the existence of the -CCC- motifs, which are rare in fungal MTs (García et al., 2002).

In the last two decades, the number of known fungal MTs has increased exponentially; among them, those of a set of plant and human pathogenic fungi, including mycorrhizal, mushrooms and even aquatic fungi. With the promising results that we obtained in the characterization of CnMTs discussed above, our group decided to expand the current knowledge on pathogenic fungi MTs, which may reveal important features in order to understand the fungus infectivity mechanisms and their MT involvement as virulence determinants. Our approach to identify new fungal MTs was based on a combination of literature searches and *in silico* analysis. Unsatisfactory initial results about putative pathogenic fungal MT were obtained after multiple searches in the available literature; and also initially poor results were retrieved in the *in silico* BLAST searches using as query the huge number of fungal MTs know to date. A most careful scanning allowed us to identify annotated MT sequences, in which only a part matched with real MT peptide features. The subsequent analyses of EST databases, allowed us to decipher the real encoding sequence and corroborate the presence of mis annotated MTs in databases. This scenario already shown in the characterization of the *C. neoformans* MTs, turned to be quite usual in all the performed searches, probably as a result of automatic genome sequencing. The MT sequences finally identified and clarified, belong to different opportunistic human pathogenic fungi with medical interest, such as: *Histoplasma capsulatum*, *Aspergillus flavus* or *Coccidioides immitis* (the causing agents of several systemic mycosis in immunocompromised people) among others, and plant pathogenic fungi with agronomic impact such as: *Fusarium oxysporum*, *Fusarium graminearum* or *Moniliophthora perniciosa* (responsible of important crop pests). The comparative analysis between these new MT peptides and the already known fungal MT, allowed us to establish different groups of fungal MTs, depending on their sequence similarity and the number of cysteine residues that they contain. Thus, the Subfamily 1 includes the shortest sequences containing 6-7 cysteines, being *N. crassa* MT the classic model of this group. Subfamily 2, comprises new identified fungal MT, with a medium-length sequence, 9 cysteines and *H. capsulatum* MT as the representative model. Subfamily 3, represented by the well known Cup1 from *S. cerevisiae*, include a set of past and recently described fungal MTs identified by other members of our group; these MTs possess long sequences and a total of 12-18 cysteine residues. Finally, the Subfamily 4 contains the longest reported fungal MTs, whose cysteine number surpasses the 22 residues; that is: both CnMTs from *C. neoformans* and the largest MT described ever, belonging to the saprophyte fungus *Tremella mesenterica*, which was also recently described and characterized in our group. At this point, it is clear that divergences in fungal MTs are great, probably not so much in cysteine distributions, but in

length, which can be more advantageous for the fungus than the rearrangement of its Cys-pattern.

As a result of all this information, we aimed at characterizing a new pathogenic fungal MT, whose sequence was not found in the *in silico* results. Starting from the point that the fungal MT encoding sequences of *F. oxysporum* and *F.graminearum* were known, we followed the strategy used in our group (discussed above) to analyze the putative MT from *F. verticillioides*, an important human-plant pathogen. The FvMT cDNA, obtained from total mRNA of the fungus, encoded a protein with a sequence exact to those of *F. oxysporum* and *F. graminearum* MTs, containing 6 cysteine residues. When recombinantly synthesized, it yielded major Zn_2-FvMT species (Zn-supplemented cultures); no Cd-FvMT complexes Cd-supplemented cultures; and homometallic Cu_5-FvMT species from both normal and low-aerated Cu-supplemented cultures. These results indicate a genuine Cu-thionein behaviour of FvMT and match perfectly those obtained for each Cys-building block of CnMTs (publication 4), confirming once again what looks like a general rule dogma for fungal MTs: a basic unit containing 7 cysteine residues binds 5 Cu^+ forming a Cu_5-cluster. In that case, the need to review the Cu_6-MT of *N. crassa* becomes a priority in which our group is currently working.

Overall, this PhD thesis work contributes to enlarge the current limited knowledge about molecular evolution of unicellular eukaryote MTs. Two different MT systems, belonging to the protist *T. thermophila* and the fungus *C. neoformans*, were characterized. Their MT systems revealed different strategies used by these organisms; whereas each *T. thermophila* MT shows a preference to bind high amounts of a specific heavy metal ion, *C. neoformans* MTs exhibit the capacity to bind high amounts of a single metal ion (Cu^+) as part of its detoxification machinery. Be that as it may, in both organisms the evolving events may explain the structural architecture of their MTs to better understand their particular functions. As general conclusion, it could be said that according to what has been here exposed, divalent metal ion-MTs seem to have evolved through two main strategies: basic module duplications, and cysteine duplications with subsequent rearrangements. Contrarily, monovalent metal-ion MTs seem apparently evolved to increase their capacity basically by unit duplication phenomena, with isolated episodes of cysteine rearrangement also observed. However, these conclusions should be corroborated by future works; at the same time that it would be interesting decipher the enigma that can answer the question: What are the main reasons why some unicellular organisms have evolved to possess long MT sequences, after having been

described that pathogenic and non-pathogenic fungi exhibit extremely different number of residues in their MTs?

CONCLUSIONS

5. CONCLUSIONS

5.1. METAL BINDING PREFERENCES OF *Tetrahymena thermophila* MTS.

1. The previous classification of MTT1, MTT3 and MTT5 as Cd-thioneins and MMT2 and MTT4 as Cu-thioneins is correct, but not completely accurate. Both the diverse Cd-thioneins and the diverse Cu-thioneins exhibit substantial differences among them.

2. The analysis of Zn-, Cd- and Cu-binding abilities revealed the pronounced Zn/Cd-thionein character of MTT1, which is unable to yield stable, unique Cu-complexes. MTT1 yielded a major Zn_{17}- with minor Zn_{18}- and Zn_{16}-MTT1 together with minor complexes of lower and higher stoichiometry. Contrarily, an almost unique Cd_{17}-, together with a very minor Cd_{12}-MTT1 was recovered.

3. A very atypical behaviour of MTT3 is described, with poor yield results in which mixtures of species were detected in Zn- and Cd-supplemented cultures. Thus, a range of major Zn_{12}-, and minor Zn_9- to Zn_{15}-MTT3 were identified; and predominant $Cd_{16}S$- $Cd_{15}S$- and Cd_{18}-MTT3 together with identifiable $Cd_{13}S$-, $Cd_{14}S$-, Cd_{15}-, Cd_{16}-, Cd_{17}- and Cd_{19}-MTT3 were recovered. The synthesis in Cu-supplemented cultures also rendered poor results, consisting of heterometallic Zn,Cu-complexes, where Cu_8- and Cu_4- with minor Cu_{12}-cores were identified.

4. Contrarily, MTT5 rendered stable complexes with the three metal ions, but with better results for Zn^{2+} and Cd^{2+}, for which Zn_6- and Zn_5- as major species, together with minor Zn_7-, Zn_8-, Zn_4- and Zn_3-MTT5 were detected; and almost a unique Cd_8- with a very minor Cd_9-MTT5 were recovered. Samples from Cu-supplemented cultures analyzed at neutral ESI-MS yielded heterometallic M_{12}-, followed by M_9- and M_8-complexes (M= Zn or Cu) that were identified as Cu_9-, Cu_8- and minor Cu_{12}-MTT5 species by acidic ESI-MS.

5. The analysis of Zn-, Cd, and Cu-binding preferences of MTT2 revealed its incapacity of to fold into stable Zn- or Cd-complexes. Contrarily, the Cu-supplemented cultures yielded stable heterometallic complexes at normal oxygenation: major M_{20}- together with minor M_{16}- and M_{17}-MTT2, according to neutral ESI-MS, which corresponded to Cu_{20}-, Cu_{16}- and Cu_{12}-conatining complexes. The low oxygenated cultures rendered homometallic Cu_{20}-, Cu_{21}- and Cu_{23}-MTT2 complexes.

6. From MTT4 synthese in Zn-supplemented cultures, a major Zn_{10}- and minor Zn_8- to Zn_{12}-MTT4 complexes were retrieved. MTT4 was unable to yield recombinant Cd-complexes. In Cu-supplemented cultures at normal oxygenation, the species detected by neutral ESI-MS were major Zn_{16}- and M_{13}- together with significantly intense M_9- to M_{14}-MTT4 complexes (M= Zn or Cu), whereas acidic ESI-MS revealed major Cu_8-, and minor Cu_{12}- and Cu_{14}-MTT4 cores. In low aeration, major homometallic Cu_{20}-MTT4 together with higher nucleation species were produced.

7. All the gathered results allow to draw a Zn/Cd-thionein to Cu-thionein gradation of the *T. thermophila* MTTs as follows: MTT1>MTT5>MTT3>MTT4>MTT2.

8. It appears that evolution may have modulated the amino acid sequences and the Cys motif patterns in these long MTs. Cys doublets and triplets in the modular structures of MTT1, MTT3 and MTT5 seem associated to the Zn/Cd-thionein character. Nevertheless the absence of Cys doublets and triplets, as well as a difference of one single amino acid (an Asn in MTT2 by a Lys in MTT4 at position 89), confer a major Cu-thionein character to MTT2 than a MTT4. All these information constitutes an invaluable model for MT metal preference and evolution studies.

5.2. METAL BINDING ABILITIES AND MODULAR STRUCTURE ANALYSIS OF THE TWO *Cryptococcus neoformans* MTS. COMPARISON WITH OTHER FUNGAL MTS.

1. CnMT1 and CnMT2 are atypical fungal MTs with long sequences, being the largest MTs described so far. They contain multiple Cys residues, resulting in a peculiar architecture of three and five 7-Cys modular segments separated by three and four spacer regions, respectively.

2. The analysis of the Zn-, Cd- and Cu-binding abilities of CnMTs reveals genuine Cu-thionein features. For Zn, CnMT1 major Zn_8-CnMT1, or equimolar Zn_7- and Zn_8-CnMT1 complexes were recovered in different productions. In parallel, major Cd_8- with minor Cd_9- and significantly Cd_8S-CnMT1, were detected from Cd-supplemented cultures. Finally, normally oxygenated Cu-supplemented cultures produced major heterometallic M_{11}- and M_8-CnMT1 complexes followed by M_9-CnMT1 and other minor species (M=Zn or Cu), as revealed by neutral ESI-MS. By acidic ESI-MS, a very

predominant, almost unique Cu_5-CnMT1 was identified in these samples. In low oxygenation biosynthesis, CnMT1 folded into Cu homometallic species, that were identified as major Cu_{16}-CnMT1, together with minor Cu_{15}- and Cu_{17}-CnMT1.

3. Also CnMT2 exhibits Cu-thionein features yielding a mixture of major Zn_{11}- and minor Zn_{12}- and Zn_{10}-CnMT2 complexes in Zn-supplemented cultures; and major Cd_{13}- and Cd_{15}-CnMT2, among multiple minor species, in Cd-supplemented cultures. From Cu-supplemented cultures grown at normal oxygenation, heterometallic species ranging from M_6- to M_{17}-CnMT2 (M=Zn or Cu) were obtained, formed mainly by Cu_5-, but also Cu_9- and Cu_{10}-cores, as indicated by acidic ESI-MS. Under low oxygenation conditions a major M_{24}-CnMT2 (M=Zn or Cu), with a myriad of minor species, was recovered, among which acidic ESI-MS identified Cu_{20}- and Cu_{24}-CnMT2 as major species.

4. The overall consideration of Zn-, Cd- and Cu-abilities of CnMTs reveals a genuine Cu-thionein character for both of them, due to the ability to render unique, homometallic Cu-species in Cu-rich media (*i.e.* low oxygenation), the production of a mixture of species of different stoichiometry when synthesized as Zn- or Cd-complexes, and significantly the presence of S^{2-} ligands in their Cd-complexes.

5. The Zn/Cu displacement reactions in Zn-CnMTs corroborate the extraordinary capacity of both MTs to bind Cu. The results of these reactions are compatible with each 7-Cys segment incorporating 5 Cu(I) ions cooperatively, forming stable Cu_5-clusters until the final Cu_{16}-CnMT1 and Cu_{24}-CnMT2 complexes.

6. Seven different CnMT1 truncated segments (Sx) were synthesized containing different 7-Cys combinations: (7-Cys), (7-Cys)+2, 2x(7-Cys) and 3x(7-Cys). Their Zn- and Cu-binding abilities exhibit the genuine Cu-thionein character shown by the entire CnMT1 whole sequence. In Zn-supplemented cultures the segments with one 7-Cys box (S1, S2 and S3) yielded Zn_2-Sx complexes; S4 ((7-Cys)+2) rendered a major Zn_3- and a minor Zn_4-complex; for S6 (with a 2x(7-Cys) content), a unique Zn_6-complex was recovered; while for S7 (3x(7-Cys)), a major Zn_7- and a minor Zn_8-complex were detected. No Zn-complexes were obtained in S5 (which contains 2+(7-Cys)).

7. Contrarily, in Cu-supplemented cultures, S1 to S3 and S4 rendered Cu_5-complexes; and S6, a major Cu_5- with minor Cu_9- and Cu_{10}-complexes, at both aeration conditions. S7,

at normal oxygenation, rendered heterometallic major M_{10}- and minor M_{11}- and M_{13}-species (neutral ESI-MS), containing major Cu_9- and minor Cu_5- and Cu_{10}-cores (acidic ESI-MS). Finally, in low oxygenated cultures, S7 yielded homometallic species, being Cu_9-S7 the major species, and Cu_{14}- and Cu_{12}-S7 the minor complexes recovered. No Cu-complexes were retrieved from S5 syntheses.

8. The Zn/Cu displacement reactions in Zn-CnMTs-Sx rendered Cu_5-Sx complexes for S1 to S4, whereas in S6 and S7 the final complexes were Cu_{10}- and Cu_9-Sx, respectively; this results corroborate that each 7-Cys segment incorporate 5 Cu(I) ions cooperatively, forming stable Cu_5-clusters.

9. It is worth to note that the presence of glutamic acid residues in the flanking regions seems to contribute to enlarge the basic 2:7 Zn:Cys coordination relationship, as observed for some constructs (S4 and S7). In the case of Cu(I) coordination, one of the Cu(I) ions of the Cu5-cluster appears quite unstable if the segment is devoid of a flanking spacer. When several 7-Cys boxes are tandemly combined, always one of them seems unable to remain filled with Cu(I). Therefore, the presence of flanking amino acids appears necessary to ensure enough stability for the Cu5-clusters in in vivo environments.

10. Comparison of CnMTs genes and protein sequence features, as well as their metal-binding abilities, support the theory of the emergence of the long *C. neoformans* MTs by ancient tandem repetition of a primeval fungal MT unit, currently represented by *Neurospora crassa* and *Agaricus bisporus* MTs.

11. New fungal MT ORFs have been identified using BLAST tools and manual genome screening. Similarities between their sequences and MTs already known, allowed to classify them in four different subfamilies attending to their length and their Cys-distribution.

12. The human and plant pathogen *Fusarium verticillioides* MT sequence was also identified. The corresponding cDNA was selectively amplified in a total cDNA population retrotranscribed from total *F. verticillioides* mRNA isolated from fungus cultures. The characterization of its MT showed extremely coincidence with the *N. crassa* MT in terms of length, number of Cys residues and their distribution, and the

capacity to bind 5 Cu. Subsequently, FvMT can also be considered a typical Cu-thionein.

13. Fungal MTs have become and interesting field of study to understand the molecular basis of MT Cu preference. Fungal MTs can perform essential roles not only in pathogenic fungi, but also in other harmless fungal species and for other purposes. The comparison between long and short fungal MTs, as well as the analysis of their possible modular architecture, facilitates a better understanding of MT evolution.

REFERENCES

Amaro F, Turkewitz AP, Martín-González A, Gutiérrez JC (2011). Whole-cell biosensors for detection of heavy metal ions in environmental samples based on metallothionein promoters from *Tetrahymena thermophila*. Microbial Biotechnology 4: 513–522.

Andreini C, Bertini I, Rosato A (2009) Metalloproteomes: a bioinformatic approach. Accounts of Chemical Research 42: 1471–1479.

Andrews GK (2000) Regulation of metallothionein gene expression by oxidative stress and metal ions. Biochemical Pharmacology 59: 95–104.

Antonissen G, Martel A, Pasmans F, Ducatelle R, Verbrugghe E, Vandenbroucke V, et al. (2014) The impact of *Fusarium mycotoxins* on human and animal host susceptibility to infectious diseases. Toxins 6: 430–452.

Artells E, Palacios Ò, Capdevila M, Atrian S (2013) Mammalian MT1 and MT2 metallothioneins differ in their metal binding abilities. Metallomics 5: 1397–1410.

Artells E, Palacios Ò, Capdevila M, Atrian S (2014) In vivo-folded metal-metallothionein 3 complexes reveal the Cu-thionein rather than Zn-thionein character of this brain-specific mammalian metallothionein. The FEBS Journal 281: 1659–1678.

Atrian S, Capdevila M (2013) Metallothionein-protein interactions. Biomolecular concepts 2: 143-160.

Balamurugan K, Schaffner W (2006) Copper homeostasis in eukaryotes: teetering on a tightrope. Biochimica Et Biophysica Acta 1763: 737–746.

Bellion M, Courbot M, Jacob C, Guinet F, Blaudez D, Chalot M (2007) Metal induction of a *Paxillus involutus* metallothionein and its heterologous expression in *Hebeloma cylindrosporum*. New Phytologist 174: 151–158.

Beltramini M, Lerch K (1986) Primary structure and spectroscopic studies of *Neurospora* copper metallothionein. Environmental Health Perspectives 65: 21–27.

Berg JM, Shi Y (1996) The galvanization of biology: a growing appreciation for the roles of zinc. Science 271: 1081–1085.

Bermingham-McDonogh O, Gralla EB, Valentine JS (1988) The copper, zinc-superoxide dismutase gene of *Saccharomyces cerevisiae*: cloning, sequencing, and biological activity. Proceedings of the National Academy of Sciences of the United States of America 85: 4789–4793.

Bertin G, Averbeck D (2006) Cadmium: cellular effects, modifications of biomolecules, modulation of DNA repair and genotoxic consequences (a review). Biochimie 88: 1549–1559.

Binz PA, Kägi JHR (1999) Chapter 1: Metallothionein: molecular evolution and classification. In Klaassen. Metallothionien IV. Basel: Brikhäuser Verlag.

Blackwell M (2011) The fungi: 1, 2, 3 … 5.1 million species?. American Journal of Botany 98: 426-438.

Bleackley MR, MacGillivray RTA (2011) Transition metal homeostasis: from yeast to human disease. Biometals : an International Journal on the Role of Metal Ions in Biology, Biochemistry, and Medicine 24: 785–809.

Bleackley MR, Young BP, Loewen CJR, MacGillivray RTA (2011) High density array screening to identify the genetic requirements for transition metal tolerance in *Saccharomyces cerevisiae*. Metallomics 3: 195–205.

Blencowe DK, Morby AP (2003) Zn(II) metabolism in prokaryotes. FEMS Microbiology Reviews 27: 291–311.

Blindauer CA, Leszczyszyn OI (2010) Metallothioneins: unparalleled diversity in structures and functions for metal ion homeostasis and more. Natural Product Reports 27: 720–741.

Blindauer CA, Harrison MD, Parkinson JA, Robinson AK, Cavet JS, Robinson NJ, Sadler PJ (2001) A metallothionein containing a zinc finger within a four-metal cluster protects a bacterium from zinc toxicity. Proceedings of the National Academy of Sciences of the United States of America, 98: 9593–9598.

Blindauer CA, Harrison, MD, Robinson AK, Parkinson JA, Bowness PW, Sadler PJ, Robinson NJ (2002) Multiple bacteria encode metallothioneins and SmtA-like zinc fingers. Molecular Microbiology, 45: 1421–1432.

Blindauer CA (2014) Chapter 21: Metallothioneins. In Maret W, Wedd A. Binding, Transport and Storage of Metal Ions in Biological Cells. London: Royal Society of Chemistry.

Bofill R, Capdevila M, Atrian S (2009) Independent metal-binding features of recombinant metallothioneins convergently draw a step gradation between Zn- and Cu-thioneins. Metallomics 1: 229–234.

Bofill R, Palacios Ò, Capdevila M, Cols N, Gonzàlez-Duarte R, Atrian S, Gonzàlez-Duarte P (1999) A new insight into the Ag+ and Cu+ binding sites in the metallothionein β domain. Journal of Inorganic Biochemistry 73: 57–64.

Boldrin F, Santovito G, Formigari A, Bisharyan Y, Cassidy-Hanley D, Clark TG, Piccinni E (2008) MTT2, a copper-inducible metallothionein gene from *Tetrahymena thermophila*. Comparative Biochemistry and Physiology. Toxicology & Pharmacology: CBP 147: 232–240.

Boldrin F, Santovito G, Gaertig J, Wloga D, Cassidy-Hanley D, Clark TG, Piccinni, E (2006) Metallothionein gene from *Tetrahymena thermophila* with a copper-inducible-repressible promoter. Eukaryotic Cell 5: 422–425.

Bonfante P, Genre A (2010) Mechanisms underlying beneficial plant-fungus interactions in mycorrhizal simbiosis. Nature Communications 1:48.

Bongers J, Walton CD, Richardson DE, Bell JU (1988) Micromolar protein concentrations and metalloprotein stoichiometries obtained by inductively coupled plasma atomic emission spectrometric determination of sulfur. Analytical Chemistry 60: 2683–2686.

Borrelly GPM, Harrison MD, Robinson AK, Cox SG, Robinson NJ, Whitehall SK (2002) Surplus zinc is handled by Zym1 metallothionein and Zhf endoplasmic reticulum transporter in *Schizosaccharomyces pombe*. Journal of Biological Chemistry 277: 30394–30400.

Bourdineaud JP, Baudrimont M, Gonzalez P, Moreau JL (2006) Challenging the model for induction of metallothionein gene expression. Biochimie 88: 1787–1792.

Brown GD, Denning DW, Gow NAR, Levitz SM, Netea MG, White TC (2012) Hidden Killers: Human Fungal Infections. Science Translational Medicine 4: 165rv13–165rv13.

Buchanan-Wollaston V (1994) Isolation of cDNA clones for genes that are expressed during leaf senescence in *Brassica napus*. Identification of a gene encoding a senescence-specific metallothionein-like protein. Plant Physiology 105: 839–846.

Bulteau AL, O'Neill HA, Kennedy MC, Ikeda-Saito M, Isaya G, Szweda LI (2004) Frataxin acts as an iron chaperone protein to modulate mitochondrial aconitase activity. Science 305: 242–245.

Burkhead JL, Reynolds KAG, Abdel-Ghany SE, Cohu CM, Pilon M (2009) Copper homeostasis. The New Phytologist 182: 799–816.

Calderone V, Dolderer B, Hartmann HJ, Echner H, Luchinat C, Del Bianco C, et al. (2005) The crystal structure of yeast copper thionein: the solution of a long-lasting enigma. Proceedings of the National Academy of Sciences of the United States of America 102: 51–56.

Capdevila M, Atrian S (2011) Metallothionein protein evolution: a miniassay. Journal of Biological Inorganic Chemistry 16: 977–989.

Capdevila M, Bofill R, Palacios Ò, Atrian S (2012) State-of-the-art of metallothioneins at the beginning of the 21st century. Coordination Chemistry Reviews 256: 46–62.

Capdevila M, Cols N, Romero-Isart N, Gonzàlez-Duarte R, Atrian S, Gonzàlez-Duarte P (1997) Recombinant synthesis of mouse Zn 3 - ? and Zn 4 - ? metallothionein 1 domains and characterization of their cadmium(II) binding capacity. Cellular and Molecular Life Sciences 53: 681–688.

Capdevila M, Domènech J, Pagani A, Tió L, Villarreal L, Atrian S (2005) Zn- and Cd-metallothionein recombinant species from the most diverse phyla may contain sulfide (S2−) ligands. Angewandte Chemie 117: 4694–4698.

Carpenè E, Andreani G, Isani G (2007) Metallothionein functions and structural characteristics. Journal of Trace Elements in Medicine and Biology. Organ of the Society for Minerals and Trace Elements (GMS) 21: 35–39 (Suppl 1).

Casas-Finet JR, Hu S, Hamer D, Karpel R L (1991) Spectroscopic characterization of the copper(I)-thiolate cluster in the DNA-binding domain of yeast ACE1 transcription factor. FEBS Letters, 281: 205–208.

Chang Y, Feng LF, Xiong J, Miao W (2011) [Function comparison and evolution analysis of metallothionein gene MTT2 and MTT4 in *Tetrahymena thermophila*]. *Dong Wu Xue Yan Jiu = Zoological Research* 32: 476–484.

Chaudhry R, Shakoori AR (2010) Isolation and characterization of a novel copper-inducible metallothionein gene of a ciliate, *Tetrahymena tropicalis lahorensis*. Journal of Cellular Biochemistry 110: 630–644.

Chiaverini N, De Ley M (2010) Protective effect of metallothionein on oxidative stress-induced DNA damage. Free Radical Research 44: 605–613.

Clemens S (2001) Molecular mechanisms of plant metal tolerance and homeostasis. Planta 212: 475–486.

Clemens S (2006a) Evolution and function of phytochelatin synthases. Journal of Plant Physiology 163: 319–332.

Clemens S (2006b) Toxic metal accumulation, responses to exposure and mechanisms of tolerance in plants. Biochimie, 88: 1707–1719.

Clemens S, Naumann B, Hippler M (2009) Proteomics of metal mediated protein dynamics in plants - iron and cadmium in the focus. Frontiers in Bioscience (Landmark Edition) 14: 1955–1969.

Cobine PA, McKay RT, Zangger K, Dameron CT, Armitage IM (2004) Solution structure of Cu6 metallothionein from the fungus *Neurospora crassa*. European Journal of Biochemistry 271: 4213–4221.

Coleman JE (1998) Zinc enzymes. Current Opinion in Chemical Biology 2: 222–234.

Collingwood TN, Urnov FD, Wolffe AP (1999) Nuclear receptors: coactivators, corepressors and chromatin remodeling in the control of transcription. Journal of Molecular Endocrinology 23: 255–275.

Cols N, Romero-Isart N, Capdevila M, Oliva B, Gonzàlez-Duarte P, Gonzàlez-Duarte R, Atrian S (1997) Binding of excess cadmium(II) to Cd7-metallothionein from recombinant mouse Zn7-metallothionein 1. UV-VIS absorption and circular dichroism studies and theoretical location approach by surface accessibility analysis. Journal of Inorganic Biochemistry 68: 157–166.

Courel M, Lallet S, Camadro JM, Blaiseau PL (2005) Direct activation of genes involved in intracellular iron use by the yeast iron-responsive transcription factor Aft2 without its paralog Aft1. Molecular and Cellular Biology 25: 6760–6771.

Cox GM, Harrison TS, McDade HC, Taborda CP, Heinrich G, Casadevall A, Perfect JR (2003) Superoxide dismutase influences the virulence of *Cryptococcus neoformans* by affecting growth within macrophages. Infection and Immunity 71: 173–180.

Coyle P, Philcox JC, Carey LC, Rofe AM (2002) Metallothionein: the multipurpose protein. Cellular and Molecular Life Sciences 59: 627–647.

Culotta VC, Howard W R, Liu XF (1994) CRS5 encodes a metallothionein-like protein in *Saccharomyces cerevisiae*. Journal of Biological Chemistry 269: 25295–25302.

Das P, Samantaray S, Rout GR (1997) Studies on cadmium toxicity in plants: a review. Environmental Pollution 98: 29–36.

Dean R, Van Kan JA, Pretorius ZA, Hammond-Kosack KE, Di Pietro A, Spanu PD et al. (2012) 10 fungal pathogens in molecular plant pathology. Molecular Plant Pathology 13: 414-430.

Deckert J (2005) Cadmium toxicity in plants: is there any analogy to its carcinogenic effect in mammalian cells? Biometals 18: 475–481.

De Silva DM, Askwith CC, Kaplan J (1996) Molecular mechanisms of iron uptake in eukaryotes. Physiological Reviews 76: 31-47.

Di Croce L, Okret S, Kersten S, Gustafsson JA, Parker M, Wahli W, Beato M (1999) Steroid and nuclear receptors. EMBO Journal 18: 6201–6210.

Ding C, Festa RA, Chen YL, Espart A, Palacios Ò, Espín J, et al. (2014a) *Cryptococcus neoformans* copper detoxification machinery is critical for fungal virulence. Cell Host & Microbe 13: 265–276.

Ding C, Festa RA, Sun TS, Wang ZY (2014b) Iron and copper as virulence modulators in human fungal pathogens. Molecular Microbiology 93: 10–23.

Ding C, Yin J, Tovar EMM, Fitzpatrick DA, Higgins DG, Thiele DJ (2011) The copper regulon of the human fungal pathogen *Cryptococcus neoformans* H99. Molecular Microbiology 81: 1560–1576.

Díaz S, Amaro F, Rico D, Campos V, Benítez L, Martín-González A, et al. (2007) *Tetrahymena* metallothioneins fall into two discrete subfamilies. PLoS ONE, 2: e291.

Domènech J, Orihuela R, Mir G, Molinas M, Atrian S, Capdevila M (2007) The Cd(II)-binding abilities of recombinant *Quercus suber* metallothionein: bridging the gap between phytochelatins and metallothioneins. Journal of Biological Inorganic Chemistry 12: 867–882.

Dugan FM (2008) Fungi at the ancient world: How Mushrooms, Mildews, Molds, and Yeast Shaped the Early Civilizations of Europe, the Mediterranean, and the Near East. Washington: APS Press.

Dupont CL, Grass G, Rensing C (2011) Copper toxicity and the origin of bacterial resistance--new insights and applications. Metallomics, 3: 1109–1118.

Ebbole DJ, Jin Y, Thon M, Pan H, Bhattarai E, Thomas T, Dean R (2004) Gene discovery and gene expression in the rice blast fungus, *Magnaporthe grisea*: analysis of expressed sequence tags. Molecular Plant-Microbe Interactions 17: 1337–1347.

Espart A, Marín M, Gil-Moreno S, Palacios Ò, Amaro F, Martín-González A, et al. (2015) Hints for metal-preference protein sequence determinants: different metal binding features of the five *Tetrahymena thermophila* metallothioneins. International Journal of Biological Sciences 11: 456–471.

Fabris D, Zaia J, Hathout Y, Fenselau C (1996) Retention of thiol protons in two classes of protein iinc Ion coordination centers. Journal of the American Chemical Society 118: 12242–12243.

Festa R A, Thiele DJ (2011) Copper: an essential metal in biology. Current Biology 21: R877–83.

Festa RA, Thiele DJ (2012) Copper at the front line of the host-pathogen battle. PLoS Pathogens 8: e1002887.

Fogel S, Welch JW (1982) Tandem gene amplification mediates copper resistance in yeast. Proceedings of the National Academy of Sciences of the United States of America 79: 5342–5346.

Fones H, Preston GM (2013) The impact of transition metals on bacterial plant disease. FEMS Microbiology Reviews 37: 495–519.

Formigari A Boldrin F, Santovito G, Cassidy-Hanley D, Clark TG, Piccinni E (2010) Functional characterization of the 5'-upstream region of MTT5 metallothionein gene from *Tetrahymena thermophila*. Protist 161: 71–77.

Freisinger E (2008) Plant MTs-long neglected members of the metallothionein superfamily. Dalton Transactions 47: 6663–6675.

García S, Prado M, Dégano R, Domínguez A (2002) A copper-responsive transcription factor, CRF1, mediates copper and cadmium resistance in *Yarrowia lipolytica*. Journal of Biological Chemistry 277: 37359–37368.

Gałazyn-Sidorczuk M, Brzóska MM, Jurczuk M, Moniuszko-Jakoniuk J (2009) Oxidative damage to proteins and DNA in rats exposed to cadmium and/or ethanol. Chemico-Biological Interactions 180: 31–38.

Gauthier GM, Keller NP (2013) Crossover fungal pathogens: the biology and pathogenesis of fungi capable of crossing kingdoms to infect plants and humans. Fungal Genetics and Biology 61: 146-157.

Gonzalez-Fernandez R, Jorrin-Novo JV (2012) Contribution of proteomics to the study of plant pathogenic fungi. Journal of Proteome Research 11: 3–16.

González-Guerrero M, Cano C, Azcón-Aguilar C, Ferrol N (2007) GintMT1 encodes a functional metallothionein in *Glomus intraradices* that responds to oxidative stress. Mycorrhiza 17: 327–335.

Grass G, Rensing C (2001) Genes involved in copper homeostasis in *Escherichia coli*. Journal of Bacteriology 183: 2145–2147.

Guirola M, Jiménez-Martí E, Atrian S (2014) On the molecular relationships between high-zinc tolerance and aconitase (Aco1) in *Saccharomyces cerevisiae*. Metallomics 6: 634–645.

Guirola M, Pérez-Rafael S, Capdevila M, Palacios Ò, Atrian S (2012) Metal dealing at the origin of the Chordata phylum: the metallothionein system and metal overload response in amphioxus. PLoS ONE 7: e43299.

Guarro J, Gené J, Stchigel AM (1999) Developments in fungal taxonomy. Clinical Microbiology Reviwes 12:454-500.

Guo L, Fu C, Miao W (2008) Cloning, characterization, and gene expression analysis of a novel cadmium metallothionein gene in *Tetrahymena pigmentosa*. Gene 423: 29–35.

Guo WJ, Bundithya W, Goldsbrough PB (2003) Characterization of the *Arabidopsis* metallothionein gene family: tissue-specific expression and induction during senescence and in response to copper. New Phytologist 159: 369–381.

Gutiérrez JC, Amaro F, Martín-González A (2009) From heavy metal-binders to biosensors: ciliate metallothioneins discussed. BioEssays 31: 805–816.

Gutiérrez JC, Amaro F, Díaz S, de Francisco P, Cubas LL, Martín-González A (2011) Ciliate metallothioneins: unique microbial eukaryotic heavy-metal-binder molecules. Journal of Biological Inorganic Chemistry 16: 1025–1034.

Hall JL (2002) Cellular mechanisms for heavy metal detoxification and tolerance. Journal of Experimental Botany 53: 1–11.

Hall JL, Williams LE (2003) Transition metal transporters in plants. Journal of Experimental Botany 54: 2601–2613.

Hamer DH (1986) Metallothionein. Annual Review of Biochemistry 55: 913–951. h

Haq F, Mahoney M, Koropatnick J (2003) Signaling events for metallothionein induction. Mutation Research 533: 211–226.

Hawksworth DL (2004) Fungal diversity and its implications for genetic resource collections. Studies in Mycology 50: 9-18.

Hibbett DS, Binder M, Bischoff JF, Blackwell M, Cannon PF, Eriksson OE, Huhndorf S et al. (2007) A higher level phylogenetic classification of the Fungi. Mycological Research 111: 509–547.

Hildebrandt U, Regvar M, Bothe H (2007) Arbuscular mycorrhiza and heavy metal tolerance. Phytochemistry 68: 139–146.

Hood MI, Skaar EP (2012) Nutritional immunity: transition metals at the pathogen-host interface. Nature Reviews. Microbiology 10: 525–537.

Hope W, Natarajan P, Goodwin L (2013) Invasive fungal infections. Clinical Medicine 13: 507–510.

Horng YC, Cobine PA, Maxfield AB, Carr HS, Winge DR (2004) Specific copper transfer from the Cox17 metallochaperone to both Sco1 and Cox11 in the assembly of yeast cytochrome C oxidase. Journal of Biological Chemistry 279: 35334–35340.

Hosiner D, Gerber S, Lichtenberg-Fraté H, Glaser W, Schüller C, Klipp E (2014) Impact of acute metal stress in Saccharomyces cerevisiae. PLoS One 9: e83330.

Hussain D, Haydon MJ, Wang Y, Wong E, Sherson SM, Young J, et al. (2004) P-type ATPase heavy metal transporters with roles in essential zinc homeostasis in *Arabidopsis*. The Plant Cell Online 16: 1327–1339.

Jensen LT, Howard WR, Strain JJ, Winge DR, Culotta VC (1996) Enhanced effectiveness of copper ion buffering by CUP1 metallothionein compared with CRS5 metallothionein in *Saccharomyces cerevisiae*. Journal of Biological Chemistry 271: 18514–18519.

Jo WJ, Loguinov A, Chang M, Wintz H, Nislow C, Arkin AP, et al. (2008) Identification of genes involved in the toxic response of *Saccharomyces cerevisiae* against iron and copper overload by parallel analysis of deletion mutants. Toxicological Sciences 101: 140–151.

Jung WH, Hu G, Kuo W, Kronstad JW (2009) Role of ferroxidases in iron uptake and virulence of *Cryptococcus neoformans*. Eukaryotic Cell 8: 1511–1520.

Kang YJ (2006) Metallothionein redox cycle and function. Experimental Biology and Medicine 231: 1459–1467.

Kägi JH, Vallee BL (1960) Metallothionein: a cadmium- and zinc-containing protein from equine renal cortex. Journal of Biological Chemistry 235: 3460–3465.

Kägi JH, Kojima Y, Kissling MM, Lerch K (1979) Metallothionein: an exceptional metal thiolate protein. Ciba Foundation Symposium 72: 223–237.

Kägi JHR, Kojima Y (1987) Chemistry and biochemistry of metallothionein. Experientia Supplementum Metallothionein II 52: 26-61.

Kameo S, Iwahashi H, Kojima Y, Satoh H (2000) Induction of metallothioneins in the heavy metal resistant fungus *Beauveria bassiana* exposed to copper or cadmium. Analusis 28: 382, 385.

Karin M, Najarian R, Haslinger A, Valenzuela P, Welch J, Fogel S (1984) Primary structure and transcription of an amplified genetic locus: the CUP1 locus of yeast. Proceedings of the National Academy of Sciences of the United States of America 81: 337-341.

Kelly EJ, Quaife CJ, Froelick GJ, Palmiter RD (1996) Metallothionein I and II protect against zinc deficiency and zinc toxicity in mice. The Journal of Nutrition 126: 1782–1790.

Kim BE, Nevitt T, Thiele DJ (2008) Mechanisms for copper acquisition, distribution and regulation. Nature Chemical Biology 4: 176–185.

Kim S, Ahn IP, Lee YH (2001) Analysis of genes expressed during rice-*Magnaporthe grisea* interactions. Molecular Plant-Microbe Interactions 14: 1340–1346.

Kim YO, Lee YG, Patel DH, Kim HM, Ahn SJ, Bae HJ (2012) Zn tolerance of novel *Colocasia esculenta* metallothionein and its domains in *Escherichia coli* and tobacco. Journal of Plant Research 125: 793–804.

King JC (2011) Zinc: an essential but elusive nutrient. Presented at the The American journal of clinical nutrition, American Society for Nutrition. 94: 679S–84S

Kleczkowski M, Garncarz M (2012) The role of metal ions in biological oxidation-the past and the present. Polish Journal of Veterinary Sciences 15: 165–173.

Kobayashi DY, Crouch JA (2009) Bacterial/Fungal interactions: from pathogens to mutualistic endosymbionts. Annual Review of Phytopathology 47: 63–82.

Krezel A, Maret W (2007) Different redox states of metallothionein/thionein in biological tissue. The Biochemical Journal 402: 551–558.

Kriek NP, Kellerman TS, Marasas WF (1981) A comparative study of the toxicity of *Fusarium verticillioides* (= *F. moniliforme*) to horses, primates, pigs, sheep and rats. The Onderstepoort Journal of Veterinary Research 48: 129–131.

Kumar KS, Dayananda S, Subramanyam C (2005) Copper alone, but not oxidative stress, induces copper-metallothionein gene in *Neurospora crassa*. FEMS Microbiology Letters 242: 45–50.

Kuźniak E, Kaźmierczak A, Wielanek M, Głowacki R, Kornas A (2013) Involvement of salicylic acid, glutathione and protein S-thiolation in plant cell death-mediated defence response of *Mesembryanthemum crystallinum* against *Botrytis cinerea*. Plant Physiology and Biochemistry 63: 30–38.

Labbé S, Zhu Z, Thiele, DJ (1997) Copper-specific transcriptional repression of yeast genes encoding critical components in the copper transport pathway. Journal of Biological Chemistry 272: 15951–15958.

Lachke SA, Srikantha T, Tsai LK, Daniels K, Soll DR (2000) Phenotypic switching in *Candida glabrata* involves phase-specific regulation of the metallothionein gene MT-II and the newly discovered hemolysin gene HLP. Infection and Immunity 68: 884–895.

Lagorce A, Fourçans A, Dutertre M, Bouyssiere B, Zivanovic Y, Confalonieri F (2012) Genome-wide transcriptional response of the archaeon *Thermococcus gammatolerans* to cadmium. PLoS ONE 7: e41935.

Lanfranco L (2002) Differential Expression of a metallothionein gene during the presymbiotic versus the symbiotic phase of an arbuscular mycorrhizal fungus. Plant Physiology 130: 58–67.

Langmade SJ, Ravindra R, Daniels PJ, Andrews GK (2000) The transcription factor MTF-1 mediates metal regulation of the mouse ZnT1 gene. Journal of Biological Chemistry 275: 34803–34809.

Leonhardt T, Sacky J, Simek P, Santrucek J, Kotrba P (2014) Metallothionein-like peptides involved in sequestration of Zn in the Zn-accumulating ectomycorrhizal fungus *Russula atropurpurea*. Metallomics 6: 1693–1701.

Li L, Chen OS, McVey Ward D, Kaplan J (2001) CCC1 is a transporter that mediates vacuolar iron storage in yeast. Journal of Biological Chemistry 276: 29515–29519.

Lin SJ, Pufahl RA, Dancis A, O'Halloran TV, Culotta VC (1997) A role for the *Saccharomyces cerevisiae* ATX1 gene in copper trafficking and iron transport. Journal of Biological Chemistry 272: 9215–9220.

Linder MC, Hazegh-Azam M (1996) Copper biochemistry and molecular biology. *T*he American Journal of Clinical Nutrition 63: 797S–811S.

Lippard SJ, Berg JM (1994) Principles of Bioinorganic Chemistry. Mill Valley, California: University Science Books.

Liu XD, Thiele DJ (1996) Oxidative stress induced heat shock factor phosphorylation and HSF-dependent activation of yeast metallothionein gene transcription. Genes & Development 10: 592–603.

Loebus J, Leitenmaier B, Meissner D, Braha B, Krauss GJ, Dobritzsch D, Freisinger E (2013) The major function of a metallothionein from the aquatic fungus *Heliscus lugdunensis* is cadmium detoxification. Journal of Inorganic Biochemistry 127: 253–260.

Lu D, Boyd B, Lingwood CA (1998) The expression and characterization of a putative adhesin B from *H. influenzae*. FEMS Microbiology Letters 165: 129–137.

Luber S, Reiher M (2010) Theoretical Raman optical activity study of the beta domain of rat metallothionein. The Journal of Physical Chemistry B 114: 1057–1063.

MacDiarmid CW, Milanick MA, Eide DJ (2002) Biochemical properties of vacuolar zinc transport systems of *Saccharomyces cerevisiae*. Journal of Biological Chemistry 277: 39187–39194.

Margoshes M, Vallee B (1957) A cadmium protein from equine kidney cortex. Journal of the American Chemical Society 17: 4813-4814.

Martelli A, Rousselet E, Dycke C, Bouron A, Moulis JM (2006) Cadmium toxicity in animal cells by interference with essential metals. Biochimie 88: 1807–1814.

Mehra RK, Garey JR, Winge DR (1990) Selective and tandem amplification of a member of the metallothionein gene family in *Candida glabrata*. Journal of Biological Chemistry 265: 6369–6375.

Mehra RK, Garey JR, Butt TR, Gray WR, Winge DR (1989) *Candida glabrata* metallothioneins. Cloning and sequence of the genes and characterization of proteins. Journal of Biological Chemistry 264: 19747–19753.

Mehra RK, Tarbet EB, Gray WR, Winge DR (1988) Metal-specific synthesis of two metallothioneins and gamma-glutamyl peptides in *Candida glabrata*. Proceedings of the National Academy of Sciences of the United States of America 85: 8815–8819.

Mir G, Domènech J, Huguet G, Guo WJ, Goldsbrough P, Atrian S, Molinas M (2004) A plant type 2 metallothionein (MT) from cork tissue responds to oxidative stress. Journal of Experimental Botany 55: 2483–2493.

Moreno MA, Ibrahim-Granet O, Vicentefranqueira R, Amich J, Ave P, Leal F, et al. (2007) The regulation of zinc homeostasis by the ZafA transcriptional activator is essential for *Aspergillus fumigatus* virulence. Molecular Microbiology 64: 1182–1197.

Mühlenhoff U, Stadler JA, Richhardt N, Seubert A, Eickhorst T, Schweyen RJ, et al. (2003) A specific role of the yeast mitochondrial carriers MRS3/4p in mitochondrial iron acquisition under iron-limiting conditions. Journal of Biological Chemistry 278: 40612–40620.

Münger K, Lerch K (1985) Copper metallothionein from the fungus Agaricus bisporus: chemical and spectroscopic properties. Biochemistry 24: 6751–6756.

Münger K, Germann UA, & Lerch, K. (1985). Isolation and structural organization of the Neurospora crassa copper metallothionein gene. *The EMBO Journal*, *4*(10), 2665–2668.

Münger K, Germann UA, Lerch K (1987) The *Neurospora crassa* metallothionein gene. Regulation of expression and chromosomal location. Journal of Biological Chemistry 262: 7363–7367.

Nathan C, Shiloh MU (2000) Reactive oxygen and nitrogen intermediates in the relationship between mammalian hosts and microbial pathogens. Proceedings of the National Academy of Sciences of the United States of America 97: 8841–8848.

Ngu TT, Stillman MJ (2009) Metalation of metallothioneins. IUBMB Life 61: 438–446.

Nies DH (1992) Resistance to cadmium, cobalt, zinc, and nickel in microbes. Plasmid 27: 17–28.

Nucci M, Anaissie E (2007) *Fusarium* infections in immunocompromised patients. Clinical Microbiology Reviews 20: 695–704.

Nyhus KJ, Wilborn AT, Jacobson ES (1997) Ferric iron reduction by *Cryptococcus neoformans*. Infection and Immunity 65: 434–438.

Orihuela R, Monteiro F, Pagani A, Capdevila M, Atrian S (2010) Evidence of native metal-S(2-)-metallothionein complexes confirmed by the analysis of Cup1 divalent-metal-ion binding properties. Chemistry 16: 12363–12372.

Osobová M, Urban V, Jedelský PL, Borovička J, Gryndler M, Ruml T, Kotrba P (2011) Three metallothionein isoforms and sequestration of intracellular silver in the hyperaccumulator *Amanita strobiliformis*. New Phytologist 190: 916–926.

Outten CE, O'Halloran TV (2001) Femtomolar sensitivity of metalloregulatory proteins controlling zinc homeostasis. Science 292: 2488–2492.

Pagani MA, Tomas M, Carrillo J, Bofill R, Capdevila M, Atrian S, Andreo CS (2012) The response of the different soybean metallothionein isoforms to cadmium intoxication. Journal of Inorganic Biochemistry 117: 306–315.

Pagani A, Villareal L, Capdevila M, Atrian S (2007) The *Saccharomyces cerevisiae* Crs5 Metallothionein metal-binding abilities and its role in the response to zinc overload. Molecular Microbiology 61: 256-269.

Palacios Ò, Atrian S, Capdevila M (2011) Zn- and Cu-thioneins: a functional classification for metallothioneins? Journal of Biological Inorganic Chemistry 16: 991–1009.

Palacios Ò, Espart A, Espín J, Ding C, Thiele DJ, Atrian S, Capdevila M (2014a) Full characterization of the Cu-, Zn-, and Cd-binding properties of CnMT1 and CnMT2, two metallothioneins of the pathogenic fungus *Cryptococcus neoformans* acting as virulence factors. Metallomics 6: 279–291.

Palacios Ò, Pérez-Rafael S, Pagani A, Dallinger R, Atrian S, Capdevila M (2014b) Cognate and noncognate metal ion coordination in metal-specific metallothioneins: the *Helix pomatia* system as a model. Journal of Biological Inorganic Chemistry 19: 923–935.

Palmiter RD (1995) Constitutive expression of metallothionein-III (MT-III), but not MT-I, inhibits growth when cells become zinc deficient. Toxicology and Applied Pharmacology 135: 139–146.

Palmiter RD (1998) The elusive function of metallothioneins. Proceedings of the National Academy of Sciences of the United States of America 95: 8428–8430.

Parfrey LW, Lahr DJG, Knoll AH, Katz LA (2011) Estimating the timing of early eukaryotic diversification with multigene molecular clocks. Proceedings of the National Academy of Sciences of the United States of America 108: 13624–13629.

Patel K, Kumar A, Durani S (2007) Analysis of the structural consensus of the zinc coordination centers of metalloprotein structures. Biochimica Et Biophysica Acta 1774: 1247–1253.

Pence NS, Larsen PB, Ebbs SD, Letham DL, Lasat MM, Garvin DF, et al. (2000) The molecular physiology of heavy metal transport in the Zn/Cd hyperaccumulator *Thlaspi caerulescens*. Proceedings of the National Academy of Sciences of the United States of America 97: 4956–4960.

Perego P, Howell SB (1997) Molecular mechanisms controlling sensitivity to toxic metal ions in yeast. Toxicology and Applied Pharmacology 147: 312-318.

Perfus-Barbeoch L, Leonhardt N, Vavasseur A, Forestier C (2002) Heavy metal toxicity: cadmium permeates through calcium channels and disturbs the plant water status. The Plant Journal : for Cell and Molecular Biology 32: 539–548.

Perotto S, Angelinic P, Bianciottob V, Bonfanteab P, Girlandaab M, Kulld T, Mellob A, Pecorarod. L, et al. (2013) Interactions of fungi with other organisms. Plant Biosystems 147: 208-218.

Piccinni E, Irato P, Guidolin L (1990) Cadmium-thionein in *Tetrahymena thermophila* and *Tetrahymena pyriformis*. European Journal of Protistology 26: 176–181.

Piccinni E, Staudenmann W, Albergoni V, De Gabrieli R, James P (1994) Purification and primary structure of metallothioneins induced by cadmium in the protists *Tetrahymena pigmentosa* and *Tetrahymena pyriformis*. European Journal of Biochemistry / FEBS 226: 853–859.

Pitt JI, Hocking AD (2009) Chapter 2: The ecology of fungal food spoilage. In Pitt JI, Hocking AD. Fungi and Food Spoilage. New York: Springer.

Porcheron G, Garénaux A, Proulx J, Sabri M, Dozois CM (2013) Iron, copper, zinc, and manganese transport and regulation in pathogenic Enterobacteria: correlations between strains, site of infection and the relative importance of the different metal transport systems for virulence. Frontiers in Cellular and Infection Microbiology 3: 90.

Prasad AS (2009) Zinc: role in immunity, oxidative stress and chronic inflammation. Current Opinion in Clinical Nutrition and Metabolic Care 12: 646–652.

Prohaska JR (2008) Role of copper transporters in copper homeostasis. The American Journal of Clinical Nutrition 88: 826S–9S.

Puig S, Thiele DJ (2002) Molecular mechanisms of copper uptake and distribution. Current Opinion in Chemical Biology 6: 171–180.

Puig S, Lee J, Lau M, Thiele DJ (2002) Biochemical and genetic analyses of yeast and human high affinity copper transporters suggest a conserved mechanism for copper uptake. Journal of Biological Chemistry 277: 26021–26030.

Quesada AR, Byrnes RW, Krezoski SO, Petering DH (1996) Direct reaction of H_2O_2 with sulfhydryl groups in HL-60 cells: zinc-metallothionein and other sites. Archives of Biochemistry and Biophysics 334: 241–250.

Ramesh G, Podila GK, Gay G, Marmeisse R, Reddy MS (2009) Different patterns of regulation for the copper and cadmium metallothioneins of the ectomycorrhizal fungus *Hebeloma cylindrosporum*. Applied and Environmental Microbiology 75 2266–2274.

Razem FA, Bernards MA (2002) Hydrogen peroxide is required for poly(phenolic) domain formation during wound-induced suberization. Journal of Agricultural and Food Chemistry 50: 1009–1015.

Rees E M, Thiele DJ (2004) From aging to virulence: forging connections through the study of copper homeostasis in eukaryotic microorganisms. Current Opinion in Microbiology 7: 175–184.

Rigby KE, Stillman MJ (2004) Structural studies of metal-free metallothionein. Biochemical and Biophysical Research Communications 325: 1271–1278.

Robinson NJ, Tommey AM, Kuske C, Jackson PJ (1993) Plant metallothioneins. The Biochemical Journal 295: 1–10.

Romero-Isart N, Vasák M (2002) Advances in the structure and chemistry of metallothioneins. Journal of Inorganic Biochemistry 88: 388–396.

Rutherford JC, Bird AJ (2004) Metal-responsive transcription factors that regulate iron, zinc, and copper homeostasis in eukaryotic cells. Eukaryotic Cell 3: 1–13.

Rutherford JC, Jaron S, Ray E, Brown PO, Winge DR (2001) A second iron-regulatory system in yeast independent of Aft1p. Proceedings of the National Academy of Sciences of the United States of America 98: 14322–14327.

Ruttkay-Nedecky B, Nejdl L, Gumulec J, Zitka O, Masarik M, Eckschlager T, et al. (2013) The role of metallothionein in oxidative stress. International Journal of Molecular Sciences 14: 6044–6066.

Sabolić I, Breljak D, Skarica M, Herak-Kramberger CM (2010) Role of metallothionein in cadmium traffic and toxicity in kidneys and other mammalian organs. Biometals 23: 897–926.

Sacky JS, Leonhardt T, Borovička J, Gryndler M, Briksí A, Kotrba P (2014) Intracellular sequestration of zinc, cadmium and silver in *Hebeloma mesophaeum* and characterization of its metallothionein genes. Fungal Genetics and Biology 67:C 3–14.

Salt De, Wagner GJ (1993) Cadmium transport across tonoplast of vesicles from oat roots. Evidence for a Cd^{2+}/H^{+} antiport activity. Journal of Biological Chemistry 268: 12297–12302.

Santovito G, Formigari A, Boldrin F, Piccinni E. (2007) Molecular and functional evolution of *Tetrahymena* metallothioneins: new insights into the gene family of *Tetrahymena thermophila*. Comparative Biochemistry and Physiology. Toxicology & Pharmacology 144: 391–397.

Schueffler A, Anke T (2014) Fungal natural products in research and development. Natural Product Reports 31: 1425-1448.

Seefelder W, Humpf HU, Schwerdt G, Freudinger R, Gekle M (2003) Induction of apoptosis in cultured human proximal tubule cells by fumonisins and fumonisin metabolites. Toxicology and Applied Pharmacology 192: 146–153.

Shang Y, Song X, Bowen J, Corstanje R, Gao Y, Gaertig J, Gorovsky MA (2002) A robust inducible-repressible promoter greatly facilitates gene knockouts, conditional expression, and overexpression of homologous and heterologous genes in *Tetrahymena thermophila*. Proceedings of the National Academy of Sciences of the United States of America 99: 3734–3739.

Sherman F, Fink GF, Hicks J (1994) Chapter 6: Yeast RNA isolation. In Grodzicker T, Hastie N. Methods in Yeast Genetics. New York: Cold Spring Harbor Laboratory Press.

Shi J, Lindsay WP, Huckle JW, Morby AP, Robinson NJ (1992) Cyanobacterial metallothionein gene expressed in *Escherichia coli*. Metal-binding properties of the expressed protein. FEBS Letters 303: 159–163.

Shuja RN, Shakoori AR (2007) Identification, cloning and sequencing of a novel stress inducible metallothionein gene from locally isolated *Tetrahymena tropicalis lahorensis*. Gene 405: 19–26.

Sigler L (2003) Chapter 11: Miscellaneous opportunistic fungi: Microascaceae and other Ascomycetes, Hyphomycetes, Coelomycetes and Basidiomycetes. In Howard DH. Pathogenic fungi in humans and animals (2nd ed.). New York: Marcel

Simpkins CO (2000) Metallothionein in human disease. Cellular and Molecular Biology 46: 465–488.

Sinclair SA, Krämer U (2012) The zinc homeostasis network of land plants. Biochimica Et Biophysica Acta 1823: 1553–1567.

Sriram K, Lonchyna VA (2009) Micronutrient supplementation in adult nutrition therapy: practical considerations. Journal of Parenteral and Enteral Nutrition 33: 548–562.

Stadler JA, Schweyen RJ (2002) The yeast iron regulon is induced upon cobalt stress and crucial for cobalt tolerance. The Journal of Biological chemistry 277: 39649-39654.

Strain J and Culotta VC (1996) Copper ions and the regulation of *Saccharomyces cerevisiae* metallothionein genes under aerobic and anaerobic conditions. Molecular and General Genetics 251: 139-45.

Sutherland DEK, Stillman MJ (2011) The "magic numbers" of metallothionein. Metallomics 3: 444–463.

Tamai KT, Liu X, Silar P, Sosinowski T, Thiele DJ (1994) Heat shock transcription factor activates yeast metallothionein gene expression in response to heat and glucose starvation via distinct signalling pathways. Molecular and Cellular Biology 14: 8155–8165.

Tang L, Qiu R, Tang Y, Wang S (2014) Cadmium-zinc exchange and their binary relationship in the structure of Zn-related proteins: a mini review. Metallomics 6: 1313–1323.

Tapiero H, Townsend DM, Tew KD (2003) Trace elements in human physiology and pathology. Copper. Biomedicine & Pharmacotherapy 57: 386–398.

Taylor JW (2014) Evolutionary perspectives on human fungal pathogens. Cold Spring Harbor Perspectives in Medicine a019588.

Templeton DM, Cherian MG (1984) Chemical modifications of metallothionein. Preparation and characterization of polymers. The Biochemical Journal 221: 569–575.

Thiele DJ (1988) ACE1 regulates expression of the *Saccharomyces cerevisiae* metallothionein gene. Molecular and Cellular Biology 8: 2745–2752.

Thomson A, Gray H (1998) Bio-inorganic chemistry. Current Opinion in Chemical Biology 2: 155–158.

Tió L, Villarreal L, Atrian S, Capdevila M (2004) Functional differentiation in the mammalian metallothionein gene family: metal binding features of mouse MT4 and comparison with its paralog MT1. Journal of Biological Chemistry 279: 24403–24413.

Tomàs M, Domènech J, Capdevila M, Bofill R, Atrian S (2013) The sea urchin metallothionein system: Comparative evaluation of the SpMTA and SpMTB metal-binding preferences. FEBS Open Bio 3: 89–100.

Tomàs M, Pagani MA, Andreo CS, Capdevila M, Atrian S, Bofill R (2015) Sunflower metallothionein family characterisation. Study of the Zn(II)- and Cd(II)-binding abilities of the HaMT1 and HaMT2 isoforms. Journal of Inorganic Biochemistry (In Press).

Tomàs M, Pagani MA, Andreo CS, Capdevila M, Bofill R, Atrian S (2014) His-containing plant metallothioneins: comparative study of divalent metal-ion binding by plant MT3 and MT4 isoforms. Journal of Biological Inorganic Chemistry 19: 1149–1164.

Trevors JT, Stratton GW, Gadd GM (1986) Cadmium transport, resistance, and toxicity in bacteria, algae, and fungi. Canadian Journal of Microbiology 32: 447–464.

Tucker SL (2004) A fungal metallothionein is required for pathogenicity of *Magnaporthe grisea*. The Plant Cell Online 16: 1575–1588.

Valko M, Morris H, Cronin MTD (2005) Metals, toxicity and oxidative stress. Current Medicinal Chemistry 12: 1161–1208.

Valls M, Bofill R, Gonzàlez-Duarte R, Gonzàlez-Duarte P, Capdevila M, Atrian S (2001) A new insight into Metallothionein (MT) classification and evolution: the *in vivo* and *in vitro* metal binding features of *Homarus americanus* recombinant MT. Journal of Biological Chemistry 276: 32835–32843.

Vasák M (2005) Advances in metallothionein structure and functions. Journal of Trace Elements in Medicine and Biology 19: 13–17.

Vasák M, Hasler DW (2000) Metallothioneins: new functional and structural insights. Current Opinion in Chemical Biology 4: 177–183.

Vido K, Spector D, Lagniel G, Lopez S, Toledano MB, Labarre J (2001) A proteome analysis of the cadmium response in *Saccharomyces cerevisiae*. Journal of Biological Chemistry 276: 8469–8474.

Vilahur N, Vahter M, Broberg K (2015) The epigenetic effects of prenatal cadmium exposure. Current Environmental Health Reports 2: 195–203.

Wagner D, Maser J, Lai B, Cai Z, Barry CE, Höner Zu Bentrup K, et al. (2005) Elemental analysis of *Mycobacterium avium*-, *Mycobacterium tuberculosis*-, and *Mycobacterium smegmatis*-containing phagosomes indicates pathogen-induced microenvironments within the host cell's endosomal system. Journal of Immunology 174: 1491–1500.

Waldron KJ, Robinson NJ (2009) How do bacterial cells ensure that metalloproteins get the correct metal? Nature Reviews. Microbiology 7: 25–35.

Walton FJ, Idnurm A, Heitman J (2005) Novel gene functions required for melanization of the human pathogen *Cryptococcus neoformans*. Molecular Microbiology 57: 1381–1396.

Waters BM, Eide DJ (2002) Combinatorial control of yeast FET4 gene expression by iron, zinc, and oxygen. Journal of Biological Chemistry 277: 33749–33757.

Westin G, Schaffner W (1988) A zinc-responsive factor interacts with a metal-regulated enhancer element (MRE) of the mouse metallothionein-I gene. The EMBO Journal 7: 3763–3770.

Winge DR, Nielson KB, Gray WR, Hamer DH (1985) Yeast metallothionein. Sequence and metal-binding properties. Journal of Biological Chemistry 260: 14464–14470.

Wysocki R, Tamás MJ (2010) How *Saccharomyces cerevisiae* copes with toxic metals and metalloids. FEMS Microbiology Reviews 34: 925–951.

Zhao H, Eide D (1996a) The yeast ZRT1 gene encodes the zinc transporter protein of a high-affinity uptake system induced by zinc limitation. Proceedings of the National Academy of Sciences of the United States of America 93: 2454–2458.

Zhao H, Eide D (1996b) The ZRT2 gene encodes the low affinity zinc transporter in *Saccharomyces cerevisiae*. Journal of Biological Chemistry 271: 23203–23210.

Zhao H, Butler E, Rodgers J, Spizzo T, Duesterhoeft S, Eide D (1998) Regulation of zinc homeostasis in yeast by binding of the ZAP1 transcriptional activator to zinc-responsive promoter elements. Journal of Biological Chemistry 273: 28713–28720.

Zhou PB, Thiele DJ (1991) Isolation of a metal-activated transcription factor gene from *Candida glabrata* by complementation in *Saccharomyces cerevisiae*. Proceedings of the National Academy of Sciences of the United States of America 88: 6112–6116.

Zhou Z, Wang C, Liu H, Huang Q, Wang M, Lei Y (2013) Cadmium induced cell apoptosis, DNA damage, decreased DNA repair capacity, and genomic instability during malignant transformation of human bronchial epithelial cells. International Journal of Medical Sciences 10: 1485–1496.